UTILIZING MICROPELLETS AS BUILDING BLOCKS IN CARTILAGE TISSUE ENGINEERING

Betul Kul Babur

B.Sc.

ID: 7673442

Submitted in fulfilment of the requirements for the degree of

Doctor of Philosophy (Research)

Institute of Health and Biomedical Innovation, Translational Research Institute

School of Biomedical Sciences, Faculty of Health

Queensland University of Technology

February 2015

Keywords

Articular cartilage treatment, articular chondrocytes, biphasic tissue, cartilage dust, cartilage particles, cartilage tissue engineering, cell aggregates, cell spheroids, chondrocyte redifferentiation, chondrogenesis, chondrogenic differentiation, hypoxia, mesenchymal stromal cells, micropellets, normoxia, osteochondral tissue, osteogenic differentiation, pellet culture, scaffold-free tissue engineering, tissue assembly, tissue building blocks.

Abstract

Osteoarthritis (OA) is considered to be one of the leading causes of disability in the western countries and it represents an enormous financial burden on healthcare systems. OA can arise as the result of cartilage tissue degeneration in response to an acute injury or idiopathic degeneration. In both cases degeneration reflects the inherent limited self-repair capacity of articular cartilage. Despite significant and broad research efforts targeting cartilage defect repair via marrow stimulation, osteochondral graft transplantation, *in vitro* expanded chondrocyte implantation, and/or the use of various biomaterials as scaffolds, successful and robust repair remains elusive. Recent studies suggest that cell-based therapies do promote the regeneration of articular cartilage, however their modest efficacy suggests that further optimization and even a change in approach is needed.

Previous research from our group demonstrated that the chondrogenic differentiation of human bone marrow-derived mesenchymal stem/stromal cells (MSC) was enhanced when the cells were assembled into micropellets, rather than traditional macroscopic pellets. Based on this critical finding, I investigated opportunities to exploit this phenomenon in cartilage tissue engineering applications. Through my Thesis, I addressed the following three specific questions:

Q1. Does the micropellet approach also enhance the redifferentiation of monolayer expanded chondrocytes?

Q2. Can the matrix content and defect filling capacity of engineered cartilage be enhanced through the inclusion of donor matrix particles in MSC micropellets?

Q3. Can chondrogenic and osteogenic micropellets be used as building blocks and assembled into macroscopic osteochondral-like tissue?

High-throughput manufacture of micropellets was facilitated via a custom-made microwell surface originally generated as a silica wafer and then replicated with soft

lithography method. According to this manufacturing process, single cells were seeded on a polydimethylsiloxane (PDMS) surface containing the microwell impression. When the cells were centrifuged or settled on this microwell surface, they were divided into small groups of 100-200 cells, which then formed micropellets within the first hours of culture. With this robust micropellet manufacturing technique, three independent but closely related studies were conducted, each addressing one of the previously mentioned questions. These three studies were reported as separate research articles in this Thesis by publication.

Chapter 3 addresses the first question and reports on the chondrogenic redifferentiation of expanded chondrocytes in macro- or micropellets and under normoxic or hypoxic atmospheres. It is a well-known phenomenon that the articular chondrocytes dedifferentiate during monolayer expansion. Similar to MSC chondrogenesis, pellet culture promotes redifferentiation, however these traditional pellets have 1-2 mm diameter, which causes diffusion gradients and mass transport issues leading to a heterogenic tissue structure. In order to overcome this problem, I tested the chondrocyte redifferentiation in micropellets that were approximately ten times smaller than the traditional pellets. According to chondrogenic assays, gene expression analyses and histological assessments, the redifferentiation of chondrocytes in micropellets was enhanced and yielded homogenous tissue structure. This work also demonstrated that micropellets could be assembled in order to engineer macroscopic cartilaginous tissue constructs.

Chapter 4 addresses the second question and reports on the effects of incorporation of microscopic cartilage pieces in macro- or micropellets of human bone marrow MSC. The fact that larger cartilage defects require a greater number of cells limits the applicability of cell-based therapies. As an alternative to articular chondrocytes, bone marrow-derived MSC can be harnessed because of their proliferation capacity, chondrogenic differentiation potential and ease of harvest. Additionally, use of xenogeneic cartilage pieces can increase the volume of engineered tissue graft in order to fill the larger defects more effectively. By combining two approaches, I tested the incorporation of microscopic bovine cartilage particles, termed as “cartilage dust”, into MSC micropellets. Chondrogenic characteristics, gene

expression profile and histological structure assessment indicated that incorporation of cartilage dust into micropellets had significantly increased the size and cartilaginous matrix content, however it did not enhance the chondrogenic differentiation of MSC. It is also demonstrated that micropellets with or without cartilage dust can be assembled in order to engineer macroscopic cartilaginous tissue constructs.

Chapter 5 addresses the third question and reports on the assembly of osteogenic and chondrogenic micropellets into a biphasic tissue. The main purpose of building an osteochondral graft is to exploit more efficient bone-bone integration that takes place at the foundation of the defect and stabilizes the cartilaginous graft in place. The method of utilizing a scaffold with biphasic characteristics in order to generate an osteochondral graft is frequently trialed. In this study, I first tested the chondrogenic and osteogenic phenotype change in MSC micropellets, and then constructed the first scaffold-free biphasic tissue utilizing micropellets as building blocks.

In conclusion, this Thesis describes the characteristics of micropellets with different cell types (chondrocytes or MSC) and compositions (with or without the cartilage dust) under different conditions (hypoxic, normoxic, chondrogenic, osteogenic). The results presented in this Thesis introduce a novel intermediate component, micropellets, between the single cells and the tissue to be engineered. Utilization of micropellets may improve tissue engineering applications and cell-based therapies, ultimately leading to development of novel approaches in cartilage defect repair.

Table of Contents

List of Figures and Tables

List of Abbreviations

2D	Two Dimensional
3D	Three Dimensional
ACI	Autologous Chondrocyte Implantation
ALP	Alkaline Phosphatase
AMIC	Autologous Matrix-induced Chondrogenesis
bFGF	basic FGF/FGF-2
BMC	Bone Marrow Concentrate
BMP	Bone Morphogenic Protein
BSA	Bovine Serum Albumin
CACI	Collage-covered ACI
CD	Cartilage Dust
cDNA	complementary DNA
CHI	Chitosan
CO_2	Carbon Dioxide
DAPI	4',6-diamidino-2-phenylindole
DMB	1,9-Dimethyl-Methylene Blue
DMEM	Dulbecco's Modified Eagle Medium
DMSO	Dimethyl sulfoxide
DNA	Deoxyribonucleic Acid
ECM	Extracellular Matrix
EDAC	1-Ethyl-3(3Dimethylaminopropyl) carbodiimide
EDTA	Ethylenediaminetetraaceticacid
FBS	Fetal Bovine Serum
FDA	Food and Drug Administration
FGF	Fibroblast Growth Factor
GAG	Glycosaminoglycan
GAPDH	Glyceraldehyde 3-phosphate dehydrogenase
HA	Hyaluronic Acid
HIF	Hypoxia-Inducible Factor
IF	Immuno Fluorescence
IGF	Insulin-like Growth Factor
Ihh	Indian hedgehog

ITS-X	Insulin-Transferrin-Selenium-Ethanolamine
JNK	c-Jun N-terminal Kinase
MACI	Matrix-assisted ACI
MAP	Mitogen-activated Protein
MES	2-(N-morpholino) ethanesulfonic Acid
ML	Multilayer
MSC	Mesenchymal Stem/Stromal Cells
N-cadherin	Neural cadherin
N-CAM	Neural Cell Adhesion Molecule
NHS	N-Hyrdoxysuccinimide
O_2	Oxygen
OA	Osteoarthritis
OCT	Optimum Cutting Temperature
PBS	Phosphate Buffered Saline
PCL	Polycaprolactone
PCR	Polymerase Chain Reaction
PDMS	Polydimethylsiloxane
PEG	Polyethylene Glycol
PEO	Polyethylene Oxide
PGA	Poly Glycolic Acid
PLA	Poly Lactic Acid
PLGA	Poly (Lactic-co-Glycolic Acid)
PRP	Platelet Rich Plasma
PS	Penicillin-Streptomycin
PTHrP	Parathyroid Hormone related Protein/Peptide
qPCR	quantitative PCR
RGD	Arg-Gly-Asp peptide motif
RNA	Ribonucleic Acid
RT	Room Temperature
RUNX2	Runt-related transcription factor 2
sGAG	sulfated GAG
SOX9	(Sex determining region Y)-box 9
TGFβ	Transforming Growth Factor beta
UV	Ultraviolet

Statement of Original Authorship

The work contained in this thesis has not been previously submitted to meet requirements for an award at this or any other higher education institution. To the best of my knowledge and belief, the thesis contains no material previously published or written by another person except where due reference is made and appropriate permission to reuse is obtained.

QUT Verified Signature

Signature:

Date: 20.01.2015

"I do not know what I may appear to the world; but to myself I seem to have been only like a boy playing on the seashore, and diverting myself in now and then finding a smoother pebble or a prettier shell than ordinary, whilst the great ocean of truth lay all undiscovered before me."

Isaac Newton

Chapter 1: Introduction

1. Osteoarthritis

Osteoarthritis (OA) is the most common form of joint diseases affecting 250 million people worldwide [1]. It is even more prevalent in developed countries with aging population such as USA, Canada, Europe and Australia [2,3]. In Australia, an estimated 1.9 million people were affected by OA in 2012 and it is projected that this number will rise to 3 million by 2032 [4]. The financial cost of OA in Australia was estimated to be 3.7 billion dollars in 2012, which was equivalent to 6.8% of the total health expenditure [4]. In OA, the articular cartilage that is the tissue covering the ends of long bones loses its integrity and resilience followed by complications and further degeneration until the function of the joint is impaired. Some would even argue that OA is similar to an organ failure, if articular cartilage is considered as an organ [5]. OA can be classified as primary (idiopathic/unknown cause) or secondary in which the cause of disease is another primary disease or a traumatic injury [5]. Hereditary components, sex (more prevalent in females) [6], ageing, obesity [7] and injury [8] are the leading risk factors of OA. Weight loss and exercise are the highly encouraged lifestyle changes for prevention of OA, but the compliance rate is very low [9]. The diagnosis rate peaks around the age of 50 and the general symptoms are pain, stiffness, clicking, locking and

loss of joint function [10]. At advanced stages, OA causes disability to perform daily life activities decreasing the quality of life, therefore causing psychological distress in patients. Once diagnosed with OA, patients do not have many options other than joint replacement surgery, which is the amputation of damaged cartilage and resurfacing of the joint with metal and plastic components (see Chapter 2). This fact has motivated efforts to develop tissue engineering approaches that enable the repair of damaged articular cartilage at earlier stages so that the prevalence of OA can be minimized in the future.

2. History of articular cartilage focused medical research

The unusual characteristics of cartilage were realized around second century. Early scientists and physicians were utterly puzzled with the properties of this inscrutable tissue. The following historical quotations describing the first scientific impressions of cartilage are taken from the paper by Benedek [11], where more of similar quotations can be found.

Galen described the articular cartilage for the first time in 175 as follows: "*Cartilages are spread on some parts of them [bones], such as the joints, to make them smooth, and Nature also uses cartilages occasionally as moderately yielding bodies… Cartilage serves as a grease for the joints* [12][a]". Galen also noted the function of synovial fluid together with the cartilage: "*... Nature has again searched out a double remedy, first covering each member of the joint with cartilage and then pouring over the cartilages themselves a sort of oily substance, a greasy, glutinous fluid, which gives every joint an easy movement and protection against wear* [12][b]".

Later in 1536, Niccolo Massa drew attention to the function of the articular cartilage: "*cartilage is a certain substance like bone, but softer which you will find at the extremities of all the bones, large and small according to the need of the member… This cartilaginous portion was reserved for many bones at their extremities in order to keep two hard surfaces from coming into contact and being broken by movement and to maintain something between the final hardness of the bone and the soft flesh…*[13]". Interestingly, Massa used the term "reserved" for articular cartilage, however the

developmental process, where a thin layer of cartilage is literally reserved, was only discovered three centuries later [14].

Morgagni described the state of osteoarthritic cartilage and the osteophytes for the first time in an autopsy report in 1741: "*The head of the right os femoris was not rounded into a globular form: and was depress'd, and not cover'd by a smooth and white cartilage, but by one of a pale ash-colour: and, indeed, this cartilage was totally deficient in the posterior part of the head; so that the bone appear'd naked in that part, and form'd into many roundish and protuberant particles* [15]".

In 1743, Hunter was the first to report the different orientation of the collagen fibers, synovial membrane, and lack of self-healing in the case of injury: *"... We may compare the Texture of a Cartilage to the Pile of Velvet, its Fibres rising up from the Bone, as the silky Threads of that rise from the woven Cloth or Basis… Now these perpendicular Fibres make the greatest Part of the cartilaginous Substance; but without Doubt there are likewise transverse Fibrils which connect them, and make the Whole a solid Body, though these last are not easily seen, because being very tender, they are destroyed in preparing the Cartilage… Every Joint is invested with a Membrane, which forms a complete Bag, and gives a Covering to everything within the Articulation… The Blood-vessels are so small, that they do not admit the red Globules of the Blood; so that they remain in a great measure unknown… an ulcerated Cartilage is universally allowed to be a very troublesome Disease; that it admits of a Cure with more difficulty than a carious Bone; and that, when destroyed, it is never recovered* [16]" (Quotations are re-used with permission from Elsevier, see App. A).

In the nineteenth century the biochemistry of the cartilage was revealed and individual matrix components were identified [11]. In the twentieth century researchers started to develop treatments to heal cartilage injuries (see Chapter 2). With the advancements in scientific technology, such as microscopes and analysis instruments, today in the twenty-first century we know a lot more about the structure, biomechanical function, development and injury of the articular cartilage (see Chapter 2). Currently, it is possible to treat injured cartilage in different ways, however none of the existing treatment options guarantee full-recovery yet, which perhaps makes the articular cartilage the "Achilles' heel" of the human body.

3. Thesis overview

3.1. Description of research problem

OA is one of the leading causes of pain and disability worldwide. The biomedical research to find the ultimate cure for articular cartilage injuries is still in progress at present. Articular cartilage tissue has limited self-healing capacity, therefore there is a legitimate need to develop biological therapies to treat cartilage injuries and minimize onset of OA and associated financial burden.

3.2. Overall objectives of the study

This study aims to improve existing cell-based therapies and introduce novel approaches to treat cartilage defects. The most significant contribution of this study to the accumulating body of knowledge in cartilage research is the idea of using "micropellets" as discrete units to engineer macroscopic cartilage tissue grafts. An analogy of constructing a wall and engineering a tissue can be useful in order to understand the significance of the micropellets as an intermediate step between the single cells and the whole tissue. One cannot construct a wall directly from sand but needs discrete units such as bricks, and then the clay is used to adhere and seal the individual bricks. Similarly, this study suggests that adequate building blocks for tissue engineering applications is not single cells but micropellets. The tissues with great size and high complexity can be generated utilizing multicellular micropellets as the bricks and the produced extracellular matrix acts as the clay.

3.3. Specific aims of the study

In this Thesis, the following specific aims were addressed in three independent research articles:

- To test the micropellet approach in redifferentiation of monolayer expanded human articular chondrocytes
- To increase matrix content and defect filling properties of human bone marrow MSC micropellets with incorporation of donor cartilage particles
- To assemble osteogenic and chondrogenic micropellets in order to generate a scaffold-free osteochondral-like tissue

3.4. Linking research papers

In this project, first an in-house fabricated, custom made microwell platform was developed to enable cost effective, high throughput generation of micron size micropellets for all studies. After setting up the microwell platform, different ways of utilizing micropellets in cartilage tissue engineering were explored. Three specific examples of micropellet use, which could potentially be useful in cell-based therapies, were reported as three research articles. In the first study, the articular chondrocytes were tested in micropellet platform because of their clinical relevance. Autologous chondrocyte is seen as the primary cell source for most of the cell-based therapies. However, monolayer expansion of chondrocytes causes loss of chondrogenic phenotype and a redifferentiation step is required to restore cell phenotype before implantation. Chapter 3 demonstrated how micropellet culture enhances this redifferentiation process [17]. The fabrication of microwell platform was also included in Chapter 3. Previously, our group demonstrated that bone marrow MSC chondrogenesis was enhanced in hypoxic micropellets [18]. In the second study, bone marrow MSC micropellets were further examined. Most of the MSC studies conclude that the replication of high matrix content found in native cartilage is quite challenging. Chapter 4 explained how the cartilaginous matrix content and defect filling properties of MSC micropellets were increased with incorporation of donor cartilage particles. Another common challenge in cartilage treatment is the inefficient integration of the tissue graft to the defect site. Some studies focus on generating osteochondral tissue grafts in order to overcome this problem. In the third study, a scaffold-free osteochondral-like tissue was engineered using osteogenic and chondrogenic micropellets. Previously, our group reported that MSC osteogenesis was also more efficient in micropellets [19]. Chapter 5 demonstrated how MSC derived osteogenic and chondrogenic micropellets were assembled to generate a scaffold-free osteochondral-like tissue exemplifying the use of micropellets as building blocks. In this project, articular chondrocyte micropellets (Chapter 3), donor matrix incorporated MSC micropellets (Chapter 4) and a scaffold-free biphasic tissue generated with MSC micropellets (Chapter 5) were characterized *in vitro*. Testing these different micropellets in animal defect models is the next vital step in order to expose the potential of micropellet use in clinical applications.

3.5. Chapter contents

In Chapter 1, the greatest clinical motivation for cartilage research, osteoarthritis, and its effects are described in order to justify the scientific effort and the financial expenses spared for finding alternative ways to treat cartilage injuries. Then some historical quotations describing the first scientific and clinical impressions of articular cartilage and its injury are provided. Finally, the Thesis overview is listed.

In Chapter 2, a detailed literature review is compiled. The literature review starts with the description of articular cartilage, its components, development and state in injury. Then, the existing surgical techniques, including joint replacement, microfracture, mosaicplasty and autologous chondrocyte implantation (ACI) are explained. Next, cartilage tissue engineering and its components are introduced and advancements in the area are discussed. Finally, the significance of using micropellets as building blocks in scaffold-free cartilage tissue engineering is explained.

Chapters 3, 4 and 5 are the result chapters, each exemplifying a specific way of using micropellets in *ex vivo* cartilage tissue generation. Each chapter is in the format of a research article therefore includes individual abstract, introduction, materials and methods, results, discussion, and conclusion sections.

In Chapter 3, the redifferentiation of monolayer expanded human articular chondrocytes in macro- or micropellets and in normoxic or hypoxic atmosphere is reported. Additionally, the amalgamation of the discrete micropellets is investigated with the assembly of the micropellets at different time points. The feasibility of chondrocyte micropellet use in cartilage tissue engineering is studied.

In Chapter 4, the incorporation of the microscopic donor cartilage particles, termed as “cartilage dust” (CD), into macro- and micropellets of human bone marrow derived mesenchymal stem/stromal cells (MSC) is reported. Additionally, the amalgamation of the discrete micropellets with and without the CD is investigated with the assembly of the micropellets at different time points. The feasibility of CD use in order to increase the volume and defect filling capacity of MSC derived chondrogenic micropellets is studied.

In Chapter 5, the differentiation of human bone marrow derived MSC micropellets when exposed to chondrogenic and osteogenic media is tested. The

chondrogenic and osteogenic characteristics of micropellets is reported in the following culture conditions: two weeks of chondrogenic media, one week of chondrogenic followed by another week of osteogenic media, one week of osteogenic followed by another week of chondrogenic media and two weeks of osteogenic media. Additionally, a scaffold-free osteochondral-like tissue is generated with layer by layer assembly of the chondrogenic and osteogenic micropellets. The feasibility of engineering a composite tissue using different phenotype micropellets as building blocks is studied.

In Chapter 6, the findings are summarized, discussed and the future perspectives, including *in vivo* experiments, mass production of micropellets and complex tissue engineering with micropellets, are outlined.

"I am among those who think that science has great beauty. A scientist in his laboratory is not only a technician: he is also a child placed before natural phenomena which impress him like a fairy tale."

Marie Curie

Chapter 2: Literature Review

1. Articular cartilage

Articular/hyaline cartilage is the tissue covering the ends of the articulating joints (Fig. 1). Its function is to provide almost frictionless gliding surfaces in between bones and absorb the impact during joint movement. Articular cartilage lacks blood vessels, lymphatic vessels and neurons, therefore it relies on diffusion of signal molecules and metabolites from the synovial fluid [20]. Whilst the histological assessment of the native articular cartilage suggests a relatively simple tissue structure at first glance, decades of research have proven that this tissue has a remarkably complex and elegant design. It is this complexity that has made replicating and repairing this tissue an unmet challenge.

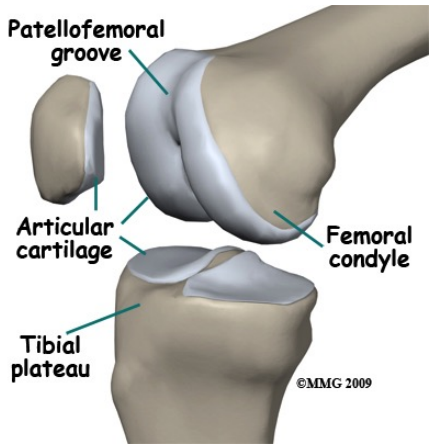

Figure 1. Anatomical structure of the articular cartilage of knee. Image is courtesy of Medical Multimedia Group LLC, www.eOrthopod.com , see App.B for permission.

1.1. Chondrocyte

Articular cartilage mostly consists of extracellular matrix (ECM) that is produced and maintained by a single cell type, the chondrocyte. Each individual chondrocyte has high metabolic activity, however since all chondrocytes only correspond to 1-5% of the total volume, the overall metabolic activity of the tissue is very low [21]. The chondrocytes are mostly spherical in morphology, sparsely distributed and entrapped by matrix in compartments called lacuna (Fig. 2A). The fluid filling the lacuna (pericellular matrix) and the chondrocyte residing in that lacuna are referred as "chondron" [22,23]. It is suggested that the pericellular matrix mediates the transduction of biomechanical and biochemical signals to the chondrocytes [24] and altered permeability of the chondrons in disease might have a role in biomechanical failing of the tissue [25].

1.2. Extracellular matrix

The ECM is comprised of different molecules organized in a hierarchical order (Fig. 2A). The collagen is the main component of the ECM, type II dominating other types such as type IX, X and XI, which are unique to cartilage [26]. Collagen molecules form fibers and cross-linked collagen fibers form a network that entraps the other ECM components. The collagen network also provides the tensile strength of the tissue. Hyaluronic acid (HA) is a large non-sulfated glycosaminoglycan (GAG) molecule that aggregates proteoglycan monomers such as aggrecan in the presence of link protein [27]. Aggrecan aggregates keratin sulfate and chondroitin sulfate that are small, negatively charged, sulfated GAG (sGAG) molecules (Fig. 2A). The net negative charge of the tissue generated by high number of sGAG molecules attracts the positively charged cations such as Na^+, K^+ that causes an influx of water into the tissue in a non-loaded state, which is described as Donnan effect [20]. This effect endows articular cartilage its compressive strength, and in fact the instant efflux of the water retained in the tissue provides the very first shock absorbance. It is this unique and highly organized combination of each ECM component in different proportions that makes articular cartilage a multi-phasic, non-linearly permeable, viscoelastic tissue [28]. The simple histological appearance of this tissue is an illusion.

1.3. Ultrastructure

The multi-phasic nature of articular cartilage is highly studied, and it is concluded that there are four different zones defined by the alignment of the collagen fibers and the chondrocyte morphology (Fig. 2B). The superficial zone is the thin uppermost layer with horizontally aligned collagen fibers and flattened chondrocyte morphology. This horizontal alignment of the collagen fibers in superficial zone provides the greatest tensile strength, which is critical for the integrity of the whole tissue. Additionally, the densely packed horizontal collagen fibers act as a barrier from synovial fluid, giving the cartilage its immune-privileged status [29]. The middle zone is known for the randomly aligned collagen fibers and sparsely distributed spherical chondrocytes. The deep zone is distinguished by the perpendicular alignment of collagen fibers and the columnar orientation of spherical chondrocytes. The last layer that connects the cartilage tissue to underlying bone is the calcified zone, which has hypertrophic enlarged chondrocytes that synthesize collagen X. Also the perpendicular collagen fibers from deep zone penetrate into calcified zone strengthening the connection between the articular cartilage and the underlying bone. A visible line stained by basic dyes called ‘tidemark’ separates the deep zone from calcified zone (Fig. 2B). Overall, the ultrastructure of articular cartilage provides the greatest tensile strength in superficial zone while providing the greatest compressive strength in middle and deep zones.

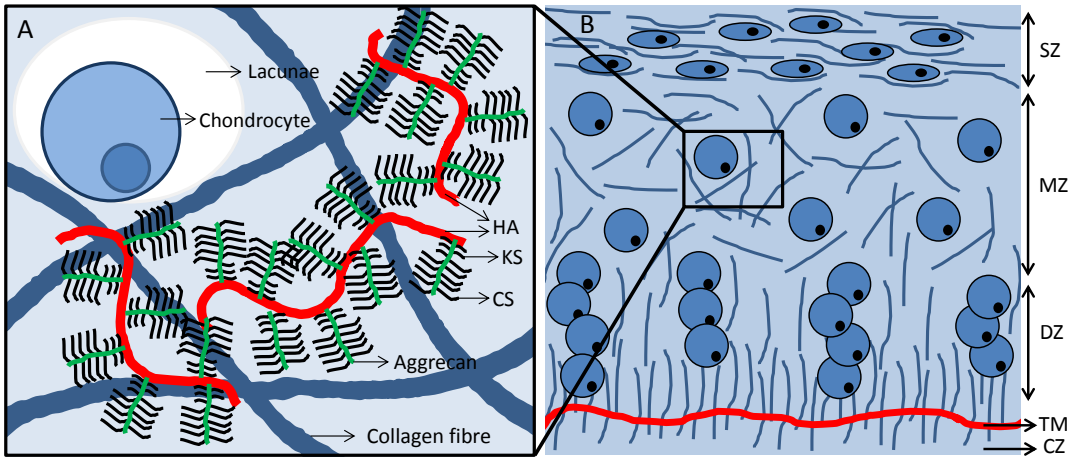

Figure 2. Chondrocyte, ECM and ultrastructure of articular cartilage. Chondrocytes are surrounded by lacuna and ECM molecules such as hyaluronic acid (HA), aggrecan, keratin sulfate (KS), chondroitin sulfate (CS) are entrapped by the collagen II fibers (A). Chondrocytes and collagen fibers are aligned horizontally in superficial zone (SZ), randomly in middle zone (MZ) and vertically in deep zone (DZ); tidemark (TM) separates the deep zone and the calcified zone (CZ) (B). Figure is not to scale.

1.4. Mechanical properties

The thickness of the articular cartilage in the knee changes between 1-5 mm [28]. The tensile modulus can decrease from 125 to 40 MPa from the age of 20 to 85 [30] while the compressive modulus of the femoral condyles is in the range of 4.3-13 MPa [31]. During normal walking the articular cartilage bears ~ 2.5 times the body-weight [32], however when climbing stairs or during deep knee bends it could bear up to 3.3 or 7.8 times the body-weight, respectively [33].

1.5. Development

The development of articular cartilage during embryogenesis is a unique process. First, hyaline cartilage templates for the long bones are generated at specific locations, sizes and shapes, then converted into bone tissue with a process called endochondral ossification (Fig. 3) [34]. Interestingly, the articular cartilage, which has a critical function throughout the life, is the “reserved” tissue layer from the primitive cartilage skeleton template.

Limb development is extensively studied, specifically in chick models, in order to understand the molecular mechanisms that drive chondrogenesis, which is then followed by endochondral ossification (Fig. 3, 4) [35-37]. During limb development, first the mesenchymal stem cells from the mesenchyme migrate to the site where the

limb is going to be generated. The cells do not interact at that point because of the HA-rich matrix that facilitates cell movement [38]. Next, HA is degraded [35] enabling the formation of cell clusters in which cell-cell interactions are mediated via neural cadherin (N-cadherin) and neural cell adhesion molecule (N-CAM) [39]. Next, the gap junctions are established to facilitate small molecule exchange in between the cells [40,41]. Meanwhile, a chondrogenesis specific isoform of fibronectin is detected around the cell clusters [42], which is thought to have a role in translocation of the cells into the clusters [43]. This step is referred as "condensation" and shown to be critical for the initiation of chondrogenesis and the molecules mediating the process are downregulated or switched off as soon as the chondrogenic differentiation initiates (Fig. 4) [44,45].

The limb growth is a gradual and dynamic process initiated by mesoderm, however the ectoderm layer covering the limb mesoderm also has a critical role in extension of the limb facilitated by growth factors [46,47]. By the time cells on the more proximal area undergo condensation step and chondrogenesis, a group of undifferentiated mesenchymal cells on the distal side, under the paracrine effects (mostly FGF-2, -4, -8) of the extending ectoderm, continue proliferating and migrating towards distal side of the limb [46,48]. Both the epithelial cells of the ectoderm and the mesenchymal cells produce BMP-2, -4, -7 that helps maintaining the limb growth [49].

After mesenchymal condensation, chondrogenic differentiation is initiated. Cells liberated from clusters, with the downregulation of the cell attachment molecules [44], proliferate and produce cartilage specific matrix molecules such as collagen II, aggrecan and link protein until the individual cells are sparsely distributed and entrapped in cartilaginous matrix. After maturation and hyaline cartilage formation, the chondrocytes undergo a process called hypertrophy, which is then followed by the ossification of the cartilage template generating the bone tissue. There are two main regulators of the hypertrophy. The first one, parathyroid hormone-related protein/peptide (PTHrP) originating from the periarticular region prevents the hypertrophy preserving the mature chondrocytes close to the articular surface. The second one, Indian hedgehog (Ihh) promotes hypertrophy by initiating the collagen X production, which then leads to the vascular invasion and bone formation (Fig. 4) [50]. The opposing effects of these molecules were nicely shown in previous studies. PTHrP receptor knockout in a mouse

model resulted in early hypertrophy, led to formation of short bones and lack of unmineralized cartilage tissue [51], whilst the Ihh misexpression led to the prevention of hypertrophy resulting in the cartilaginous skeletal elements failed to be replaced by bone [50]. With the initiation and progression of the hypertrophy, blood vessels enter the tissue and replace most of the cartilage template with bone leaving the thin layers of cartilage at the ends of the bones (Fig. 3), which then act as shock absorbers for a comfortable joint movement throughout the life.

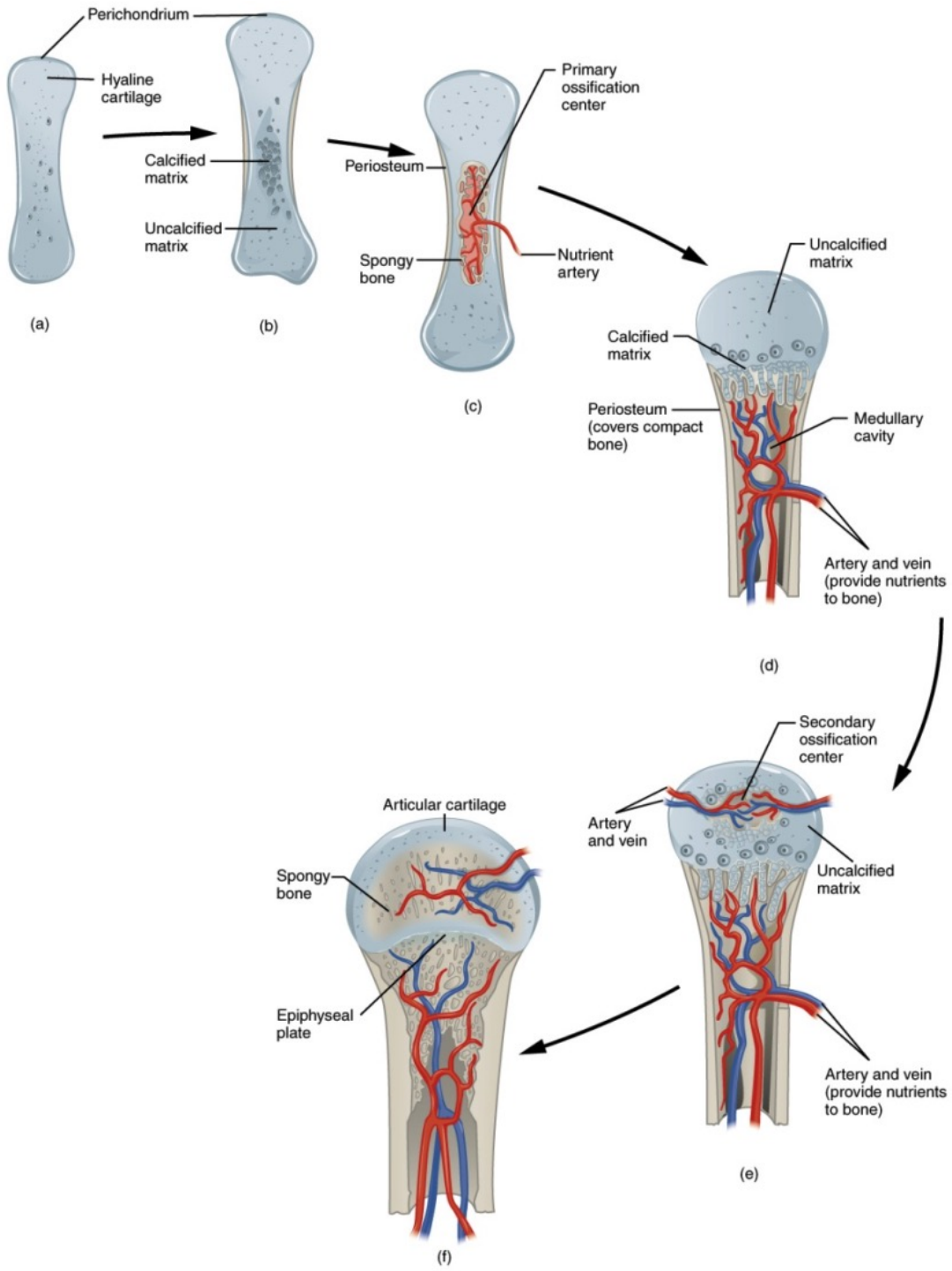

Figure 3. Embryonic bone formation via endochondral ossification. A hyaline cartilage template is formed (a), hypertrophy is initiated in the middle region (b), blood vessel invasion starts in the primary ossification center (c), bone formation and blood vessel invasion continues until the heads of the bone (d), blood vessels penetrate to the secondary ossification centers (e), maturation of bone tissue and vascularization leaving only thin sections of hyaline cartilage on the articulating surfaces (f). Image is courtesy of Creative Commons CC-BY, OpenStax College, Bone Formation and Development. OpenStax CNX June 28, 2013, see App. C for permission.

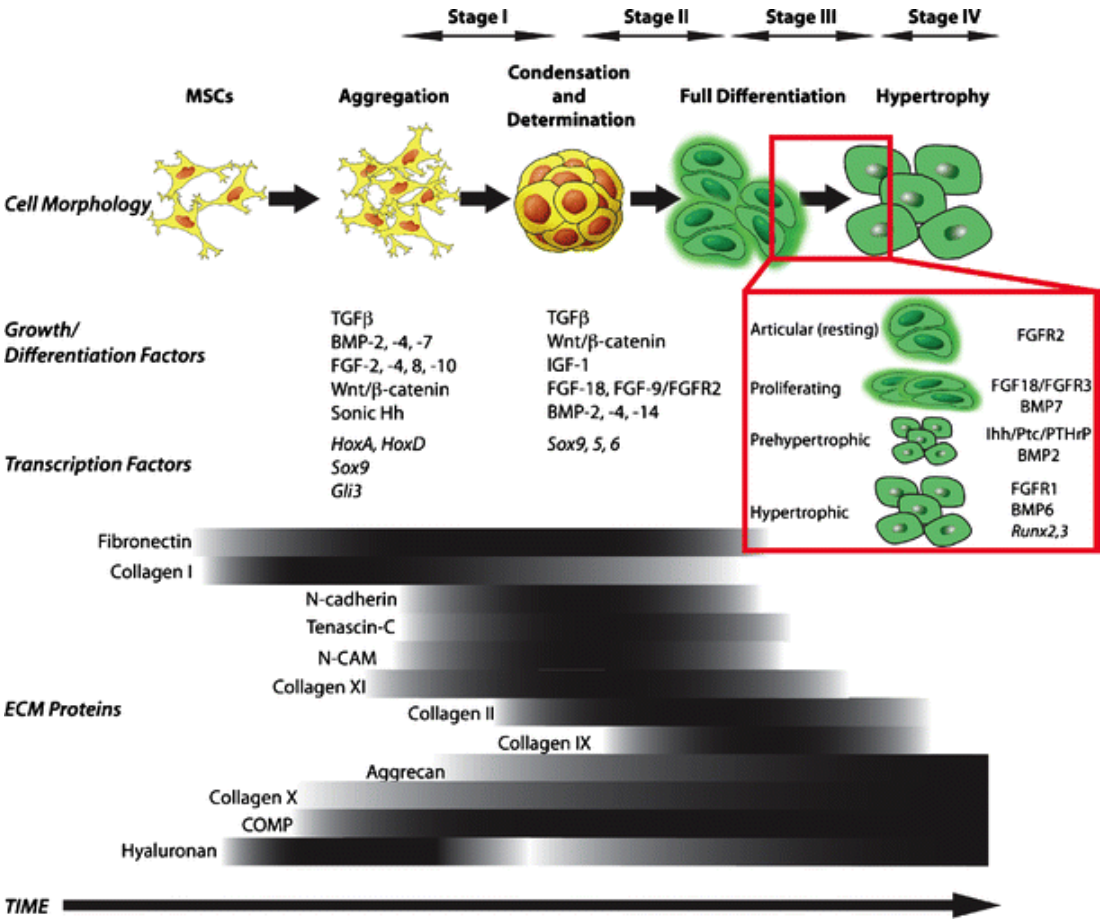

Figure 4. Molecular cross-talk during endochondral ossification. The critical changes in the expression of growth factors, transcription factors and ECM molecules during aggregation, condensation and determination, hypertrophy during bone formation. Image is courtesy of Springer, taken from [52], see App. D for permission.

1.6. Injury

The resilience of the cartilage tissue provides painless joint movement for almost half a century in normal health conditions. However, the unique properties such as avascularity and low cellularity that are critical for its resilience also limit the self-healing capacity of the tissue. Articular cartilage can only heal microscopic damage to the ECM that can be compensated by surrounding chondrocytes, however for macroscopic injuries a surgical intervention is required (Fig. 5A) [21]. Once articular cartilage is damaged and degenerated, further complications including the synovial fluid and the underlying bone are observed. Bone spur (osteophyte) formation at the outer rim of the joint surface and the imbalances in pro- and anti- inflammatory cytokines in synovial fluid are some of the complications [53]. It is also suggested that the imbalance

in cytokine profile may cause the activation of the proteolytic degradation of cartilage matrix [54] initiating a self-destructive phase rather than self-repairing. The size of the cartilage injury is generally defined in affected surface area (top view) and the depth of the defect (side view). According to depth, the defect is described as chondral (partial-thickness or full-thickness) and osteochondral (Fig. 6). The partial-thickness defects are the superficial injuries on the surface exposing middle or deep layers of articular cartilage (Fig. 6A) whereas the full-thickness defects affect all layers of cartilage and expose the underlying bone (Fig. 6B). The osteochondral defects affect both the full-thickness cartilage and underlying bone (Fig. 6C). The size and depth determination of the injury is critical in decision making for defect treatment and it is assumed that a macroscopic defect bigger than 1 cm^2 can lead to further degeneration if left untreated [29]. There are a number of surgical treatment options for acute injuries (Fig. 5A) or degenerative OA (Fig. 5B), which will be listed in the following section.

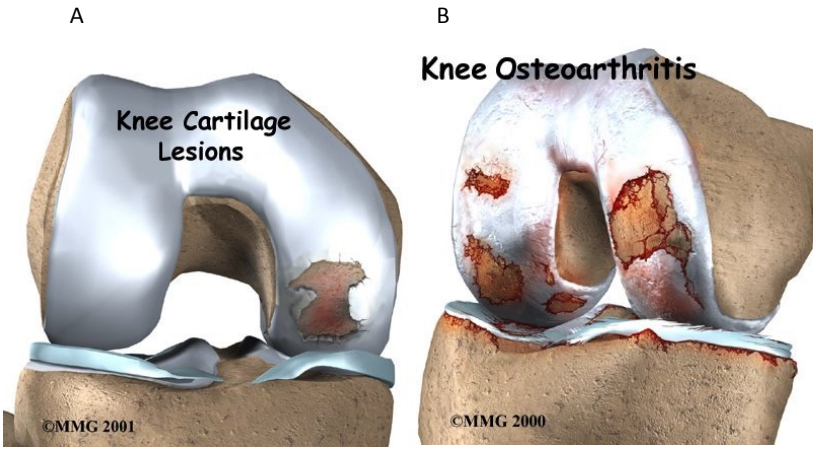

Figure 5. Articular cartilage defect/lesion and osteoarthritic cartilage. A full-thickness cartilage lesion that could occur after an acute injury (A). The state of articular cartilage in an osteoarthritic knee (B). Images are courtesy of Medical Multimedia Group LLC, www.eOrthopod.com , see App.B for permission.

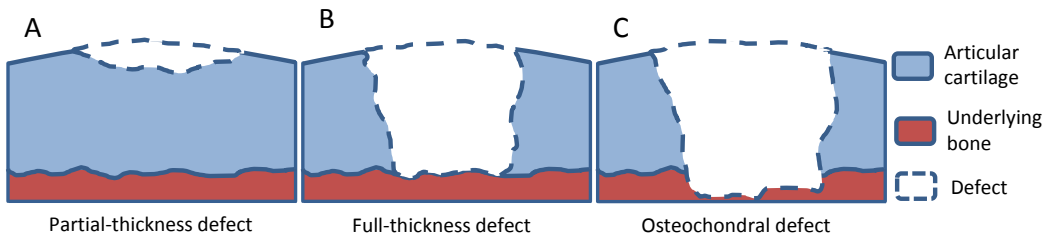

Figure 6. Cartilage defect types. According to the affected area cartilage defects could be partial-thickness (A), full-thickness (B) or osteochondral (C).

2. Existing surgical treatments

2.1. Symptomatic approach

These methods do not repair or stimulate regeneration of the tissue but provide temporary (debridement and lavage) or long-term (joint replacement) pain relief in the damaged joint [55].

2.1.1. Debridement and lavage

Arthroscopic debridement (removal of damaged tissue) and lavage (irrigation of joint) are the first surgical treatments offered in early phases of OA. Since "shaving and washing" the defect does not initiate a repair response, it is speculated that the pain relief after treatment may be due to a placebo effect [56]. To test this, double-blind trials were conducted and no significant difference was found between the control and the treatment groups [57,58] confirming the placebo effect. However, these treatments are not completely futile, they could be utilized for different purposes. The cell count in the synovial fluid obtained by lavage could be informative about the inflammatory state of the joint [59]. The debridement could be useful in order to remove loose pieces and flaps in the defect area that might compromise the success of a following treatment [60]. Debridement also might help revealing or changing the precise geometry of the defect when necessary. Therefore, arthroscopic debridement and lavage might serve as a preparatory step for following procedures.

2.1.2. Joint replacement

Depending on the cartilage damage site hip, knee, shoulder or ankle joints can be replaced. Specifically in knee joint, a partial or a total replacement can take place. In a total knee replacement procedure, the joint is exposed and the ends of femur and tibia,

together with the damaged cartilage are removed. The prosthetic femoral and tibial components are cemented to the ends of the bones generating an artificial joint (Fig. 7). The joint replacement procedure is still the gold standard and cost-effective clinical treatment for advanced OA [61]. It significantly reduces the pain and improves the life quality of the patients. However, the prosthetics generally last for a limited time (10-15 years) and additional replacements may be necessary for younger patients. The number of knee replacements performed in Australia, only in 2012 was reported to be 48,502 [62]. Despite cost-effectiveness of the procedure itself, when combined with indirect costs (including hospital bedding etc.) and the high prevalence of the disease, the joint replacements are huge financial burdens on national health care systems and patients [61,63,64]. Since joint replacements are the last resort with no further future repair possibilities, it is necessary to improve early regeneration techniques in order to delay and minimize the onset of OA.

Figure 7. Artificial joint. In the knee arthroplasty/replacement surgery, the affected cartilage surfaces are removed and replaced by metal and plastic components creating an artificial joint. Image is courtesy of Medical Multimedia Group LLC, www.eOrthopod.com , see App.B for permission.

2.2. Reparative approach

2.2.1. Marrow stimulation

The partial-thickness defects of articular cartilage do not demonstrate any spontaneous repair response whereas the full-thickness defects are immediately filled with a blood clot originating from the subchondral bone. This “super clot” is thought to

recruit stem cells from bone marrow to form a repair tissue [65]. Some techniques are developed exploiting this phenomenon.

First, Magnuson described abrasion arthroplasty where a surgical instrument was used to abrade the subchondral bone surface to induce a repair response [66,67]. Later, Pridie described a drilling technique to induce repair response from underlying bone marrow [68]. Finally, Steadman *et al.* introduced microfracture where a surgical awl is used to create microscopic fractures at the subchondral bone surface (Fig. 8) [69]. Microfracture method was found to be more reproducible and less traumatizing when compared to Pridie drilling with thermal necrosis or abrasion arthroplasty with extra bone removal [70].

Despite the rapid blood clot formation, marrow stimulating techniques mostly fail to induce the regeneration of hyaline cartilage, which is collagen II abundant, but instead yield a fibrocartilage repair tissue, which is collagen I abundant and inferior in biomechanical properties [71]. Because the newly formed repair tissue is fragile, compliance with the following rehabilitation protocol, which reduces weight-bearing for an extended period, is one of the critical factors determining the success of microfracture [72]. The temporary nature of the repair tissue was demonstrated with histology images in a rabbit model [73] where the efficient integration of the fibrocartilage with native tissue was observed at the end of 24 weeks, however the cartilage was further degenerated and fissures appeared between the repair tissue and native cartilage after 48 weeks [74]. Therefore, the repair tissue generated by marrow microfracture is not equivalent to the mechanically resilient hyaline cartilage and a repair tissue without efficient integration and functionality would eventually fail [75]. From a tissue engineering perspective, this technique attracts attention to the potential use of bone marrow-derived MSC in cartilage defect treatment.

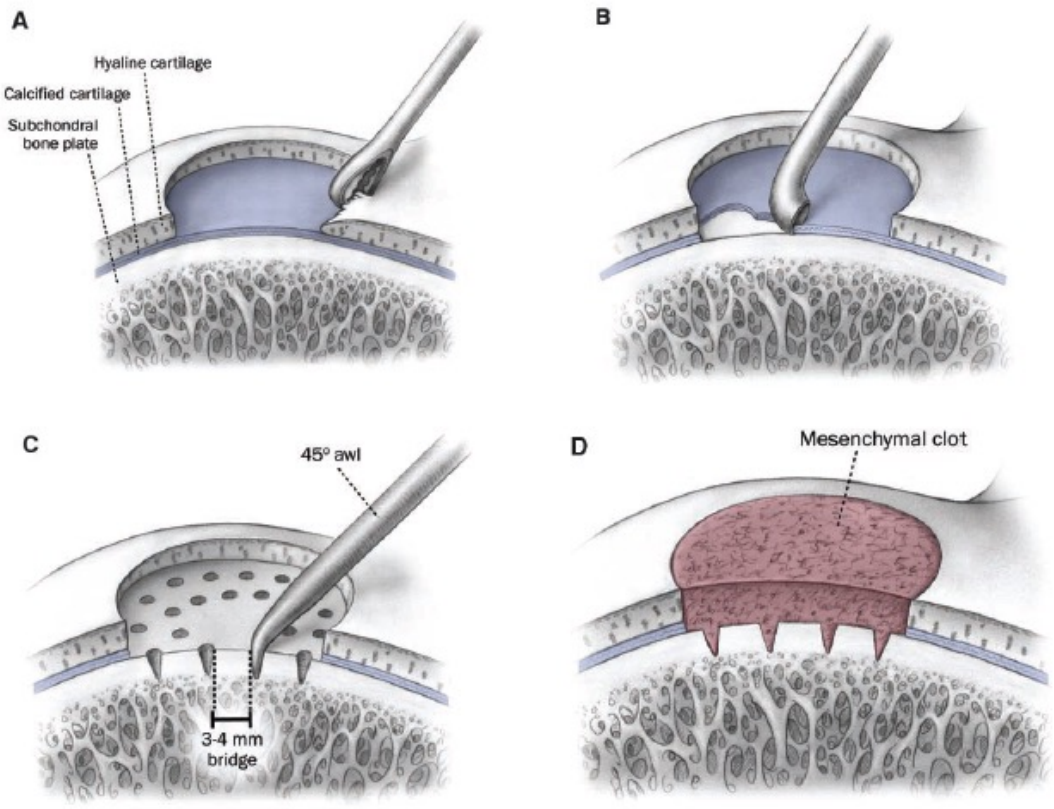

Figure 8. Microfracture procedure. First the defect region is debrided to obtain a smooth and vertical edge (A) then the base of the defect is abraded in order to reveal underlying bone (B) then with a surgical awl microfractures of 3-4 mm apart are introduced (C) and the bleeding from underlying bone forms a clot filling the defect area (D). Image is courtesy of SAGE, taken from [76], see App. E for permission.

2.2.2. Perichondral or periosteal graft transplantation

The perichondral graft used to treat cartilage lesions of the knee is harvested from the cartilaginous part of the lower rib [77]. It was previously shown that perichondral graft can regenerate hyaline-like cartilage when tested in a rabbit defect model [78]. The results of the first human trial conducted by Homminga *et al.* were optimistic [77]. Similarly, the use of a periosteal flap taken from the tibia to treat cartilage lesions was trialed by Niedermann *et al.* [79]. The rationale for using the periosteal flap was the discovery of the chondroprogenitor cells in the cambium layer, which is the inner layer of the periosteal flap [80] and the hyaline cartilage formation facilitated by the cells originating from the flap when transplanted in rabbit defect model [81]. Both techniques had reparative outcomes to some extent, however the limited graft size with donor site morbidity, delamination of the grafts, lack of graft harvest

reproducibility, the varying graft nature and failure of hyaline cartilage formation due to hypertrophy intrinsic to the graft were the limitations of the techniques that led to research looking for alternative treatment options.

2.3. Restorative approach

2.3.1. Osteochondral tissue transplantation (Mosaicplasty)

Allogeneic or autologous osteochondral tissue transfer is another way to treat large or small cartilage defects, respectively. Allogeneic tissue is generally obtained from cadavers, therefore larger size defects could be restored with this approach; however, immune response or disease transmission risks and the low chondrocyte viability in stored tissue grafts are the challenges which make this method less preferable [70,82].

Autologous osteochondral tissue transfer was first described in 1993 [83] and gained wide popularity over the years with the name "mosaicplasty" [84-87]. In this procedure, multiple cylindrical osteochondral plugs were taken from the non-load-bearing site of the same joint and inserted to the primary defect site revealing a mosaic-like pattern (Fig. 9). Different size plugs could be utilized in order to maximize the defect coverage [72]. The method was generally performed as an open surgery because of the challenging task of harvesting osteochondral plugs, however keyhole surgery versions were also described [88,89]. The procedure had varying clinical success and because of the donor site morbidity it was recommended for defects smaller than 4 cm^2 [29]. The vertical integration of the transferred plugs were relatively fast since it required bone to bone integration, however the horizontal integration of the plugs with each other and the defect site mostly failed due to chondrocyte necrosis around the edges of the grafted tissue [90]. Other problems associated with the procedure were the void space in between the cylindrical plugs and difficulty of matching the thickness and height of the plugs at the defect site. Critically, the need for larger grafts to treat larger defects made this method less promising.

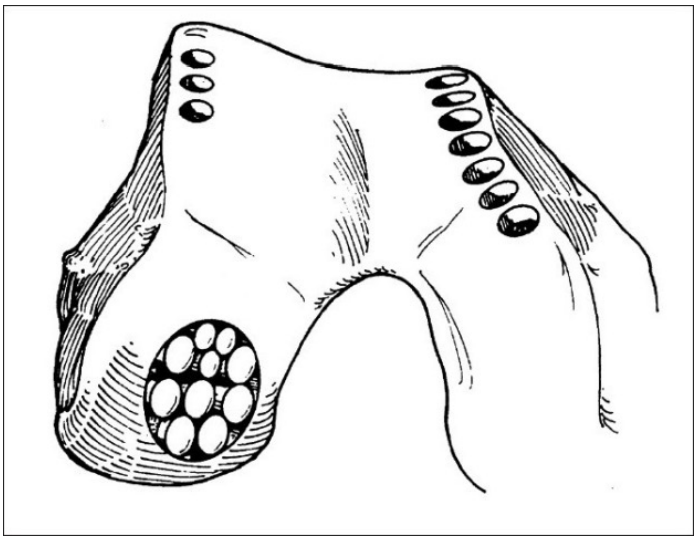

Figure 9. Mosaicplasty procedure. In mosaicplasty, a number of osteochondral plugs are taken from the non-weight bearing site of the cartilage and inserted into the defect site revealing a mosaic like pattern. Image is courtesy of BMJ, taken from [91], see App. F for permission.

2.4. Regenerative approach

Unlike previously described conservative methods, these techniques include innovative *ex vivo* steps in order to facilitate de novo tissue generation or true regeneration to replace the damaged cartilage tissue. Some of the innovative steps are the enzymatic isolation, monolayer expansion, redifferentiation of human articular chondrocytes and the use of biomaterials enabling efficient delivery or distribution of the cells in the defect site.

2.4.1. Autologous chondrocyte implantation

The very first cell-based therapy for cartilage repair called Autologous Chondrocyte Implantation (ACI) was first described by Grande *et al.* [92] in a rabbit model and the first human trial results were reported by Brittberg *et al.* in 1994 [93]. In ACI, a biopsy of articular cartilage (300-500 mg) was taken from the non-load-bearing site of the tissue, then the chondrocytes were liberated enzymatically (180,000-455,000 cells) and expanded in monolayer for 2-3 weeks (up to 2.6-5 million cells), then in an open surgery first the defect was covered with a periosteal flap taken from tibia and sutured to the rim of the defect, then finally the chondrocyte suspension (50-100 μl) was injected beneath the flap (Fig. 10A). After 16-66 months of follow up good-to-excellent results were obtained for most of the patients and regeneration of hyaline-like cartilage

was reported [93]. It was an innovative breakthrough because for the first time patient's own cells were expanded *ex vivo* and high number of cells were delivered to the defect site effectively. However, the following clinical trials revealed that the method had some limitations [94,95]. In addition to donor site morbidities and chondrocyte dedifferentiation, the complications associated with periosteal flap use were criticized. A second donor site was created with periosteal flap harvest and early delamination of the flap was reported in some cases. Additionally, the cells originating from the flap caused hypertrophy in the defect site compromising the desired hyaline cartilage regeneration by injected chondrocytes [96,97]. Therefore, new generations of ACI [97] were described to eliminate some of the complications. The second generation ACI, later referred as collagen-covered ACI (CACI) had aimed to replace the periosteal flap with a bilayer collagen I/III membrane [98]. CACI had clinical success [99] with reduced surgery duration and morbidity, however the collagen membrane still required sutures to the defect site, therefore the ultimate need to improve the existing procedures lead to other versions of ACI.

2.4.2. Matrix-assisted autologous chondrocyte implantation

Matrix-assisted ACI (MACI) was first described by Behrens *et al.* in 1999 [100]. The CACI and MACI procedures were very similar (both utilizing collagen I/III membrane instead of a periosteal flap), however the critical difference that made MACI more mainstream today was the way cells were delivered; in CACI the chondrocytes were injected beneath the collagen membrane in a suspension (similar to ACI) whereas in MACI the chondrocytes were harvested from monolayer then seeded and cultured on the membrane for an additional 3 days before implantation [101]. In MACI, the collagen scaffold with chondrocytes was fixed to the defect site only with fibrin glue and no suturing or watertight sealing was required because the cells had already adhered to the collagen membrane (Fig. 10B). With MACI, the invasiveness and the operation length were dramatically reduced. After ACI, MACI was another breakthrough because the tissue engineering techniques (chondrocytes seeded and cultured on a biomaterial) were used to treat cartilage defects for the first time. MACI is widely applied in orthopedics as a routine procedure with successful results in Europe and Australia [101-107] but not yet in USA (pending Food and Drug Administration approval) [108]. However, the risk

of disease transmission by porcine derived collagen membrane, intensive cost and the long duration of cartilage regeneration by monolayer expanded chondrocytes (up to 24 months[106]) are the drawbacks of the technique, all of which are reasons stimulating further improvement of the existing procedures.

2.4.3. Autologous matrix-induced chondrogenesis

Another method called Autologous Matrix-Induced Chondrogenesis (AMIC) using the same collagen I/III membrane was introduced by again Behrens *et al.* at the end of a MACI follow-up report [101]. Authors drew attention to the cost-intensiveness of the MACI procedure and changed their strategy of using monolayer expanded chondrocytes (which causes the cost-intensiveness) into utilizing bone marrow derived cells similar to marrow stimulating techniques. In this method, microfracture technique was combined with the use of a collagen membrane. First, microfracture was performed recruiting the cells from the bone marrow to the defect site, and then the collagen membrane was fixed into "bleeding" defect with fibrin glue (Fig. 10C). The advantages of implanting a collagen membrane into the defect after microfracture were more homogenous defect filling, additional mechanical strength and chondrogenic induction of marrow derived cells [109]. When compared to MACI, this one-step technique successfully prevented donor site morbidity and increased the practicality and cost effectiveness of the procedure. The follow up study with a mean of 37 months revealed promising results [109], however the histological assessment of the repair tissue and long term follow up reports are required in order to demonstrate effectiveness of the technique.

2.4.4. Autologous chondrocyte spheroid implantation

Another autologous chondrocyte implantation method was developed by co.don (Germany). In this method, the chondrocytes are harvested and expanded similar to ACI procedure, however the expanded cells are then used to form spheroids of 200,000 cells each (termed as chondrosphere®), cultured in patient's own serum, then implanted into the defect site arthroscopically (Fig. 10D) [110]. The use of animal derived or synthetic materials is purposely avoided to offer a complete autologous, biological procedure. The culture of chondrocytes in 3D spheroids before implantation is critical because it helps

the chondrocytes to redifferentiate and regain their chondrogenic phenotype, which was diminished during monolayer expansion [111-113]. Additionally, the arthroscopic delivery of spheroids makes this procedure minimally invasive and provides faster recovery time. The company is recruiting patients for phase III clinical trials and pending approval from European Medicines Agency for this procedure to be routinely practiced in Europe.

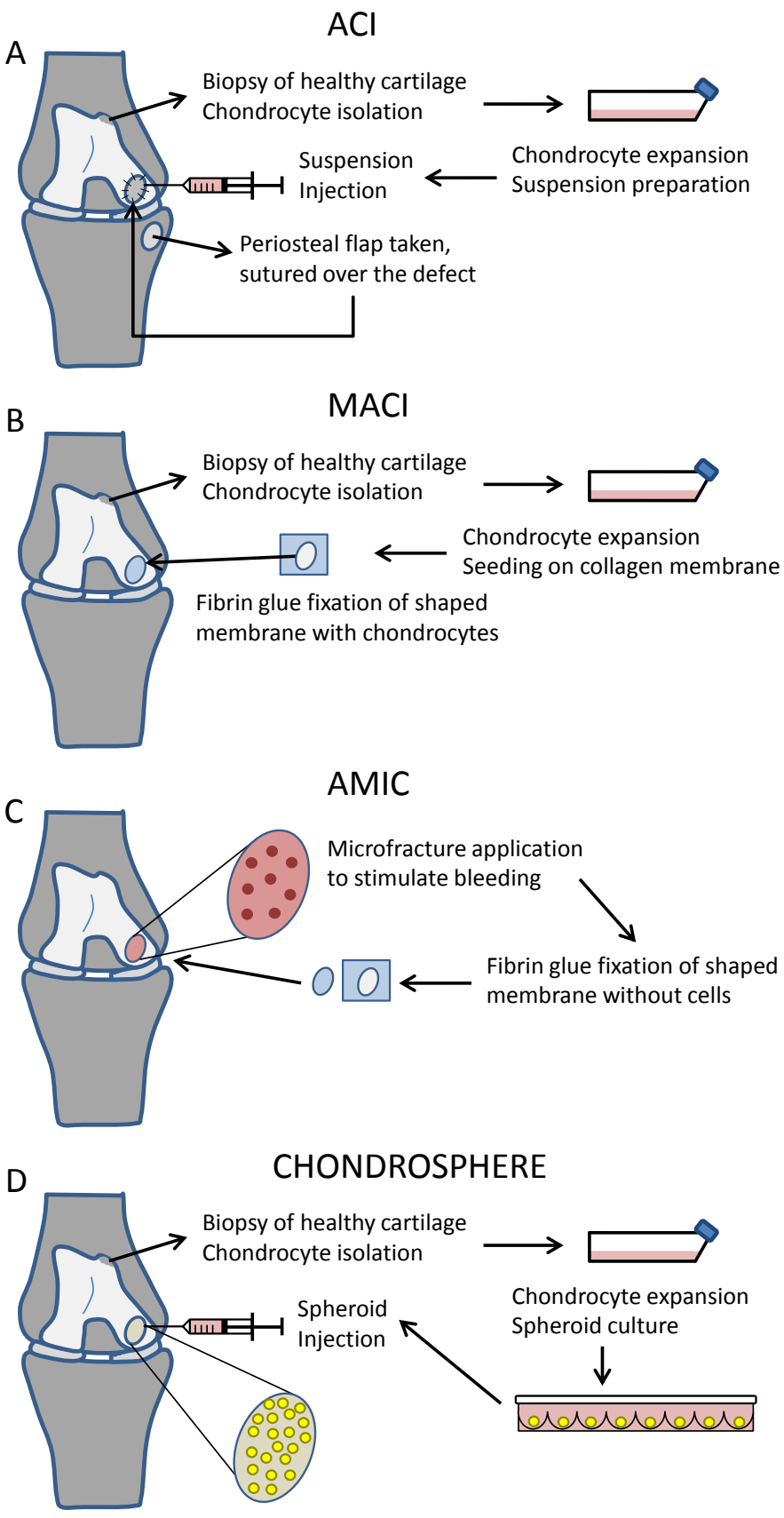
ACI
A
Biopsy of healthy cartilage
Chondrocyte isolation
Chondrocyte expansion
Suspension preparation
Suspension
Injection
Periosteal flap taken,
sutured over the defect
MACI
B
Biopsy of healthy cartilage
Chondrocyte isolation
Chondrocyte expansion
Seeding on collagen membrane
Fibrin glue fixation of shaped
membrane with chondrocytes
AMIC
C
Microfracture application
to stimulate bleeding
Fibrin glue fixation of shaped
membrane without cells
CHONDROSPHERE
D
Biopsy of healthy cartilage
Chondrocyte isolation
Chondrocyte expansion
Spheroid culture
Spheroid
Injection

Figure 10. Existing cell-based therapies to treat cartilage injuries. The critical steps and the differences of following procedures are demonstrated: Autologous Chondrocyte Implantation (A), Matrix-assisted Chondrocyte Implantation (B), Autologous Matrix-induced Chondrogenesis (C) and chondrosphere (D).

3. Cartilage tissue engineering

The relative success of cell-based therapies is stimulating cartilage regeneration focused-tissue engineering research more than ever. There is also a tremendous commercial motivation in finding better treatment options for cartilage defects [114] since OA is considered to be an epidemic with increasing age. Therefore, numerous researchers from around the globe are seeking alternative ways to treat cartilage defects, which would ideally improve clinical outcomes. This led to the accumulation of a great body of work in cartilage tissue engineering of which a brief summary will be given in this section.

There are three components considered as cornerstones of cartilage tissue engineering: cells, chondrogenic signals and scaffolds (Fig. 11).

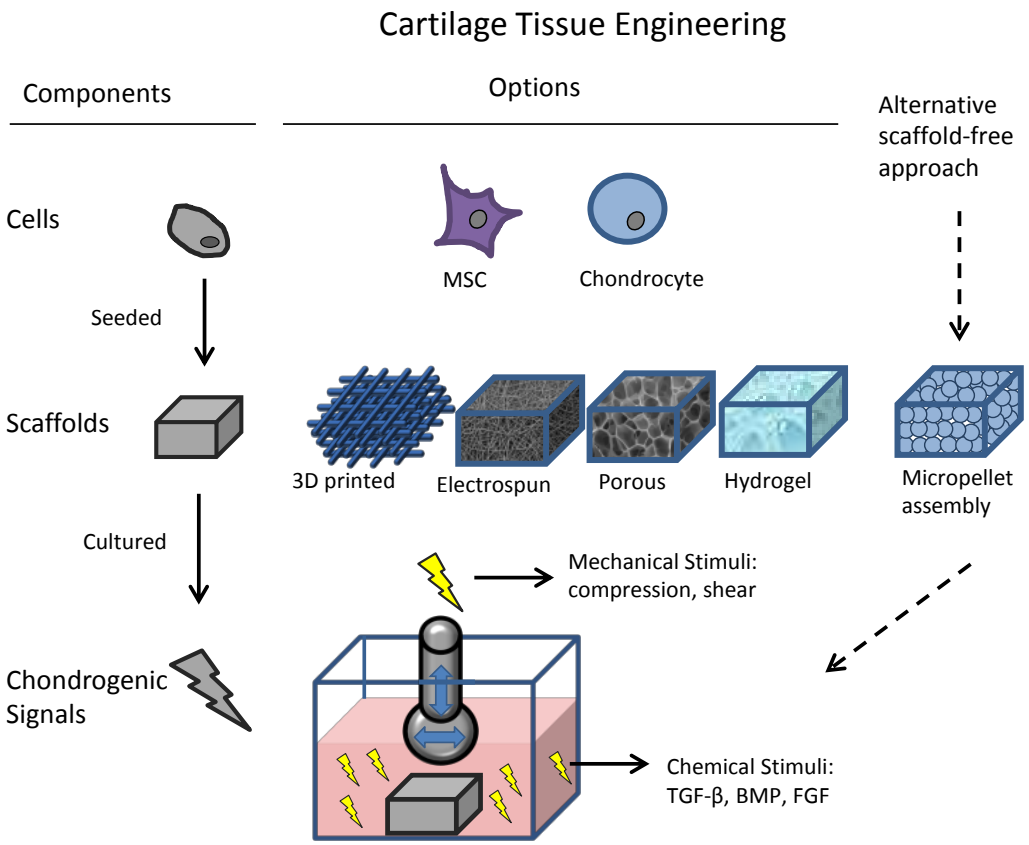

Figure 11. Cartilage tissue engineering overview. In order to obtain an *in vitro* engineered cartilage graft generally cells (chondrocytes or MSC) are seeded on various scaffolds then cultured under chemical and mechanical stimuli. This project introduces a scaffold-free approach for *in vitro* cartilage tissue generation.

3.1. Cell source

3.1.1. Articular chondrocytes

Autologous articular chondrocytes are often preferred on the basis that they are the cartilage-generating units of patient's own tissue, which requires treatment. These cells are ideal because they have the right phenotype and capabilities to be used in cartilage regeneration. However, chondrocytes are obtained at a cost of introducing another minor injury to the non-healing cartilage and the hypocellular nature of the tissue causes low cell yield. This is why the harvested cells are generally expanded on monolayer but this process leads to an even more critical problem; rapid dedifferentiation and loss of chondrogenic phenotype [115]. It is noted that collagen II expression is substantially downregulated during the first few passages [116] and the spherical morphology is replaced by fibroblast-like shape [117]. Some studies focused

on redifferentiating the expanded chondrocytes in 3D culture environment with addition of growth factors [118], however the general notion is that the full chondrogenic capacity is never regained. Alternatively, the use of MSC in cartilage regeneration is also investigated.

3.1.2. Mesenchymal stem/stromal cells (MSC)

MSC are highly utilized in regenerative medicine mostly because of their relative ease of harvest, proliferation and differentiation capacity. MSC can be isolated from various tissues [119] but generally bone marrow- and adipose-derived MSC are preferred in cartilage regeneration studies since some similarities are observed between these two cell populations [120,121]. However, comparative studies concluded that the proliferation capacity of adipose derived MSC is higher [122] whilst the chondrogenic and osteogenic differentiation capacity of bone marrow-derived MSC is found to be superior [123]. Epigenetic alterations studies in different origin MSC reveals that promoter DNA hypermethylation occurs at the progenitor state and that may restrict the expression of other lineage-specific genes limiting the generation of tissues other than the tissue of origin [124,125]. This epigenetic memory phenomenon, described as memory from the tissue of origin, supports the use of bone marrow derived MSC in cartilage regeneration since it has intrinsic chondrogenic and osteogenic differentiation capacity.

The major challenge associated with the use of MSC in cartilage regeneration is the difficulty of obtaining and maintaining a chondrogenic phenotype. One of the reasons is the unique way the skeleton is generated from hyaline cartilage during development and then replaced by bone via a process called endochondral ossification (Development section) [126]. During this process chondrocytes arise from condensed MSC and generate a hyaline cartilage template then undergo hypertrophy and apoptosis that is synchronized with the ossification of the tissue resulted with the bone formation [127]. In theory, this process is mimicked for the chondrogenic differentiation of MSC; therefore the chondrogenic characteristics are generally transient and not stable enough to regenerate functional cartilage tissue. Numerous studies are still focusing on optimizing the culture conditions of MSC to enhance and stabilize chondrogenic differentiation and prevent hypertrophy [128-130].

Another drawback associated with MSC use is the heterogenic nature of the cell population isolated with plastic adherence method [131,132]. Either the presence of osteogenic cells in the initial cell population, or the monolayer expansion on a stiff plastic surface [133] is enhancing the osteogenic differentiation potential while simultaneously compromising the ability to obtain a homogenous chondrogenic population. In order to overcome this problem, some studies aimed to isolate more "stem-like" cells by sorting them according to the presence or absence of specific cell surface markers. However, the inconsistency in the selected markers in different studies increased the debate in the field. Finally, the International Society for Cellular Therapy published the minimal criteria for defining MSC [134] where the following requirements were listed: (1) plastic-adherence, (2) expression of CD 105, CD 73, CD 90 and lack of expression of CD 45, CD 34, CD 14 or CD 11b, CD 79α or CD 19 and HLA-DR surface molecules, (3) *in vitro* tri-lineage (chondrogenic, osteogenic, adipogenic) differentiation. This report emphasizes the importance of initiating differentiation studies with more homogenous and potent cell population in order to have better quality tissue regeneration. However, since the criteria above only define the mesenchymal stromal cells, the search for true "stemness" markers continues. One of the highly studied cell surface antigens is STRO-1 and fibroblast colony forming cells (CFU-F) were exclusively found in this STRO-1^+ cell population [135]. Following studies revealed that the STRO-1^+ cells were rich in osteogenic precursors [136], which suggests that STRO-1 may be a marker for osteogenic lineage [137]. A recent study reported the presence of STRO-1 expression in tissues other than the bone marrow, and this finding may raise questions about the specificity of STRO-1 as the mesenchymal stem cell marker [138]. Another MSC marker Nestin was identified in mouse MSC and it is claimed that Nestin$^+$ cells mostly contained self-renewing, CFU-F cells [139]. However, the intracellular localization of Nestin led to search for surface markers associated with the presence of Nestin. In a recent report, it is demonstrated that PDGFRα and CD51 surface markers can be used to identify Nestin$^+$ MSC populations [139]. There are other studies suggesting that the Nestin$^+$ cells may be biased towards neural fate [140,141]. Similarly, there is a search for a specific marker, which helps to identify the cells with higher chondrogenic differentiation potency. In one study, a subset of MSC (CD271^{bright}

MSCA-1^{+} CD56^{+}) were suggested to have higher chondrogenic differentiation capacity [142]. While the use of the discussed markers appear to enable enrichment for MSC populations, it is still not possible to definitively identify and isolate MSC. The next step after isolation is the expansion of MSC, which is also known to be critical. One of the factors that help maintaining the stemness and the differentiation capacity is the continuous provision of hypoxic atmosphere during cell expansion [143]. It is claimed that hypoxia mimics the native stem cell niche preserving the undifferentiated state of the stem cells. Another factor is the geometry of the culture. Expanding MSC in 3D culture has been trialed and the idea was to better mimic the developmental chondrogenesis process [144]. The undifferentiated state of MSC was preserved in 3D spheroids, however cell expansion rate was substantially lower in 3D culture when compared to 2D [145]. The expansion media composition is also known to be effective in the maintenance of the stemness and multipotency. Numerous studies suggested that serum free expansion medium is beneficial for preserving stemness and crucial for clinical applications [146,147]. One of the studies emphasized that the serum free MSC expansion enhances chondrogenic and adipogenic differentiation capacity [148]. In this project, MSC were not isolated based on surface marker profiles because of the limited access to clinical samples, however MSC expansion was performed under hypoxic conditions and the differentiation was facilitated in 3D micropellets in order to maximize the chondrogenic features of the generated tissues.

3.1.3. Coculture of chondrocytes and MSC

Since both chondrocytes and MSC have complementary advantages, some suggest combining the two cell populations to harness the benefits of both. The suggested mechanisms explaining how coculture enhances chondrogenesis are controversial. Some studies suggest that the trophic effects of MSC help proliferation and redifferentiation of chondrocytes whereas others argue that the presence of chondrocytes in the culture enhances chondrogenic differentiation and prevents hypertrophy of MSC [149-153]. Wu *et al.* demonstrated compelling evidence that presence of human bone marrow MSC enhanced bovine chondrocyte proliferation and matrix production, also they reported preferential MSC apoptosis within the first weeks of the coculture supplemented with serum containing proliferation media [154].

However, when they repeat the coculture study with chondrogenic media, MSC apoptosis was decreased [155]. Therefore, the interplay between two cell types in accordance with the coculture microenvironment and the actual mechanisms driving the benefit of coculture remain to be elucidated. Further studies need to investigate the effects of combining the two cells populations in order to justify the extra effort required to use both cells types in clinical applications.

3.2. Chondrogenic signals

Chondrocytes are highly differentiated and specialized cells that maintain the fine balance between the anabolism and catabolism of the unique ECM of hyaline cartilage. Similarly, MSC require very specific "directions" in order to acquire chondrogenic characteristics. In chondrogenic differentiation studies it is soon realized that obtaining and maintaining this specific phenotype requires more than an undefined, batch-to-batch varying serum containing medium. This realization led to the formulations of a serum-free, chemically-defined medium generically referred as "chondrogenic differentiation/induction medium" that combines specific growth factors and chemical species at specific concentrations [156,157]. There are also other factors such as oxygen concentration and mechanical stimuli that effects chondrogenesis.

3.2.1. Growth factors

Growth factors that are known to be critical during cartilage development are considered the most effective chondrogenic medium additive. Some of the well-known growth factors with chondroinductive effect are transforming growth factor beta (TGF-β 1,3), bone morphogenic protein (BMP-2,4,7), basic fibroblast growth factor (bFGF/FGF-2) and insulin-like growth factor (IGF-1). TGF-β 1 plays role in chondrocyte differentiation, maturation, proliferation and chondrogenic matrix synthesis [158-163]. Recently another isoform, TGF-β 3, has gained popularity in chondrocyte redifferentiation and chondrogenic differentiation of MSC [164-167]. BMP isoforms are known for upregulating N-cadherin expression required for MSC condensation before chondrogenic differentiation (BMP-2) [168], inducing Smad1 or Smad5 mediated chondrogenesis (BMP-4) [169] and increasing cartilage ECM synthesis whilst decreasing catabolic effects of interleukins and matrix metallopeptidases (BMP-7) [170].

FGF-2 expansion medium supplementation has been shown to increase MSC proliferation and subsequent chondrogenic capacity [171]. IGF-1 was also reported to enhance both MSC chondrogenesis and prevent chondrocyte dedifferentiation [172,173] and additive effects were observed when used in combination with TGF-β 1 [172]. Generally, most studies start with investigating the chondrogenic effects of a single growth factor as a continuous supplement in culture medium, however it is more rational to think that the combination of growth factors, ideally with spatial and temporal control, would better mimic the well-orchestrated, strictly-regulated cartilage development process [34,174]. Additionally most of the growth factors of which chondrogenic effect is demonstrated *in vitro*, appear to have deleterious side effects such as synovial fibrosis and osteophyte formation when injected *in vivo* [174]. Therefore, more autologous and benign ways of concentrated growth factor delivery strategies, such as platelet-rich plasma (PRP)[175] or bone marrow concentrate (BMC)[176] injections, are being trialed, however more extensive research regarding those novel techniques is required in order to validate their effectiveness when compared to growth factor supplements.

3.2.2. Oxygen concentration and other chemicals

It is well-known that the oxygen concentration also affects chondrogenesis [177,178] and low oxygen (hypoxic) atmosphere (2-5% O_2) is generally preferred since the oxygen concentration in native cartilage is low and the chondrocytes obtain energy through glycolysis [179]. It is shown that during both expansion and redifferentiation of chondrocytes, hypoxic atmosphere helps preserving chondrogenic properties [17,180]. Similarly, the chondrogenesis of the bone marrow MSC is enhanced when cultured under low oxygen atmosphere during both expansion and differentiation [18,181]. This effect is thought to be related to the original niche of MSC in the bone marrow being also hypoxic [182]. The chondrogenic effect of hypoxia is mediated via hypoxia-inducible factor (HIF) molecules. HIF-1α is known to mediate chondrocyte growth arrest and survival in low oxygen microenvironment [183,184] whereas specifically HIF-2α is shown to mediate the upregulation of chondrogenic gene expression via SOX9 dependent and independent pathways [185,186].

Some other additives are suggested to further enhance chondrogenesis when supplemented in chondrogenic differentiation medium. The well-known additives are

dexamethasone, which upregulates cartilage ECM expression [187], ascorbic acid that takes role in collagen synthesis pathway [188], parathyroid hormone-related peptide, which is shown to be critical in prevention of hypertrophy [189].

3.2.3. Mechanical stimulation

In addition to the chemical cues in the environment, engineered cartilage tissue is also known for its sensitivity to mechanical stimuli, which simulate the aspects of joint movement. Mechanical stimulation can be applied in different ways including direct mechanical compression [190-192], surface motion [193,194], hydrostatic pressure [195] or ultrasound [196,197]. However, it is critical to finely tune the magnitude, duration and the frequency of the mechanical stimuli because weak stimuli might fail to demonstrate any effect or strong stimuli might have deleterious effects on cultured cells and the tissue. The mechanical forces affect the cultured tissue in two ways; (1) by enhancing the diffusion of medium and its contents in a more dynamic microenvironment hence increasing cell viability, proliferation and matrix production [198], (2) by activating certain signaling pathways with a process called mechanotrunsduction, which is critical in maintaining the integrity of the articular cartilage [199]. It is reported that the single cilium found in the chondrocytes act as a mechanoreceptor [200] and at a molecular level it is suggested that the integrins convey the mechanical forces to the inner cell activating critical pathways including mitogen-activated protein (MAP) kinase/JNK pathway [201]. The exact details of this complex interaction between the cartilage ECM and the chondrocyte mediated via mechanical forces are not yet fully understood. Once these details are clarified, it may be possible to partly mimic the mechanotrunsduction effects by media supplements.

Mechanical stimulation in cartilage tissue engineering studies will likely require a sterile closed system such as a bioreactor combined with the mechanical components, which might be costly and less practical. Additionally to be able to introduce forces to the culture, the tissue needs to be mature enough to endure the loadings, which may require longer culture duration increasing the cost intensiveness; therefore the clinical relevance of such applications is questionable. Nevertheless, these systems are useful tools in order to mimic the natural dynamics of an articulating joint *in vitro* to better understand the interplay between the cells and the biomechanical forces.

3.3. Scaffolds

Scaffolds are commonly utilized in cartilage tissue engineering. The primary role of a scaffold is to provide a structure for cells to colonize. The use of a scaffold is also considered as a practical strategy to improve the mechanical properties of the engineered tissue that facilitates the manual handling during subsequent procedures. In addition, the specific characteristics of the selected scaffold may contribute to cell proliferation, differentiation and ECM production [202]. Ideally, scaffolds must meet the criteria of being non-toxic, non-immunogenic, biocompatible, biodegradable, reproducible, easily-manufactured and mechanically strong to be appropriate for tissue engineering [203]. According to the origin of their materials scaffolds are classified as natural or synthetic and according to their manufacturing process and structure they can be 3D-printed, porous, nanofibrous, microspheres hydrogels or hybrids.

3.3.1. Natural scaffolds

Natural scaffolds are generally preferred because of their inherent biocompatibility, however they may still stimulate antigenic responses. The most commonly used protein-based natural materials are collagen, gelatin, fibrin and the carbohydrate-based ones are hyaluronic acid (HA), chitosan and alginate. Collagen is widely used as it is naturally found in most of the tissues, biodegradable, cell adhesive with RGD (arginine-glycine-aspartic acid) peptide sequence and can easily be combined with other materials [204]. It can also be manufactured in different forms such as a porous sponge [205], a hydrogel [206] or a nanofibrous scaffold [207]. As collagen can easily modify surfaces, it is generally used to coat the other types of scaffolds to increase their biocompatibility [208,209]. Gelatin is the denatured form of collagen and has a thermo-reversible gelling ability, which makes it a practical and attractive hydrogel for encapsulation of cells in cartilage tissue engineering. However, the mechanical strength of gelatin is very low at body temperature, therefore functionalized versions of gelatin emerged mostly with the photocurable/photocross-linkable properties [210-212]. One of the methods introduces methacrylamide groups, which can be cross-linked with UV light yielding a gelatin hydrogel with tunable curing properties [213]. Fibrin glue is a biological hydrogel of which components (human fibrinogen and thrombin, critical elements of blood coagulation) are commercially available (Tissel, Austria) and widely

used in surgeries to stop local bleeding or immobilize/glue the biological implants in place [214]. It is generally used to encapsulate the cells *in vitro* [215,216] or to aid the precise and efficient delivery of the cells to the defect site *in vivo* [217]. However, the rapid enzymatic degradation of the fibrin makes it only useful for short-term applications. Hyaluronic acid/hyaluronan (HA) is present in native cartilage and the synovial fluid, therefore, is a widely used scaffold material, however it is water soluble and lacks mechanical integrity in aqueous environment [218]. Fortunately, the hydroxyl and carboxyl-rich chemical structure allows different types of chemical or photo crosslinking to obtain water insoluble scaffolds [219,220]. The esterification of HA with different alcohols yielded an FDA-approved commercial HA product called HYAFF® (Italy), which was then used for cartilage tissue engineering applications and cell-based therapies [221,222]. In a HA-based scaffold, Jacobsen *et al.* showed that bone marrow MSC were able to express collagen II 600 times higher than the chondrocytes [223]. It is suggested that the highly porous, open microenvironment facilitates the condensation step required for MSC chondrogenesis [218], however that also leads to the escape of collagen II molecules to the culture media [223]. Chitosan derived from chitin (found in the exoskeleton of arthropods) is used in cartilage tissue engineering because of its extreme chemical structure similarity to the sGAG and HA found in native cartilage [224]. It is reported that the chondrocytes can maintain their spherical morphology when grown on a chitosan membrane and minimize the dedifferentiation at a cost of 4.7 times less growth when compared to tissue culture plastic [225]. Chitosan is soluble in acidic environment and the solution is freeze-dried to obtain a simple porous scaffold [226] or it can also be used as a stimulus-responsive "smart" injectable hydrogel [227]. Alginate, derived from brown seaweed, is a widely used, practical hydrogel that can be reversibly cured with the addition of a cation ion such as Ca^{2+} [228]. Alginate gained wide popularity in cell encapsulation studies after it is suggested that geometry of the cells affects their chondrogenic properties and spherical morphology is generally accompanied by enhanced chondrogenic characteristics [229,230]. However, alginate lacks cell adhesion sites and it is known that the cell-cell or cell-matrix interactions are critical for the communication between the cells and their microenvironment. Therefore, encapsulation of single cells in alginate may cause cell stress. Additionally, alginate is

not biodegradable; it is claimed that the mechanical strength is lost due to uncontrolled dissociation of Ca^{2+} ions overtime [231]. However, alginate is also used to reverse insulin-dependent diabetes with encapsulation of islet cells to prevent immunogenicity [232] and the long term success of this application indicates that alginate enables diffusion of molecules but physically stays intact *in vivo,* which could potentially compromise the regeneration of cartilage tissue in the defect site.

Overall, batch-to-batch variation of the materials, no control over the biodegradation and mechanical weakness are the limitations of the natural scaffolds.

3.3.2. Synthetic scaffolds

Synthetic biodegradable polymers are used in cartilage tissue engineering to overcome some of the problems associated with the natural materials. Synthetic materials are relatively easier to reproduce, mass-produce and have uniform, predictable, robust, tunable mechanical properties. Some of the frequently used synthetic materials are linear aliphatic polyesters such as poly(lactic acid) (PLA), poly(glycolic acid) (PGA), and their copolymers poly(lactic acid-co-glycolic acid) (PLGA), polycaprolactone (PCL) and polyethers such as poly(ethylene glycol) (PEG) and poly(ethylene oxide) (PEO). PLA and PGA are degraded by hydrolysis producing lactic acid and glycolic acid, respectively, which increases the acidity of the microenvironment [233]. PLA is known to be more hydrophobic than PGA, therefore it degrades slower [234] and has milder toxicity on cells [235]. However, the slow degradation of the PLA delays the proliferation of cells compromising rapid regeneration of the tissue [236]. Therefore, copolymers of those materials are produced (PLGA) with varying PLA-PGA ratios to tailor the biodegradation rate and acidic by-product release. PLGA is an FDA approved material and is commonly used in cartilage tissue engineering as a scaffold in the form of microspheres [237,238], porous sponge [239,240] or fibrous mesh [241,242]. Polycaprolactone (PCL) is another type of polyester used in cartilage tissue engineering. It is one of the most commonly electrospun materials [243] and known to be non-toxic and inexpensive [244]. It is shown that by changing the modulus of the electrospun PCL scaffold, MSC can be differentiated in to chondrogenic or osteogenic lineages on soft or stiff scaffolds, respectively [245]. However, the low swelling and slow biodegradation (described in terms of years) are the shortcomings of this material

[243]. PEG and its high molecular weight version PEO are highly hydrophilic and generally used in the form of a hydrogel in cartilage tissue engineering applications. The hydroxyl end-groups and the overall chemical structure make PEG a widely chemically modified synthetic material so that the modification of therapeutic agents with PEG chains referred as "pegylation" [246,247]. For example, the biodegradation can be tuned with the incorporation of PLA whilst photocross-linking can be achieved with the addition of dimethacrylate groups yielding a biodegradable and photocurable PEG hydrogel to be used in cartilage regeneration studies [248,249]. Photopolymerizable PEG hydrogels are also used as injectable scaffolds delivered in a minimally invasive way and then cured in the defect with transdermal UV light exposure [250]. However, in addition to its lack of biodegradability, PEG is also biologically very inert with no cell attachment sites. To overcome this problem cell attachment sites, RGD peptides, can be chemically incorporated into the PEG hydrogels in varying concentrations [251].

Overall, their high immunogenicity, lack of biological property/degradability and cytotoxic by-products are the limitations of the synthetic scaffolds.

3.3.3. Hybrid scaffolds

The natural scaffolds may be used on their own in clinical applications (collagen I/III membrane used in MACI), however most of the synthetic materials require some modifications to gain more biological properties and to hinder their immunogenic nature before implantation. Also, combining natural and synthetic materials may be necessary to finely tune the scaffold properties such as biodegradation rate, rigidity, pore size and biocompatibility. This leads to the common hybrids of natural/synthetic scaffolds used for cartilage regeneration [202,241,252]. The modification can take place in different ways such as simple mixing or blending, crosslinking the components or surface coating, layer-by-layer localizing the specific components. The PLGA/collagen scaffolds are common and it is shown that the chondrogenic properties of the tissue cultured on hybrid scaffolds were enhanced when compared to collagen or PLGA only scaffolds [241,253-256]. Similarly PCL/collagen/chondroitin sulfate scaffolds were able to increase the proliferation and ECM production of chondrocytes when compared to PCL only scaffolds [257]. More combinations with different types of natural and

synthetic materials need to be trialed, optimized and compared to be able to decide which scaffold is ideal for which tissue engineering approach.

3.3.4. Decellularized cartilage

The use of decellularized ECM as a scaffold is now a common strategy for a wide variety of organ/tissue engineering studies [258]. Autologous [259], allogeneic [260] or xenogeneic [261-265] ECM can be used for repairing the original tissue the ECM is derived from [261-263,265-267] or it can be used in a novel way to repair a different organ with similar biological properties [268-271]. Decellularized ECM use is even more prevalent in orthopedic tissue repair [272] since these tissues are endowed with resilient mechanical properties mainly by their ECM-rich structure. Decellularization and recellularization of articular cartilage has been described in some studies, however the intact, non-porous, ECM-rich tissue structure makes this process inefficient.

The aim of decellularization step is to remove the foreign material that could cause infection, disease transmission or immune reaction [263]. Extensive research is focusing on optimizing decellularization of cartilage while preserving the mechanical strength of the native tissue [263,273-276]. Recellularization, however, is necessary to vitalize the tissue graft before implantation because repopulation of the implanted decellularized tissue by native chondrocytes is less likely since these cells have limited migration capacity. Recellularization of 1 mm thick cartilage pieces was shown to be limited to the periphery of the tissue [277,278] whereas cell penetration rate was increased when thinner tissue sections were used [279]. Based on these findings, powdered cartilage matrix use was trialed to enhance the repopulation of the decellularized tissue. In two studies, physically crushed donor cartilage particles were used to manufacture porous scaffolds [280,281]. Similarly, our group previously explained the benefits of using powdered microscopic donor cartilage particles referred as “cartilage dust”, where the cells and the cartilage dust were directly mixed and cocultured [282]. In Chapter 4, the use of cartilage dust in tissue engineering applications is further investigated where the incorporation of cartilage dust into MSC micropellets is reported.

3.3.5. Limitations of scaffolds

In addition to their many advantageous properties, the scaffolds also have their downsides. Despite they are considered an essential component for cartilage tissue engineering; the problems associated with the use of a scaffold cannot be underestimated.

The natural scaffolds such as collagen membranes are derived from xenogeneic sources, which is associated with disease transmission risks. Generally, porcine derived collagen is utilized, and the material is treated with strong alkaline solutions to inactivate any nucleic acid residue that may cause disease transmission [283]. Additionally, the telopeptide regions of collagen, which are known to be antigenic, are removed to prevent immune response [283]. However, the companies never assure the 100% safety of the product, therefore even low, there are immune response and disease transmission risks.

The use of synthetic scaffolds is even more questionable since there are no effective strategies to prevent immune response when implanted *in vivo*. The surface modification with biological materials may serve as a short term solution effective only during the first weeks of the implantation [284]. Most of the synthetic materials lack biodegradability; therefore the implanted material may act as a barrier preventing the cell proliferation and new tissue formation. There are some synthetic materials with biodegradability, however the challenge in this case is to control the biodegradation rate because most of the common materials used in cartilage tissue engineering such as PLA, PLGA undergo bulk erosion rather than the ideal surface erosion [285]. This effect causes rapid loss of the mechanical strength but more importantly the accumulation of the acidic by-products decreases the pH in the microenvironment, which may diminish the cellular activity in surrounding tissue and can cause immune response [286]. The avascular nature is thought to provide cartilage an immune-privileged status, however it is the intact superficial layer preventing the infiltration of the immune cells from the synovial fluid and in the case of an injury this mechanism is impaired. Therefore, the biocompatibility and the control of biodegradation rate in synthetic scaffolds need further optimization before they are routinely used in clinical treatments.

Most of the 3D printed or porous scaffolds are considered to be a pseudo-3D culture platform since they can only provide the cells a “surface” to attach to, similar to

monolayer culture. Specifically in low cell seeding densities, where the cell-cell interaction is limited, the cell morphology seems to be similar to the monolayer culture. Alternatively, hydrogels are preferred because the spherical cell morphology, one of the key characteristics of the chondrocytes, can easily be mimicked in such platforms. However, single cell encapsulation in a hydrogel almost completely blocks the cell-cell interactions, which are known to be essential for MSC chondrogenesis (see 1.5. Development section). At that point, the scaffolds seem inefficient in mimicking the critical elements of biological microenvironment.

In conclusion, it is the lack of complete autologous and biological solutions that motivate the use of scaffolds in cartilage tissue engineering. The biological components such as cells on their own lack the strength to mimic the natural resilience of articular cartilage, therefore the scaffold use has a merit in order to provide a temporary support to the regenerating tissue. However, it is still important to search for more biological strategies and ideally eliminate the use of foreign materials in clinical treatments.

3.4. Scaffold-free cartilage tissue engineering, micropellets as building blocks

In order to engineer a tissue without the mechanical support of a scaffold, an entity reasonably greater than a single cell is required, because it is simply impractical trying to shape a tissue structure using the single cells as building blocks. Cell pellets/spheroids/aggregates, which contain certain number of cells attached with the help of cell-cell and/or cell-ECM interactions, are the ideal candidates for being building blocks in scaffold-free tissue engineering approaches.

It is known that the chondrogenic differentiation of MSC and redifferentiation of expanded chondrocytes are enhanced when the cells obtain a round morphology similar to the chondrocytes in native cartilage [287-289]. It is also shown that the cell-cell interactions are essential in order to initiate MSC chondrogenesis. Hence a conventional method was first described by Johnstone *et al.* [157] where 200,000 MSC were centrifuged in a tube to form a 3D high-density cell aggregate, later this method was commonly referred as pellet culture. Despite still being the gold-standard method for MSC chondrogenesis and chondrocyte redifferentiation, pellet culture often yields a radially heterogenic histological appearance for matrix distribution. The common heterogeneity patterns are the uneven matrix distribution, necrotic core and fibrous outer

layer. It is highly possible that the large pellet size (~1 mm diameter) causes diffusion gradients throughout the pellet and this effect is exacerbated with the accumulating cartilaginous matrix resulting in uneven matrix distribution [18]. The diffusion gradients may form for chondrogenic factors, metabolites, waste products and oxygen concentration. Using smaller size pellets can mitigate diffusion gradient formation and yield more homogenous chondrogenesis [18]. The small size pellets termed as micropellets in this study are made of 150-200 cells with a diameter of 100-200 μm each.

The micron size pellets have some advantages when compared to traditional large pellets. It is anticipated that large pellets cultured under atmospheric oxygen have a decreasing oxygen gradient from surface to the core, yielding cartilaginous tissue in the interior region whereas the well-oxygenated outer layer has a fibrous appearance. It is assumed that the concentrations of both oxygen and chondrogenic factors are more predictable and less changing throughout the micropellets provided by their micron-scale size. Therefore, micropellet culture is geometrically superior in providing more homogenous conditions while mimicking 3D culture microenvironment.

Another challenge in cartilage regeneration is replicating the matrix abundant low cellularity of the native tissue. Hydrogel systems mimic the low cellularity too early by diluting single cells in a large volume of hydrogel, which is hardly ever replaced by cartilaginous matrix. The aggregation of fewer cells in individual micropellets may allow rapid matrix accumulation and increase in size, yielding low cellular and matrix rich chondrogenic building blocks of micropellets.

Previously, our group showed that when reduced pellet size was coupled with low oxygen atmosphere MSC chondrogenesis was enhanced [18]. Similarly, in Chapter 3, the enhancement of expanded chondrocyte redifferentiation in micropellets coupled with low oxygen is demonstrated. In Chapter 4, it is shown that the micropellets mediated more efficient incorporation of cartilage particles into the engineered tissue. Finally, in Chapter 5 osteogenic and chondrogenic micropellets are used as building blocks to engineer a composite osteochondral-like tissue. In this Thesis, I suggest that the chondrogenic micropellets can be arthroscopically delivered to fill non-uniform complex-geometry defects of articular cartilage. I also suggest and demonstrate that

various types of micropellets can be utilized as building blocks to engineer large and composite structures such as a biphasic tissue, bypassing the scaffold use (Fig. 11). In this Thesis, I report that micropellets with different characteristics can be manufactured and assembled in an organized fashion to be able to obtain continuous composite macrotissues.

Next three chapters are independent research articles with significant common elements such as micropellet manufacturing and a subsequent assembly. Each one of these studies address one of the specific aims of this study, also represent an example of utilizing micropellets as building blocks.

- Chapter 3 aims to test the micropellet approach in redifferentiation of monolayer expanded human articular chondrocytes
- Chapter 4 aims to increase matrix content and defect filling properties of human bone marrow MSC micropellets with incorporation of donor cartilage particles
- Chapter 5 aims to assemble osteogenic and chondrogenic micropellets in order to generate a scaffold-free osteochondral-like tissue

Chapter 3: Statement of Contribution of Co-Authors for Thesis by Published Paper

In the case of this chapter

Title: **The interplay between chondrocyte redifferentiation pellet size and oxygen concentration**

Date, status, journal: March 2013, Published, PLOS ONE

Full citation: Babur BK, Ghanavi P, Levett P, Lott WB, Klein T, Cooper-White JJ, Crawford R, Doran MR. (2013) PLoS One. The interplay between chondrocyte redifferentiation pellet size and oxygen concentration; 8(3):e58865. Epub 2013 Mar 15.

Contributor	Statement of contribution
Betul Kul Babur Signature Date 20.01.2015	wrote the manuscript (M), experimental design (D), conducted experiments (E), and data analysis (A)
Parisa Ghanavi	aided with E, A
Peter Levett	aided with D, E, A
William B. Lott	aided with M, A
Travis Klein	aided with M, D, A and materials
Justin Cooper-White	aided with D, A
Ross Crawford	aided with D and materials
Michael Robert Doran	aided with M, D, A and materials

Principal Supervisor Confirmation

I have sighted email or other correspondence from all Co-authors confirming their certifying authorship.

Michael Robert Doran		20.01.2015
Name	Signature	Date

"One thing I have learned in a long life: that all our science, measured against reality, is primitive and childlike and yet it is the most precious thing we have."
Albert Einstein

Chapter 3: The interplay between chondrocyte redifferentiation pellet size and oxygen concentration

1. Abstract

Chondrocytes dedifferentiate during *ex vivo* expansion on 2-dimensional surfaces. Aggregation of the expanded cells into 3-dimensional pellets, in the presence of induction factors, facilitates their redifferentiation and restoration of the chondrogenic phenotype. Typically $1x10^5$-$5x10^5$ chondrocytes are aggregated, resulting in "macro" pellets having diameters ranging from 1-2 mm. These macropellets are commonly used to study redifferentiation, and recently macropellets of autologous chondrocytes have been implanted directly into articular cartilage defects to facilitate their repair. However, diffusion of metabolites over the 1-2 mm pellet length-scales is inefficient, resulting in radial tissue heterogeneity. Herein we demonstrate that the aggregation of $2x10^5$ human chondrocytes into micropellets of 166 cells each, rather than into larger single macropellets, enhances chondrogenic redifferentiation. In this study, we describe the development of a cost effective fabrication strategy to manufacture a microwell surface for the large-scale production of micropellets. The thousands of micropellets were manufactured using the microwell platform, which is an array of 360x360 μm microwells cast into polydimethylsiloxane (PDMS) that has been surface modified with an electrostatic multilayer of hyaluronic acid and chitosan to enhance micropellet

formation. Such surface modification was essential to prevent chondrocyte spreading on the PDMS. Sulfated glycosaminoglycan (sGAG) production and collagen II gene expression in chondrocyte micropellets increased significantly relative to macropellet controls, and redifferentiation was enhanced in both macro and micropellets with the provision of a hypoxic atmosphere (2% O_2). Once micropellet formation had been optimized, we demonstrated that micropellets could be assembled into larger cartilage tissues. Our results indicate that micropellet amalgamation efficiency is inversely related to the time cultured as discrete micropellets. In summary, we describe a micropellet production platform that represents an efficient tool for studying chondrocyte redifferentiation and demonstrate that the micropellets could be assembled into larger tissues, potentially useful in cartilage defect repair.

2. Introduction

Cartilage is an avascular tissue with poor regenerative capacity. Existing surgical repair strategies are limited in their efficacy [290-292], and largely function only to delay the onset of osteoarthritis [293,294]. It is envisaged that autologous cell-based therapies will overcome these regenerative barriers, enabling defect repair and restoration of long-term joint function [93,295]. However, in practice, cell-based therapies have demonstrated only modest efficacy relative to less complex and less costly treatment protocols such as microfracture [296,297]. Nevertheless, the capacity of cell-based therapies to deliver more cells of an appropriate phenotype into defect sites is seen as a unique feature that will ultimately enable their efficacy. Notably, manufacturing this ideal cell population remains a challenge [298].

Clinically approved cell-based cartilage defect strategies utilize autologous chondrocytes harvested from non-weight bearing regions of the joint targeted for repair [93,299]. Selection of articular chondrocytes as a starting population is rational, as these cells have a phenotype appropriate for articular cartilage tissue formation. However, this “optimal” phenotype is lost when the finite number of donor chondrocytes is expanded using traditional 2-dimensional (2D) tissue culture methodologies [300,301]. A number of research groups have explored alternatives to conventional 2D expansion processes [302-304], but avoiding chondrocyte

dedifferentiation whilst also achieving the necessary expansion in a clinically relevant time frame has not yet been achieved.

During *in vitro* studies, expanded chondrocytes are commonly redifferentiated through the aggregation of $1x10^5$-$5x10^5$ cells into a 3-dimensional (3D) pellet in the presence of TGF-ß or other induction factors [305-310]. The resulting "macropellet" is macroscopic, having diameters of 1-2 mm. Significant diffusion gradients develop over such length-scales and as a result the redifferentiation phenotype and matrix deposition vary radially through the pellet [306,311-313]. Despite this artefact, macropellet cultures remain the gold standard for studying chondrocyte redifferentiation *in vitro,* and in recent clinical trials they have been directly implanted into articular cartilage defects to facilitate tissue regeneration by co.don® AG (Teltow, Germany) [313,314]. Macropellets' popularity as a redifferentiation platform, and now potentially as a clinical tool, reflects the simple and robust methods used in their manufacture. The cells are easily pelleted via centrifugation in polypropylene tubes or v-bottom plates. Whilst being an inexpensive process, the heterogeneous product derived from pellet cultures limits our capacity to investigate and optimize redifferentiation mechanisms for clinical application.

In previous work we outlined how a commercial microwell product could be utilized to manufacture thousands of micropellets (166 cells each, diameters of ~100 µm each) of mesenchymal stem/stromal cells (MSC) and subsequently differentiate them into chondrocytes [18]. The reduced diameter of the micropellets mitigated diffusion gradients, enhanced MSC chondrogenic differentiation and generated a more uniform cell product [18]. We reasoned that a similar strategy should also enhance chondrocyte redifferentiation, and that optimized chondrocyte micropellets should be capable of subsequent assembly into larger tissues, thereby demonstrating their potential in tissue engineering applications. To further optimize the redifferentiation process, and to better understand the role of hypoxia in relation to pellet dimension, redifferentiation studies were performed in hypoxic (2% O_2) and normoxic (20% O_2) atmospheres.

Identifying a cost effective platform for micropellet formation is essential for routine and thorough micropellet experimentation. To address this need, an in-house process for the manufacture of a microwell platform from polydimethylsiloxane

(PDMS) was developed. This custom PDMS microwell platform was then surface modified with an electrostatic multilayer of hyaluronic acid (HA) and chitosan (CHI) to promote micropellet formation. Such surface modification was essential to prevent chondrocyte spreading on the PDMS, and the HA/CHI multilayer ensured robust micropellet formation. Using this platform, the redifferentiation of $2x10^5$ 2D-expanded chondrocytes, either assembled into single macropellets or into 1200 micropellets (166 cells each), in 2% and 20% oxygen atmospheres were contrasted over 14 days. Macropellets and micropellets were characterized for metabolic activity, total sulfated glycosaminoglycan (sGAG), DNA production, gene expression and histology. In subsequent experiments, the optimal micropellet manufacturing protocol (2% O_2) was utilized to characterize the capacity of micropellets of different maturity to amalgamate into a single cartilage tissue. Micropellets from day 4, 8, 11 or 14 cultures were amalgamated up to 21 days, and integration was assessed via histology.

3. Materials and methods

All materials were purchased from SIGMA-ALDRICH® unless otherwise stated.

Fabrication of microwell surface

Soft lithography was used to prepare custom microwell surfaces [315]. A silica wafer having an array of microwells with the dimensions of 360 µm x 360 µm x 180 µm (Fig. 12A) was prepared via deep reactive ion etching [316] by the Australian National Fabrication Facility-Queensland (ANFF-Q). PDMS (Slygard®, silicone elastomer kit) was used to generate a negative imprint of the microwell surface on the silica wafer (Fig. 12A, B), as per the manufacturer's protocol. This PDMS negative was then used as a mold to generate a replica of the original microwell surface. First, the PDMS negative was coated with a 5% solution of Pluronic-F127 to act as a release agent. The Pluronic-F127 coated surface was permitted to air-dry overnight. It was then used to cast the replica surface in a 2 mm thick layer of PDMS (Fig. 12C). This layer was cured at 60˚C for one hour and then pealed from the negative. As this process was not sufficiently reproducible to enable reliable mass production of such surfaces, a hot embosser was used to cast this replica PDMS shape into polystyrene. This polystyrene surface then

functioned as a mold that could be used repeatedly to cast microwell sheets (Fig. 12D, E). The polystyrene hot embossing was achieved by taking a sheet of polystyrene cut from a culture flask and pressing the PDMS replica surface into it (at 160˚C for 15 minutes with minimal pressure, POWER TEAM hydraulic heat press), PDMS sheets with microwells were mass-produced (Fig. 12E), and 2 cm^2 disks were punched from the PDMS sheets (Fig. 12F), which were inserted into 24-well plates (Nunc™).

Surface modification of microwells

We previously showed that cells cultured on unmodified PDMS microwell surfaces have a propensity to spread rather than form pellets [317], and this microwell platform exhibited similar problems when culturing chondrocytes in serum-free chondrogenic redifferentiation medium (Fig. 12H). To minimize cell attachment to the microwell surface (Fig. 12I), the PDMS insert surface was chemically modified using a variation of our electrostatic multilayer (ML) technique [318] (Fig. 12G). Prior to ML deposition, a net negative charge was imparted on the PDMS microwell surface utilizing a hand-held high frequency plasma generator (Model BD-20, ETP) [319]. Immediately following plasma modification, the inserts were submerged in an electropositive poly-L-lysine solution (50 μg/mL in MES buffer, pH 5.5) and centrifuged at 4000xg for 5 minutes to ensure that the fluid entered the microwells. The poly-L-lysine was adsorbed onto the PDMS surface for 30 minutes at room temperature (RT). The wells were then rinsed twice with MES buffer, and ML deposition was initiated by adsorbing electronegative hyaluronic acid (HA) (50 μg/mL in MES buffer, pH 5.5) plus 1:100 dilution of fresh cross-linker stock. N-Hydroxysuccinimide (NHS) and *N*-Ethyl-*N*′-(3-dimethylaminopropyl) carbodiimide hydrochloride (EDAC) cross-linker stock solution contained 50 mg/mL EDAC plus 70 mg/mL NHS in DMSO. We found that the DMSO stock solution could be effectively frozen and stored at -20ºC in aliquots as long as the aliquots were used immediately upon thawing. The HA layers were adsorbed and cross-linked to the poly-L-Lysine for 20 minutes, and then the surfaces were washed twice with MES. Next, a layer of electropositive chitosan (CHI, 50 μg/mL CHI in MES buffer) was adsorbed to the HA layer for 20 minutes at RT. This process was repeated until 4 bilayers of HA-CHI were deposited, with the top layer being HA. The inserts

were then sterilized overnight in 70% ethanol, washed three times with PBS, placed into sterile 24-well cell culture plates and kept hydrated in PBS at 4ºC overnight.

The stability of the multilayer was tested by incubating multilayered and non-multilayered flat PDMS disks under different conditions and assessing cell attachment. Briefly, disks were incubated in 100% ethanol, 70% ethanol, acetone, liquid nitrogen, air, distilled water, PBS, boiling water for 24 hours, then ventilated for 15 minutes. The cells were seeded at a density of 3000 per cm^2, incubated overnight in chondrogenic redifferentiation media. The next day, cell attachment was assessed (Fig. 19). For further information regarding characteristics of HA-CHI multilayer please see references [320,321].

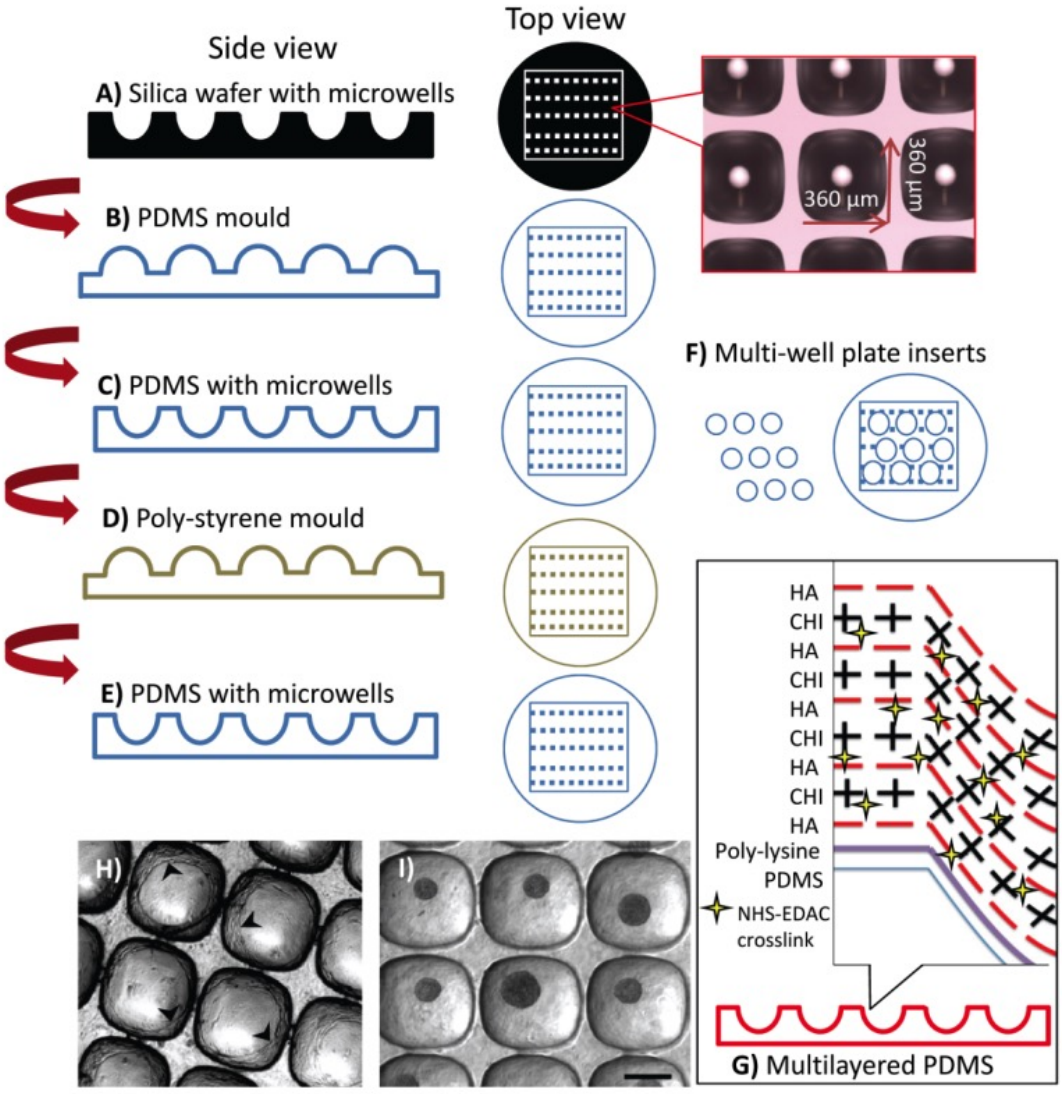

Figure 12. Fabrication of the microwell surface from PDMS replica molding and surface modification. A silica wafer having an array pattern of microwells was formed via deep reactive ion etching. The dimensions of the microwells on silica wafer were 360 x 360 x 180 (depth) µm (A). This surface was used to cast PDMS, generating a negative surface. PDMS mold having an inverted microwell pattern (B). This surface was then coated in 5% pluronic acid solution, which functioned as a release agent. The coated surface was used to cast a 2 mm thick PDMS sheet having a microarray pattern identical to the original silica wafer (C). Because PDMS-PDMS casting was not reproducible, the PDMS sheet with the microwells was cast with a polystyrene sheet to obtain a plastic mold (D). Using polystyrene mold PDMS sheets with microwells were produced (E). A punch was used to create 2 cm^2 discs, which fit snuggly into the bottom of a 24-well plate (F). Individual microwell inserts were subsequently surface modified using a CHI/HA electrostatic multilayer; see text for details (G). The chondrocytes spreading on non-modified PDMS microwell surface (cell layers marked with arrowheads) (H). Robust micropellet formation on CHI/HA multilayered PDMS surface (I). Scale bar: 200 µm.

Human articular chondrocyte isolation and expansion

Articular chondrocytes were isolated from intact articular cartilage tissue remaining on the knee joints donated following total joint replacement surgery. Ethical approval for this tissue recovery was granted through the Queensland University of Technology Ethics Committee and the Prince Charles Hospital in accordance with the Australian National Health and Medical Research Council's Statement on Ethical Conduct in Research Involving Humans. Articular cartilage was minced into 3-4 mm pieces using a sterile scalpel. Tissue pieces were washed 3 times in phosphate-buffered saline (PBS; Gibco®). Pieces were suspended in 200 U/mL of Collagenase (Gibco®) diluted in low glucose Dulbecco's modified Eagle's medium (DMEM-LG; Gibco®), and then incubated overnight at 37ºC. The digest was filtered through a 40 μm cell strainer (BD Falcon™) to separate tissue fragments. The filtered suspension was washed 3 times, each in 10 mL of DMEM-LG.

Chondrocytes were expanded in monolayer using T175 cm^2 culture flasks (Nunc™) in 35 mL/flask volume of medium composed of DMEM-LG (Gibco®) supplemented with 10% fetal bovine serum (FBS; Gibco®), 100 U/mL penicillin and 100 μg/mL streptomycin (1% PS, Gibco®), 1% Glutamax (Gibco®), 40 μM ascorbic acid 2-phosphate, 40 μg/mL L-proline, in a humidified incubator having a 2% O_2 and 5% CO_2 atmosphere at 37ºC. For the first two passages, 50 μg/mL gentamicin (Amersham Biociences©) and 2% PS were added to the medium. When monolayer cultures approached 80% confluence, the cells were harvested via 5-minute incubation with 3 mL 0.25% trypsin (Trypsin-EDTA; Gibco®) at 37ºC. To inactivate the trypsin, 9 mL of expansion media containing 10% FBS and 1% PS was added. The cell suspension was centrifuged at 500xg for 5 minutes, the supernatant was discarded, and the cells were diluted into 3 times the previous growth medium volume and seeded into 3 T175 cm^2 flasks, giving a split ratio of 1:3. The experiment was repeated with three different donor chondrocytes, and passage 3 cells were used.

Chondrogenic redifferentiation medium

Chondrogenic redifferentiation medium was composed of high-glucose DMEM (DMEM-HG; Gibco®), 10 ng/mL recombinant human Transforming Growth Factor- β1

(TGF-β1, Gibco®), 10^{-7} M dexamethasone, 200 μM ascorbic acid 2-phosphate, 100 μg/mL sodium pyruvate, 40 μg/mL L-proline, 1% ITS-X (Gibco®) and 1% PS.

Formation of macropellets

Macropellets were formed using a conventional pellet culture method [18]. In brief, $2x10^5$ cells were suspended in 1 mL of chondrogenic induction medium, then centrifuged in a 15 mL tube (LabServ®) at 500xg for 5 minutes, and then placed into a 2% or 20% O_2 - 5% CO_2 cell culture incubator at 37ºC with the tube lid loosened to facilitate gas exchange.

Formation of micropellets

Micropellets were formed as described previously [18,19,317]. This design was modeled after work described by Ungrin *et al.* [322]. In brief, microscopic pellets of approximately 166 cells were formed using the patterned surface having 600 microwells/cm^2 (described in Fig. 12). Approximately 1200 micropellets were formed from $2x10^5$ cells by suspending these cells in 1 mL of chondrogenic induction medium over 2 cm^2 microwell inserts in the bottom of 24-well plates. Plates were centrifuged for 5 minutes at 500xg to facilitate pellet formation. Following centrifugation, an even distribution of cells within the microwells was confirmed via microscopy, and the plates were carefully transferred to a cell culture incubator set at 5% CO_2 and either 2% or 20% O_2 at 37ºC.

Assembly of micropellets

The micropellets were transferred into a 15 mL tube then centrifuged at 500xg for 5 minutes to facilitate assembly after the culture of discrete micropellets, in microwells, for 4, 7, 11 or 14 days. The total culture time, including both micropellet culture and assembled culture, was 21 days. This part of the study was performed in only 2% O_2 and 5% CO_2 atmosphere at 37ºC.

Sulfated glycosaminoglycan (sGAG) quantification

Chondrogenic medium was exchanged twice weekly, and the medium from the macropellet and micropellet cultures was collected and stored at -80ºC. When the culture was terminated, the recovered macropellets and micropellets were digested by adding 25 μg papain per sample directly to each tube or microwell plate then the pellet/enzyme mixtures were incubated at 60ºC overnight. DMB dye (1,9-Dimethyl-Methylene Blue zinc chloride double salt) was used to quantify the sGAG content in the collected media and digested tissues using an established protocol [323]. In brief, a 30 μL volume of each sample of was dispensed into a single well of a 96-well clear plate (Nunc™), followed by the addition of 170 μL of DMB dye. The amount of sGAG was quantified by measuring the blue to purple color shift at 530 nm and 590 nm, respectively, in a plate reader (Benchmark Plus plate reader, Bio-Rad). Shark cartilage extract was used to generate a standard curve.

Metabolic activity assay

AlamarBlue® (Invitrogen™) was used to assess the metabolic activity of the pellets as per the manufacturer's protocol. The 10X alamarBlue® solution was diluted in the culture media of the pellets and incubated for 3 hours. Then the medium was removed and analyzed in a plate reader (POLARstar OPTIMA, BMG Labtech) at an excitation and emission of 544 nm and 590 nm, respectively.

DNA quantification

A Quant-iT™ PicoGreen® dsDNA Reagent and Kit (Invitrogen™) was used to determine DNA content in the cultures, as per the manufacturer's protocol. In brief, 50 μL of papain digest was mixed with 50 μL of PicoGreen dye in a fluorescence plate (Nunc™) and analyzed in a plate reader (POLARstar OPTIMA, BMG Labtech) at an excitation and emission of 480 nm and 520 nm, respectively.

Relative gene expression analysis

TRIzol® (Invitrogen™) was used for RNA extraction, as per the manufacturer's protocol. RNA concentration was determined using a Nanodrop ND-1000

spectrophotometer (Bio-Lab). cDNA was synthesized from RNA template using SuperScript III RT and oligo(dT)20 (Invitrogen™) as per the manufacturer's protocol, and stored at -80ºC until analysis. Real-time polymerase chain reaction (qPCR) was performed using Platinum® SYBR® Green qPCR SuperMix-UDG (Invitrogen™) using the primer sequences shown in Table 1 (Geneworks). The master mix was dispensed into the 384-well reaction plate and combined with cDNA samples using an epMotion 5057 (Eppendorf) liquid handling robot. The plates were processed in a 7900HT Fast Real-Time PCR System (Applied Biosystems). PCR cycling parameters were 50ºC for 2 minutes, 95ºC for 3 minutes, 95ºC for 15 seconds and 60ºC for 30 seconds, repeated for a total of 40 cycles. The results were analyzed using the ΔCt method normalized to the geometric mean of two housekeeping genes (cyclophilin A and glyceraldehyde 3-phosphate dehydrogenase (GAPDH)) [324].

Histological analysis

Harvested tissues were embedded in optimum cutting temperature compound (OCT, Tissue-Tek®), and stored at -80ºC. 10 µm-thick sections of samples were generated using a microtome-cryostat (Leica®), and then adsorbed onto poly-lysine glass slides (Thermo Fisher Scientific) and stored at -20ºC until further analysis.

For Alcian blue staining, the slides were fixed with 4% paraformaldehyde for 20 minutes at RT then rinsed with PBS 3 times. Following rinsing, slides were dried and the sections submerged in fresh filtered 1% Alcian blue solubilized in 3% acetic acid (pH 2.5) for 10 minutes. The slides were then rinsed thoroughly with PBS and observed under Laborlux S microscope (Leitz®) using bright field illumination. For immunofluorescence (IF), the slides were fixed with 4% paraformaldehyde for 20 minutes at RT, and then rinsed with PBS 3 times. The slides were dried and borders drawn around sections using a PAP pen. The sections were blocked (3% goat serum, 0.3% Triton X-100 in 1% BSA/PBS) for 20 minutes at RT. The blocked sections were incubated with collagen I, II and X primary antibodies (raised in mouse, rabbit and rabbit respectively, Abcam®) at 4ºC overnight in a humidity chamber. The slides were washed with 0.3% Triton X-100 in PBS for 3 minutes, and then rinsed with PBS. The sections were incubated with corresponding secondary antibodies (FITC conjugated anti

mouse IgG2b and Cy-3 conjugated anti rabbit IgG, Abcam®) for 30 minutes at RT. Slides were washed twice with 0.3% Triton X-100 in 1% BSA/PBS and once with PBS. Coverslips were mounted onto slides using the ProLong Gold Antifade Reagent (Invitrogen™), and assessed under an Eclipse TE2000-U (Nikon) fluorescence microscope using NIS Elements (F 3.2) software.

Statistical analysis

All experiments contained $n = 4$ biological replicates. Studies were repeated using chondrocytes derived from three donors. Data were represented as mean ± standard deviation. Data were analyzed using SPSS (statistical software package: SPSS® Inc.) and one-way analysis of variance (ANOVA) with Tukey post-hoc tests to identify statistical significance, (*) represents $p < 0.05$ and (***) represents $p < 0.001$.

4. Results

Morphology and size of the pellets

Chondrocytes aggregated into micropellets within 24 hours (data not shown). At day 14 of culture, both hypoxic macropellet and micropellet diameters were greater than normoxic pellet diameters (Fig. 13A, B). The estimated average diameter of the hypoxic micropellets was 193 ± 20 μm ($n = 20$), whilst the normoxic micropellets had an estimated average diameter of 87 ± 10 μm ($n = 20$).

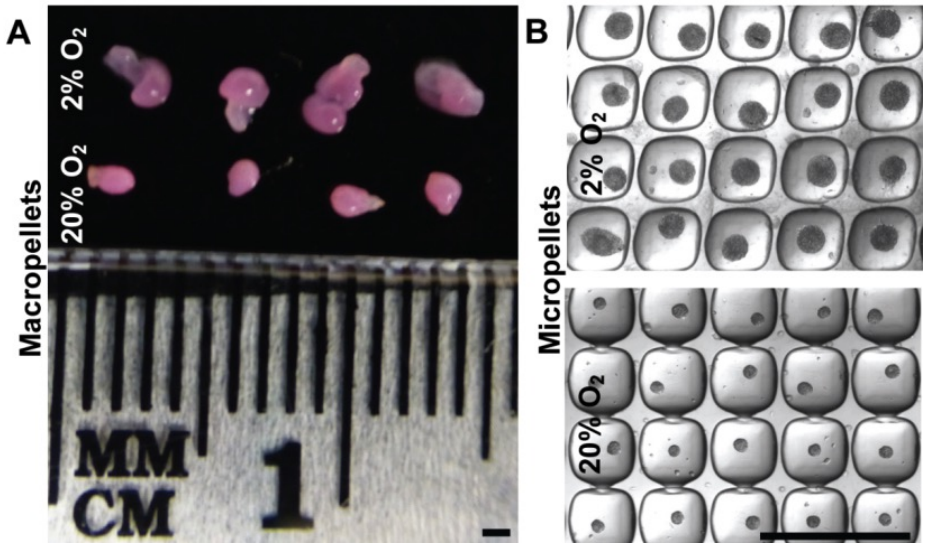

Figure 13. Morphology and size of the pellets. At the end of the 14-day culture, both hypoxic macropellets (A) and micropellets (B) were bigger than the normoxic pellets. The estimated mean diameter for hypoxic micropellets was 193 ± 20 μm (*n = 20*) whilst the estimated mean diameter of the normoxic micropellets was 87 ± 10 μm (*n = 20*). Scale bars: 1 mm.

Metabolic activity, DNA and sGAG production

Hypoxic micropellets were significantly more metabolically active than the other pellets over the culture period, as assessed by alamarBlue® (Fig. 14A). DNA quantification demonstrated that the proliferation of the cells did not differ significantly in different conditions (Fig. 14B). To assess the recovery of the chondrogenic phenotype, the amount of sGAG secreted into the medium over the culture duration and in the final tissues was quantified. The amount of the sGAG retained inside the pellet was significantly higher for the hypoxic macropellets at day 7, 11 and 14 (Fig. 14C). However, the amount of sGAG released into the media was highest for the hypoxic micropellets at all time points (Fig. 14D). The sGAG/DNA ratio was calculated by dividing the total amount of sGAG produced during the culture to the amount of DNA measured at the end of the culture. Hypoxic micropellets had the greatest ratio when compared to other pellets; hypoxic macropellets also had a significantly higher ratio than normoxic pellets (Fig. 14E). The amount of total sGAG measured in the media was higher than the amount measured in the pellets for all conditions (Fig. 14F). The retained sGAG was the highest for the hypoxic macropellets; whilst the overall produced sGAG was greater for the hypoxic micropellets (Fig. 14F).

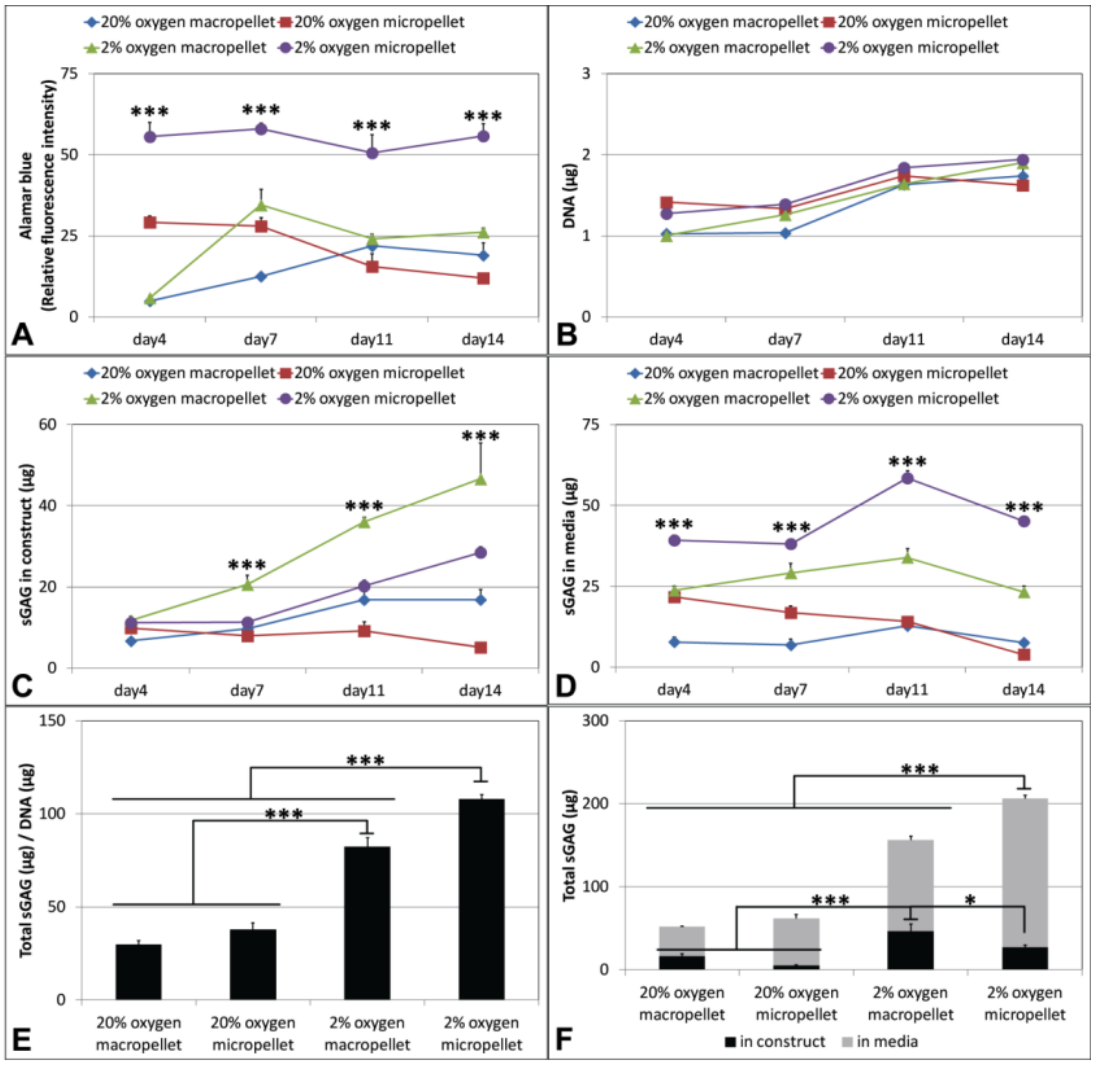

Figure 14. Metabolic activity, growth and sGAG production in pellets. AlamarBlue® graph for metabolic activity (A), DNA quantification (B), sGAG in construct (C) and sGAG in media (D) measurements on days 4, 7, 11, 14. The sGAG/DNA ratio (calculated by dividing the total amount of sGAG produced during the culture to the amount of DNA measured on day 14) (E) and the total sGAG graph demonstrating the total sGAG in media and in construct separately (F).

Chondrogenic and hypertrophic gene expression

Chondrocyte-associated expression of Sox9, aggrecan and collagen II and hypertrophy associated expression of Runx2, collagen I, collagen X, osteocalcin, versican [18] were assessed. Key matrix genes like aggrecan and collagen II had the highest expression in the hypoxic micropellets (Fig. 15A, B). Collagen I was significantly downregulated in macropellets, but remained unchanged in micropellet cultures relative to day 0 controls (Fig. 15C). Runx2 (Fig. 15F) expression was greater in normoxic micropellets, as was collagen X expression in hypoxic micropellets (Fig.

15D). Sox9 expression was lower in hypoxic macropellets (Fig. 15E). Macropellets maintained in a normoxic atmosphere had the highest expression of versican (Fig. 15G) and osteocalcin (Fig. 15F).

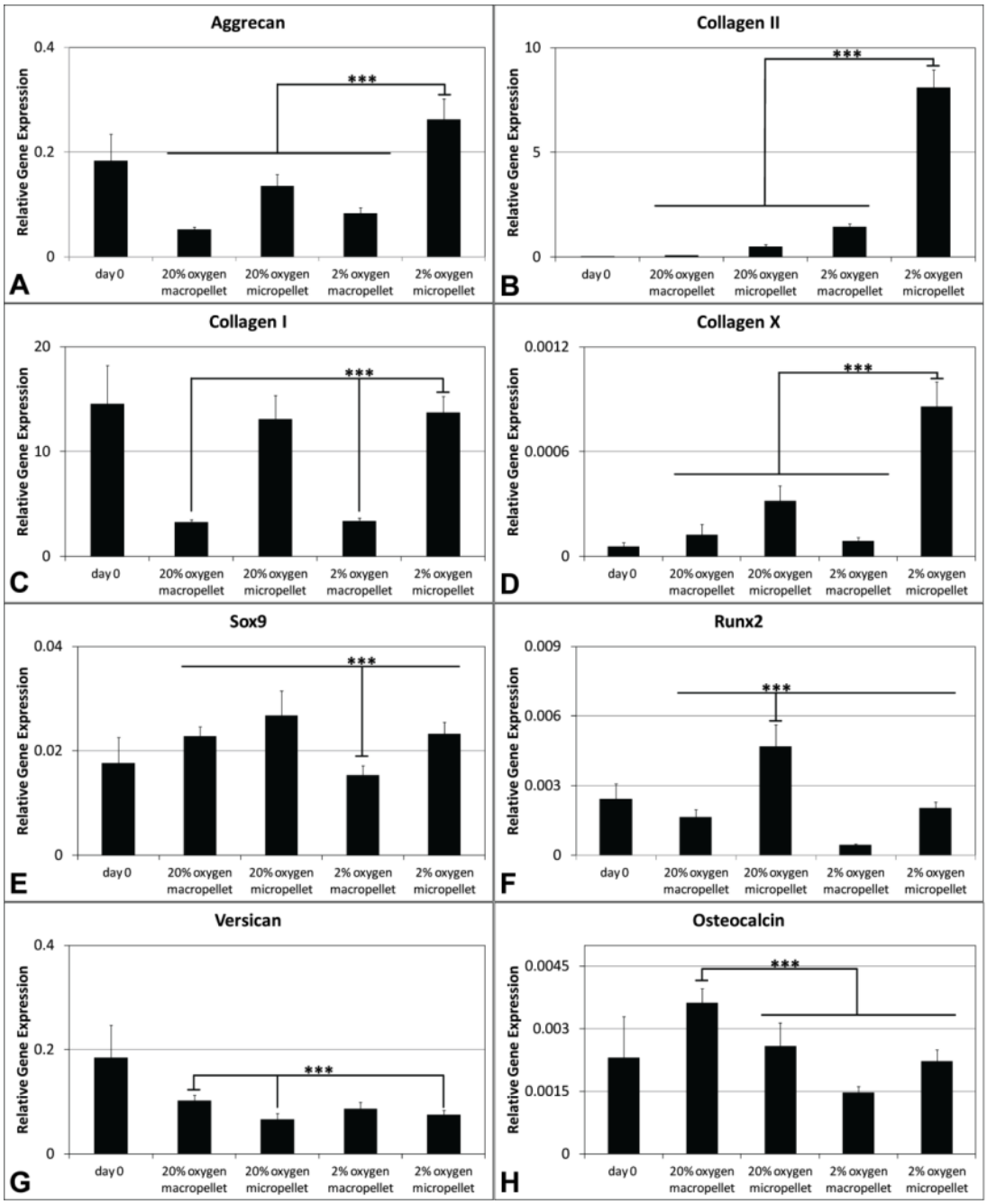

Figure 15. Gene expression in pellets. Aggrecan (A), collagen II (B), collagen I (C), collagen X (D), Sox9 (E), Runx2 (F), versican (G), and osteocalcin (H) expressions relative to the geometric mean of housekeeping genes cyclophilin A and GAPDH

Chondrogenic and hypertrophic matrix deposition and distribution

To visualize the distribution of the ECM molecules within the macro and micropellets, Alcian blue staining and IF analysis for collagen I, II and X were performed. DAPI staining was used to visualize the nuclei (Fig. 16A). Collagen I accumulation was minimal in all conditions, but appeared even lower in hypoxic cultures (Fig. 16B). Collagen X was more intense in normoxic cultures relative to cultures maintained in hypoxic atmospheres (Fig. 16C). By contrast, collagen II staining was stronger in hypoxic cultures. Collagen II matrix distribution in hypoxic macropellets appeared non-uniform, whilst individual micropellets were stained more homogeneously (Fig. 16D). Alcian blue staining revealed that sGAG was lower in normoxic macropellets and staining was more homogeneous in micropellets relative to macropellets (Fig. 16E).

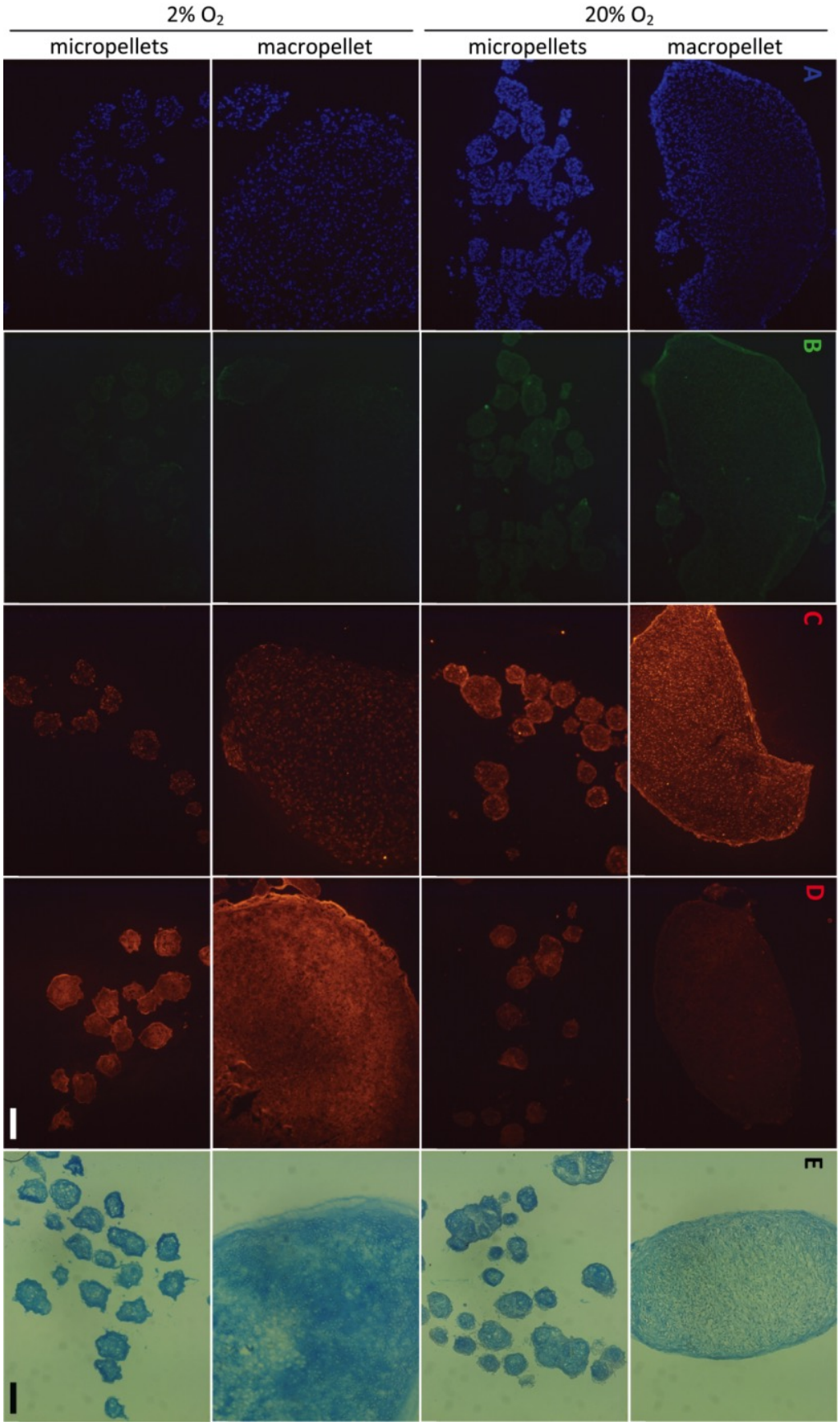
2% O2
20% O2
micropellets
macropellet
micropellets
macropellet
A
B
C
D
E

Figure 16. Cell and matrix localization throughout pellets following 14 days of culture. DAPI staining of nuclei in pellets (A).Immunofluorescence images for collagen I (B), collagen X (C), and collagen II (D), Alcian blue staining for sGAG (E). Scale bars: 100 μm.

Micropellet assembly into macrotissues

To assess the interaction between individual micropellets, they were collected from the microwell surface and centrifuged into a single aggregate at different time points during the chondrogenic redifferentiation process. Micropellets collected from day 4 cultures that were assembled into larger tissue constructs integrated in a uniform manner, such that discrete micropellets were virtually indistinguishable via Alcian blue staining. By contrast, it was still possible to identify individual micropellets collected from day 14 cultures that had been assembled into larger tissue constructs, indicating that full integration had not yet occurred in these constructs (Fig. 17).

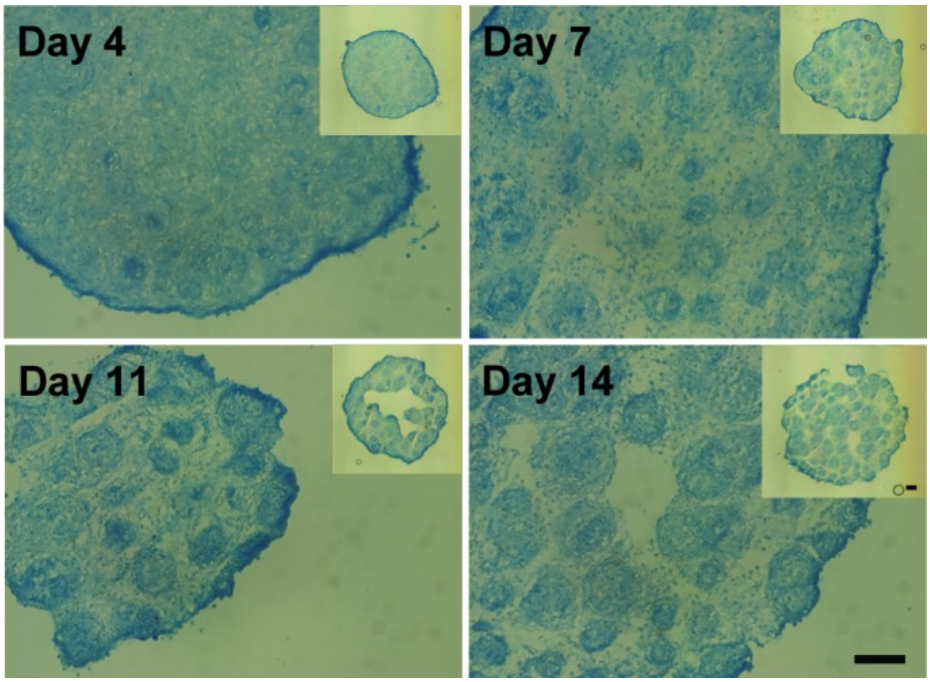

Figure 17. Hypoxic micropellets assembled into macrotissues. Alcian blue staining for hypoxic micropellets assembled at different time points (indicated days). The total culture duration was 21 days. Scale bars: 100 μm.

5. Discussion

A number of strategies are available to facilitate cell aggregate manufacture (reviewed in [325]), including hanging drop and various rotary bioreactors. Our group

favors microwells, as they offer an unparalleled capacity to facilitate robust and precise high-throughput cell aggregate manufacture. Previous studies utilized a commercial microwell product (Aggrewell^{TM}, STEMCELL Technologies) to efficiently manufacture micropellets [18,19,317]. However, if the unmodified PDMS microwell surface is utilized directly in micropellet manufacture, the chondrocytes will adhere to the surface rather than form micropellets (Fig. 12H). In our studies, modifying the surface to prevent cell attachment further enhanced the performance of Aggrewell^{TM}. Minimizing cell attachment favored aggregate formation and facilitated aggregate harvest. As a cost effective strategy, also to enable full control and to ease the optimization of the surface properties, we designed and fabricated our own microwell surface. Figure 12 outlines the fabrication process that was used to generate PDMS microwell inserts that fit into 24-well plates. Following surface modification with the HA/CHI ML (Fig. 12G), the microwell surface enabled robust chondrocyte micropellet formation and harvest (Fig. 12I). Additionally, the stability of the multilayer was tested, and the surface modification remained functional even after 24 hour incubation in 100% ethanol, 70% ethanol, liquid nitrogen, air, distilled water, PBS or boiling water (Fig. 19).

Other available microwell platforms are also suitable for chondrocyte micropellet manufacture. For example, the development of a microwell platform in which the microwells were cast in an agarose gel rather than PDMS was recently described [326]. In this clever strategy, the agarose surface promoted cell aggregate formation by resisting protein adsorption and subsequent cell attachment to the agarose surface. However, a more mechanically robust PDMS microwell platform is compatible with centrifugation, which enables more rapid and efficient micropellet manufacture than the gravity settling method required with an agarose platform. Additionally, there is comparatively less risk of damaging the PDMS microwell structure during medium exchange or culture manipulation processes.

Enhanced sGAG synthesis is critical for effective cartilage tissue regeneration, as the sGAG content endows cartilage with its compressive strength [18]. The sGAG outputs in both micropellet and macropellet cultures were significantly enhanced when these cultures were maintained in hypoxic atmospheres (Fig. 14E). These results are consistent with previous studies demonstrating that hypoxia enhances chondrocyte

redifferentiation by stabilizing the hypoxia inducible factor 1 alpha (HIF-1α), which is translocated into nucleus and activates chondrogenic gene expression [327,328]. However, this is the first study comparing the sGAG production between micropellets and macropellets, under both hypoxic and normoxic environments. Consistent greater sGAG production is observed in hypoxic micropellets, whilst greater sGAG retention occurs in the hypoxic macropellets (Fig. 14F). The loss of the sGAG to the medium is a commonly reported challenge in cartilage tissue engineering, and solutions have been suggested in previous papers [329,330]. The high surface-area-to-volume ratio in the micropellets contributes to the significant loss of sGAG to the medium. However the greater sGAG production and superior gene expression indicate that the chondrocyte redifferentiation was enhanced in hypoxic micropellets. If it is possible to improve the quality of the redifferentiation process, then this short term *in vitro* loss of sGAG should be insignificant relative to the overall clinical benefits. The retention of sGAG would likely be enhanced during a cartilage repair procedure where a large number of micropellets would be implanted into a sealed cartilage defect (Fig. 18A).

Consistent with the sGAG results, chondrogenic gene expression also indicated that the redifferentiation was enhanced in hypoxic micropellets. No significant difference was observed in hypoxic micropellet expression profile for collagen I, Sox9, Runx2, versican and osteocalcin when compared to day 0 measurements (Fig. 15C, E, F, G, H). The expression of some osteogenic genes was elevated in the day 0 cultures, and this reflects the fact that the chondrocytes used in this study were all derived from tissue discards harvested from elderly patients suffering from severe osteoarthritis. Whilst collagen X expression was significantly upregulated in hypoxic micropellets, the overall magnitude of the expression was very low (0.0012 times) relative to the expression of housekeeping genes (Fig. 15D). By comparison, collagen II gene expression was ~10-fold greater in the hypoxic micropellet cultures than the housekeeping gene expression (Fig. 15B). Despite having some hypertrophic properties, the hypoxic micropellets exhibit superior redifferentiation when data are considered cumulatively. The hypoxic micropellets had a larger volume (Fig. 13B), greater metabolic activity, sGAG production (Fig. 14A, E) and higher collagen II expression (Fig. 15B). Importantly, the deposition of the collagen II and sGAG was

more uniform in the micropellets relative to macropellets (Fig. 16D, E). More uniform cell behavior is consistent with a smaller diameter pellet with reduced diffusion gradients. These data mirror our previously reported results indicating that the micropellet strategy enhanced uniformity in MSC chondrogenic cultures [18].

Co.don® AG (Teltow, Germany) is currently evaluating the potential of macropellets for cartilage defect repair in on-going trials [313,314]. We suggest that there may be legitimate benefits in using micropellets rather than macropellets, as this should provide for a more uniform and potent clinical product. Additionally, because of their smaller geometry, micropellets may be able to accommodate more complex defect geometries and ultimately produce a smoother articular surface. This is a rational expectation, as smaller diameter spheres will always more uniformly fill a void than larger diameter spheres. A prerequisite to such applications is that micropellets must demonstrate the capacity to amalgamate into a contiguous repair tissue. Here we tested the amalgamation efficiency of cartilage micropellets that had been cultured for 4, 7, 11 or 14 days. The amalgamation efficiency depended on the time that the micropellets had been cultured before assembly (Fig. 17), and the most primitive day 4 micropellets proved the most efficient. This outcome is also rational, as temporal matrix deposition in the micropellets would be expected to stabilize with time. These results reflect only short-term observation, and it may be possible to observe excellent integration of even day 14 micropellets over an extended time period. Given that micropellets contain significant matrix content, we reason that they may be superior to single cell suspensions lacking any legitimate matrix component, as in procedures like Autologous Chondrocyte Implantation (ACI). Unlike macropellets, micropellets could easily be injected under ACI-type membranes, thus facilitating delivery.

Using our microwell system, it is possible to generate 36,000 cartilage micropellets in a single 6-well plate. This manufacturing efficiency enables the evaluation of micropellets either in the direct repair of cartilage defects (Fig. 18A), or as a building block in the *in vitro* assembly of complex zonal osteochondral tissues (Fig. 18B). Typically, osteochondral tissues have been made from single cell suspensions seeded into gels or onto solid scaffolds [331-334], although a recent study used spheroids of rabbit MSCs differentiated into osteoblasts and chondrocytes, which were

subsequently assembled into a zonal tissue [335]. In this study, the spheroids were manufactured by manually dispensing cells in collagen droplets. Our more efficient manufacturing process should enable more sophisticated zonal tissues such as those shown schematically in Figure 18B. Data from our group indicated that a similar micropellet manufacturing strategy enabled enhanced MSC osteogenesis and the generation of bone spheroids [19] ideal for the assembly of an osteochondral tissue. Ultimately, the small dimensions of micropellets make them ideal for identifying the culture conditions necessary to recapitulate the various zonal tissues found in cartilage [336], and therefore, micropellets will likely become the preferred building blocks for reconstructing such tissues.

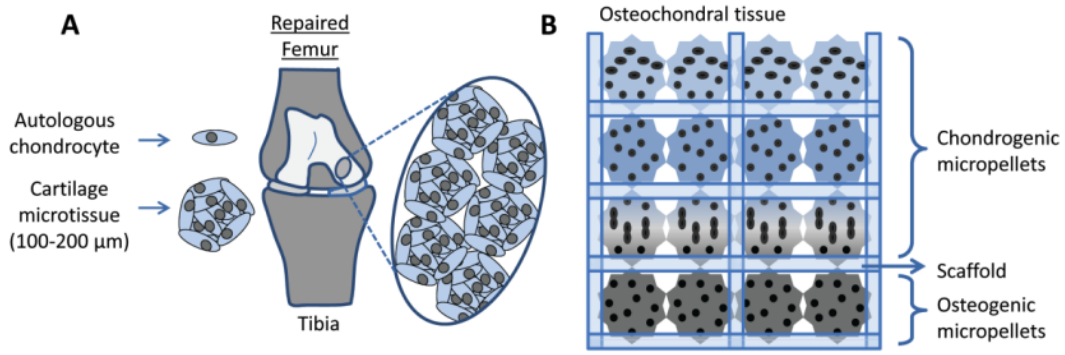

Figure 18. Potential applications of the chondrocyte micropellets. The direct use of chondrocyte micropellets in articular cartilage defect repair (A). The use of cartilage micropellets in the manufacture of osteochondral tissues *in vitro* (B).

6. Conclusion

Herein we describe the fabrication of a custom microwell system and a surface modification that enables the efficient manufacture of thousands of cartilage micropellets. Hypoxic micropellet culture was shown to be a superior chondrocyte redifferentiation platform, relative to traditional macropellet cultures. We rationalized that the micropellets might offer a unique strategy for enhanced cartilage defect repair, and to investigate this potential the efficiency of the micropellet amalgamation was examined. Micropellets that had been cultured for 4-7 days most efficiently amalgamated, and the composite tissue was nearly seamless at the end of the 21-day culture. Cumulatively, our results indicate that the redifferentiation of expanded human

articular chondrocytes can be enhanced using micropellet culture, and that these micropellets can be assembled into larger more clinically relevant dimensions.

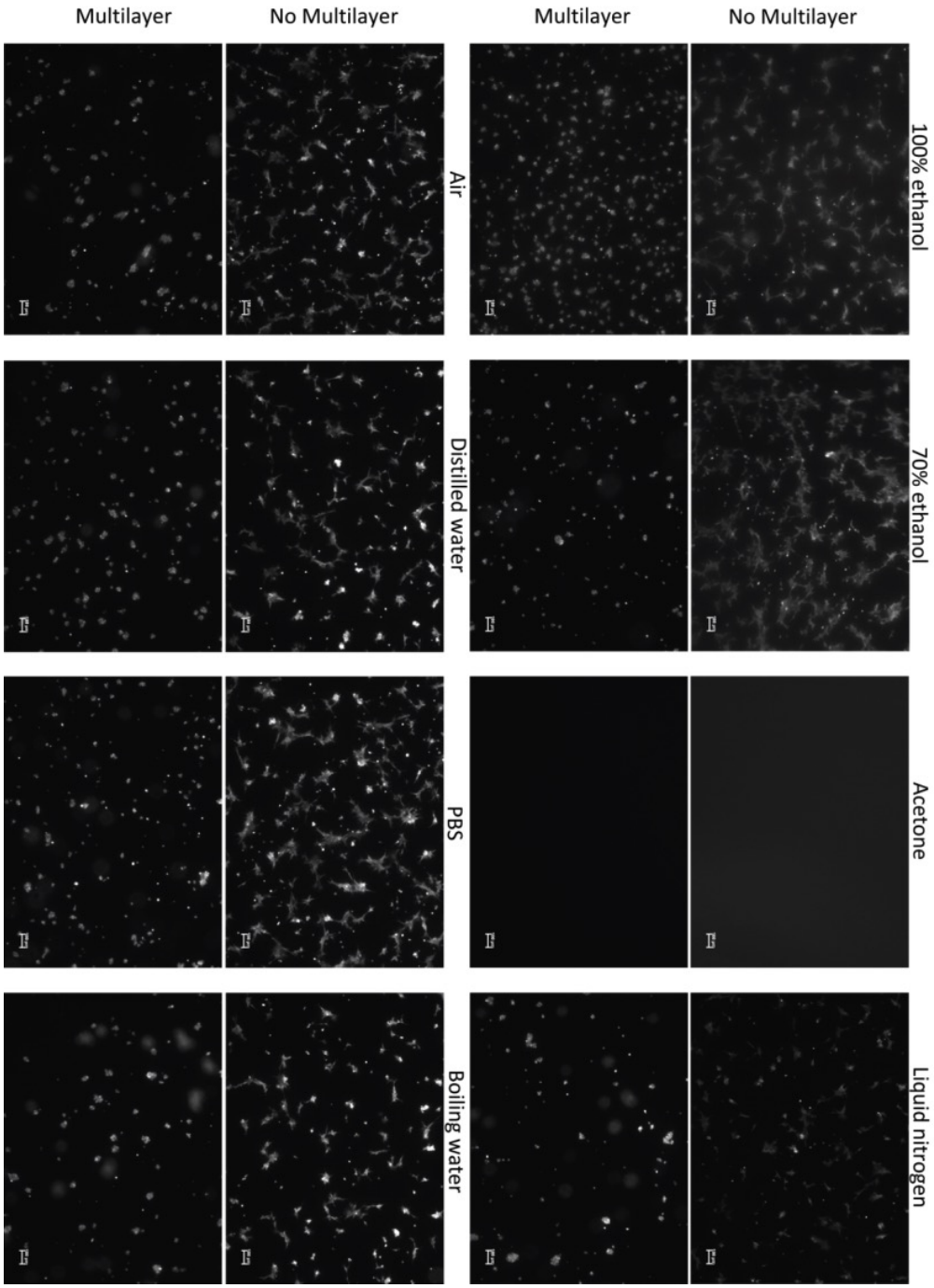

Figure 19. Surface modification testing. To assess the stability and functionality of the surface modification after incubation in ethanol and PBS, a testing platform was set up as follows: flat 24 well plate PDMS disks were produced and half of them were multilayered as explained in the Materials and Methods section. The disks were incubated under conditions stated (in 100% ethanol, in 70% ethanol, in acetone, in liquid nitrogen, in air, in distilled water, in PBS, in boiling water) for 24 hours and the

functionality of the surface was assessed by imaging cell attachment. After 15 minutes of ventilation, cells were seeded at a density of 3000/cm^2, incubated in chondrogenic redifferentiation media overnight. Surface modification was not affected by any of the conditions. However acetone sensibly decreased the transparency of the PDMS itself, therefore the cell attachment could not be assessed. For all other conditions the cell spreading was observed for the surface with no multilayer whereas the cells were not spreading on the surfaces with multilayer.

Gene (Amplicon size in basepair)	Primers
Cyclophilin A (164)	Forward CTCGAATAAGTTTGACTTGTGTTT
	Reverse CTAGGCATGGGAGGGAACA
GAPDH (119)	Forward ATGGGGAAGGTGAAGGTCG
	Reverse TAAAAGCAGCCCTGGTGACC
SOX9 (77)	Forward TTCCGCGACGTGGACAT
	Reverse TCAAACTCGTTGACATCGAAGGT
Aggrecan (85)	Forward TCGAGGACAGCGAGGCC
	Reverse TCGAGGGTGTAGCGTGTAGAGA
Collagen II, COL2A1 (79)	Forward GGCAATAGCAGGTTCACGTACA
	Reverse CGATAACAGTCTTGCCCCACTT
Collagen I, COL1A1 (83)	Forward CAGCCGCTTCACCTACAGC
	Reverse TTTTGTATTCAATCACTGTCTTGCC
Versican (98)	Forward TGGAATGATGTTCCCTGCAA
	Reverse AAGGTCTTGGCATTTTCTACAACAG
Collagen X, COL10A1 (70)	Forward CAAGGCACCATCTCCAGGAA
	Reverse AAAGGGTATTTGTGGCAGCATATT
Runx2 (113)	Forward GGAGTGGACGAGGCAAGAGTTT
	Reverse AGCTTCTGTCTGTGCCTTCTGG
Osteocalcin (70)	Forward GAAGCCCAGCGGTGCA
	Reverse CACTACCTCGCTGCCCTCC

Table 1. Primers used for gene expression analysis.

Chapter 4: Statement of Contribution of Co-Authors for Thesis by Published Paper

In the case of this chapter

Title: **The rapid manufacture of uniform composite multicellular-biomaterial micropellets, their assembly into macroscopic organized tissues, and potential applications in cartilage tissue engineering**

Date, status, journal: January 2015, Submitted, PLOS ONE

Contributor	Statement of contribution
Betul Kul Babur Signature Date 20.01.2015	wrote the manuscript (M), experimental design (D), conducted experiments (E), and data analysis (A)
Mahboubeh Kabiri	aided with D, E
William B. Lott	aided with M, A
Travis Klein	aided with M, D, A
Michael Robert Doran	aided with M, D, A and materials

Principal Supervisor Confirmation

I have sighted email or other correspondence from all Co-authors confirming their certifying authorship.

Michael Robert Doran		20.01.2015
Name	Signature	Date

"To invent, you need a good imagination and a pile of junk."
Thomas Edison

Chapter 4: The rapid manufacture of uniform composite multicellular-biomaterial micropellets, their assembly into macroscopic organized tissues, and potential applications in cartilage tissue engineering

1. Abstract

We and others have published on the rapid manufacture of micropellet tissues, typically formed from 100-500 cells each. The micropellet geometry enhances cellular biological properties, and in many cases the micropellets can subsequently be utilized as building blocks to assemble complex macrotissues. Generally, micropellets are formed from cells alone, however when replicating matrix-rich tissues such as cartilage it would be ideal if matrix or biomaterials supplements could be incorporated directly into the micropellet during the manufacturing process. Herein we describe a method to efficiently incorporate donor cartilage matrix into tissue engineered cartilage micropellets. We lyophilized bovine cartilage matrix, and then shattered it into microscopic pieces having average dimensions < 10 μm diameter; we termed this microscopic donor matrix "cartilage dust (CD)". Using a microwell platform, we show that ~0.83 μg CD can be rapidly and efficiently incorporated into single multicellular aggregates formed from 180 bone marrow mesenchymal stem/stromal cells (MSC) each. The microwell platform enabled the rapid manufacture of thousands of replica composite micropellets, with each micropellet having a material/CD core and a cellular surface. This micropellet organization enabled the rapid bulking up of the micropellet

core matrix content, and left an adhesive cellular outer surface. This morphological organization enabled the ready assembly of the composite micropellets into macroscopic tissues. Generically, this is a versatile method that enables the rapid and uniform integration of biomaterials into multicellular micropellets that can then be used as tissue building blocks. In this study, the addition of CD resulted in an approximate 8-fold volume increase in the micropellets, with the donor matrix functioning to contribute to an increase in total cartilage matrix content. Composite micropellets were readily assembled into macroscopic cartilage tissues; the incorporation of CD enhanced tissue size and matrix content, but did not enhance chondrogenic gene expression.

2. Introduction

Cartilage tissue lacks reliable self-repair. Consequently, cartilage injuries often further degenerate rather than healing spontaneously. The tendency to degenerate makes osteoarthritis (OA) the leading cause of pain and disability in developed nations [2,337-339]. Currently, the repair of osteoarthritic lesions is not possible and joint replacements are the only surgical interventions that successfully restore OA joint function [340]. However, surgical repair of acute cartilage injuries and delayed onset of OA is possible to a limited extent. A range of surgical methodologies has been developed and the most promising methods utilize cell-based tissue engineering approaches.

The two clinically approved tissue engineering methodologies are Autologous Chondrocyte Implantation (ACI) [93] and Matrix-Assisted Chondrocyte Implantation (MACI) [341]. In both ACI and MACI, autologous chondrocytes are isolated from a biopsy of a non-load bearing site of the damaged cartilage. The isolated chondrocytes are then expanded *ex vivo*, before being transplanted into the primary defect site beneath a periosteum membrane isolated from the patient's tibia (ACI) or on a manufactured type I/III collagen membrane (MACI). In both cases, the initial repair tissue lacks any cartilage matrix and is extremely fragile; typically the repaired joint is protected from full weight bearing for 2-3 months [342-344].

The initial fragility of the ACI/MACI repair tissue is related to the lack of mature cartilage ECM at the time of implantation. To overcome this problem a number of groups have explored strategies that involve the direct incorporation of mature cartilage

matrix into engineered tissue. Peretti *et al.* assessed the bonding of 1 mm thick cartilage slices or chips with expanded chondrocytes; the bonding was successful however the repopulation of the cartilage pieces was inefficient [277,278,345]. The dense ECM network in donor cartilage matrix prevents effective cell infiltration, and as a result the repopulation of the 1 mm thick cartilage pieces was only successful on the superficial or in regions adjacent to outer exposed areas [277,278,345]. Using a refined approach Gong *et al.* combined thinner (10-30 μm) sections of donor cartilage and chondrocytes [279]. They reported that the repopulation of the cartilage sections was significantly enhanced in 10 μm thick sections even relative to the 30 μm thick sections [279]. This body of work indicated that donor cartilage matrix might not be efficiently repopulated unless used in units with dimensions approaching 10 μm in thickness. This characteristic suggests that unlike tissues such as skin, large pieces of donor cartilage matrix cannot be used to provide a template for the effective generation of larger 3D tissue structures.

An alternative to using large pieces of donor cartilage to provide macroscopic structure is the incorporation of cartilage matrix particles into scaffolds formed via conventional scaffold manufacture. Yang *et al.* described the fabrication of a natural porous ECM derived scaffold made of physically crushed, lyophilized and cross-linked native cartilage tissue [280]. Similarly, Zheng *et al.* compared porous scaffolds made of PLGA versus porous scaffolds made of pulverized cartilage versus a composition of both [281]. They identified the composite scaffold as optimal, and suggested that this was related to the combination of biomimetic natural nanofibrous cartilage pieces and the mechanically strong PLGA component [281]. Additionally, Shin *et al.* used a freezer mill to crush porcine cartilage pieces, then cross-linked the particles to obtain a porous scaffold which was then seeded with chondrocytes for tracheal implantation in a rabbit model [346]. The use of donor matrix to enhance engineered cartilage tissue quality appears to be a rational and promising approach.

Our team has previously utilized micropellet cultures to generate cartilage-like tissue [17,18]. Micropellets differ from conventional pellets, with micropellets typically having 100-1000 cells each, whilst macropellets typically have 100,000-500,000 cells each. Chondrogenesis appears to be enhanced and more homogeneous in micropellets,

and this likely reflects the improved mass transport enabled by their smaller diameter [18]. Whilst chondrogenesis appears to be improved in the micropellet system, relative to conventional pellet cultures, the rapid formation of cartilage matrix equivalent to native tissue remains challenging. We reasoned that the incorporation of microparticles of donor matrix into micropellets would provide a mechanism to rapidly increase the cartilage-like matrix volume of the micropellets, and ultimately enhance the tissue quality.

Herein we describe the optimization of a method to incorporate lyophilized donor bovine matrix particles into microtissues or macrotissues formed from bone marrow-derived mesenchymal stem/stromal cells (MSC). Hereafter we call the cartilage matrix particles Cartilage Dust (CD). We contrasted the volume contribution and chondrogenic induction capacity enabled through the incorporation of CD into microtissues or macrotissues formed from 180 cells or 200,000 cells each, respectively. To demonstrate the potential utility of this concepts in tissue engineering applications, we used a high throughput microwell system to manufacture thousands of micropellets containing CD, and demonstrated that these tissues could be amalgamated into larger tissues in a manner that might have utility in the engineering of larger repair tissues or perhaps in direct cartilage defect filling.

3. Materials and Methods

Microwell fabrication and surface modification

In previous work we outlined detailed methods for microwell insert manufacture [17]. In brief, using deep reactive ion etching a silica wafer was etched to have a microwell pattern of 600 microwells/cm^2. Individual microwells had dimensions of 360x360x180 μm (Fig. 26). Polydimethylsiloxane (PDMS) replica molding was used to generate a negative that was then heat pressed into a sheet of polystyrene. The resulting polystyrene mold was used to manufacture PDMS sheets of microwells surfaces, from which discs were punched out to use as inserts within 24-well plates [17]. The 2 cm^2 discs containing microwells were fit and glued with PDMS into 24-well plates (Fig. 26). Each 24-well plate insert contained 1200 microwells. The plates with microwell inserts were sterilized for 1 hour in 70% ethanol then rinsed multiple times with sterile PBS.

Before cells were seeded, the inserts were treated with 5% pluronic acid (Sigma) solution for 5 minutes to block protein adhesion and prevent cell attachment to the PDMS surface. Then, the inserts were rinsed again with PBS and the cells were seeded into the wells containing the microwell inserts.

Human bone marrow MSC isolation and expansion

Ethics: Bone marrow aspirate was collected from the iliac crest of healthy donors with full informed written consent in all cases. Mater Health Services Human Research Ethics Committee approved the consent procedure and held the consent documents. All tissue samples were provided to the research team in a de-identified manner. Ethical approval for this research was granted through the Mater Health Services Human Research Ethics Committee (Ethics number: 1541A) and the Queensland University of Technology Ethics Committee in accordance with the Australian *National Statement on Ethical Conduct in Human Research*.

Bone marrow MSCs were isolated directly from bone marrow aspirates. The collected bone marrow aspirate was diluted 1:1 with PBS and underlayed with 12 mL Ficoll Paque Plus (GE healthcare). The solution was centrifuged at 535xg for 20 minutes. Interface cells were collected, washed and resuspended in low glucose DMEM (DMEM-LG, Invitrogen) with PS and 10% fetal bovine serum (FBS, Invitrogen), then seeded in tissue culture flasks (T175, Nunc). After 48 hours, the non-adherent cells were removed and the adherent cells were further cultured to 80% confluence with medium changes every 3-4 days.

MSCs were expanded in monolayer in DMEM-LG supplemented with 10% FBS and PS in an incubator with 2% O_2 and 5% CO_2 atmosphere at 37°C. The cells were dissociated via 5-minute incubation with 0.25% TrypLE (Invitrogen) at 37°C when they reached confluence. The cells dissociated from one flask were divided equally into four and then seeded into new flasks until passage 3, and then the cells were used in the described studies.

Chondrogenic differentiation medium

Chondrogenic medium was composed of DMEM-HG with 110 μg/mL sodium pyruvate (Invitrogen), 10 ng/mL recombinant human Transforming Growth Factor β1 (TGF- β1, Peprotech), 10^{-7} M dexamethasone (Sigma), 200 μM ascorbic acid 2-phosphate (Sigma), 40 μg/mL L-proline (Sigma), 1% Insulin-Transferrin-Selenium-Ethanolamine (ITS-X, Invitrogen) and PS. The chondrogenic medium was changed 75% every second day, the collected media was stored at -20°C for sulfated glycosaminoglycan (sGAG) analysis.

Cartilage dust preparation

Bovine knee articular cartilage (obtained from a local butcher, animals were ~12 month-old) was used to generate cartilage dust. The cartilage tissue was harvested aseptically from femoral condyle as thin sections. The collected tissue was washed three times with sterile phosphate-buffered saline (PBS, Invitrogen) containing 100 U/mL penicillin and 100 μg/mL streptomycin (PS, Invitrogen). The tissue was frozen at -80°C overnight then lyophilized (Christ Alpha 1-2 LDplus). The lyophilized tissue was aseptically pulverized into a powder using a marble pestle and mortar (10 cm inner diameter) by vigorous crushing for 30 minutes. The powdered cartilage was stored dry at -20°C until use. The powdered cartilage was suspended in high glucose Dulbecco's modified Eagle's medium (DMEM-HG, Invitrogen) with PS immediately prior to initiating cultures, and the wetted cartilage pieces were filtered using a 40 μm cell strainer (BD Falcon) to eliminate pieces larger than 40 μm. The filtered micron size fraction of the powdered cartilage, referred as cartilage dust (CD), was washed twice with DMEM-HG including PS to generate a concentrated CD solution (~20 mg/mL). A 50 μL sample of that solution was added to each CD-containing macro or micropellets delivering ~1 mg (dry weight) CD per culture. Monochrome phase contrast images of the CD on a glass slide were taken with a Nikon DS-Qi1Mc camera using ECLIPSE Ti microscope at 4X magnification (Nikon, Japan). Cartilage dust particle size was measured using Feret's diameter (ImageJ, NIH, USA).

Macropellet formation

Macropellets were formed in 15-mL tubes (BD Falcon) using the conventional method. MSC macropellets contained only 2.2 x 10^5 MSCs in 1mL chondrogenic media in tubes. MSC+CD macropellets contained both 2.2 x 10^5 MSCs in 1 mL chondrogenic media and 1 mg CD, described in previous section, in tubes. CD macropellets contained only 1 mg CD in 1 mL chondrogenic media in tubes. Then the tubes were centrifuged at 400xg for 5 minutes. The macropellets were cultured in a 2% O_2 and 5% CO_2 incubator at 37°C for 14 days with loosened lids to enable gas exchange.

Micropellet formation

Micropellets of ~180 cells each (a total of 2.2x10^5 cells in 1200 micropellets) were formed using microwell PDMS discs in 24-well plates (Nunc) (Fig. 26) [17]. Each disc contained 1200 microwells therefore a single macropellet described in previous section was equivalent and compared to 1200 micropellets. Similar to macropellets, MSC micropellets contained only 2.2 x 10^5 MSCs in 1mL chondrogenic media in wells. MSC+CD micropellets contained both 2.2 x 10^5 MSCs in 1mL chondrogenic media and 1mg CD in wells. CD micropellets contained only 1mg CD in 1mL chondrogenic media in wells. Then the plates were centrifuged at 400xg for 5 minutes. The micropellets were cultured in a 2% O_2 and 5% CO_2 incubator at 37°C for 14 days. Monochrome phase contrast images of the cultures at day 1 and 14 were taken with a Nikon DS-Qi1Mc camera using ECLIPSE Ti microscope (Nikon, Japan). The diameters of the micropellets were then estimated from the images using ImageJ software.

Micropellet assembly

In the second part of the study, the micropellets were assembled at different time points. Day 0 assembly was equivalent to macropellet formation. The other cultures were initiated as micropellets and subsequently assembled after either day 4, 7, 10 or 14 of culture as discrete micropellets. The assembly process was achieved by dislodging the micropellets from the microwells, via pipette aspiration, and pelleting the micropellets in a 15-mL tube by centrifuging at 400xg for 5 minutes. The assembled micropellets were then cultured in a 2% O_2 and 5% CO_2 incubator at 37°C with loosened lids to enable gas

exchange. The total duration of chondrogenic culture was 22 days for the assembled tissues in this study.

Sulfated glycosaminoglycan (sGAG) and DNA quantification

Tissues were digested through the addition of 0.25 mg papain (Sigma) solution directly to each tube or well followed by overnight incubation at 60°C. The digest was used to quantify both the DNA and the sGAG in tissue constructs. The medium collected during the medium exchanges was analyzed to determine the quantity of secreted sGAG. 1,9 Dimethyl methylene blue zinc chloride double salt (DMB, Sigma) was used for sGAG quantification. Digests or culture medium were dispensed in clear 96-well plates (Nunc), then DMB dye was added and the signal was measured at 590 using a plate reader (MULTISKAN GO, Thermo Fischer). Shark chondroitin sulfate (Sigma) was used to generate a standard curve.

PicoGreen dsDNA Reagent and Kit (Invitrogen) was used to quantify the DNA content in the micropellet digests. The papain digest and the PicoGreen solution was mixed in a black 96-well plate (half-area, Costar) and measured in a plate reader (FLUOstar OMEGA, BMG Labtech) at an excitation and emission of 480 nm and 520 nm, respectively.

Gene expression

Trizol (Invitrogen) was used to extract mRNA from pellets as per the manufacturer's protocol. The RNA concentration was measured using spectrophotometer (Nanodrop 1000, Thermo Scientific). Complementary DNA (cDNA) was synthesized from the mRNA template using SuperScript III RT and oligo(dT)20 kit (Invitrogen) as per the manufacturer's instructions. The quantitative polymerase chain reaction (qPCR) was performed using Platinum SYBR Green qPCR SuperMix-UDG kit (Invitrogen). The primers (5' to 3', Geneworks) listed in Table 2 were used.

The qPCR reactions mixes were aliquoted using a liquid handler (epMotion M5073, Eppendorf). SYBR Green master mix was dispensed into 384-well plates (Applied Biosystems) and combined with cDNA template. The qPCR reaction was performed using ViiA real time PCR system (Applied Biosystems). The qPCR reaction

was initiated with a 2-minute 50°C hold, followed by a 3-minute 95°C hold, and then proceeded with 40 cycles of 15-second at 95°C, 30-second at 60°C. The qPCR results were analyzed using ΔCt method and the gene expression was normalized to the geometric mean of two housekeeping genes (cyclophilin A and glyceraldehyde 3-phosphate dehydrogenase (GAPDH)).

Histology

Cultured tissues were fixed in 4% paraformaldehyde (PFA, Sigma) for 30 minutes. Then collected in micro centrifuge tubes and embedded in optimum cutting temperature compound (OCT, Tissue-Tek) and frozen at -20°C. Embedded frozen tissues were sectioned in 10 μm thickness using a cryostat (Leica) then the sections were adsorbed on poly-lysine glass slides (Thermo Fisher), dried at room temperature, stored at -20°C. Before staining, the slides were brought to room temperature and the sections were fixed with 4% PFA for 20 minutes then rinsed with PBS.

For alcian blue staining, the sections were covered with filtered 1% alcian blue (Sigma) dissolved in 3% acetic acid with pH of 2.5 for 10 minutes. Then the slides were rinsed with PBS until the excess alcian blue was removed from the slides. The sections were counter stained using 4', 6 diamidino-2-phenylindole (DAPI, Sigma). The sections were imaged using a Nikon ECLIPSE Ti microscope and images were taken using a Nikon DS-Fi1 camera. Alcian blue and DAPI images were merged using Photoshop (Adobe CS5) software.

For immunofluorescence (IF) staining, the slides were dried and borders were drawn around the sections using a hydrophobic PAP pen (Sigma). Then the sections were blocked using 3% goat serum (Invitrogen), 0.3% Triton X-100 (Sigma) in 1% BSA (Sigma) for 20 minutes at room temperature. Then the sections were incubated with primary antibodies for human collagen II and X both 1:100 dilution and raised in rabbit (Abcam) at 4°C overnight in a humidified chamber. Then the slides were washed twice with 0.3% Triton X-100 in PBS for 3 minutes, then rinsed once with PBS. Next, the sections were incubated with the secondary antibody (Cy-3 conjugated anti rabbit IgG, Abcam) diluted 1:500 in 1% BSA for 30 minutes at room temperature. The slides were washed twice with 0.3% Triton X-100 in PBS for 3 minutes, counter stained with DAPI

then rinsed once with PBS. The sections were mounted using CC/Mount (Sigma) and cover slipped. The slides were imaged using an ECLIPSE Ti epifluorescent microscope (Nikon, Japan) and monochrome images were taken with a Nikon DS-Qi1Mc camera, and then colored using NIS Elements BR 3.2 software. The images were merged using Photoshop (Adobe CS5) software.

Live imaging

A parallel 24-well plate containing MSC micropellets and MSC+CD micropellets was prepared and live imaging was utilized to track the assembly of the micropellets over the first 92 hours of culture. Medium was not changed during imaging and micropellets were cultured at 37°C under 5% CO_2 and atmospheric oxygen instead of 2% O_2. All live imaging was performed on a Live cell microscope (ZEISS, Germany), and image stacks were converted to AVI format using ImageJ software, then the videos were compressed and converted to mp4 using Movie Maker (Microsoft Windows, USA) software.

Statistical analysis

All experiments were performed with $n = 4$ biological replicates. Studies were repeated using 3 different donor MSCs. Data in graphs were represented as mean + standard deviation (SD). The significance was analyzed using SPSS software (SPSS Statistics 21, IBM, USA) and one-way analysis of variance (ANOVA) with Tukey's post-hoc test was used to identify the statistical significance with a p-value smaller than 0.05. The significance was indicated using Roman numerals or symbols on the corresponding graphs, any two groups with same numerals or symbols were statistically equivalent and the groups not marked with the same numerals or symbols were statistically different.

4. Results and Discussion

Cartilage dust

CD particle size was first characterized via image analysis. A gradient in particle size was observed in cartilage dust (Fig. 20A), and overall size distribution graph

indicated that particle size was mainly less than 10 μm (Fig. 20B). However even in low numbers, there were still particles greater than 10 μm since CD solution was filtered with a 40 μm cell strainer. In total 10,000 particles were characterized. The overall particle size average was estimated to be 5.53 ± 6.02 μm (Fig. 20B) and the median particle size was 3.73 μm.

Devitalized xenogeneic matrix has been utilized in tissue engineering previously, but this particular approach has never been described. Here we pulverized lyophilized bovine cartilage and used only micron size particles, which provided efficient cell infiltration and repopulation of the donor matrix [282], since the size of the CD particles was in the same range with the mammalian cell size. The individual collagen fibers in CD particles might still be intact, however the overall collagen fiber organization was likely to be abolished during pulverization. Our pulverization method yielded different sizes of particles in CD (Fig. 20A, B). The smaller particles tend to rapidly lose both the unwanted residual DNA as well as leach the desired sGAG molecules. The release of both DNA and sGAG increases proportionally to the increased surface area to volume ratio that occurs as the particle diameter is reduced. This phenomenon was noted nearly three decades ago; although at the time pulverizing cartilage into microparticles was done purposefully to enhance the extraction of sGAG from cartilage [347]. In our hands, it was necessary to store the CD dry and frozen to prevent loss of sGAG and only rinse it immediately before use to remove the bulk of the residual DNA.

Pellet size

The addition of CD during the manufacturing of MSC+CD macro and micropellets always resulted in a significant increase in the pellet size, and this relative increase in size was maintained over the 14-day culture period (Fig. 20C). The average diameters of the MSC micropellets and MSC+CD micropellets on day 1 were 100.8 ± 7.8 μm and 176.1 ± 9.9 μm, respectively. On day 14, the average diameters of the MSC micropellets and MSC+CD micropellets were 82.6 ± 10.8 μm and 183.8 ± 16.2 μm, respectively. The addition of CD to the tissue effectively doubled the diameter, significantly increasing the micropellet volume. The MSC micropellets were slightly smaller following 2 weeks of culture compared to day 1, whereas MSC+CD micropellets

were slightly larger in size following 2 weeks of culture. MSC+CD micropellets appeared to have a darker core in phase contrast images at day 14 (Fig. 20C). The CD appeared to be homogenously distributed within the MSC+CD micropellets at day 1, however CD was increasingly concentrated within the core of the micropellets throughout the culture (Fig. 20C). MSC and MSC+CD micropellet formation was captured for the first 92 hours and the mechanism of MSC/CD self-assembly was documented in Video 1 [348] and Video 2 [349]. In videos, it is seen that the micropellet formation was completed within the first 4 hours, and that cell proliferation occurred at the periphery of the micropellets following micropellet assembly. Perhaps the most interesting outcome from this paper is the impressive mechanism by which the micropellet rolls around the microwell, attaches to the biomaterial/matrix, and then internalizes it. This feature may have potential utility in a number of tissue engineering and micropellet tissue mimic applications. It is foreseeable that this technology could readily be used to incorporate biomaterial particles that elute chondrogenic induction factors or other signal molecules. Alternatively, this approach could be used to rapidly incorporate bone matrix, for example, into micropellets to enable the rapid formation of bone tissue mimics for *in vitro* study or *in vivo* tissue repair.

The substantial volume increase in MSC+CD macro and micropellets supports the concept of using CD as an agent to rapidly increase the matrix content of engineered cartilage tissue. Utilizing CD, larger cartilage defects could be filled with reduced total number of cells. This would enable the rapid filling of defects with matrix-rich artificial tissue that had cell density and matrix composition similar to native cartilage tissue. A fortunate outcome of having the CD localize within the core is that the cellular surface of the MSC+CD micropellet makes individual micropellets very adhesive and readily assembled into larger tissues. Based on these observations, we reason that assembling MSC+CD micropellets will enhance the capacity of this concept to have utility in cartilage defect repair.

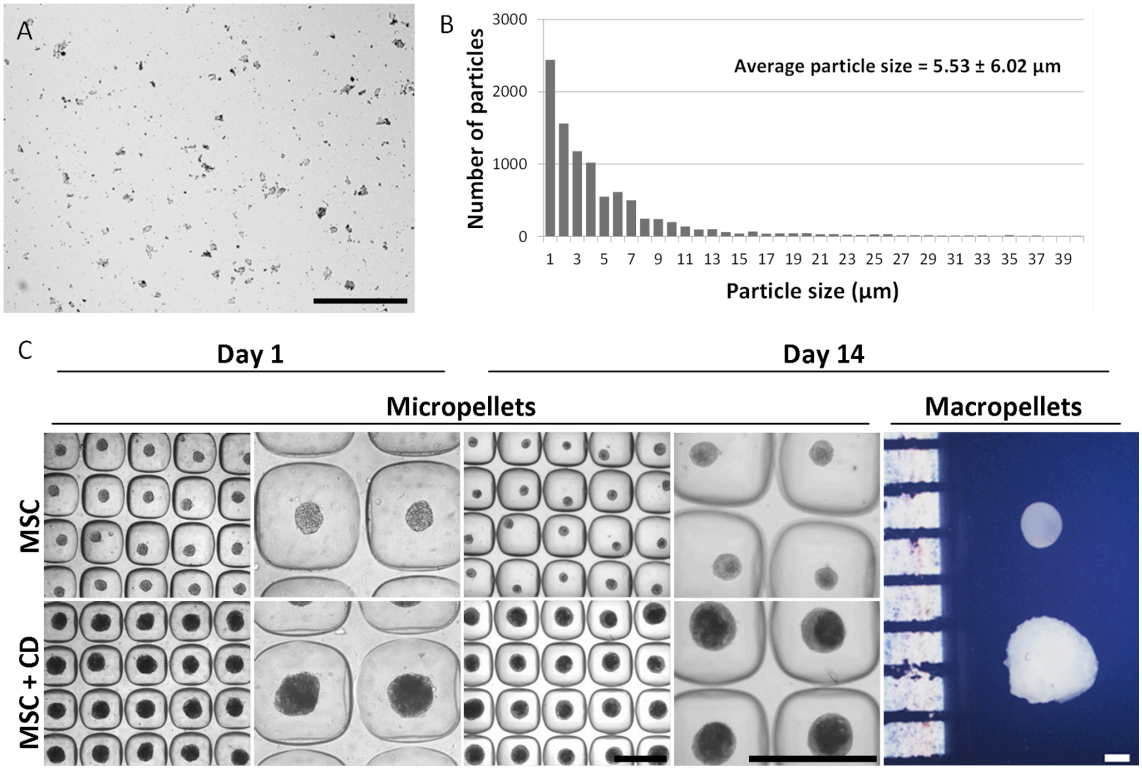

Figure 20. Cartilage dust (CD) characterization and micropellet morphology. Phase contrast image of CD demonstrated a gradient in particles size (A). The particles size distribution indicated that most of the particles had a size smaller than 10 µm and the average particle size was estimated to be 5.53 µm (B). Phase contrast images of MSC and MSC+CD micropellets on day 1 and 14 and macroscopic images of MSC and MSC+CD macropellets (C), the average diameters for MSC micropellets on day 1 was 100.8 ± 7.8 µm and on day 14 was 82.6 ± 10.8 µm, the average diameters for MSC+CD micropellets on day 1 was 176.1 ± 9.9 µm and on day 14 was 183.8 ± 16.2 µm Overall, MSC+CD macro and micropellets were greater in size. Abbreviations: MSC, cell only control; MSC+CD, composite (cell and cartilage dust). Scale bars: 500 µm.

DNA and sGAG production

There was residual DNA retained within CD only control samples (Fig. 21B). At day 14 MSC micropellets had increased total DNA compared to day 0, indicating some cell proliferation. By contrast, there was no increase in DNA content in the MSC+CD macro and micropellets when compared to day 0 (Fig. 21B).

Some DNA is retained possibly in greater size CD particles. In previous work, using human-derived CD, we were able to exclusively generate particles less than 10 µm in size and the human material retained only trace quantities of residual DNA [282]. In this study, the bovine cartilage was less malleable and tended not to be as easily pulverized, resulting in greater retention of DNA. Residual DNA could be removed through DNAse treatment, however additional processing of the CD would have also

depleted sGAG content and chondrogenic cues therefore CD was minimally processed and not decellularized to maximize its biological potential on MSC chondrogenesis.

The quantity of sGAG measured in the media for the CD and MSC+CD macro and micropellets was greater during the early days of the culture (Fig. 21A). The elution profiles from CD macro and micropellet controls indicate that the sGAG content in the medium over the first few days for MSC+CD macro and micropellets largely reflects elution from the CD rather than *de novo* sGAG synthesis by the MSC. Similarly, this time course also indicates that the sGAG elution from CD is completed by the end of the first week of culture (day 8). By contrast, MSC micropellets continuously increased their sGAG secretions over the first and second week of culture. It is clear that the sGAG secretion profile of the micropellets (MSC and MSC+CD) is superior to the macropellets (MSC and MSC+CD) in the second week of culture (Fig. 21A).

Figure 21C outlines the total sGAG content in each of the tissue constructs. The sGAG values represent the actual quantity of sGAG produced by MSC and as well as the sGAG content that originated from CD. The calculations used to estimate these values accounted for the fact that we only performed a 75% volume medium exchange (rather than 100% exchange) every second day. CD macro and micropellets were able to retain the majority of their sGAG within the constructs while both MSC and MSC+CD micropellets eluted approximately twice as much sGAG as they retained (Fig. 21C). Nevertheless, the overall sGAG retained and released to the media was significantly greater in micropellets relative to macropellets (Fig. 21C). The loss of sGAG into bulk media only occurs during the micropellet culture and ceases when the micropellets are assembled (see "Micropellet assembly" section).

The total quantity of sGAG (both in media and in the tissue digest) from each sample was normalized to the total DNA. The greatest sGAG/DNA content was found in the MSC+CD micropellets followed by MSC micropellets (Fig. 21D). The total sGAG content in these constructs was equivalent to the summation of the sGAG in the MSC micropellet plus the CD controls (Fig. 21D). Previously published studies have reported synergistic benefits through the incorporation of donor cartilage matrix [350-352]. In our micropellet system the sGAG production is upregulated by 3-4 fold relative to the macropellet. It is possible that the increase in chondrogenesis resulting from the

micropellet culture and TGFβ supplementation superseded the more subtle changes reported to be induced by the inclusion of donor matrix. Additionally, bovine-derived cartilage matrix was used in this study rather than human-derived cartilage matrix as described previously [282]. In our system, it appears that the increase in MSC+CD tissue volume and sGAG quantity represents the primary contribution of the CD to the cultures.

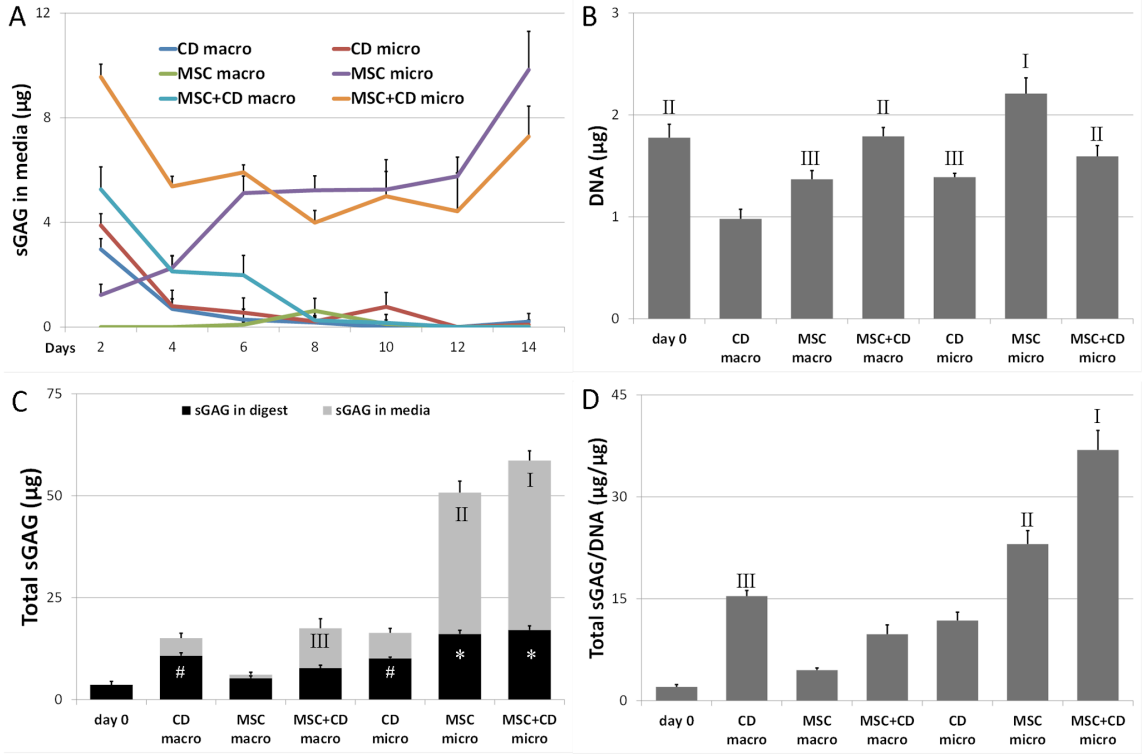

Figure 21. DNA quantification and chondrogenic differentiation. The quantity of sGAG in the media throughout the culture was higher for micropellets in general (A). The quantity of DNA at day 14 was the greatest for MSC micropellets and residual DNA was detected in CD macro and micropellets (B). The overall sGAG quantification in digest and in media demonstrated that the greatest quantity of sGAG was contained and eluted by MSC and MSC+CD micropellets (C). Total sGAG/DNA was calculated by dividing the quantity of the total sGAG (in digest and media) by DNA and this ratio was the greatest for MSC+CD micropellets (D). Abbreviations: CD, cartilage dust only control; MSC, cell only control; MSC+CD, composite (cell and cartilage dust); macro, macropellet; micro, micropellet.

Matrix deposition and distribution

Alcian blue staining demonstrated that all macro and micropellets contained sGAG (Fig. 22). MSC macropellets demonstrated a heterogeneous sGAG distribution where some parts of the pellets were more intensely stained than others, and DAPI staining revealed that the less stained areas had more concentrated nuclei than sGAG

rich areas (Fig. 22). MSC+CD macropellet had less intense staining, reduced number of nuclei and the tissue structure appeared to be less intact (Fig. 22). The staining for MSC and MSC+CD micropellets appeared similar, although it was evident that MSC+CD micropellets had a greater overall diameter.

Collagen II immunolocalizing suggested that CD itself was rich in collagen II, and MSC+CD macro and micropellets stained intensely for collagen II (Fig. 22). The antibody manufacturer indicates that their human anti-collagen II antibody cross-reacts with bovine collagen II and we expected to be able to visualize the contribution of the bovine collagen. MSC macro and micropellets also stained positively for collagen II, however the intensity of the staining was substantially lower than the MSC+CD macro and micropellets indicating that the increase in collagen II content is mainly provided by the CD incorporation rather than *de novo* collagen II biosynthesis. Collagen X staining was relatively weak and similar for all conditions (Fig. 22). The legitimate next step in future studies is the biomechanical characterization of generated tissues in order to measure the additional mechanical strength provided by CD incorporation.

Gene expression

A panel of chondrogenic, hypertrophic and osteogenic (aggrecan, versican, SOX9, RUNX2, collagen II, collagen I, collagen X, osteocalcin) gene expression was assessed for samples on day 0, day 7 and day 14 (Fig. 23). Aggrecan expression was greatest in MSC micropellets on both days 7 and 14 (Fig. 23A). Versican was significantly downregulated in all cultures relative to day 0, and the lowest expression was seen in the MSC+CD macropellets (Fig. 23B). SOX9 was upregulated in MSC macropellets on day 7 (Fig. 23C). RUNX2 was upregulated in MSC+CD macropellet and MSC micropellets on day 7 (Fig. 23D). Collagen II expression was only upregulated in MSC micropellets on both day 7 and 14, being significantly higher on day 14 than on day 7 (Fig. 23E). The low collagen II expression in MSC+CD micropellets also supports that the increase in collagen II content of these tissues (Fig. 22) was mainly provided by the incorporation of CD. Collagen I expression was the lowest in MSC and MSC+CD macropellets (Fig. 23F). The greatest relative collagen I expression was observed in MSC micropellets on day 7 (Fig. 23F). Collagen X expression, similar to collagen II,

was only upregulated in MSC micropellets on both day 7 and 14 (Fig. 23G). Osteocalcin expression was the highest in MSC micropellets on day 7 but was significantly downregulated on day 14 (Fig. 23H).

Overall the chondrogenic gene expression was not elevated in MSC+CD micropellets as much as it was in MSC micropellets confirming the previous results; no chondroinductive effects were observed as a result of CD supplementation (Fig. 23). This observation suggests that chondrogenic factor supplement is superior to CD addition in inducing chondrogenic differentiation.

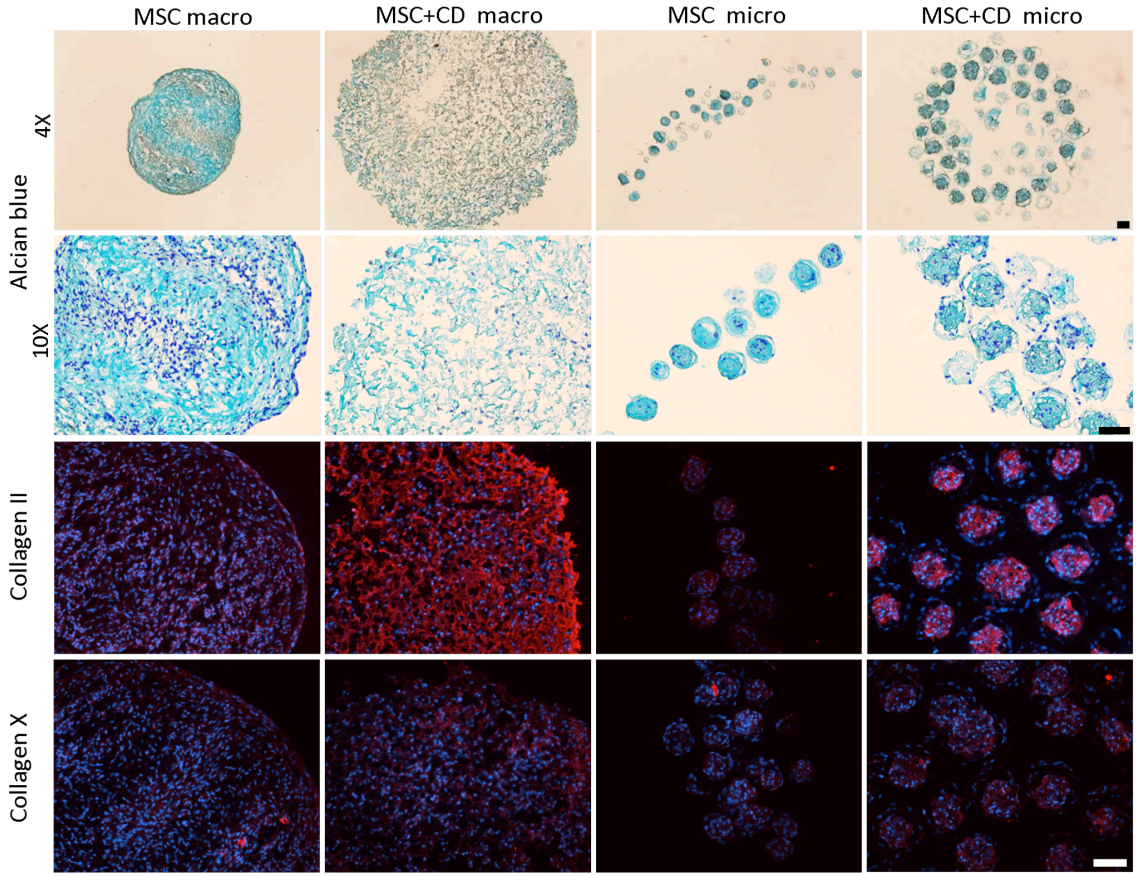

Figure 22. Histological assessment of MSC and MSC+CD macro and micropellets at day 14. The alcian blue staining demonstrated that MSC+CD macropellet was less intact when compared to MSC macropellet. Collagen II staining was stronger in MSC+CD macro and micropellets when compared to MSC macro and micropellets indicating that CD itself contained high quantity of collagen II. Collagen X staining was similar in all conditions. All the images were overlayed with DAPI staining. Abbreviations: MSC, cell only control; MSC+CD, composite (cell and cartilage dust); macro, macropellet; micro, micropellet. Scale bars: 100 μm.

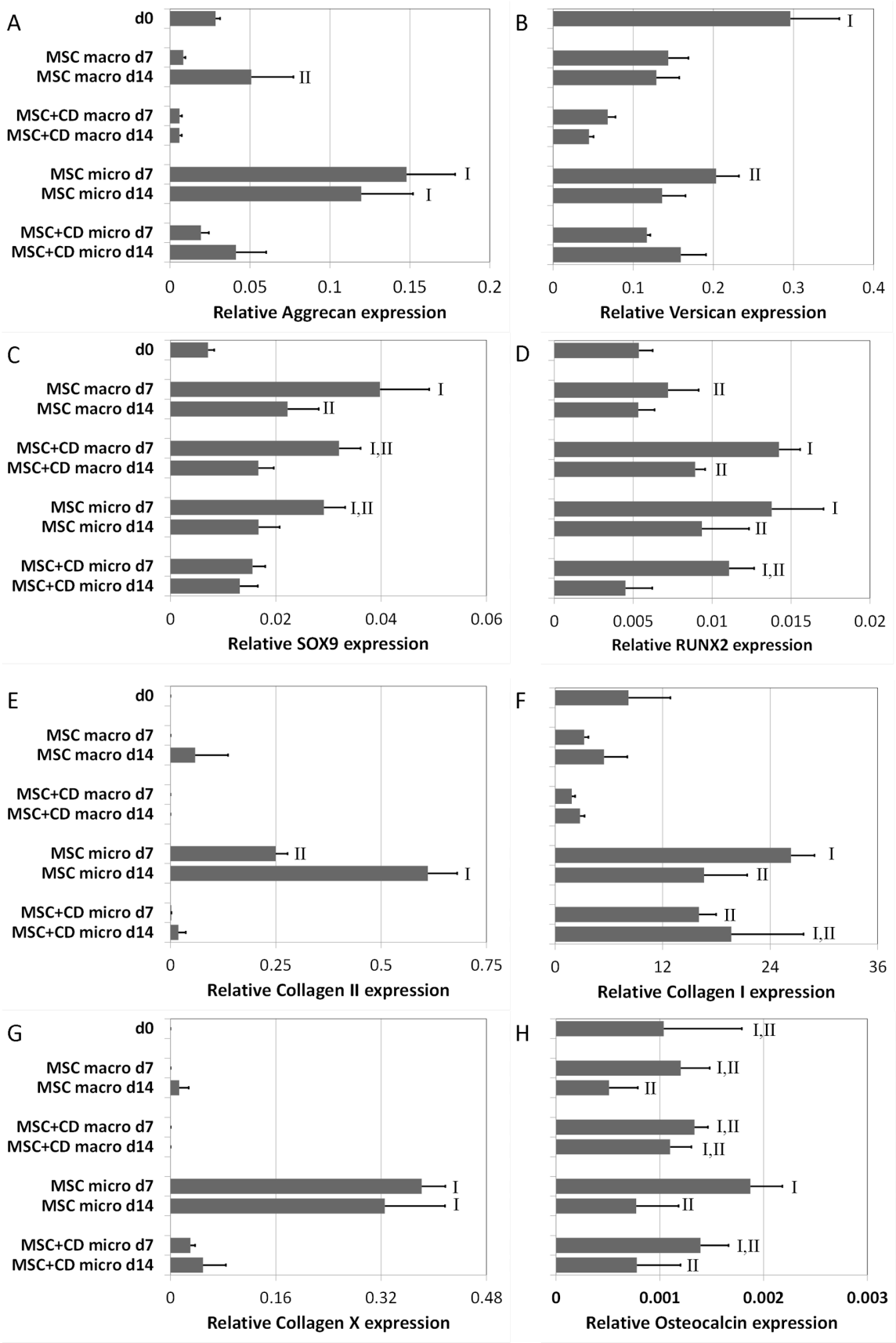
A
d0
MSC macro d7
MSC macro d14
MSC+CD macro d7
MSC+CD macro d14
MSC micro d7
MSC micro d14
MSC+CD micro d7
MSC+CD micro d14
I
II
I
I
0
0.05
0.1
0.15
0.2
Relative Aggrecan expression
B
I
II
0
0.1
0.2
0.3
0.4
Relative Versican expression
C
I
II
I,II
I,II
0
0.02
0.04
0.06
Relative SOX9 expression
D
II
I
II
I
II
I,II
0
0.005
0.01
0.015
0.02
Relative RUNX2 expression
E
II
I
0
0.25
0.5
0.75
Relative Collagen II expression
F
I
II
II
I,II
0
12
24
36
Relative Collagen I expression
G
I
I
0
0.16
0.32
0.48
Relative Collagen X expression
H
I,II
I,II
II
I,II
I,II
I
II
I,II
II
0
0.001
0.002
0.003
Relative Osteocalcin expression

Figure 23. Gene expression analysis of MSC and MSC+CD macro and micropellets at day 7 and 14. Aggrecan (A), Versican (B), SOX9 (C), RUNX2 (D), Collagen II (E), Collagen I (F), Collagen X (G) and Osteocalcin (H) gene expressions were analyzed to assess the chondrogenic, hypertrophic and osteogenic characteristics of the generated macro and micropellets. Abbreviations: MSC, cell only control; MSC+CD, composite (cell and cartilage dust); macro, macropellet; micro, micropellet; d7, day 7; d14, day 14.

Micropellet assembly

Assembly of macropellets is previously utilized in order to engineer macroscopic cartilage tissues [353,354]. Similarly in this study, the relative capacity of micropellets to be assembled into macroscopic tissues was compared at multiple time points in order to help predict the time point that would enable optimal tissue integration in defect repair applications. Specifically, MSC micropellets and MSC+CD micropellets were assembled into macrotissues following 4, 7, 10, or 14 days of culture as discrete micropellets. The assembled macrotissues were then matured in culture until day 22. Alcian blue staining revealed that MSC-only micropellets appeared to be more efficiently integrated into continuous and seamless macrotissues relative to MSC+CD micropellets (Fig. 24). MSC+CD micropellet integration appeared to be more efficient at early time points (Fig. 24). This is consistent with our previously published results, which demonstrated that the more mature a cartilage micropellet was, the less efficient it was at seamlessly integrating with other micropellet into a continuous macrotissue [17].

The collagen II staining confirmed the rich collagen II content of CD and if assembled at early time points, MSC+CD micropellets could form a collagen II rich cartilaginous tissue (Fig. 24). Additionally, DAPI staining showed that few nuclei were observed for the day 0 MSC+CD assembly when compared to later assembly time points (Fig. 24). Therefore, first generating composite MSC+CD micropellets then assembling them into macroscopic constructs can enhance revitalization of CD with MSC.

The macroscopic appearance indicated that MSC+CD assembled tissues were more opaque while the MSC assembled tissues appeared more transparent (Fig 25A). Day 0 assembled MSC tissue was noticeably smaller than the other assembled MSC tissues (Fig 25A). This observation may indicate that MSC micropellets can rapidly increase their size resulting in a greater total tissue volume relative to tissues formed immediately through the pelleting of a single cell suspension.

The quantity of sGAG released into the media was measured before and after the assembly of micropellets. Previously, it has been reported that the retention of sGAG is enhanced when chondrocyte macropellets are assembled into larger constructs [354]. Similarly, we observed that when MSC micropellets were assembled into macroscopic constructs, their sGAG elution slowed after the assembly time point (Fig. 25B). This result is rational, as the surface area to volume ratio, from which the sGAG is eluted, decreases when larger tissues are formed. However elution pattern was different for MSC+CD micropellet assembly where a high quantity of sGAG was released to the media during the first week (Fig. 25C), which suggest that the gradual sGAG loss was mainly originating from CD itself. Nevertheless, the elution of sGAG from both MSC and MSC+CD micropellets appears to be a transient event occurring during the early stage of discrete micropellet culture.

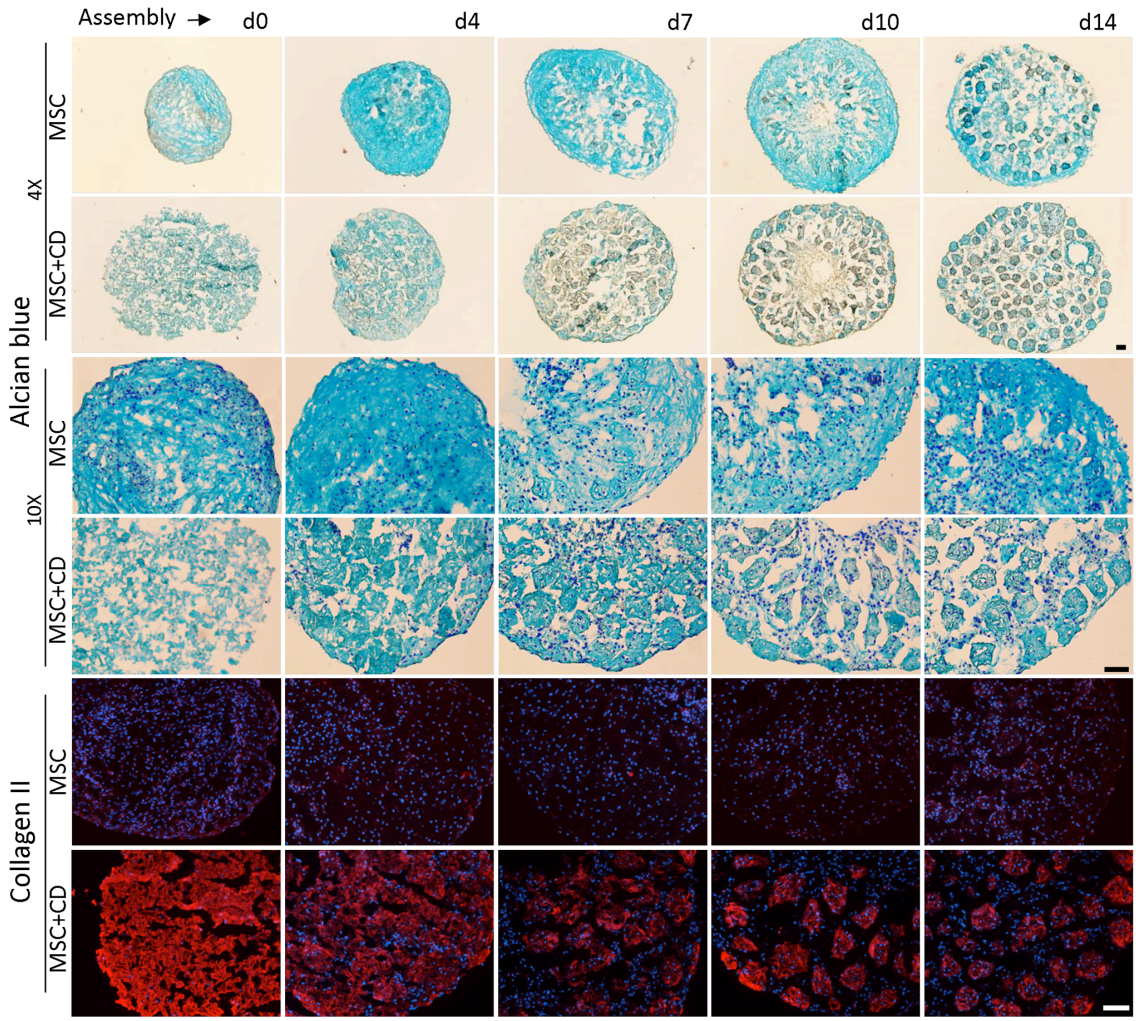

Figure 24. Histological assessment of the assembled tissues. Alcian blue staining showed inefficient integration of the CD particles in day 0 MSC+CD assembly (equivalent to MSC+CD macropellets) and decreasing integration efficiency was observed when the assembly day increased. Collagen II staining confirmed that the quantity of collagen II in MSC+CD assembled tissues was higher than the collagen II in MSC assembled tissues. Abbreviations: MSC, cell only control; MSC+CD, composite (cell and cartilage dust); d0, day 0; d4, day 4; d7, day 7; d10, day 10; d14, day 14. Scale bars: 100 µm.

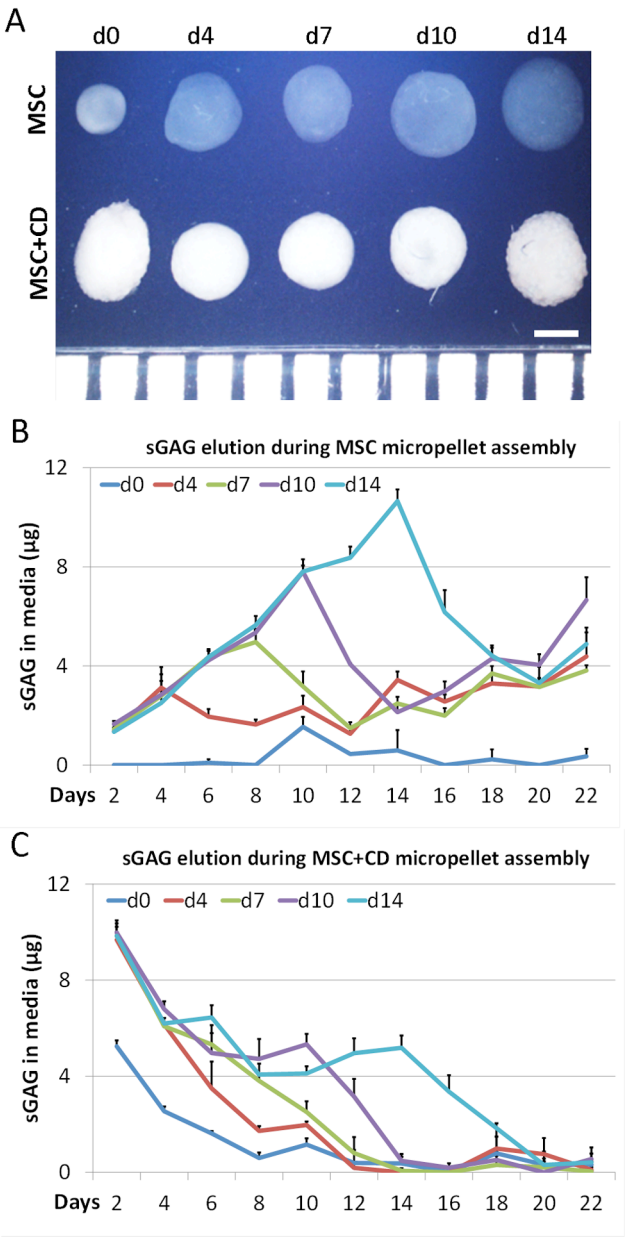

Figure 25. Morphology of the assembled tissue and quantification of the sGAG in media during assembly. MSC assembled tissues looked transparent whereas MSC+CD assembled tissues were more opaque and the day 0 MSC tissue was smaller than the rest of the assembled tissues. (A). The graph of sGAG in media during assembly of the MSC micropellets showed that the sGAG release to the media was diminished after assembly time points (B). The sGAG in media for the MSC+CD assembled tissues showed a decreasing trend in the first week, which is mostly the sGAG originating from CD (C). Abbreviations: MSC, cell only control; MSC+CD, composite (cell and cartilage dust); d0, day 0; d4, day 4; d7, day 7; d10, day 10; d14, day 14. Scale bar: 1 mm.

5. Conclusion

Replicating native cartilage tissue ECM properties in tissue engineered cartilage remains a significant challenge in the field [355]. In approved therapies, such as ACI, chondrocytes are implanted into defects without the benefit of any previously established mature cartilage matrix. A cartilage defect site is a challenging microenvironment for tissue regeneration and expecting the rapid and efficient generation of functional repair tissue may not be rational, and thus successful cartilage defect repair strategies may require the combined use of donor and *de novo* cartilage matrix. Here we have described a novel strategy to incorporate mature donor cartilage matrix into engineered cartilage tissue. By supplying donor cartilage matrix in the form of microscopic cartilage dust (CD) we were able to overcome previously reported limitations in cell penetration and repopulation of larger dimension donor cartilage matrix pieces. To enable the uniform CD distribution in the engineered tissue, we first manufactured composite MSC+CD micropellets. Composite micropellets self-assembled into structures with a core of CD, and a cellular surface that facilitated the bridging of micropellets into macrotissues when they were in contact with each other. The logical next step in future studies is to assess biomechanical features of the generated tissues to further verify the benefits of utilizing CD in cartilage repair. Whilst the addition of CD did not enhance MSC chondrogenic differentiation, this delivery strategy resulted in uniform and rapid loading of donor cartilage matrix particles into MSC micropellets that may offer a mechanism to enhance cartilage defect repair. In a clinical setting, xenogeneic CD can be used as an off-the-shelf product, and the patient's own bone marrow MSC can be harvested and expanded for two weeks, then MSC+CD micropellets can be manufactured within a week. Three weeks after the bone marrow harvest, the prepared micropellets can be injected into the defect site where CD will provide temporary mechanical support and MSC will contribute to *de novo* tissue regeneration. The exploitation of the described micropellet and biomaterial composite strategy may offer a unique template for the addition of other nano/microparticles capable of enhancing chondrogenesis through the release of growth factors or other signal molecules. Such strategies could enable control over cellular organization and the

continued release of induction factors following implantation of the micropellets *in vitro*.

Gene (Amplicon size in basepair)	Primers
Cyclophilin A (164)	Forward CTCGAATAAGTTTGACTTGTGTT
	Reverse CTAGGCATGGGAGGGAACA
GAPDH (119)	Forward ATGGGGAAGGTGAAGGTCG
	Reverse TAAAAGCAGCCCTGGTGACC
SOX9 (77)	Forward TTCCGCGACGTGGACAT
	Reverse TCAAACTCGTTGACATCGAAGGT
Aggrecan (85)	Forward TCGAGGACAGCGAGGCC
	Reverse TCGAGGGTGTAGCGTGTAGAGA
Collagen II, COL2A1 (79)	Forward GGCAATAGCAGGTTCACTGACA
	Reverse CGATAACAGTCTTGCCCCACTT
Collagen I, COL1A1 (83)	Forward CAGCCGCTTCACCTACAGC
	Reverse TTTTGTATTCAATCACTGTCTTGCC
Versican (98)	Forward TGGAATGATGTTCCCTGCAA
	Reverse AAGGTCTTGGCATTTTCTACAAAG
Collagen X, COL10A1 (70)	Forward CAAGGCACCATCTCCAGGAA
	Reverse AAAGGGTATTTGTGGCAGCATATT
Runx2 (113)	Forward GGAGTGGACGAGGCAAGAGTTT
	Reverse AGCTTCTGTCTGTGCCTTCTGG
Osteocalcin (70)	Forward GAAGCCCAGCGGTGCA
	Reverse CACTACCTCGCTGCCCTCC

Table 2. Primers used for gene expression analysis.

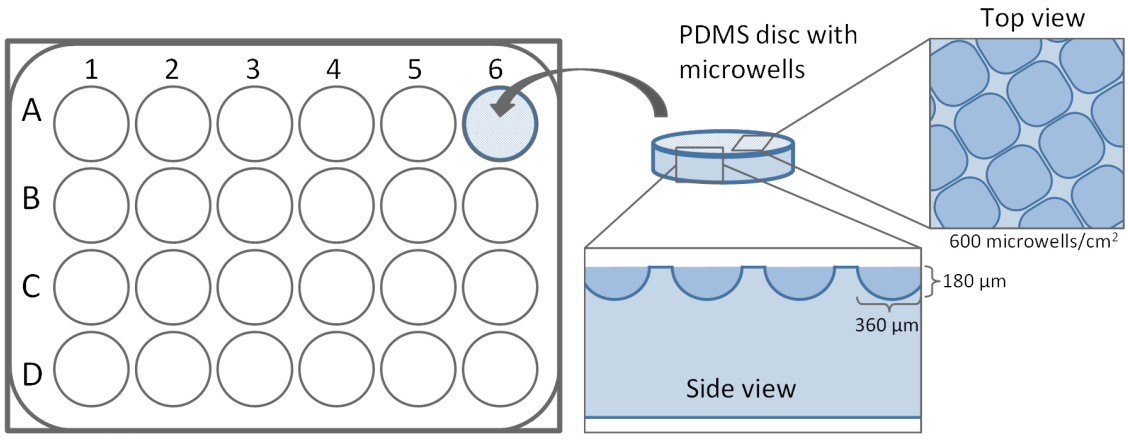

Figure 26. Schematic demonstrating the details of the microwell discs.

CD size distribution (Fig. 20B)

Particle size (μm) - x axis	1	2	3	4	5	6	7	8	9	10
Number of particles - y axis	2442	1561	1178	1021	550	616	501	246	239	197
Particle size (μm) - x axis	11	12	13	14	15	16	17	18	19	20
Number of particles - y axis	139	97	101	61	41	69	39	42	42	44
Particle size (μm) - x axis	21	22	23	24	25	26	27	28	29	30
Number of particles - y axis	31	34	26	21	28	31	18	17	18	13
Particle size (μm) - x axis	31	32	33	34	35	36	37	38	39	40
Number of particles - y axis	13	15	15	10	20	9	13	8	7	10

sGAG in media (Fig. 21A)

Conditions - y axis	sGAG in media Mean					
Days - x axis	CD macro	CD micro	MSC macro	MSC micro	MSC+CD macro	MSC+CD micro
2	2.972776688	3.883592156	0	1.226780719	5.265261938	9.558345375
4	0.692260781	0.799397156	0	2.264625188	2.124713344	5.377400719
6	0.283911187	0.551493844	0.090084656	5.120479687	1.982941875	5.912734219
8	0.17647575	0.215379	0.620349	5.22804675	0.253215	3.99003675
10	0.001620469	0.775510313	0.119172656	5.256480938	0.160095938	4.99909125
12	0	0	0	5.762797219	0	4.425272813
14	0.204325	0.088777	0.018327	9.836309	0	7.283201
	sGAG in media SD					
2	0	0.854370616	0.407338812	0.494253765	0.408157058	0.452246709
4	0	0.608513382	0.451093882	0.382822206	0.71632335	0.278875603
6	0.097730741	0.754601956	0.653538162	0.285388063	0.403931717	0.559003326
8	0.476292951	0.305559777	0.551041477	0.466649088	0.25605942	0.159225068
10	0.154942238	0.320191875	1.141370398	0.947978112	0.003240938	0.547090903
12	0	0	0.732053943	1.465343649	0	0
14	0.036654	0	1.46614287	1.159650656	0.315444511	0.177554

DNA (Fig. 21B)

Conditions - x axis	day 0	CD macro	MSC macro	MSC+CD macro	CD micro	MSC micro	MSC+CD micro
DNA Mean - y axis	1.776973608	0.981319964	1.368836081	1.79034104	1.38973187	2.210923494	1.594000115
DNA SD	0.13290329	0.093223984	0.086063894	0.087508626	0.03777488	0.152798852	0.10530326

Total sGAG (Fig. 21C)

	Total sGAG Mean						
Conditions - x axis	day 0	CD macro	MSC macro	MSC+CD macro	CD micro	MSC micro	MSC+CD micro
sGAG in digest - y axis (black)	3.66803625	10.78598725	5.296019625	7.731108125	10.14415963	16.1244505	17.127134
sGAG in media - y axis (grey)	0	4.331369875	0.847933312	9.786228094	6.243503125	34.6955195	41.54608213
	Total sGAG SD						
	0.830490886	0.722895338	0.539372176	0.73675105	0.317742541	0.912076263	0.992807002
	0	1.211719974	0.582689347	2.341712726	1.104154892	2.788330602	2.398654515

Total sGAG/ DNA (Fig. 21D)

Conditions - x axis	day 0	CD macro	MSC macro	MSC+CD macro	CD micro	MSC micro	MSC+CD micro
Total sGAG/DNA Mean - y axis	2.051542897	15.40735177	4.503288236	9.793679776	11.81423028	23.04989717	36.92345935
Total sGAG/DNA SD	0.338739052	0.83104324	0.333145192	1.372414077	1.2331806	1.99606069	2.870746073

Gene expression (Fig. 23)

Relative gene expression - x axis	Gene expression Mean							
Conditions - y axis	Aggrecan (Fig. 23A)	Versican (Fig. 23B)	Sox 9 (Fig. 23C)	Runx2 (Fig. 23D)	Col I (Fig. 23F)	Col II (Fig. 23E)	Col X (Fig. 23G)	Osteocalcin (Fig. 23H)
MSC+CD micro d14	0.041249167	0.15928649	0.013168423	0.00450951	19.66655951	0.018971088	0.049431972	0.000777859
MSC+CD micro d7	0.019395302	0.117070141	0.015580249	0.011074219	16.05265291	0.002091582	0.030437476	0.001391523
MSC micro d14	0.119628577	0.135985124	0.016742476	0.009356104	16.61536192	0.61077304	0.325578793	0.000772288
MSC micro d7	0.147984306	0.203332614	0.029137531	0.01377469	26.33207606	0.249702151	0.381665587	0.001872898
MSC+CD macro d14	0.005928658	0.044775999	0.016692754	0.00892704	2.780884598	1.52953E-05	0.000122195	0.001098905
MSC+CD macro d7	0.005962409	0.068159876	0.032001645	0.014240243	1.854222295	1.65041E-05	0.000236096	0.00133397
MSC macro d14	0.050808842	0.128836997	0.022237641	0.005328402	5.454949455	0.058810946	0.013399238	0.000510641
MSC macro d7	0.008345466	0.14363354	0.039774719	0.007207111	3.24478076	0.000154071	0.000186668	0.001201627
d0	0.028472483	0.296021537	0.007151873	0.005362364	8.191271934	2.66049E-06	4.84755E-06	0.001037553
	Gene expression SD							
MSC+CD micro d14	0.01893115	0.031584641	0.003418478	0.00169978	8.061006451	0.017428758	0.034844207	0.000421305
MSC+CD micro d7	0.004931078	0.004167333	0.002424744	0.001584744	1.917623165	0.000205975	0.007043007	0.000270851
MSC micro d14	0.032391112	0.029240949	0.003994321	0.002984179	4.821128418	0.069743272	0.091456497	0.000408488
MSC micro d7	0.030407047	0.028560114	0.004028969	0.003286186	2.616840634	0.028348308	0.0359078	0.000308233
MSC+CD macro d14	0.001443255	0.005731784	0.002933673	0.000630861	0.49530209	7.06622E-06	6.44366E-05	0.000205159
MSC+CD macro d7	0.001536055	0.009671057	0.004106253	0.001337315	0.381987334	1.15132E-06	0.00017071	0.000129575
MSC macro d14	0.026408797	0.028656881	0.005923434	0.001029282	2.60054007	0.078083635	0.014394629	0.000276827
MSC macro d7	0.00134004	0.025235375	0.009365887	0.001943515	0.46696334	0.00012397	0.000100374	0.000279366
d0	0.002844536	0.061189478	0.00115335	0.000875945	4.676250324	2.95025E-06	7.16061E-06	0.000752905

Table 3. Data used to generate Figures 20, 21, 23.

sGAG elution during MSC micropellet assembly (Fig. 25B)

sGAG elution - y axis		sGAG elution Mean										
Days - x axis		2	4	6	8	10	12	14	16	18	20	22
Assembly time points	d0	0.004468	0	0.09467	0.003169	1.545339	0.450282	0.592758	0	0.232364	0	0.353014
	d4	1.368675	3.122325	1.955823	1.638867	2.344224	1.266054	3.435384	2.562456	3.293793	3.172986	4.383654
	d7	1.450512	2.798874	4.356375	4.968204	3.174285	1.490781	2.484516	1.99869	3.699081	3.153501	3.815991
	d10	1.655754	2.841741	4.229073	5.35011	7.803921	4.069296	2.135085	2.978136	4.299219	4.044615	6.660801
	d14	1.343994	2.510496	4.365468	5.650179	7.810416	8.368986	10.655226	6.171078	4.417428	3.315876	4.885068
		sGAG elution SD										
	d0	0.0077388	0	0.1427927	0.00548887	0.39860678	0.0390349	0.82193299	0	0.40246625	0	0.30772435
	d4	0.14299034	0.54293383	0.30793698	0.19902698	0.45650379	0.23704526	0.33673177	0.28669669	0.35224943	0.33761008	0.9719793
	d7	0.19814754	0.59623251	0.27426132	0.4662252	0.60343549	0.24325314	0.27129204	0.30052415	0.29551322	0.1384578	0.21238948
	d10	0.019485	1.11447614	0.37887846	0.15173299	0.24960075	0.0250542	0.35398405	0.40046929	0.52656147	0.42867	0.9167922
	d14	0.43672488	0.3158574	0.31499076	0.36885882	0.49708268	0.44525392	0.46902355	0.89104488	0.31616977	0.65138212	0.66233334

sGAG elution during MSC+CD micropellet assembly (Fig. 25C)

sGAG elution - y axis		sGAG elution Mean										
Days - x axis		2	4	6	8	10	12	14	16	18	20	22
Assembly time points	d0	5.243592	2.54427	1.62198	0.598368	1.156938	0.39531	0.372499	0.016159	0.793375	0.316799	0.316642
	d4	9.680976	6.15549	3.491241	1.7259	1.974009	0.185443	0	0	0.990823	0.7609	0.103763
	d7	9.848547	6.081447	5.325429	3.810795	2.513094	0.804338	0.06869	0	0.310304	0.212308	0.038085
	d10	9.97455	6.793299	4.964307	4.722693	5.330625	3.157398	0.477561	0.194693	0.516531	0	0.5568
	d14	9.842052	6.19446	6.446466	4.070595	4.11606	4.96041	5.183838	3.356145	1.840212	0.307549	0.415937
		sGAG elution SD										
	d0	0.24752342	0.19237922	0.09682562	0.23046178	0.26280924	0.53566618	0.39278156	0.02798821	0.6966341	0.54871196	0.14251641
	d4	0.68002743	0.27238144	1.11852047	0.20049677	0.14267136	0.21977757	0	0	0.8580978	0.67065468	0.10827582
	d7	0.14277777	0.14420655	0.8009765	0.25339491	0.44060234	0.66555579	0.10435064	0	0.38292403	0.36772824	0.00811225
	d10	0.51248637	0.32357618	0.82927391	0.83168773	0.42776565	0.73141544	0.17236609	0.18045381	0.33799221	0	0.48316514
	d14	0.38310371	0.01190553	0.50524922	0.45287991	0.29722982	0.61745011	0.51063094	0.68627413	0.20703061	0.14872859	0.36765448

Table 4. Data used to generate Figure 25.

Chapter 5: Statement of Contribution of Co-Authors for Thesis by Published Paper

In the case of this chapter

Title: **High throughput bone and cartilage micropellet manufacture, followed by assembly of micropellets into a biphasic osteochondral tissue**

Date, status, journal: January 2015, Submitted, Cell and Tissue Research

Contributor	Statement of contribution
Betul Kul Babur Signature Date 20.01.2015	wrote the manuscript (M), experimental design (D), conducted experiments (E), and data analysis (A)
Kathryn Futrega	aided with E,A
William B. Lott	aided with M, A
Travis Klein	aided with M, D, A
Justin Cooper-White	aided with D, A
Michael Robert Doran	aided with M, D, A and materials

Principal Supervisor Confirmation

I have sighted email or other correspondence from all Co-authors confirming their certifying authorship.

Michael Robert Doran		20.01.2015
Name	Signature	Date

"An expert is a person who has made all the mistakes that can be made in a very narrow field."
Niels Bohr

Chapter 5: High throughput bone and cartilage micropellet manufacture, followed by assembly of micropellets into a biphasic osteochondral tissue

1. Abstract

Engineered biphasic osteochondral tissues may have utility in cartilage defect repair. As bone marrow-derived mesenchymal stem/stromal cells (MSC) have the capacity to make both bone-like and cartilage-like tissues, they are an ideal cell population for use in the manufacture of osteochondral tissues. Effective differentiation of MSC to bone-like and cartilage-like tissues requires two unique medium formulations, and this presents a challenge in both in achieving initial MSC differentiation and in maintaining tissue stability when the unified osteochondral tissue is subsequently cultured in a single medium formulation. In this proof-of-principle study we used an in-house fabricated microwell platform to manufacture thousands of micropellets formed from 166 MSC each. We then characterized the development of bone-like and cartilage-like tissue formation in the micropellets maintained for 8 to 14-days in sequential combinations of osteogenic or chondrogenic induction medium. Our data indicate that bone-like and cartilage-like micropellets induced for only 8-days displayed significant phenotypic changes when the osteogenic or chondrogenic induction medium, respectively, was swapped. Based on these data we developed an extended 14-day protocol for the pre-culture of bone-like and cartilage-like micropellets in their respective induction medium. A unified osteochondral tissue was then formed by layering 12,000 osteogenic micropellets and 12,000 chondrogenic micropellets into a

biphasic structure and cultured in chondrogenic induction medium. The assembled tissue was cultured for a further 8-days and then characterized via histology. The micropellets had amalgamated into a continuous structure with distinctive bone-like and cartilage-like regions. This proof-of-concept study demonstrates the feasibility of micropellet assembly for the formation of osteochondral-like tissues that may have utility in osteochondral defect repair.

2. Introduction

Articular cartilage has limited intrinsic regeneration capacity. The degeneration of articular cartilage leads to osteoarthritis (OA), which is the most common form of joint disease and one of the leading causes of disability worldwide [2,337-339]. The capacity to effectively repair acute cartilage defects could delay or prevent the development of OA for many patients. A number of acute cartilage defect repair strategies have been proposed and these range from filling of the defect with cells, with natural/synthetic hydrogels/scaffolds, or combinations of both [93,101,110]. There are a number of challenges associated with any cartilage defect repair, and perhaps most significant is the effective integration of the repair tissue with the adjacent native tissue [356,357]. Because chondrocytes are low in number and have a limited capacity to migrate through cartilage matrix at wound edges, the borders surrounding the repair tissue may not be iteratively remodeled and effectively integrated into the adjacent repair tissue. Additionally, the underlying bone often incurs simultaneous damage during the initial injury, and building new tissue on this damaged foundation can be problematic [358]. In procedures such as mosaicplasty, the underlying bone and associated cartilage is harvested from a donor location and transplanted into a critical defect site [83]. The inclusion of the bone layer is essential as it facilitates tissue integration and provides a foundation for the donor cartilage tissue [90]. Whilst the bone layer rapidly and iteratively remodels, the integration of the cartilage layer can be delayed or even remain incomplete. A ring of dead tissue can often be observed around the perimeter of a mosaicplasty tissue plug [90]. Nevertheless, the inclusion of the bone layer does enhance integration and the probability of a successful repair. A fundamental drawback in mosaicplasty is the limited supply of autologous donor tissue available for

harvest and the associated damage at the donor site. These limitations are driving the development of tissue engineering solutions that will enable the manufacture of either synthetic or biosynthetic osteochondral tissues.

Approaches trialed in the manufacture of artificial osteochondral tissues include the use of bilayer scaffolds, separate scaffolds for bony and chondral layers, scaffold for bony layer scaffold-free for chondral layer, and single homogenous or heterogeneous scaffolds [359]. There are also cell-free studies that utilize scaffolds to fill the defect site, with the anticipation that biological "cues" incorporated into the scaffold will direct host cells to repopulate the scaffold in a useful and organized manner [360-362]. This cell-free approach is likely not suitable for large chondral defects for reasons similar to the failure of mosaicplasty plugs to integrate; because chondrocytes have limited capacity to migrate from the dense matrix in the adjacent native tissue, the probability that cells would be able to populate a large scaffold is remote. For this reason, cell-free studies are often coupled with microfracture technique, which stimulates bleeding and recruits cells from within the underlying bone marrow [109,363,364]. Additionally, most scaffold approaches aim to use the scaffolds as a temporary extracellular matrix (ECM) support and assume that the scaffold biodegradation will be synchronized with the *de novo* tissue formation. This synchronization is technically challenging when the scaffold has multiple phases or components. Other studies have explored repairing full-thickness osteochondral defects with scaffold-free approaches. However, in such cases the repair tissue only includes a cartilage phase [365,366], and the *de novo* tissue relies on the existing bone to function as both the tissue foundation and interface.

Bone marrow-derived mesenchymal stem/stromal cells (MSC) are frequently utilized in osteochondral defect studies [367-370], because it is assumed that these cells have the potential to differentiate into either chondrocyte or osteoblast-like cells. The chondrogenic or osteogenic phenotype derived from MSC populations is very sensitive to the medium formulation, and chondrogenic or osteogenic medium traditionally has different formulations [371]. Constructing a continuous osteochondral tissue *in vitro* presents a very real challenge as it obligates the culture of both tissue types in a single medium cocktail. Some groups have attempted to overcome this challenge by culturing composite tissues in custom-made double chamber bioreactors that aim to physically

isolate each tissue type in their unique medium formulations [372,373]. We reason that a more rational approach might be to manufacture MSC micropellets, and induce chondrogenic or osteogenic differentiation in discrete culture systems, and then assemble the partially mature micropellet into a biphasic tissue in a common culture. Based on this rationale, we described the method for high throughput manufacture of discrete bone-like and cartilage-like micropellets with the subsequent assembly of the micropellets into a biphasic osteochondral-like tissue.

Bone-like and cartilage-like micropellets were manufactured using a modified microwell platform previously described by our group [18,19]. Using this modified method, we systematically characterized the phenotypic change of bone marrow-derived MSC micropellets exposed sequentially to osteogenic and/or chondrogenic medium. Following characterization and optimization of this process, we assembled bone-like and cartilage-like micropellets into an osteochondral tissue and cultured this construct in a single medium formulation.

3. Materials and Methods

Experimental design

This study has two parts. In the first part, the phenotypic characteristics of micropellets formed from human bone marrow-derived MSC cultured for 14 days under four different sequential medium conditions were characterized. The medium conditions are described in Table 5, and defined using the following abbreviations: CC (chondrogenic media for 14 days), CO (chondrogenic media for first 8 days and osteogenic media for last 6 days), OC (osteogenic media for first 8 days and chondrogenic media for last 6 days), OO (osteogenic media for 14 days). After 14 day exposure to osteogenic and/or chondrogenic media, micropellets were assessed for DNA, chondrogenic and osteogenic differentiation, histological features and gene expression. In the second part of the study, chondrogenic and osteogenic micropellets were assembled at different time points to form a continuous biphasic osteochondral-like tissue as depicted in Figure 30. The biphasic tissue was assessed for cartilage and bone histological features.

Abbreviation	Medium-first 8 days	Medium-last 6 days
CC	Chondrogenic	Chondrogenic
CO	Chondrogenic	Osteogenic
OC	Osteogenic	Chondrogenic
OO	Osteogenic	Osteogenic

Table 5. The abbreviations used in the study. According to the media type, and culture duration, each condition is stated with two letters. The first letter "C" or "O" indicates the culture medium formulation over the first 8 days of culture, and the second letter "C" or "O" indicates the culture medium formulation over the subsequent 6 days of culture. The media types were swapped at day 8 but not 7 because the media was changed every second day throughout the culture.

Microwell fabrication and surface modification

We used an in-house fabricated microwell surface to efficiently manufacture micropellets [17]. In brief, a polystyrene microwell mold having an array of microwells (each with dimensions of 360x360x180 μm, and 600 microwells per cm^2) was used to generate sheets of polydimethylsiloxane (PDMS, Slygard) with microwells. The process of fabricating the mold is described in detail here [17]. Discs (2 cm^2 or 10 cm^2) were punched from the sheets of PDMS and used to make multiwell inserts with 1200 and 6000 microwells, respectively. The PDMS discs were glued (Silicone Glue) into 24-well plates and 6-well plates (Nunc), respectively. The plates with the microwell inserts were sterilized in 70% ethanol for 1 hour and then rinsed with sterile phosphate-buffered saline (PBS, Invitrogen). To prevent cell attachment, the surface was treated with surfactant, 5% pluronic F-127 (Sigma) solution, for 5 minutes then rinsed with sterile PBS once before the cells were seeded.

Human bone marrow MSC isolation and expansion

Ethics: Bone marrow aspirates were obtained from the iliac crest of volunteer donors with written consent. This documentation is held by the ethics committee and all tissue samples were provided to the research team in a de-identified manner. Mater Health Services approved this consent procedure. Ethical approval for these studies was granted by the Mater Health Services Human Research Ethics Committee (Ethics number: 1541A) and the Queensland University of Technology Human Research Ethics

Committee in accordance with the Australian *National Statement on Ethical Conduct in Human Research*.

The bone marrow aspirates were processed as described previously [18]. Aspirates (~20 mL) were diluted 1:1 using sterile PBS, and 12 mL Ficoll Paque Plus (GE Healthcare) was underlayed beneath the diluted aspirates. The Ficoll and bone marrow mixture was centrifuged at 535xg for 20 minutes. The cells accumulated at the interface of the Ficoll and bone marrow were aspirated carefully and washed with sterile PBS. The cells were resuspended in low glucose Dulbecco's modified Eagle's medium (LG DMEM, Invitrogen) with 100 U/mL penicillin and 100 μg/mL streptomycin (PS, Invitrogen) and 10% fetal bovine serum (FBS, Invitrogen) and seeded in T175 flasks (Nunc) and incubated for 48 hours before removing the non-adherent cells. The plastic adherent cells (MSC) were cultured until confluent with media changes every 3-4 days and passaged with 1:4 ratio three times (until passage 3), and then used in micropellet studies. MSC were expanded at 37°C in a hypoxic incubator (2% O_2 and 5% CO_2 atmosphere) as this has been previously demonstrated to enhance proliferation and differentiation capacity [143,374]. Passage 2 expanded cells were characterized for their expression of CD marker profiles associated with MSC [375]. Specifically, we confirmed that the cell populations used were CD90, CD73, CD105, CD44 and CD146 positive, and CD45, CD34, and HLA-DR negative. Antibodies were purchased from Miltenyi Biotech and used as per the manufacturers instructions. Stained cells were analyzed on a BD LSR-II flow cytometer.

Micropellet formation

Micropellets were formed in the multi-well plates containing microwell inserts. In the first part of the study 24-well plates containing 2 cm^2 microwell inserts each containing 1200 microwells were used. For each sample, 1 mL medium containing $2x10^5$ human MSC was dispensed to each well (166 cells/microwell) and settled for micropellet formation inside the incubator. In the second part of the study 6-well plates containing 10 cm^2 microwell inserts each containing 6000 microwells were used. For each well 5 mL medium containing 1 million human MSC was dispensed to each well

(166 cells/microwell) and then transferred into the incubator. Micropellet formation was confirmed via microscopy the following day.

Chondrogenic and osteogenic differentiation

Chondrogenic media contained high glucose (HG) DMEM with 110 μg/mL sodium pyruvate (Invitrogen), PS, 10^{-7} M dexamethasone (Sigma), 200 μM ascorbic acid 2-phosphate (Sigma), 40 μg/mL L-proline (Sigma), 1% insulin-transferrin-selenium-ethanolamine (ITS-X, Invitrogen) and 10 ng/mL recombinant human Transforming Growth Factor β1 (TGF β1, Peprotech). Cultures containing chondrogenic media were incubated in a 2% O_2 5% CO_2 atmosphere at 37°C.

Osteogenic media contained HG DMEM (Invitrogen), PS, 10% FBS, 10^{-7} M dexamethasone, 50 μM ascorbic acid 2-phosphate, 10 mM β-glycerol phosphate (Sigma). Cultures containing osteogenic media were incubated in a 20% O_2 5% CO_2 atmosphere at 37°C.

In the first part of the study, the media was exchanged 75% every second day for 14 days except at day 8. At day 8, the media was exchanged 100% in all samples. This is because at day 8 the media type was switched (i.e. osteogenic to chondrogenic) and cultures were placed into different incubators at different oxygen concentrations appropriate for the medium type and corresponding differentiation process.

Biphasic tissue assembly

In the second part of the study, the MSC micropellets were differentiated in chondrogenic and osteogenic media separately, and then assembled at different time points to form a continuous osteochondral-like tissue. The chondrogenic media was exchanged 75% every second day until day 8, and the chondrogenic micropellets were assembled to form a macroscopic chondrogenic tissue on day 8. Similarly, the osteogenic media was exchanged 75% every second day until day 14, and then the osteogenic micropellets were assembled on top of the macroscopic chondrogenic tissue to form a biphasic tissue. The assembly of micropellets into larger tissues was achieved using customized PDMS funnel and layering cylinder shown schematically in Figure 30. This device was formed using the tip of a 10 mL syringe (Terumo) inside a 6-well plate

as a mold to cast PDMS around. The tip of the syringe was cut and glued to the middle of the well and the outer space left between the syringe and the well was filled with PDMS and cured (Fig. 33) then the extra PDMS around the edges of the mold was removed to accommodate more medium in the same well. The mold was sterilized in 70% ethanol for 1 hour, and then rinsed repeatedly with sterile PBS prior to use in biphasic tissue formation. On day 8, chondrogenic micropellets (12,000) were concentrated in 2 mL media then transferred into the funnel mold in two steps (1 mL each time, followed by 300xg centrifugation for 2 minutes and removal of excess media). The accumulation of micropellets at the bottom of the funnel mold was visually confirmed and the remaining portion of the well was then filled with 5mL chondrogenic media. Following the first assembly step, the assembled tissue was cultured in a 20% O_2 5% CO_2 atmosphere at 37°C with 75% of the medium volume exchanged daily. On day 14 osteogenic micropellets (12,000) were transferred into the funnel mold using the above approach in order to generate a layer of bone tissue. Following the addition of osteogenic micropellets, the amalgamating tissue was cultured in chondrogenic media for 2 more days in the funnel mold, and then gently relocated into a 6-well plate. This 6 well plate was coated with PDMS and treated with 5% pluronic F-127 to prevent cell attachment to the underlying tissue culture treated polystyrene, but otherwise had a standard geometry. The biphasic tissue was cultured for a further 6 days in chondrogenic media and then characterized via histology.

Chondrogenic and osteogenic analyses

Each sample for the first part of the study consisted of $2x10^5$ cells (initially) in the form of 1200 micropellets. DNA, sGAG, calcium, alkaline phosphatase activity and gene expression quantifications were performed on ~1200 micropellets to obtain a single measurement. sGAG quantification in media was performed on 0.75 mL media collected after each media change on every second day.

For DNA quantification the micropellets were digested in 0.25 mg/mL papain (Sigma) solution at 60°C overnight. DNA was quantified using PicoGreen dsDNA Reagent and Kit (Invitrogen) according to the manufacturer's protocol. The signal was

measured using a fluorescent plate reader (BMG Labtech) with the excitation of 480 nm and emission of 520 nm.

The quantity of sulfated glycosaminoglycan (sGAG) in the micropellets was measured from the papain digests and sGAG in media was measured from the media collected during culture. The media or digest was mixed with 1,9 Dimethyl methylene blue zinc chloride double salt (DMB, Sigma) and the color change was measured using a plate reader (Thermo Fischer) at 590 nm. Shark chondroitin sulfate (Sigma) was used to generate a standard curve.

Calcium quantification of the micropellets was achieved by incubating the tissues overnight in a tube shaker (Eppendorf) at 900 rpm in 10% acetic acid (RCI Labscan) at room temperature. A 1 mg/mL o-Cresolphthalein Complexone (OCPC, Sigma) solution was combined with 14.8 M ethanolamine-boric acid buffer (pH 11, Sigma) and 8-hydroxyquinoline (50 mg/mL in 95% ethanol, Merck) in following ratios 5:5:2, then diluted 10X with ddH2O. The samples were mixed with OCPC solution, incubated at room temperature for 10 minutes and measured using a plate reader at 575 nm. A standard curve was generated using serial dilutions of pure $CaCl_2$ (Sigma).

Alkaline phosphatase activity was quantified in the micropellets by first lysing them in a 0.1% Triton X-100 (Sigma) Tris buffer solution (pH 10.1, Sigma) contained in a tube placed in a shaker at 900 rpm for 1 hour at room temperature. The recovered lysate was mixed with substrate solution (1 mg/mL P-Nitrophenyl phosphate disodium salt, Sigma) and incubated at room temperature for 30 minutes in the dark. The absorption of the incubated solution was measured in a plate reader at 405 nm.

Gene expression analyses

RNA was extracted from micropellets using Trizol (Invitrogen) as per the manufacturer's suggested protocol. The isolated RNA was quantified with Nanodrop 1000 (Thermo Scientific). Reverse transcription was performed with SuperScript III RT and oligo(dT)20 kit (Invitrogen) as per the manufacturer's protocol to obtain complementary DNA (cDNA). Platinum SYBR Green qPCR SuperMix-UDG kit (Invitrogen) was used to perform quantitative polymerase chain reaction (qPCR). The primer sequences (5' to 3', Geneworks) in Table 6 were used to perform the qPCR.

SYBR Green master mix and cDNA were combined in a 384-well plate (Applied Biosystems) using liquid handler (epMotion M 5073, Eppendorf). The qPCR reaction was initiated with 2 minutes hold at 50°C, continued with 3 minutes hold at 95°C, then continued with 40 cycles of 95°C for 15 seconds, and 60°C for 30 seconds. This reaction was completed in a ViiA real time PCR machine (Applied Biosystems). The gene expression was quantified using ΔCt method and the relative gene expression was calculated by normalizing the gene expression with the geometric mean of two housekeeping genes (Cyclophillin A and GAPDH).

Histological analyses

The micropellets and the biphasic tissues analyzed via histology were first fixed in 4% paraformaldehyde (PFA, Sigma) for 30 minutes to preserve the tissue structure, then embedded in optimum cutting temperature compound (OCT, Tissue-Tek) then frozen at -20°C prior to sectioning. Using a cryostat (Leica) at -25°C, 10 µm thick sections were cut. The sections were captured on poly-lysine slides (Thermo Fischer), dried at room temperature, and then stored at -20°C. For staining, the sections were brought to room temperature and to prevent detachment, the sections were fixed second time onto glass slides with 4% PFA for 20 minutes then rinsed with PBS.

Alcian blue staining was performed to identify the presence of sGAG in the tissues. Sections were covered and incubated for 10 minutes with 1% alcian blue (Sigma) solution in 3% acetic acid (pH 2.5). Then the sections were rinsed with PBS and counterstained with 4',6 diamidino-2-phenylindole (DAPI, Sigma) for 5 minutes, rinsed with PBS and mounted (CC/mount, Sigma) for imaging.

Alizarin red staining was performed to assess osteogenic matrix deposition. The sections were rinsed with ddH_2O then dried at 37°C for 10 minutes. Slides were incubated with Alizarin Red S stain (Sigma) for 10 minutes then washed with PBS, and counterstained with DAPI for 5 minutes. Sections were washed with PBS and then mounted for imaging.

For immunofluorescence (IF) analyses, borders were drawn around the sections with a PAP pen (Sigma). A solution of 3% goat serum (Invitrogen), 0.3% Triton X-100 in 1% bovine serum albumin (BSA, Sigma) was used to block sections for 20 minutes.

The sections were incubated in primary antibody dilutions for human Collagen type I, II and X (raised in mouse, rabbit, rabbit respectively, Abcam) overnight at 4°C in a humidified environment. Negative controls for collagen type I, II and X were treated the same except their solution did not contain any primary antibody. Next day, the primary antibody solution was washed with 0.3% Triton X-100 for 3 minutes twice then rinsed with PBS once. Then, the corresponding secondary antibody solutions (Cy-3 conjugated anti rabbit IgG, FITC conjugated anti mouse IgG2b, Abcam) were added on sections and incubated for 30 minutes at room temperature, washed with 0.3% Triton X-100 for 3 minutes twice counterstained with DAPI for 5 minutes, then rinsed with PBS. The sections were then mounted for imaging.

OsteoImage mineralization assay (Lonza) was used as per the manufacturer's protocol to specifically stain the inorganic hydroxyapatite component of bone matrix. For the biphasic tissues, the sections were stained and imaged. For micropellet tissues the whole micropellets were stained and imaged via confocal microscope. All samples were counterstained with DAPI.

Microscopy

The imaging of sections was performed using an ECLIPSE Ti epifluorescent microscope (Nikon, Japan) and assessed with NIS Elements BR 3.2 software. The micropellet images and fluorescent histology images were taken with a Nikon DS-Qi1Mc camera whereas the color images (alcian blue and alizarin red staining) were taken by Nikon DS-Fi1 camera. The 3D images of whole micropellets stained with OsteoImage were acquired using a confocal microscope (ZEISS, Germany).

Statistical analyses

The experiments were repeated with 3 different MSC donor populations, some differences in differentiation efficiency were observed for different donors however the relations between different experimental groups were reproducible therefore a representative data set is presented. In each experiment, each condition had $n = 4$ biological replicates. Data were represented in graphs as mean + standard deviation (SD). The significance analyses were performed using SPSS Statistics 21 (IBM, USA),

one-way analysis of variance (ANOVA) with Tukey's post-hoc tests. For multiple comparisons, a p-value smaller than 0.05 was represented as significantly different. The significance was indicated with Roman numerals, the groups indicated with same numerals were statistically similar whereas the groups indicated with different numerals were statistically different.

4. Results and Discussion

Flow cytometry characterization of MSC

MSC from four different de-identified bone marrow donations were utilized in this study. Donations were received from a 55 year old male, a 20 year old male, and a 23 year old female. Two donations from the same 55 year old donor were collected at different times. The CD marker expression for donor MSC at Passage 2 are displayed in Figure 32. All MSC cultures contained <5% populations positive for either CD45, CD34 or HLA-DR. All MSC cultures contained >95% populations positive for CD90, CD73, CD105, CD44 and CD146.

Chondrogenic and osteogenic features of micropellets

The size of the CC and OO micropellets were noticeably different following 14 days of culture (Fig. 27A). OO micropellets were smaller and had opaque cores, whereas CC micropellets were greater in size. When compared to OO, OC micropellets had relatively greater size and less opaque cores (Fig. 27A). DNA quantification revealed that all cultures had less DNA than the day 0 samples. However, the cultures initiated with osteogenic media, OC and OO, had significantly less DNA than the cultures initiated with chondrogenic media, CC and CO (Fig. 27B). DNA content is not the only factor affecting the micropellet size; the accumulation of matrix can also vary size of the micropellets. In this case however both the micropellet size and DNA content are lower in OC and OO micropellets, which may suggest that greater cell death occurred in those micropellets.

The quantity of sGAG in the micropellets and the culture medium was measured, as this is a common approach used to indirectly quantify chondrogenesis. Figure 27C was plotted using the sGAG quantity found in the media after each media exchange

therefore it demonstrates the elution pattern of sGAG into the media over the two week culture. The quantity of sGAG in medium was incrementally increased in CC and CO micropellets, while it was lower and constant for OC and OO micropellets over the first 8 days (Fig. 27C). Following day 8, OC and OO micropellets continued to elute only minor quantities of sGAG into the media. Over the second week of the culture, sGAG elution in CO micropellets tapered slowly at first and then significantly at day 12 because of the switch to osteogenic medium (Fig. 27C). Figure 27D demonstrates the sGAG found in the tissue on day 14 (sGAG in digest) and the accumulation of sGAG eluted into the media, which is the summation of sGAG quantities found in the media after media exchanges (sGAG in media). The quantity of sGAG retained in the micropellets was the greatest for CC, although the total quantity of sGAG eluted into the culture medium was similar for both CO and CC micropellet cultures (Fig. 27D). Figure 27E demonstrates the ratio of the total sGAG quantity (which is summation of sGAG in digest and total sGAG in media) to the corresponding DNA quantity for each sample. The sGAG/DNA ratio was the greatest for CC and CO micropellets, and lesser for OC and OO micropellets (Fig. 27E). Overall, DNA and sGAG/DNA data indicated that the cultures initiated with a similar media type over the first 8 days had similar phenotype following 14 days total culture.

In contrast to chondrogenic characterization, osteogenic characterization provided greater resolution and indicated that the change in medium composition did influence micropellet phenotype substantially. The calcium/DNA ratio was the greatest for OO micropellets, significantly lower for OC micropellets, and it was the lowest for CC and CO micropellets (Fig. 27F). Interestingly, the alkaline phosphatase (ALP) activity/DNA ratio was markedly greater in the CO micropellets (Fig. 27G). ALP is considered a key early indicator of osteogenesis, and it is upregulated during early osteogenesis, and then ALP activity is diminished as the cells continue to mature [376]. The elevated ALP activity observed in the CO micropellets may suggest that these tissues acquire a pre-osteogenic phenotype in response to the change from chondrogenic to osteogenic medium.

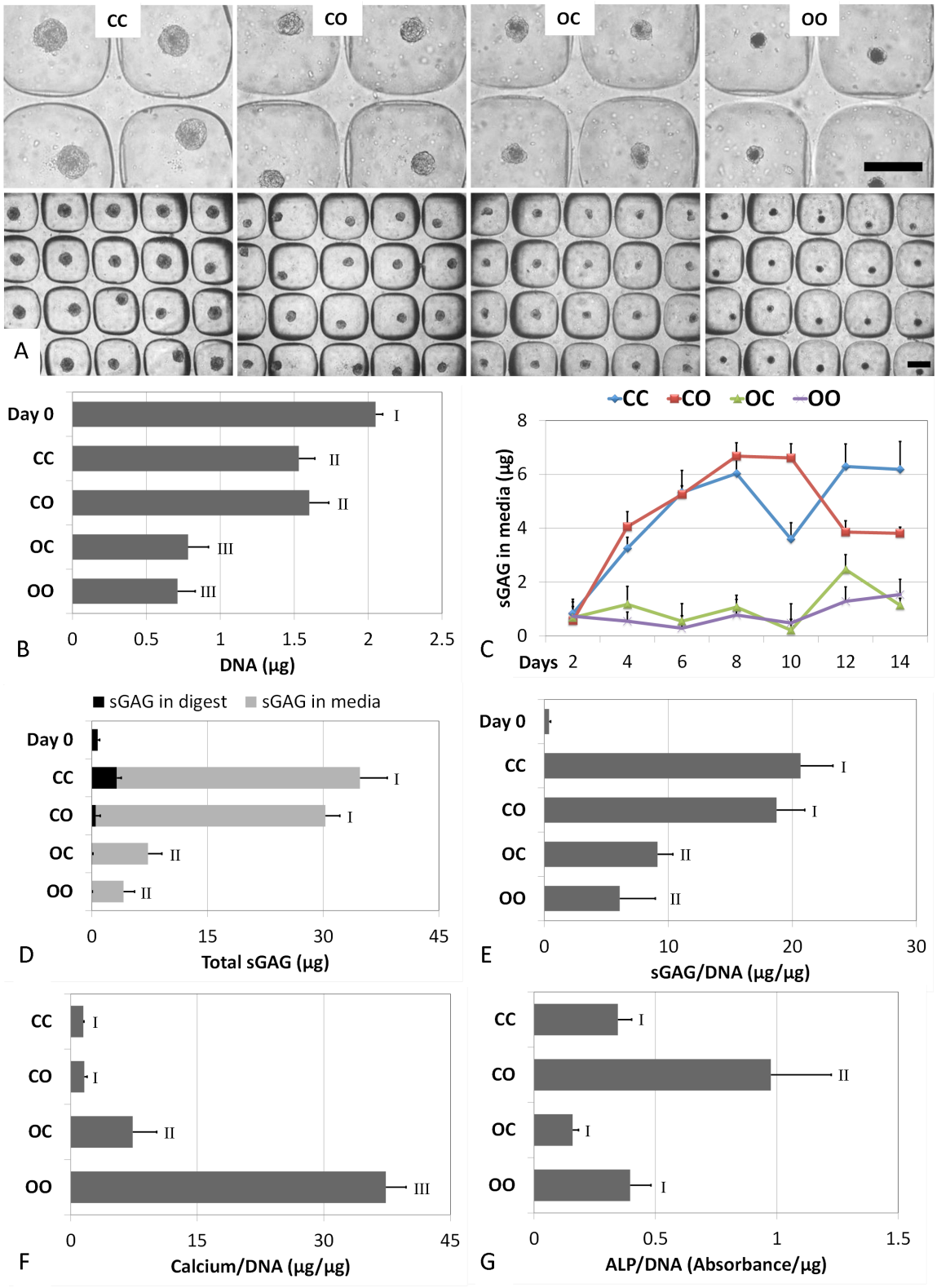

Figure 27. Morphology of micropellets, chondrogenic/osteogenic differentiation and DNA content assessment. The size of the micropellets was greatest for CC and smallest for OO micropellets. The core of OO micropellets appeared more opaque (A). The quantity of DNA was lower than day 0 control in all conditions, and it was significantly reduced for the cultures initiated with osteogenic medium; OC and OO

(B). Elution of sGAG into the media was monitored throughout the culture; sGAG in media followed an increasing pattern for micropellets initiated with chondrogenic media (CC, CO), whereas it was lower and steady for OC and OO micropellets (C). The quantity of sGAG retained in the tissue at the end of day 14 (sGAG in digest) was the greatest for CC micropellets, however the quantity of total sGAG eluted into the media (sGAG in media) was substantially greater than the quantity retained within the micropellets (D). The total sGAG/DNA ratio, which is equal to (sGAG in digest + sGAG in media) / DNA, indicated that cultures initiated with chondrogenic media, CC and CO, were able to produce greater quantity of sGAG during the two week culture (E). Calcium/DNA ratio indicated that OO micropellets had the greatest calcium content (F) whereas alkaline phosphatase activity was significantly greater only in CO micropellets (G). Data were represented in graphs as mean + SD, $n = 4$. Scale bars = 200 μm.

Histological features of micropellets

Alcian blue staining indicated that all micropellets contained sGAG, whereas a lack of alizarin red staining indicated that there was no mineralization in CC or CO micropellets (Fig. 28). Positive alcian blue staining of OC and OO micropellets likely reflects the expression of sGAG molecules commonly found in the bone (chondroitin sulfate), and the fact that the biphasic tissue had been cultured in chondrogenic induction medium for 8 days [377,378]. As expected, alizarin red staining was the most intense for OO micropellets (Fig. 28). The presence of mineralized matrix in OO micropellets was further validated with OsteoImage fluorescent stain, which is specific to hydroxyapatite portion of bone matrix (Fig. 28). OC micropellets also stained positive with OsteoImage, marking very small and localized hydroxyapatite nucleation points (Fig. 28) indicating that when the media was changed to chondrogenic their osteogenic differentiation was brought to a halt. Collagen II was present in CC, CO and OC micropellets, which suggests that chondrogenic media exposure may be required for collagen II accumulation therefore OO micropellets were stained less intense for collagen II (Fig. 28). Collagen X was present in all micropellets, which indicates that MSC micropellets were hypertrophic regardless of media type (Fig. 28). Collagen I was present in CO, OC and OO micropellets, which suggests that osteogenic media exposure may be necessary to trigger collagen I accumulation therefore CC micropellets had less intense collagen I staining.

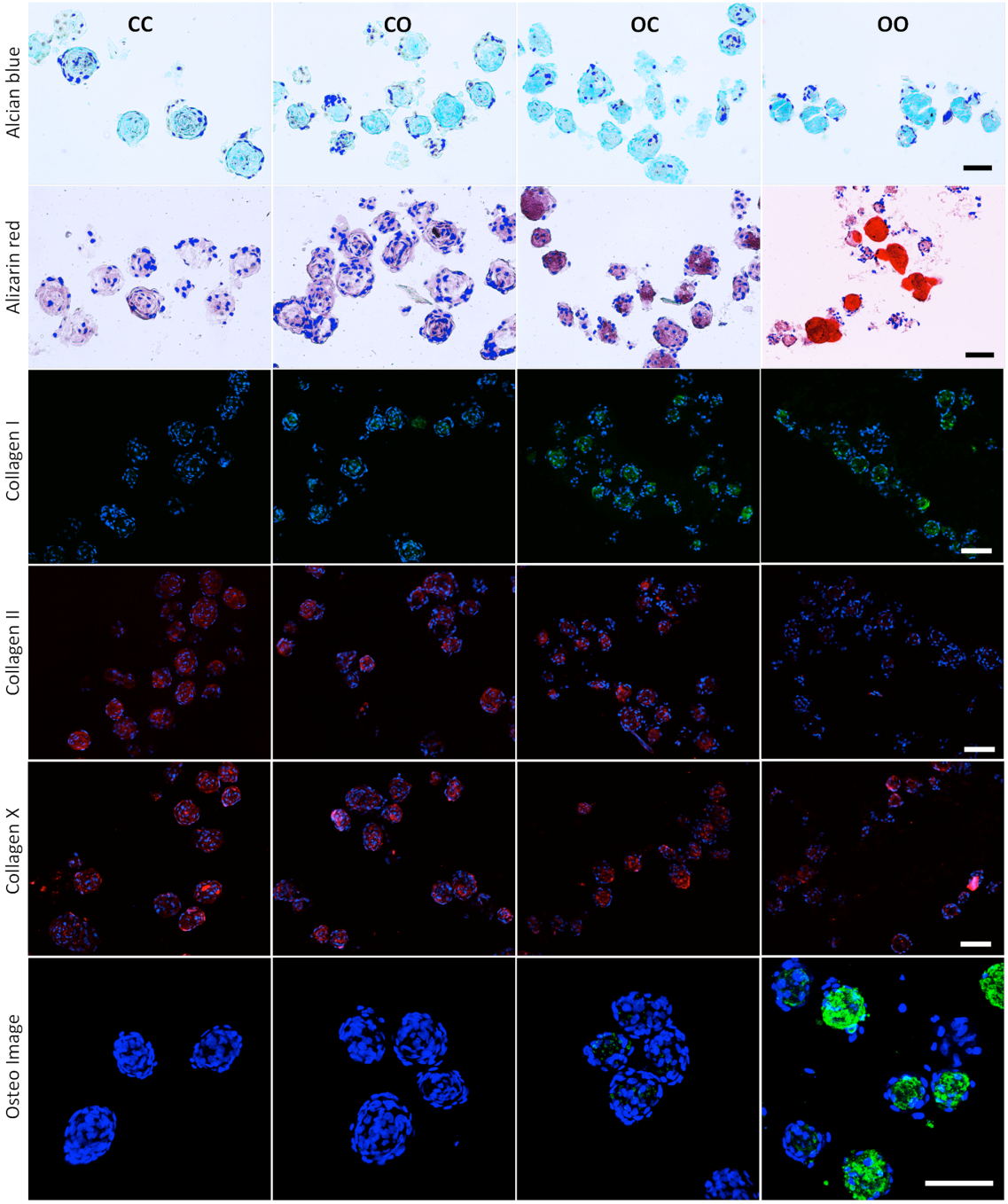

Figure 28. Histological assessment of micropellets. Alcian blue staining was similar for all conditions, whereas alizarin red staining indicated that calcification only occurred in OO micropellets. Accumulation of collagen II was less in OO micropellets, whereas collagen X was present in all cultures. Collagen I staining was less intense in CC micropellets, and OsteoImage, specific for hydroxyapatite, intensely stained OO micropellets but only marked hydroxyapatite nucleation points in OC micropellets. Scale bars = 200 μm.

Gene expression in micropellets

The gene expression for chondrogenic, hypertrophic and osteogenic markers (aggrecan, SOX9, collagen II and X, versican, RUNX2, collagen I, osteocalcin, ALP and BMP2) were assessed. Aggrecan, SOX9 and collagen II were similarly upregulated at the end of 8-day chondrogenesis, and the expression of those genes was further elevated following 14 days of chondrogenic differentiation (Fig. 29A, C, E). These results indicate that chondrogenesis continues to progress over the full 14 days of chondrogenic culture. SOX9, but not the chondrogenic matrix molecules (aggrecan or collagen II), was upregulated in CO and OC micropellets exposed to chondrogenic differentiation media for the first 8 days or in the last 6 days, respectively. This suggests that the short term exposure to chondrogenic media may upregulate SOX9 expression but it is insufficient to generate a stable chondrogenic phenotype with high collagen II expression. This is parallel to a previous report where the lack of correlation between SOX9 and collagen II expressions was shown in articular chondrocytes [379]. Collagen X expression was upregulated during the first 8-day chondrogenic culture, and then remained at a similar level in CO micropellets but increased in CC micropellets (Fig. 29G). Versican expression was significantly downregulated in micropellets initiated with chondrogenic media, CC and CO when compared to day 0. By contrast, versican expression was similar to day 0 at the end of culture for tissues initiated in osteogenic media, OC and OO (Fig. 29B). The expression of collagen I was elevated with chondrogenic media supplementation (Fig. 29F). This pattern suggests that exposure to chondrogenic media in the culture directs collagen I expression. The TGF β1 contained in the chondrogenic medium is known to upregulate collagen I expression specifically during development in various tissues including bone [380-382]. RUNX2 was upregulated in CO and OO conditions (Fig. 29D). Osteocalcin, ALP and BMP2 expressions had a similar pattern, significantly higher in CO micropellets when compared to others (Fig. 29H, I, J). This finding is quite interesting, because despite the lack of calcification in CO tissues when compared to OO, ALP activity and also gene expression for osteogenic factors such as ALP, BMP2, osteocalcin and RUNX2 were significantly elevated in CO micropellets. This parallels recent findings [62,383,384], which suggest that pre-conditioning MSC with chondrogenic medium prior to

osteogenic differentiation may enhance bone formation by better mimicking the natural process of endochondral ossification.

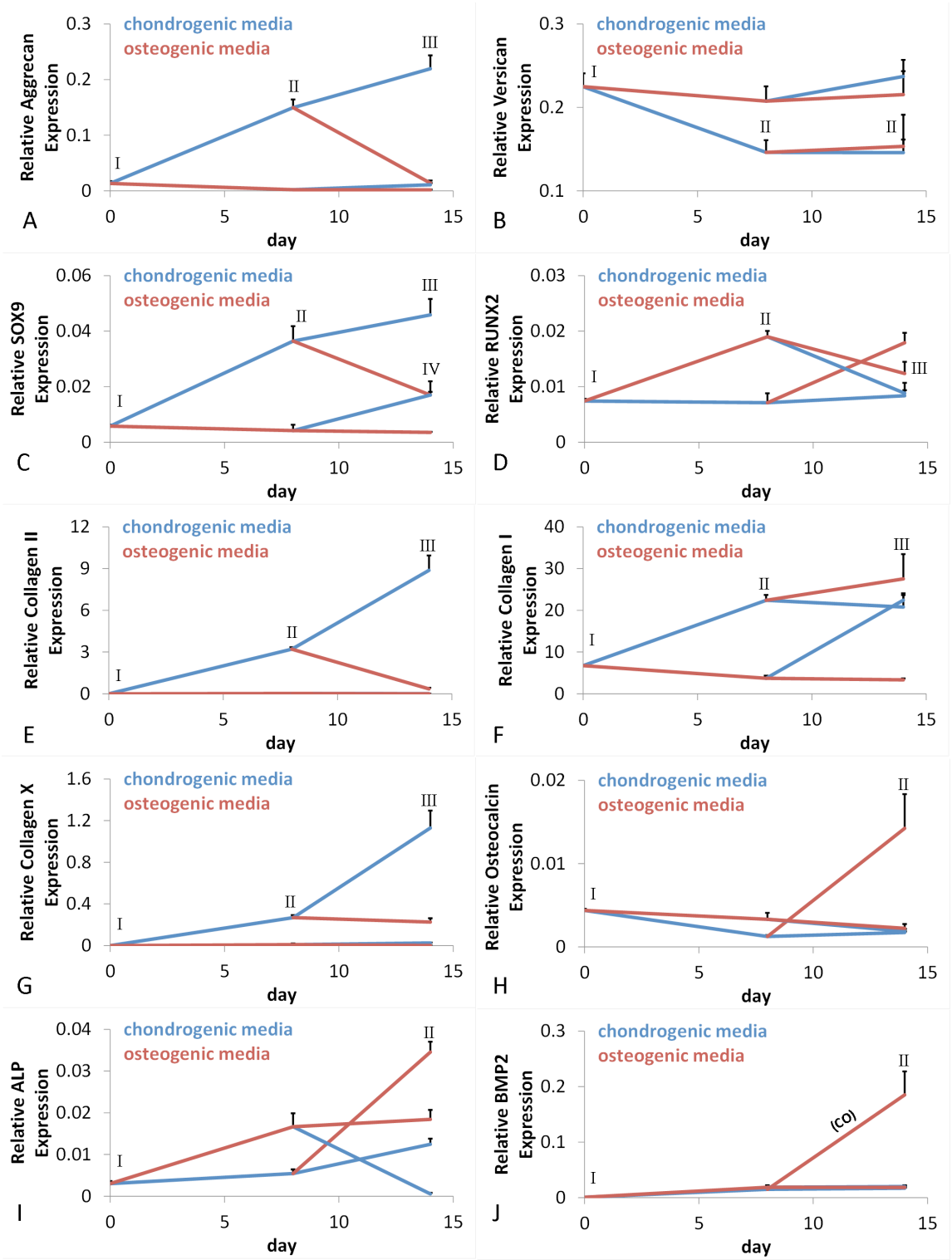

Figure 29. Gene expression analysis of micropellets. The gene expression was assessed at three different time points; day 0, day 8 and day 14. The lines connecting time points were colored either blue for chondrogenic media or red for osteogenic media. For example a continuous blue line represents CC

and a continuous red line represents OO. Aggrecan, SOX9, collagen II and X were upregulated in CC micropellets (A, C, E, G), and versican was downregulated in chondrogenic media initiated cultures (B). RUNX2 was greatest in CO micropellets (D) whereas collagen I was upregulated in CC, CO, OC micropellets (F). Osteocalcin, alkaline phosphatase and BMP2 expressions were significantly greater in CO micropellets at day 14 (H, I, J). Data were represented in graphs as mean + SD, $n = 4$.

Biphasic tissue assembly and histology

Results from the first part of our study indicated that an 8-day differentiation cycle was insufficient for MSC micropellets to acquire chondrogenic and osteogenic phenotypes required for use in the assembly of a biphasic tissue. Specifically, whilst the OC micropellets did not demonstrate chondrogenic features after the media was swapped, they also did not achieve a similar state of tissue mineralization as the OO micropellets. This implies that the osteogenic phenotype was not acquired after only 8 days in osteogenic induction medium. Similarly, the CO micropellets showed chondrogenic features after the first 8 days of culture, however when the media was altered from chondrogenic to osteogenic they rapidly became pre-osteogenic, parallel to previous findings [62,383,384]. This result implies that the chondrogenic phenotype is particularly unstable, and that exposure of early stage chondrogenic micropellets to osteogenic medium would result in osteogenic phenotype. Based on these observations, we reasoned that the separate differentiation cultures would need to be maintained for 14 days before assembling the micropellets into a biphasic tissue cultured in a common medium formulation.

Our own work in this area indicates that the first phase of discrete culture cannot be drawn out indefinitely, as the capacity of cartilage micropellets to amalgamate is reduced as the tissues mature and matrix accumulates [17]. Similarly, more efficient fusion of human MSC conventional pellets at earlier days of chondrogenic culture was shown [353]. Taking these observations together, we elected to initiate the chondrogenic and osteogenic micropellet differentiation cultures on the same day (day 0), assemble the chondrogenic micropellets into a cartilage-only tissue at day 8 in chondrogenic induction medium, then layer the osteogenic micropellets onto the cartilage tissue at day 14, and continue the biphasic tissue culture in chondrogenic induction medium for an additional week (Fig. 30).

The PDMS mold used for osteochondral tissue formation had a diameter of 4 mm and a total of 12,000 chondrogenic micropellets filled the mold to a height of 2 mm, and the same number of smaller osteogenic micropellets filled it an additional 0.5 mm high (Fig. 30). As the biphasic tissue matured the total diameter decreased slightly to ~3 mm, although the chondrogenic layer remained ~2 mm deep, the osteogenic layer shrunk slightly to ~0.3 mm deep. The shrinkage in tissue size and deviation from a perfect cylinder in tissue morphology (Fig. 30) may be caused by MSC aggregate "compaction" phenomenon [385].

The cross sectional area of the osteochondral tissue was assessed for histological features of bone and cartilage. Alcian blue stained the tissue throughout (Fig. 31A, B). This staining highlighted individual micropellets, although discrete micropellets were much more visible in the cartilage portion of the tissue (Fig. 31A, B). By contrast, the alizarin red exclusively stained the bony side of the tissue however staining revealed that mineralization was not always continuous (Fig. 31C, D). In higher magnification images it is clear that individual cells are bridging the two tissue layers together (Fig. 31B, D). Unexpectedly, the collagen II staining was more intense in the bony layer relative to the chondral layer (Fig. 31E). This differs from the first part of our study where the micropellets were cultured for 14 days in discreet microwells, and exhibited minimal collagen II expression in OC medium combination (Fig. 29). This difference suggests that the co-culture of the osteogenic and chondrogenic tissues drives this outcome. One possible explanation is that chondrogenically induced cells from the cartilage micropellets migrated onto the osteogenic induced micropellets, forming a layer of cells that contributed to the observed intense collagen II staining. An alternative possibility is that paracrine signals from the adjacent cartilage tissues modified the behavior of the initially osteogenically induced cells, resulting in their increased expression of collagen II. There is precedent for a change in cell behavior in response to the fusion of pellets and for the signaling between adjacent fused pellets [386]. For example, Lehmann et al provide high resolution images demonstrating that the cells that form the layer that fuses pellets together contribute to a unique tissue layer with histological properties that differ from the pellets that were fused to generate the amalgamated tissue [386]. Further experiments will be required to elucidate the

mechanism that drives the enhanced collagen II staining observed in our osteogenic tissue layer.

Collagen X (Fig. 31F) and I (Fig. 31G) stainings were present in both layers, but more intense in the bony layer (Fig. 31) revealing a lower collagen content in the chondral layer, and this was consistent with our expectations for bone-like tissue [62,383,384]. The hydroxyapatite-specific OsteoImage exclusively stained the bony layer suggesting there was not an accumulation of undesirable mineralization within the chondral layer (Fig. 31H). Our work builds on previous work demonstrating that discreet cartilage microtissues could be used to Whilst a previous publication demonstrated that cartilage macropellets could be fused together to form a cartilage-like core with a bone-like exterior [387]. Specifically, our work demonstrates that it is possible to assemble cartilage-like micropellets and bone like-micropellets to make a structured bi-phasic tissue. We believe that this capacity to assemble a complex layered tissue will contribute to efforts to repair or regenerate articular cartilage.

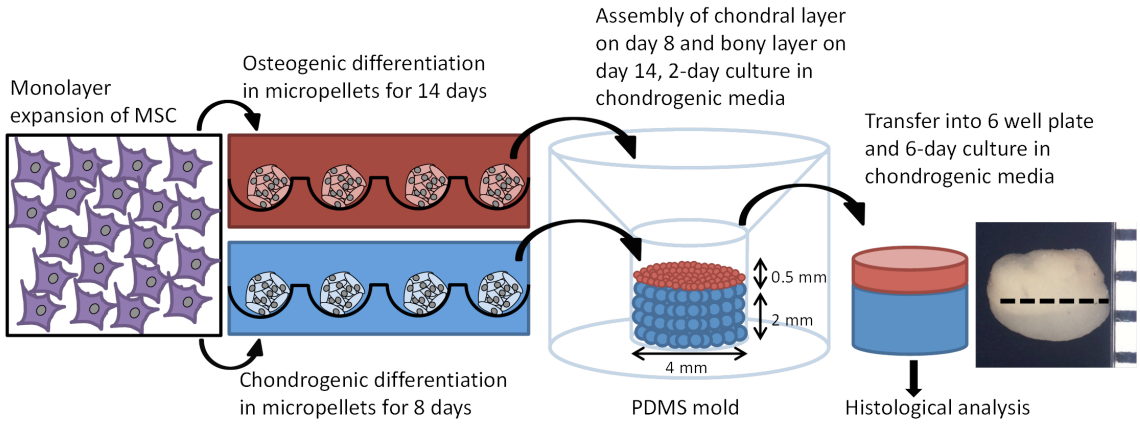

Figure 30. Biphasic tissue construction with micropellets. The monolayer expanded MSC were used to form micropellets and cultured in chondrogenic and osteogenic media separately. The chondrogenic micropellets were assembled on day 8 then the osteogenic micropellets were layered on top at day 14 using a custom-made PDMS mold. The biphasic tissue was cultured for another week then sectioned for histological analysis.

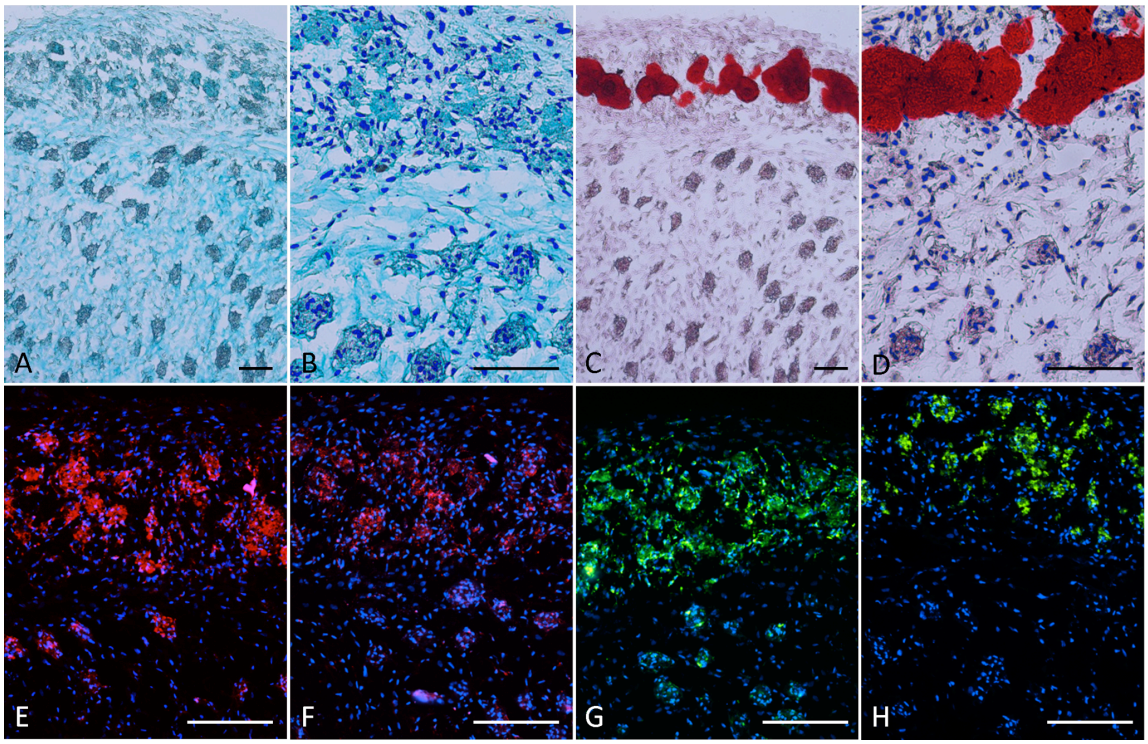

Figure 31. Histological assessment of osteochondral-like tissue. The upper section of the tissue is bony layer and the lower section is chondral layer. Alcian blue stained both chondral and bony layers (A, B), whereas alizarin red specifically stained the calcified region in the bony layer (C, D). At higher magnification, the cells migrating out of the individual micropellets and filling the void space between micropellets is visible (B, D). Collagen II (E), X (F) and I (G) were all accumulated more on bony side while being present in both sides whereas OsteoImage (H) stained exclusively bony side indicating lack of calcification on chondral layer. Scale bars = 200 μm.

5. Conclusion

Herein we described methods for the manufacture of osteogenic and chondrogenic micropellets as building blocks from bone marrow-derived MSC. Using the micropellet approach, we first assessed the impact of various medium conditions on osteogenic and chondrogenic differentiation of MSC. Then, a scaffold-free osteochondral tissue was assembled via layering osteogenic and chondrogenic micropellets in a tailored culture device. The micropellets fused into a continuous tissue retaining the two distinct original layers. Previously, the generation of an osteochondral tissue interface using collagen microencapsulated rabbit MSC spheroids was described [335]. To our knowledge, this is the first scaffold-free biphasic tissue built with a single cell type and our results are the first to demonstrate that a continuous bi-phasic structure can be generated without need for a hydrogel or polymer support structure. In future

studies, the use of micropellets should enable the precise layering of different micropellets and the more accurate replication of the complex zonal structure found in native cartilage.

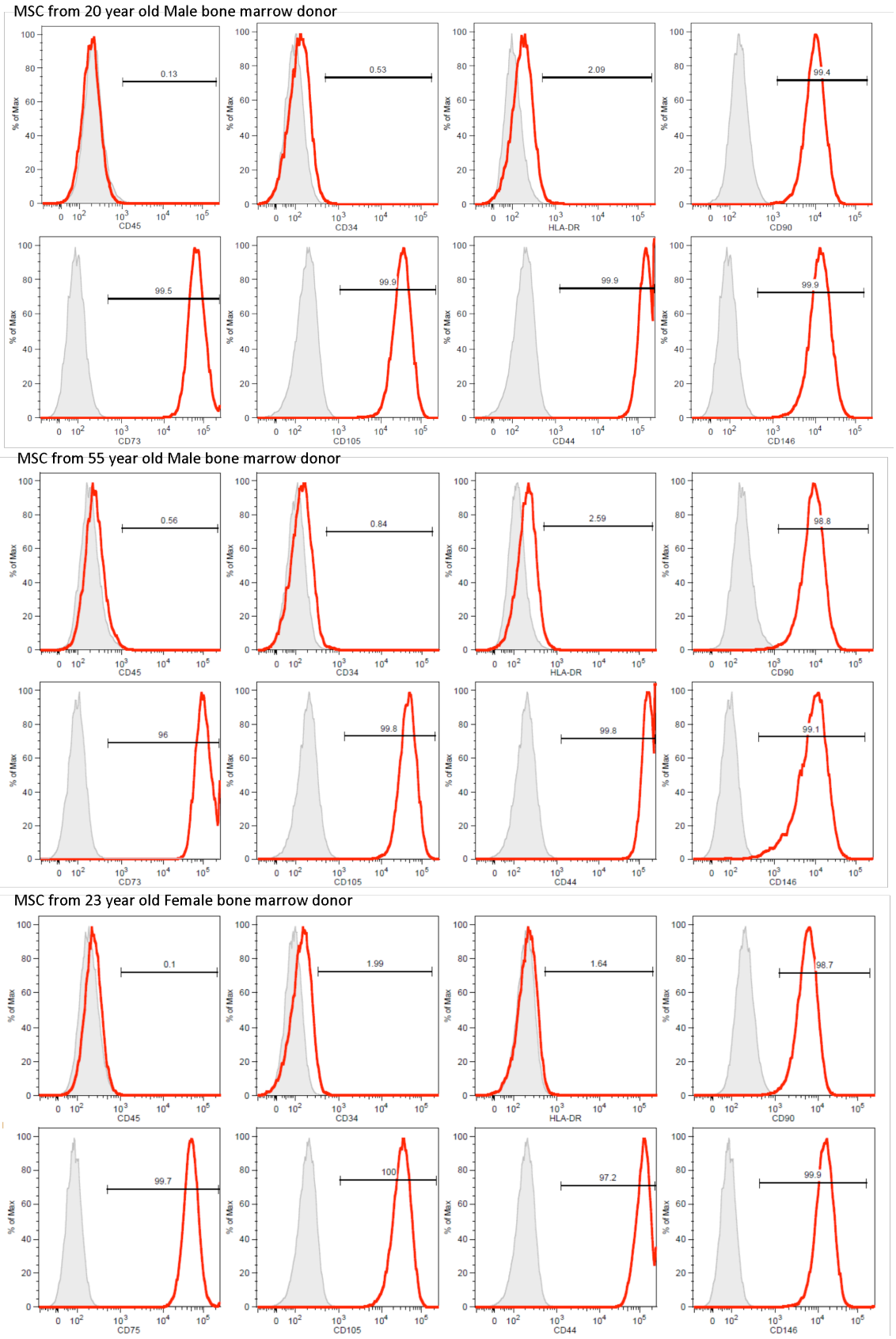
MSC from 20 year old Male bone marrow donor
0.13
0.53
2.09
99.4
99.5
99.9
99.9
99.9
CD45
CD34
HLA-DR
CD90
CD73
CD105
CD44
CD146
MSC from 55 year old Male bone marrow donor
0.56
0.84
2.59
98.8
96
99.8
99.8
99.1
CD45
CD34
HLA-DR
CD90
CD73
CD105
CD44
CD146
MSC from 23 year old Female bone marrow donor
0.1
1.99
1.64
98.7
99.7
100
97.2
99.9
CD45
CD34
HLA-DR
CD90
CD75
CD105
CD44
CD146
% of Max

Figure 32. Flow cytometry characterization of MSC. The MSC from all three donors used in these studies are characterized for their expression of CD45, CD34, HLA-DR, CD90, CD73, CD105, CD44, and CD146.

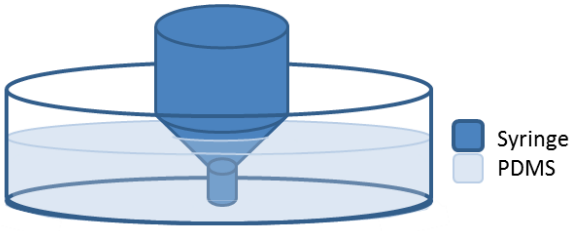

Figure 33. Fabrication of conical mold used to assemble the biphasic tissue. The tip of a 10 mL syringe was cut and glued to the middle of a single well in a 6-well plate and the space between the syringe and the well was filled with PDMS and cured. Then the syringe tip was removed and the extra PDMS layer around the mold was cut out to accommodate more medium in the same well.

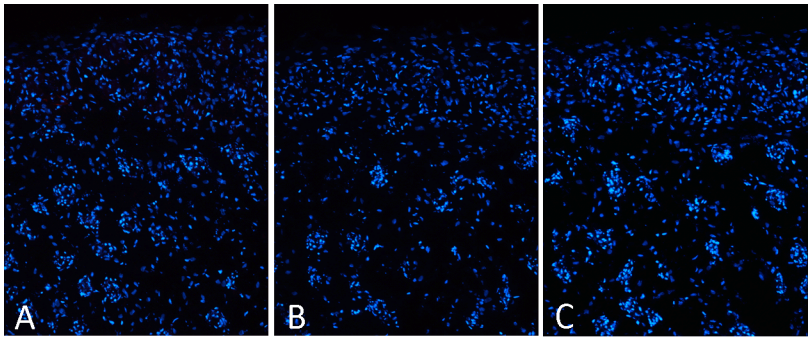

Figure 34. Negative controls for collagen staining in biphasic tissue. Negative control (no primary antibody) for collagen II (A), collagen X (B) and collagen I (C).

Gene (Amplicon size in basepair)	Primers
Cyclophilin A (164)	Forward CTCGAATAAGTTTGACTTGTGTT
	Reverse CTAGGCATGGGAGGGAACA
GAPDH (119)	Forward ATGGGGAAGGTGAAGGTCG
	Reverse TAAAAGCAGCCCTGGTGACC
SOX9 (77)	Forward TTCCGCGACGTGGACAT
	Reverse TCAAACTCGTTGACATCGAAGGT
Aggrecan (85)	Forward TCGAGGACAGCGAGGCC
	Reverse TCGAGGGTGTAGCGTGTAGAGA
Collagen II, COL2A1 (79)	Forward GGCAATAGCAGGTTCACTGACA
	Reverse CGATAACAGTCTTGCCCCACTT
Collagen I, COL1A1 (83)	Forward CAGCCGCTTCACCTACAGC
	Reverse TTTTGTATTCAATCACTGTCTTGCC
Versican (98)	Forward TGGAATGATGTTCCCTGCAA
	Reverse AAGGTCTTGGCATTTTCTACAAAG
Collagen X, COL10A1 (70)	Forward CAAGGCACCATCTCCAGGAA
	Reverse AAAGGGTATTTGTGGCAGCATATT
Runx2 (113)	Forward GGAGTGGACGAGGCAAGAGTTT
	Reverse AGCTTCTGTCTGTGCCTTCTGG
Osteocalcin (70)	Forward GAAGCCCAGCGGTGCA
	Reverse CACTACCTCGCTGCCCTCC
ALP (89)	Forward CGTGGCTAAGAATGTCATCATGTT
	Reverse TGGTGGAGCTGACCCTTGA
BMP2 (72)	Forward AAAACGTCAAGCCAAACACAAA
	Reverse GTCCACGTACAAAGGGTCTCTCT

Table 6. Primers used for gene expression analysis.

DNA		CC	CO	OC	OO	**GAG/DNA**		CC	CO	OC	OO
Donor 1	Mean	2.05027845	1.53101176	1.60205625	0.78183983	Donor 1	Mean	20.6563641	18.7179773	9.12596912	6.08157804
	SD	0.04804959	0.10806467	0.13163035	0.13845745		SD	2.61542757	2.27685284	1.23568696	2.86672799
Donor 2	Mean	0.95427188	0.8400578	0.49003736	0.28210526	Donor 2	Mean	12.7202854	8.18542708	3.24924109	4.24861085
	SD	0.0306942	0.08899185	0.05899807	0.02509655		SD	1.61921278	1.9768755	0.69832796	1.97352467
Donor 3	Mean	1.1430408	1.05114765	0.7589199	0.64725195	Donor 3	Mean	17.8826921	16.572193	11.7129252	11.0609929
	SD	0.08491509	0.16789807	0.13159206	0.11291748		SD	0.77166998	2.51333078	3.11268637	3.92149979

Calcium/DNA		CC	CO	OC	OO	**ALP/DNA**		CC	CO	OC	OO
Donor 1	Mean	1.50341292	1.62607294	7.35780659	37.3496861	Donor 1	Mean	0.34525251	0.97550356	0.15902119	0.39583005
	SD	0.07353858	0.32040183	2.84599514	2.38748149		SD	0.05676371	0.24869783	0.02425738	0.08556182
Donor 2	Mean	1.98551634	2.2819932	4.53798928	7.01688636	Donor 2	Mean	0.7291289	2.83100532	1.65706733	2.22868417
	SD	0.25351189	0.32326246	0.60788467	1.08531925		SD	0.26870077	0.29257218	0.46973419	1.10755395
Donor 3	Mean	2.02033467	2.51282267	7.57394161	41.8761768	Donor 3	Mean	0.09004894	0.10140167	0.14667912	0.25388274
	SD	0.21036379	0.66713546	2.77745867	9.70076415		SD	0.00655811	0.01724498	0.02819844	0.01888155

Gene Expression

Donor 1 - Mean	Aggrecan	Versican	Sox 9	Runx2	Col I	Col II	Col X	Osteocalcin	ALP	BMP2
CC	0.21955191	0.14585652	0.04585609	0.00837269	20.8005307	8.87748716	1.12968761	0.00172252	0.01246457	0.01707908
CO	0.01389272	0.1533135	0.01699134	0.01791073	27.5251347	0.35325963	0.22551608	0.01423678	0.03454933	0.1850758
OC	0.01090902	0.23711417	0.01698042	0.00882115	22.4280764	0.00861646	0.02539592	0.00186898	0.00056395	0.02004281
OO	0.00172744	0.21539093	0.00352271	0.01237596	3.32736075	0.00040256	0.00049373	0.00222714	0.0184183	0.01842759
Donor 1 - SD	Aggrecan	Versican	Sox 9	Runx2	Col I	Col II	Col X	Osteocalcin	ALP	BMP2
CC	0.02409777	0.01561786	0.00573684	0.00231887	3.28821875	1.06646603	0.16606624	0.00013968	0.00133337	0.00117961
CO	0.00467288	0.03783985	0.00495818	0.00178826	5.95518858	0.07932193	0.03685038	0.00409469	0.00249123	0.04229125
OC	0.00309143	0.01982998	0.00116547	0.00055289	1.21923081	0.00257982	0.00337702	0.00029038	0.00024561	0.0022704
OO	0.00057274	0.02796812	0.00020328	0.00209283	0.33458186	0.00011185	0.0002152	0.00051204	0.00227859	0.00281068

Donor 2 - Mean	Aggrecan	Versican	Sox 9	Runx2	Col I	Col II	Col X	Osteocalcin
CC	0.55481465	0.27347953	0.36787016	0.018063	114.376983	0.22957694	5.17348278	0.02114906
CO	0.01789334	0.10733799	0.19369808	0.01974532	9.8557614	0.0035489	0.36990735	0.03257208
OC	0.05416716	0.12972699	0.09293866	0.00807496	31.5223014	0.00132997	0.13917705	0.00284204
OO	0.00770769	0.04900125	0.21256182	0.02875966	3.58783203	0	0.00496683	0.06787841
Donor 2 - SD	Aggrecan	Versican	Sox 9	Runx2	Col I	Col II	Col X	Osteocalcin
CC	0.03771411	0.06170384	0.05158564	0.01058747	16.6371661	0.06069561	1.17127576	0.01001112
CO	0.01598521	0.03006616	0.05217068	0.02358799	1.2070421	0.0035489	0.06175311	0.00719858
OC	0.00709593	0.02880779	0.01202665	0.00282837	12.8749445	0.00040035	0.0156233	0.00354298
OO	0.00313174	0.09248764	0.04362818	0.00676642	1.05113912	0	0.00496683	0.01650715

Donor 3 - Mean	Aggrecan	Versican	Sox 9	Runx2	Col I	Col II	Col X	Osteocalcin
CC	0.05121239	0.21758045	0.01860672	0.01967495	30.1050171	0.13256745	0.26722254	0.00173912
CO	0.00337951	0.14556627	0.00849153	0.03011854	13.4566279	0.00048295	0.0308862	0.00237688
OC	0.0021321	0.22841739	0.01631144	0.01444447	22.332842	0.00018715	0.01008911	0.00154453
OO	0.00090629	0.08649819	0.00373291	0.02187094	1.72940737	4.6005E-05	0.0002968	0.00204155
Donor 3 - SD	Aggrecan	Versican	Sox 9	Runx2	Col I	Col II	Col X	Osteocalcin
CC	0.00785923	0.02861342	0.00507095	0.00365585	2.77040255	0.03847362	0.05582532	0.00051511
CO	0.00117818	0.01411995	0.0019039	0.00316339	2.09405668	0.00032859	0.00253737	0.00070135
OC	0.00062988	0.04177663	0.00345912	0.00321145	2.57968835	0.00012091	0.0036955	0.00050897
OO	0.00069054	0.00281783	0.00107346	0.00598759	0.56003631	4.4756E-05	0.00026189	0.00124196

Table 7. Data obtained from three different donors.

"If we knew what it was we were doing, it would not be called research, would it?"
Albert Einstein

Chapter 6: Summary, Discussion and Future Perspectives

1. Summary

Articular cartilage injuries are troublesome for both patients and orthopedic surgeons. If the injuries are not treated appropriately, the patients have the risk of living with constant joint pain or even disability. Surgeons have multiple options to treat the injuries, yet all treatments have substantial downsides and varying clinical outcomes (see Chapter 2). Overall, treatment effectiveness may depend on the surgeon's decision making [388] and talent [389], which is not ideal and likely contributes to the varying success rates in clinics.

The primary aim of cartilage tissue engineering studies is to improve the treatment procedures. During this process, a great amount of information about the biology of the cartilage tissue is also generated. Similarly, in this Thesis different ways of using micropellets in cartilage tissue engineering or cell-based therapies were investigated (Fig. 35) and at the same time, the effect of micropellet culture on different cells, under different culture conditions was reported.

The cell-based treatment procedures such as ACI and MACI are facilitated with the monolayer expanded chondrocytes isolated from a biopsy of healthy cartilage. However, it is observed that once chondrocytes are stripped of their natural, matrix intense microenvironment and expanded on tissue culture plastic they obtain fibroblast-

like characteristics and critically, their ability to generate cartilage tissue is significantly reduced with a process referred as “dedifferentiation” [116,390,391]. Therefore, some techniques are developed in order to restore the chondrogenic phenotype of chondrocytes referred as “redifferentiation” [288,392-394]. The pellet culture is one of the widely used redifferentiation methods because it helps the chondrocytes to re-obtain the 3D environment similar to native cartilage. However, the radial heterogeneity of the most pellets caused by the diffusion gradients is a concern since the chondrogenic properties are changing throughout the pellet. The use of micropellets was tested in order to overcome this heterogeneity problem. In Chapter 3, it was reported that redifferentiation of expanded articular chondrocytes was enhanced in micropellets when coupled with hypoxic microenvironment. These redifferentiated micropellets can be directly delivered into a partial-thickness defect site in order to mediate tissue regeneration (Fig. 35). Alternatively, generation of a greater size cartilaginous tissue with the assembly of chondrocyte micropellets was demonstrated, which can be useful in *ex vivo* cartilage tissue engineering applications.

The few number of chondrocytes isolated from a small biopsy limits chondrocyte use in cell-based therapies, specifically in the case of greater size injuries. As an alternative, bone marrow MSC is preferred since these cells are easier to harvest, can proliferate and have the potential to differentiate into chondrogenic lineage. Our group has previously shown that MSC chondrogenesis is enhanced in micropellets when compared to conventional pellets under hypoxic atmosphere [18]. Building on this, in Chapter 4, the incorporation of donor cartilage particles, referred as cartilage dust, into MSC micropellets was investigated. The aim of this approach was to bulk up the micropellet size, and increase the defect filling capacity of micropellets. The composite micropellets had greater size and the addition of cartilage dust enriched the collagen II content of the generated tissue. This study suggests that the composite micropellets can be used as a defect-filling agent in greater size cartilage injuries (Fig. 35).

In the case of osteochondral defects, it may be logical to exploit the nature of injury in order to facilitate better integration of the engineered construct to the defect site. In osteochondral graft transplantations, it is observed that the lateral integration occurs rapidly whereas the vertical integration mostly fails [395]. This is why in

mosaicplasty, even if the defect is not originally osteochondral, sometimes extra bone tissue is removed from subchondral region to facilitate better graft integration. Based on that, engineering an interface tissue between bone and cartilage is attempted in order to generate artificial osteochondral grafts to be implanted, eliminating the donor site morbidity associated with mosaicplasty. The most common approach is to use a biphasic scaffolds with properties mimicking the native bone and cartilage and the bone marrow MSC are preferred as a single cell source to engineer both layers. In Chapter 5, construction of a scaffold-free biphasic tissue was described where MSC derived chondrogenic and osteogenic micropellets were used as building blocks. To be able to build a biphasic tissue and culture it in a single media formulation, first the phenotypic change of MSC micropellets when cultured in chondrogenic or osteogenic media was tested. In this part of the study, chondrogenic and osteogenic characteristics of micropellets were assessed after the media were swapped from osteogenic to chondrogenic or chondrogenic to osteogenic. The exposure of chondrogenic micropellets to osteogenic medium significantly increased their osteogenic properties whereas the exposure of osteogenic micropellets to chondrogenic medium interrupted their osteogenic differentiation. Therefore, MSC micropellets were first separately differentiated into chondrogenic and osteogenic lineages, and then assembled to generate a ~2 mm thick osteochondral-like tissue. This is the first scaffold-free biphasic tissue and this method in particular embodies the idea of utilizing micropellets as building blocks in order to engineer composite tissue grafts (Fig. 35).

All studies reported in this Thesis were performed *in vitro*. In order to assess the interaction between individual micropellets, they were assembled at varying time points. The next logical step is to test the benefits of this technique *in vivo* to be able to recommend micropellet use in clinical applications (Future perspectives section).

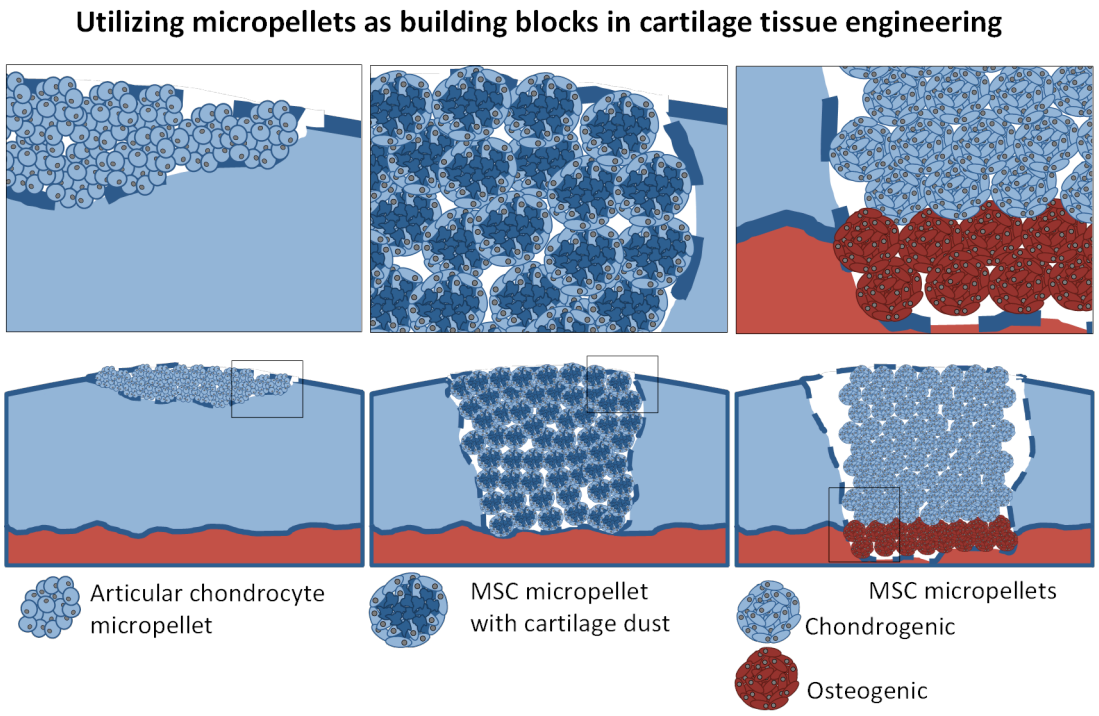

Figure 35. Utilizing micropellets as building blocks in cartilage tissue engineering. In Chapter 3, generation and assembly of chondrocyte micropellets was reported, which may lead to an efficient treatment method for partial-thickness defects. In Chapter 4, generation and assembly of bigger micropellets with addition of cartilage dust was reported, which may lead to an efficient defect filling strategy for full-thickness defects. In Chapter 5, using separately differentiated chondrogenic and osteogenic micropellets, a scaffold-free biphasic tissue was built, which may have a merit in osteochondral defect treatments.

2. General discussion

The primary aim of this project was to characterize different types of micropellets and explore their use in cartilage tissue engineering. Some significant findings were reported in three independent but theme-related studies. These studies revealed many advantages of micropellet use and also some limitations associated with it.

The initial motivation for using micropellets was solely geometrical; by increasing the surface area to volume ratio, mass transport problems were minimized. Native human cartilage is 1-5 mm thick and devoid of blood vessels [28]. Glucose, oxygen and other factors are transported to chondrocytes via diffusion of the synovial fluid into the cartilage tissue. This tissue structure gives rise to a vertically aligned diffusion gradient pattern in the native cartilage. Ideally, once the engineered tissue is

implanted, it would develop such zonal diffusion gradients, which might help the tissue to acquire a desired zonal organization. However, the diffusion gradients observed in macropellets are radial because of the spherical tissue geometry. This radial diffusion pattern is dissimilar to native cartilage. Formation of such radial diffusion gradients was mitigated in each micropellet that had 100-200 μm diameter, therefore chondrogenic factors, metabolites and the oxygen concentrations were more homogenous and predictable throughout each individual micropellet. However, the increase in total surface area was also associated with an important drawback, elution of sGAG molecules to the culture medium. Sulfated GAG loss during *in vitro* culture is a common problem in chondrogenesis studies [330] and it is exacerbated in micropellet platform where the total surface area is increased [18]. One of the possible explanations for sGAG loss to the medium may be the delay in accumulation of other critical matrix components such as aggrecan and collagen II [330]. Elution of sGAG molecules can also be facilitated by a cross-linking defect since sGAG molecules are attached to aggrecan protein and aggrecan proteins are linked to hyaluronan via linking protein (Fig. 2). Any defect interfering with these interactions may also contribute to sGAG elution. Additionally, formation of a cross-linked collagen II network is just as important because the components mentioned above are not cross-linked to collagen II molecules or attached to chondrocytes in native cartilage tissue. Therefore, their retention is solely based on the "entrapment" by the collagen network and the failure of establishing this structure can also contribute to the sGAG elution. It is now known that increasing collagen II content of the generated tissue is more challenging than upregulating sGAG production. Nevertheless, in Chapter 4 it was shown that after the assembly of micropellets the quantity of sGAG detected in the culture medium was rapidly reduced (Fig. 25). This indicates that a decrease in surface area may help retaining the produced sGAG molecules within the generated cartilage tissue [354].

All three studies contained two parts: micropellet characterization and micropellet assembly. Micropellets were only assembled in an organized fashion in Chapter 5 where an osteochondral-like tissue with two distinct layers was generated. In Chapters 3 and 4, the assembly step was performed in order to investigate the amalgamation efficiency of the individual micropellets. Micropellets were able to fuse at

all time points and single cells liberated from micropellets were able to fill the void space between individual micropellets. However, tissue integration was not always optimal since the assembled tissues were cultured for relatively short time periods (1-2 weeks). Once the micropellets were assembled into macroscopic tissues, diffusion gradient formation was mitigated because the increase in individual micropellet volume decreased the overall cell density of the generated tissue.

In all three studies, collagen II gene expression was efficiently upregulated in micropellets. However, upregulation of collagen II expression was always coupled with upregulation of unwanted hypertrophic marker collagen X expression. According to the developmental process, the chondrogenic marker collagen II expression must be observed before the hypertrophic marker collagen X [157,396] since hypertrophy takes place after chondrogenesis during endochondral ossification (Fig. 3, 4). However, in some studies it is demonstrated that collagen X is expressed prior to collagen II [396], which seems contrary to the developmental process. Similarly, in Chapter 4 in micropellets without cartilage dust, collagen X was already being expressed higher than collagen II on day 7 (Fig. 23). This uncoupling in the order of specific collagen expressions observed during *in vitro* chondrogenesis may be one of the consequences of monolayer expansion that takes place prior to differentiation. In a chicken development model, it is demonstrated that during endochondral ossification there is a timeframe where chondrocytes proliferate and generate the cartilage skeleton template but do not express collagen X [50]. The hypertrophy is later initiated in the middle of the tissue first with Ihh expression followed by collagen X expression [50]. Replicating this pure chondrogenic phenotype without collagen X expression has proven to be challenging in most MSC chondrogenesis studies. Perhaps the standard chondrogenic differentiation medium needs improvements such as addition of the hypertrophy inhibitor, PTHrP, which is suggested to alleviate collagen X expression during MSC chondrogenesis [397]. The reason for PTHrP is not being a component of the standard chondrogenic medium is that its role as the hypertrophy inhibitor is not well established yet. Therefore, including PTHrP in chondrogenic media is still considered as experimental rather than standard.

In addition to collagen X, the high expression of collagen I has been a major problem in chondrogenesis studies. Both chondrocytes and MSC seem to increase collagen I expression specifically during the monolayer expansion process. Collagen I is abundant in fibrocartilage and bone, however it is only present in insignificant amounts in hyaline cartilage. Therefore, the success of chondrogenesis is not only related to upregulation of collagen II expression but also to effective downregulation of collagen I expression. One possible way to overcome this problem would be optimization of cell expansion conditions, such as continuous provision of hypoxic atmosphere (Oxygen concentration section in Chapter 2). Additionally, some studies are focusing on developing different surface modification techniques in order to maximize chondrogenic differentiation of both chondrocytes and MSC [398,399]. In this project, the collagen II expression upregulation in micropellets was associated with the elevation of collagen I expression. This undesired increase in collagen I expression may also be caused by TGF-β 1, which is the main chondrogenic factor in the differentiation medium since this factor is also associated with collagen I expression stimulation in various tissues during development [381,382]. The chondrogenic media repeatedly used in chondrogenesis studies is perhaps optimized for the standard pellet culture, whereas the overall geometry and the total surface area are substantially changed in the micropellet platform. Therefore, customizing the chondrogenic differentiation media components and their concentrations according to the specific needs of the micropellets may have merit in order to simultaneously elevate the chondrogenic gene expression and repress the unwanted collagen X and I expressions effectively.

A recent study reported identification and specification of the mouse skeletal stem cells [400]. In this study, first a group of cells called postnatal skeletal stem cells were identified and then their specification was traced into cartilage, bone and stromal lineages. The researchers demonstrated that these skeletal stem cells can be expanded in the presence of BMP-2 and their osteogenic lineage commitment can be blocked via inhibition of VEGF signalling. Once the osteogenic lineage is blocked, these cells are able to form cartilage-like structures [400]. While being innovative, this study still must be validated with human cells. Until then, the closest adult human counterpart of these cells, bone marrow MSC, are extensively used in cartilage repair studies. In addition to

their role in contributing to the haematopoietic stem cell niche, MSC take place in long bone fracture healing process. During this process MSC are able to form a hyaline cartilage template in the fracture site, which is then replaced by newly forming bone tissue in a similar fashion observed during developmental endochondral ossification. To be able to routinely use bone marrow MSC in cartilage repair, their chondrogenic differentiation must be optimized and at the same time their hypertrophic features must be supressed [401].

The culture duration of the assembled tissues was relatively shorter (1-2 weeks) in all studies. Longer culture duration (i.e. few months) is not unusual in cartilage regeneration studies; however, the longer *ex vivo* culture duration would substantially increase the cost of a potential clinical application. Additionally, the tissue integration and maturation process may benefit from the early implantation of the micropellets or the generated tissues with provision of the true biochemical and biomechanical signals in the native cartilage microenvironment. As a result of the shorter culture period, at some cases assembled micropellets yielded an immature tissue structure and the micropellet impressions were still visible in the assembled tissues. Specifically, assembly of the osteochondral-like tissue in Chapter 5 was a worthy proof of concept demonstrating how to utilize micropellets as building blocks, but the tissue structure was suboptimal because of the deficiency in the collagen content of the chondral layer (Fig. 31). Thus, the generated scaffold-free tissues were not mechanically tested. It is possible that the large tissue geometry and high cell density may have contributed to the suboptimal tissue structure observed in the chondral layer. In future studies, mechanical testing may be applied to assembled tissues that are cultured longer preferably under dynamic conditions or tissues that are matured *in vivo*.

In general, collagen I expression was 100 times higher, collagen II expression was 10 times lower [300] and sGAG/DNA ratio was 200 times lower [402] in chondrogenic MSC micropellets when compared to native hyaline cartilage. The difference in relative ECM composition suggests that the MSC-derived cartilage tissue is deficient in cartilage-like matrix and maybe acquiring a bone-like matrix profile. Similar observations are often reported, and this reflects the current inability to

effectively differentiate MSC to enable the formation of hyaline cartilage and the mitigation of hypertrophy [401].

In Chapter 4, cartilage dust use and micropellet strategies were combined. The most common approach for direct incorporation of ECM components to the generated tissue has been single cell encapsulation in various types of hydrogels. However, there are two major drawbacks associated with that strategy; (1) lack of cell-cell interactions in single cell encapsulation, (2) lack of mechanical strength in a hydrogel. Micropellet use provided cell-cell interactions and the use of microscopic cartilage pieces increased the ECM content of the generated tissue significantly. Therefore, it is highly possible that a tissue generated with cartilage dust incorporated micropellets would be more similar to native cartilage than a hydrogel with single cell encapsulation. In this cartilage dust study, it was observed that a significant quantity of residual DNA was retained within cartilage dust (CD) particles. It is known that unmethylated CpG motifs in bacterial DNA can stimulate inflammatory response and induce arthritis [403], however it is less likely that vertebrate DNA would cause a similar response since vertebrate DNA contains less frequent CpG motifs, which are mostly methylated [404]. However, elimination of all nucleic acid content of the material is required to minimize the disease transmission risks, therefore removal of all nucleic acids is a critical step in a clinical setting, where xenogeneic or allogeneic material is transplanted. A large number of researchers are focusing on optimizing this decellularization process [273,274]. In the case of cartilage dust, removal of the residual DNA is even easier since the cartilage tissue is already crushed into microscopic pieces. However, decellularization was purposely avoided in this study because of the previous observations regarding the rapid loss of sGAG molecules in such processes. The sGAG and collagen II content of the CD was preserved because the initial aim of the study was to validate the chondroinductive effect of such matrix molecules on MSC micropellet phenotype. According to previous reports the presence of sGAG possibly enhances chondrogenesis [257,350]. However, in micropellet platform this effect could not be reproduced because the upregulation of chondrogenic gene expression was impaired in micropellets in the presence of cartilage dust (Fig. 23). This may potentially be caused by the presence of CD hindering the initial cell-cell interactions within the micropellet. This is parallel to previous findings

where superior chondrocyte redifferentiation with a significant upregulation of collagen II expression was observed in pellet culture but not in the alginate-based systems [111]. Similarly, these results may emphasize the importance of pellet culture, which allows cell-cell interactions and increases collagen II gene expression. Hence, the use of CD was promoted as a defect filling agent rather than a chondroinductive reagent in this study.

Specifically in Chapter 5, a significant upregulation of osteogenic gene expression was observed in chondrogenic-osteogenic (CO) cultured micropellets (Fig. 29). Similar effects were observed in recent studies where pre-conditioning or priming the MSC with chondrogenic medium was shown to enhance a subsequent osteogenic differentiation [62,383,384]. It was even suggested that chondrogenic priming could be exploited to accelerate tissue mineralization and bone formation after subcutaneous implantation [62,384]. This interesting finding may have the capacity to transform the traditional osteogenic differentiation methods in addition to raising questions regarding the possibility of optimizing MSC chondrogenesis.

Using micropellets as building blocks may provide numerous advantages, however at present this relatively recent method also has some limitations. The future work addressing these limitations and testing micropellet use *in vivo* may provide insight about the potential exploitation of micropellets in cell-based clinical applications.

3. Future perspectives

3.1. *In vivo* experiments and animal defect models

Before any novel approach is trialed in clinics, *in vivo* experimentation is routinely conducted in order to assure the safety of the procedure. In tissue engineering studies, the first step is generally the subcutaneous (SC) implantation of the generated tissue graft in immunodeficient mouse models. This method is widely used in order to assess the *in vivo* response to an *in vitro* generated tissue or biomaterial since the *in vitro* culture cannot always accurately mimic the *in vivo* conditions. As a result in SC implantation for most tissue types such as bone, the vascularization of the implanted tissue is a positive outcome since the new blood vessel formation throughout the newly generated tissue will be essential when the tissue is implanted into the defect site.

Controversially, the prevention of vascularization in SC implantation is a success for cartilaginous grafts since the native tissue does not bear any blood vessels. This technique is commonly used as an indicator of MSC chondrogenesis since in most cases MSC derived cartilaginous tissue is vascularized and mineralized whereas the native cartilage tissue or a tissue graft generated by chondrocytes have an intrinsic resistance to vascularization [397,405]. Therefore, it may be worthwhile to test the stability of chondrogenic phenotype in MSC micropellets via SC implantation method before moving to animal defect models.

A second, and perhaps a more reliable, approach is to test a newly developed technique in an animal defect model. Articular cartilage defect model of rabbits (lapine model) is commonly used [406-410]. The Autologous Chondrocyte Implantation (ACI) was first tested in a rabbit defect model [411] before being translated into clinics. However, in most studies conducted on small animal models, the control groups also demonstrate self-healing to some extent, raising questions about the credibility of small animal models. The reason for self-healing effect in small animals is thought to be the relatively smaller dimensions of the tissue specifically the thickness, which is in the range of few cell layers whereas the human cartilage has a thickness of few millimeters (Fig. 36) [412]. The small animal defect models are cost effective and more practical but they are dimensionally inaccurate. This is why large animal defect models are preferred, when possible, for regeneration studies of orthopedic tissues such as bone and cartilage. Most commonly used large animal models are sheep (ovine model) [413-416], goat (caprine model) [417-419], pig (porcine model) [420-422] and horse (equine model) [203,423]. Even though the cartilage thickness for most of these animals does not match the human counterpart (Fig. 36), the *in vivo* results obtained via large animal models are thought to be more reliable. In conclusion, despite cost intensiveness and requirement of access to specialized animal facilities, large animal defect models are the critical intermediate testing step between the *in vitro* engineered construct and the clinical trials for orthopedic tissues. Therefore, it is necessary to test the use of chondrocyte micropellets (Chapter 3) and MSC micropellets with cartilage dust (Chapter 4) and the osteochondral-like tissue built with micropellets (Chapter 5) preferably in a large animal model in order to predict their clinical potential and applicability in the future.

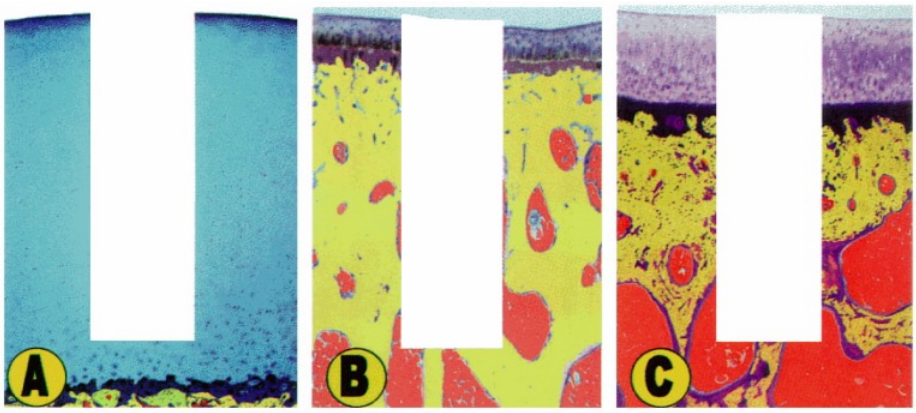

Figure 36. Articular cartilage thickness comparison. Histology section of human (A), rabbit (B) and goat (C) articular cartilage are shown. Image is courtesy of WKH, taken from [424], see App. G for permission.

3.2. Mass production of micropellets

In order to utilize them at a clinical scale, micropellets need to be generated in large numbers. In a rough estimation, to be able to fill a small size, 1 cm^3, cartilage defect ~418,000 micropellets will be required according to hexagonal close packing model (assuming that the micropellets are perfectly spherical and have a diameter of 150 μm). With the existing platform, 36,000 micropellets can be generated in a single 6-well plate (6000 each well), however the static culture and manual handling of micropellets in multiwell plates is a labor-intensive and care-demanding technique. Therefore, mass production of micropellets can be achieved via closed bioreactor systems, which can provide dynamic culture conditions. Powers *et al.* introduced a similar concept in 2001 where they described a closed perfusion bioreactor design with a microwell pattern inside, which provides dynamic culture conditions to liver cells in micropellets [425,426]. A similar, bigger scale, sterile and disposable bioreactor platform can be designed in order to generate large numbers of micropellets for clinical applications. Once the perfusion rate and media components are optimized, such platform will allow cell seeding, micropellet formation, differentiation and culture to be performed all together in an automated fashion reducing the handling and the cost of the micropellet mass production process.

3.3. Complex tissue engineering with micropellets

Unlike cartilage tissue engineering, *ex vivo* generation of complex tissues such as kidney or lung requires multiple cell types, different tissue zones with different properties and critically blood vessels in order to facilitate cell and tissue survival *ex vivo* and *in vivo*. The *ex vivo* generation of small diameter vascular graft to be used in bypass surgeries is a hot topic itself. Forgacs *et al.* introduced a novel method where they form separate micropellets of smooth muscle cells and fibroblasts then combine them using a rapid prototyping bioprinter to generate a scaffold-free small diameter vascular graft [427]. They also suggest it may be possible to engineer even more complex grafts using micropellets as building blocks (Fig. 37) [428]. Similarly, I think the micropellets enable engineering tissue grafts in higher resolution provided by their micron-scale, controllable size. In the future, using zonal chondrocyte micropellets, it may be possible to engineer cartilage constructs with biomimetic zones (Chapter 3, Fig. 18B).

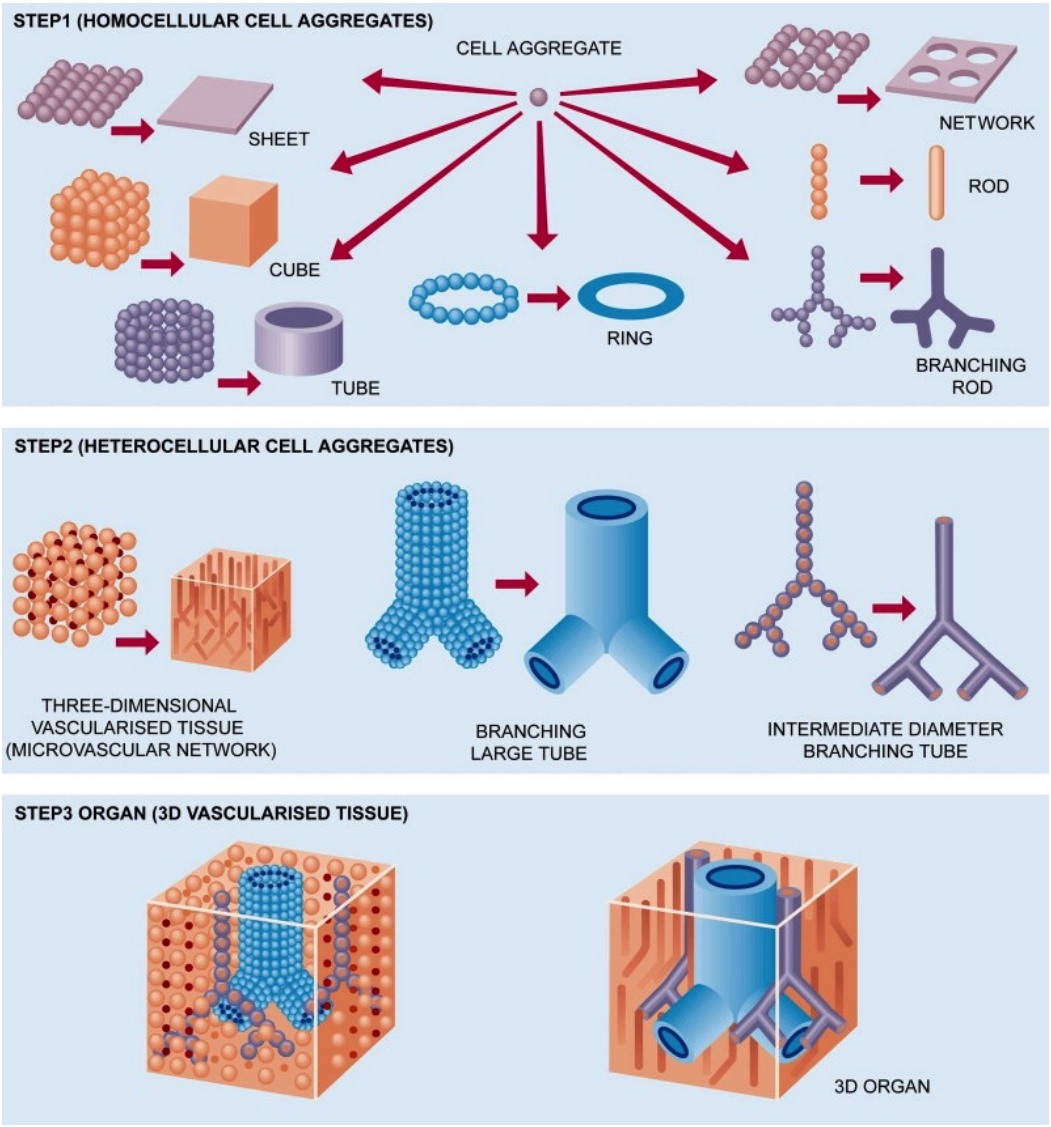

Figure 37. Complex tissue engineering using micropellets. An illustration demonstrating how to use micropellets to engineer complex tissues. Image is courtesy of Elsevier, taken from [428], see App. G for permission.

4. Closing remarks

"*Imagine that one day a patient will go to a human 'body shop' for a prescription for a lost leg, a failing liver, or a dysfunctional heart. In addition to the physiological, medical, and genetic information of the patient, the doctor will also collect three-dimensional images of the patient's remaining leg (in the case of the lost-leg patient) with detailed anatomical structures (bone, cartilage, tendons, ligaments, blood vessels, muscles, nerves, skin, and so forth) and the external shape. The doctor may collect the patient's saliva or other body fluids to extract genetic material (DNA)*

and also a tiny piece of tissue or bone marrow to obtain seeding cells for expansion. After the patient leaves the body shop, a computer is used by a tissue engineer to design the structure of the mirror leg (the lost leg) based on the symmetrical remaining leg, using various materials that simulate the extracellular matrices of the tissues of the leg (known as scaffolds or templates). Then, cells – from a universal cell source, specifically designed for the patient, or banked cells grown from the patient's own cells – are seeded onto these scaffolds. These engineered cell-scaffold components are then grown separately and/or assembled in a special chamber (bioreactor) that provides the right nutrients, regulating molecules (such as proteins, growth factors, and differentiation factors), physical and mechanical stimuli, temperature, pressure, and mass transport conditions for cell proliferation, differentiation, and tissue/organ formation. While the tissue/organ is regenerating, the scaffolding materials degrade and disappear, leaving nothing foreign to the body. The regenerated leg or leg precursor will be surgically grafted onto the patient during the second visit to the human body shop. The engineered tissues will have the capacity to grow, model, and remodel in concert with the dynamic changes of the physiological environment of the body. The grafted leg will integrate into the body. The new leg will grow and age as the body's natural leg. This scenario is an example of what the field of tissue engineering is hoping to do in the future." (Quotation is re-used with permission from Elsevier, see App. A).

Peter X. Ma explains the overall aim of tissue engineering studies in a very ideal and futuristic way in the previous paragraph [429]. Similarly, a closed bioreactor system was described by Martin *et al.,* which takes a tissue biopsy as an input then designs, generates and presents the missing body part as an output ready to be implanted into the patient's body (Fig. 38) [430]. Time will tell whether such systems are too ideal to be true or can be achieved via accumulation of research baby steps taken every day, in every laboratory all around the world, but I think the micropellets of varying size, cell type and composition will take their place as useful tools, as building blocks in the body shops or organ factories of the future.

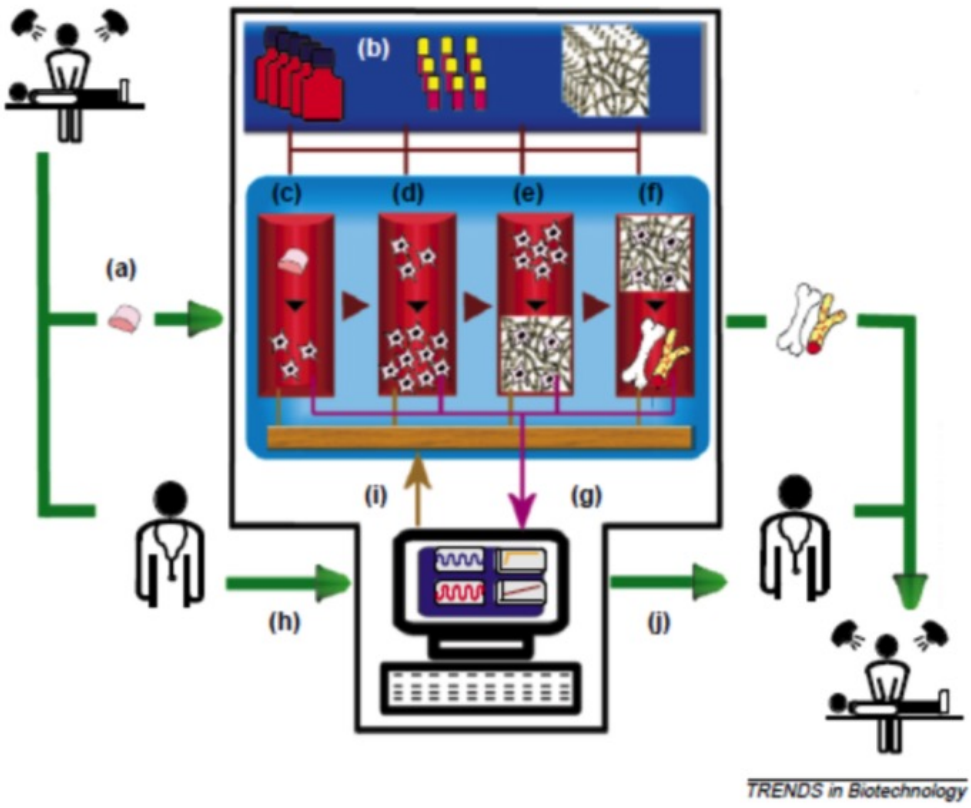

Figure 38. A theoretical "organ factory". The illustration describes where the field of tissue engineering is hoping to achieve in the future. Ideally the patients sees a doctor and a biopsy is taken, the cells are isolated, expanded, seeded on templates, cultured until the regenerated organ is mature enough to be implanted back into patient's body. Image is courtesy of Elsevier, taken from [430], see App. I for permission.

Bibliography

1. Vos T, Flaxman AD, Naghavi M, Lozano R, Michaud C, et al. (2012) Years lived with disability (YLDs) for 1160 sequelae of 289 diseases and injuries 1990-2010: a systematic analysis for the Global Burden of Disease Study 2010. Lancet 380: 2163-2196.
2. Chen A, Gupte C, Akhtar K, Smith P, Cobb J (2012) The Global Economic Cost of Osteoarthritis: How the UK Compares. Arthritis 2012: 698709.
3. Murray CJ, Lopez AD (1997) Global mortality, disability, and the contribution of risk factors: Global Burden of Disease Study. Lancet 349: 1436-1442.
4. Arthritis and Osteoporosis Victoria . (2013) A problem worth solving. Elsternwick: Arthritis and Osteoporosis Victoria.
5. Arden N, Nevitt MC (2006) Osteoarthritis: epidemiology. Best Practice & Research Clinical Rheumatology 20: 3-25.
6. Hanna FS, Teichtahl AJ, Wluka AE, Wang Y, Urquhart DM, et al. (2009) Women have increased rates of cartilage loss and progression of cartilage defects at the knee than men: a gender study of adults without clinical knee osteoarthritis. Menopause 16: 666-670.
7. Walker-Bone K, Javaid K, Arden N, Cooper C (2000) Regular review: medical management of osteoarthritis. BMJ 321: 936-940.
8. Cross M, Smith E, Hoy D, Nolte S, Ackerman I, et al. (2014) The global burden of hip and knee osteoarthritis: estimates from the Global Burden of Disease 2010 study. Ann Rheum Dis.
9. Sampson S, Reed M, Silvers H, Meng M, Mandelbaum B (2010) Injection of platelet-rich plasma in patients with primary and secondary knee osteoarthritis: a pilot study. American Journal of Physical Medicine & Rehabilitation 89: 961-969.
10. De Ceuninck F, Berenbaum F (2009) Proteomics: addressing the challenges of osteoarthritis. Drug Discov Today 14: 661-667.
11. Benedek TG (2006) A history of the understanding of cartilage. Osteoarthritis Cartilage 14: 203-209.
12. Galen. (Cited in Benedek 2006) On the usefulness of various parts of the body. Ithaca, NY: Cornell University Press, 1968. Trans. by M.T. May (a) Book 16, ii (1:683) (b) Book 12, ii (1:552).
13. Lind LR (Cited in Benedek 2006) Studies in pre-Vesalien anatomy, Niccolo Massa: Introductory book on anatomy (1536). Philadelphia: American philosophical society, 1975. Chap. 43, p. 250.
14. Tonybee J (Cited in Benedek 2006) Researches, tending to prove the non-vascularity and the peculiar uniform mode of organization and nutrition of certain animal tissues, viz. articular cartilage and the cartilage of the different classes of fibro-cartilage;... (1841). Philos Trans R Soc Lond B Biol Sci 164.
15. JB. M (Cited in Benedek 2006) The seats and the causes of diseases investigated by anatomy (1761). London: Millar and Cadell Vol. 3. Trans. by B. Alexander, p. 321.
16. Hunter W (Cited in Benedek 2006) Of the structure and diseases of articulating cartilages (1743). Philos Trans R Soc Lond 42:514-21.

17. Babur BK, Ghanavi P, Levett P, Lott WB, Klein T, et al. (2013) The interplay between chondrocyte redifferentiation pellet size and oxygen concentration. PLoS One 8: e58865.
18. Markway BD, Tan GK, Brooke G, Hudson JE, Cooper-White JJ, et al. (2010) Enhanced chondrogenic differentiation of human bone marrow-derived mesenchymal stem cells in low oxygen environment micropellet cultures. Cell Transplant 19: 29-42.
19. Kabiri M, Kul B, Lott WB, Futrega K, Ghanavi P, et al. (2012) 3D mesenchymal stem/stromal cell osteogenesis and autocrine signalling. Biochem Biophys Res Commun 419: 142-147.
20. Buckwalter JA, Mankin HJ (1998) Articular cartilage: tissue design and chondrocyte-matrix interactions. Instr Course Lect 47: 477-486.
21. Mankin HJ (1982) The response of articular cartilage to mechanical injury. J Bone Joint Surg Am 64: 460-466.
22. Poole CA, Flint MH, Beaumont BW (1988) Chondrons extracted from canine tibial cartilage: preliminary report on their isolation and structure. J Orthop Res 6: 408-419.
23. Poole CA, Flint MH, Beaumont BW (1987) Chondrons in cartilage: ultrastructural analysis of the pericellular microenvironment in adult human articular cartilages. J Orthop Res 5: 509-522.
24. Guilak F, Alexopoulos LG, Upton ML, Youn I, Choi JB, et al. (2006) The pericellular matrix as a transducer of biomechanical and biochemical signals in articular cartilage. Ann N Y Acad Sci 1068: 498-512.
25. Alexopoulos LG, Setton LA, Guilak F (2005) The biomechanical role of the chondrocyte pericellular matrix in articular cartilage. Acta Biomater 1: 317-325.
26. Watanabe H, Yamada Y, Kimata K (1998) Roles of aggrecan, a large chondroitin sulfate proteoglycan, in cartilage structure and function. J Biochem 124: 687-693.
27. Roughley PJ (2006) The structure and function of cartilage proteoglycans. Eur Cell Mater 12: 92-101.
28. Mow VC, Holmes MH, Lai WM (1984) Fluid transport and mechanical properties of articular cartilage: a review. J Biomech 17: 377-394.
29. Bhosale AM, Richardson JB (2008) Articular cartilage: structure, injuries and review of management. Br Med Bull 87: 77-95.
30. Akizuki S, Mow VC, Muller F, Pita JC, Howell DS, et al. (1986) Tensile properties of human knee joint cartilage: I. Influence of ionic conditions, weight bearing, and fibrillation on the tensile modulus. J Orthop Res 4: 379-392.
31. Shepherd D, Seedhom B (1999) The'instantaneous' compressive modulus of human articular cartilage in joints of the lower limb. Rheumatology 38: 124-132.
32. Kutzner I, Heinlein B, Graichen F, Bender A, Rohlmann A, et al. (2010) Loading of the knee joint during activities of daily living measured in vivo in five subjects. Journal of biomechanics 43: 2164-2173.
33. Hungerford DS, Barry M (1979) Biomechanics of the patellofemoral joint. Clinical orthopaedics and related research 144: 9-15.
34. DeLise A, Fischer L, Tuan R (2000) Cellular interactions and signaling in cartilage development. Osteoarthritis and cartilage 8: 309-334.

35. Toole BP (1972) Hyaluronate turnover during chondrogenesis in the developing chick limb and axial skeleton. Developmental biology 29: 321-329.
36. Pizette S, Niswander L (2000) BMPs are required at two steps of limb chondrogenesis: formation of prechondrogenic condensations and their differentiation into chondrocytes. Developmental biology 219: 237-249.
37. Linsenmayer TF, Toole BP, Trelstad RL (1973) Temporal and spatial transitions in collagen types during embryonic chick limb development. Developmental biology 35: 232-239.
38. Toole BP, Jackson G, Gross J (1972) Hyaluronate in morphogenesis: inhibition of chondrogenesis in vitro. Proceedings of the National Academy of Sciences 69: 1384-1386.
39. Chimal-Monroy J, Diaz de Leon L (1999) Expression of N-cadherin, N-CAM, fibronectin and tenascin is stimulated by TGF-beta1, beta2, beta3 and beta5 during the formation of precartilage condensations. Int J Dev Biol 43: 59-67.
40. Zimmermann B (1984) Assembly and disassembly of gap junctions during mesenchymal cell condensation and early chondrogenesis in limb buds of mouse embryos. Journal of anatomy 138: 351.
41. Coelho CN, Kosher RA (1991) Gap junctional communication during limb cartilage differentiation. Developmental biology 144: 47-53.
42. Gehris AL, Stringa E, Spina J, Desmond ME, Tuan RS, et al. (1997) The region encoded by the alternatively spliced exon IIIA in mesenchymal fibronectin appears essential for chondrogenesis at the level of cellular condensation. Developmental biology 190: 191-205.
43. Frenz DA, Jaikaria NS, Newman SA (1989) The mechanism of precartilage mesenchymal condensation: a major role for interaction of the cell surface with the amino-terminal heparin-binding domain of fibronectin. Developmental biology 136: 97-103.
44. Oberlender SA, Tuan RS (1994) Expression and functional involvement of N-cadherin in embryonic limb chondrogenesis. Development 120: 177-187.
45. Oberlender SA, Tuan RS (1994) Spatiotemporal profile of N-cadherin expression in the developing limb mesenchyme. Cell Communication and Adhesion 2: 521-537.
46. Fallon JF, Lopez A, Ros MA, Savage MP, Olwin BB, et al. (1994) FGF-2: apical ectodermal ridge growth signal for chick limb development. Science 264: 104-107.
47. Niswander L, Tickle C, Vogel A, Booth I, Martin GR (1993) FGF-4 replaces the apical ectodermal ridge and directs outgrowth and patterning of the limb. Cell 75: 579-587.
48. Summerbell D, Lewis J, Wolpert L (1973) Positional information in chick limb morphogenesis. Nature 244: 492-496.
49. Francis PH, Richardson MK, Brickell PM, Tickle C (1994) Bone morphogenetic proteins and a signalling pathway that controls patterning in the developing chick limb. Development 120: 209-218.
50. Vortkamp A, Lee K, Lanske B, Segre GV, Kronenberg HM, et al. (1996) Regulation of rate of cartilage differentiation by Indian hedgehog and PTH-related protein. Science 273: 613-622.

51. Lanske B, Karaplis AC, Lee K, Luz A, Vortkamp A, et al. (1996) PTH/PTHrP Receptor in Early Development and Indian Hedgehog--Regulated Bone Growth. Science 273: 663-666.
52. Gadjanski I, Spiller K, Vunjak-Novakovic G (2012) Time-dependent processes in stem cell-based tissue engineering of articular cartilage. Stem Cell Reviews and Reports 8: 863-881.
53. Dennison E, Cooper C (2003) Osteoarthritis: epidemiology and classification. Hochberg M, Silmon A, Smolen A, et al Rheumatology New York Mosby: 1981-1984.
54. Kuroki K, Stoker AM, Cook JL (2005) Effects of proinflammatory cytokines on canine articular chondrocytes in a three-dimensional culture. American journal of veterinary research 66: 1187-1196.
55. Jackson RW, Dieterichs C (2003) The results of arthroscopic lavage and debridement of osteoarthritic knees based on the severity of degeneration: a 4- to 6-year symptomatic follow-up. Arthroscopy 19: 13-20.
56. Wray NP, Moseley JB, O'Malley K (2003) Arthroscopic treatment of osteoarthritis of the knee. J Bone Joint Surg Am 85-A: 381.
57. Moseley JB, O'Malley K, Petersen NJ, Menke TJ, Brody BA, et al. (2002) A controlled trial of arthroscopic surgery for osteoarthritis of the knee. N Engl J Med 347: 81-88.
58. Katz JN, Brophy RH, Chaisson CE, de Chaves L, Cole BJ, et al. (2013) Surgery versus physical therapy for a meniscal tear and osteoarthritis. N Engl J Med 368: 1675-1684.
59. Edelson R, Burks RT, Bloebaum RD (1995) Short-term effects of knee washout for osteoarthritis. Am J Sports Med 23: 345-349.
60. Gobbi A, Nunag P, Malinowski K (2005) Treatment of full thickness chondral lesions of the knee with microfracture in a group of athletes. Knee Surg Sports Traumatol Arthrosc 13: 213-221.
61. Dixon T, Urquhart DM, Berry P, Bhatia K, Wang Y, et al. (2011) Variation in rates of hip and knee joint replacement in Australia based on socio-economic status, geographical locality, birthplace and indigenous status. ANZ J Surg 81: 26-31.
62. Farrell E, Both SK, Odörfer KI, Koevoet W, Kops N, et al. (2011) In-vivo generation of bone via endochondral ossification by in-vitro chondrogenic priming of adult human and rat mesenchymal stem cells. BMC musculoskeletal disorders 12: 31.
63. Dreghorn CR, Roughneen P, Graham J, Hamblen DL (1986) The real cost of joint replacement. Br Med J (Clin Res Ed) 292: 1636-1637.
64. March L, Cross M, Tribe K, Lapsley H, Courtenay B, et al. (2002) Cost of joint replacement surgery for osteoarthritis: the patients' perspective. J Rheumatol 29: 1006-1014.
65. Steadman JR, Rodkey WG, Rodrigo JJ (2001) Microfracture: surgical technique and rehabilitation to treat chondral defects. Clin Orthop Relat Res: S362-369.
66. Johnson LL (1986) Arthroscopic abrasion arthroplasty historical and pathologic perspective: present status. Arthroscopy 2: 54-69.
67. Magnuson PB (1941) Joint debridement. Surgical treatment of degenerative arthritis. Surg Gynecol Obstet 73: 61-67.

68. Pridie K, Gordon G. A method of resurfacing osteoarthritic knee joints; 1959. Journal of Bone and Joint Surgery-British Volume. pp. 618-619.
69. Steadman JR, Rodkey WG, Singleton SB, Briggs KK (1997) Microfracture technique forfull-thickness chondral defects: Technique and clinical results. Operative techniques in orthopaedics 7: 300-304.
70. Alford JW, Cole BJ (2005) Cartilage restoration, part 1: basic science, historical perspective, patient evaluation, and treatment options. Am J Sports Med 33: 295-306.
71. Buckwalter JA, Mow VC, Ratcliffe A (1994) Restoration of Injured or Degenerated Articular Cartilage. J Am Acad Orthop Surg 2: 192-201.
72. Smith GD, Knutsen G, Richardson JB (2005) A clinical review of cartilage repair techniques. J Bone Joint Surg Br 87: 445-449.
73. Khan IM, Gilbert SJ, Singhrao SK, Duance VC, Archer CW (2008) Cartilage integration: evaluation of the reasons for failure of integration during cartilage repair. A review. Eur Cell Mater 16: 26-39.
74. Shapiro F, Koide S, Glimcher MJ (1993) Cell origin and differentiation in the repair of full-thickness defects of articular cartilage. J Bone Joint Surg Am 75: 532-553.
75. Hunziker EB (2002) Articular cartilage repair: basic science and clinical progress. A review of the current status and prospects. Osteoarthritis Cartilage 10: 432-463.
76. Mithoefer K, McAdams T, Williams RJ, Kreuz PC, Mandelbaum BR (2009) Clinical Efficacy of the Microfracture Technique for Articular Cartilage Repair in the Knee An Evidence-Based Systematic Analysis. The American journal of sports medicine 37: 2053-2063.
77. Homminga GN, Bulstra SK, Bouwmeester PS, van der Linden AJ (1990) Perichondral grafting for cartilage lesions of the knee. J Bone Joint Surg Br 72: 1003-1007.
78. Homminga GN, van der Linden TJ, Terwindt-Rouwenhorst EA, Drukker J (1989) Repair of articular defects by perichondrial grafts. Experiments in the rabbit. Acta Orthop Scand 60: 326-329.
79. Niedermann B, Boe S, Lauritzen J, Rubak JM (1985) Glued periosteal grafts in the knee. Acta Orthopaedica 56: 457-460.
80. Rubak JM (1982) Reconstruction of articular cartilage defects with free periosteal grafts: an experimental study. Acta Orthopaedica 53: 175-180.
81. Rubak JM, Poussa M, Ritsilá V (1982) Chondrogenesis in repair of articular cartilage defects by free periosteal grafts in rabbits. Acta Orthopaedica 53: 181-186.
82. Tomford WW, Springfield DS, Mankin HJ (1992) Fresh and frozen articular cartilage allografts. Orthopedics 15: 1183-1188.
83. Matsusue Y, Yamamuro T, Hama H (1993) Arthroscopic multiple osteochondral transplantation to the chondral defect in the knee associated with anterior cruciate ligament disruption. Arthroscopy 9: 318-321.
84. Solheim E, Hegna J, Oyen J, Harlem T, Strand T (2013) Results at 10 to 14 years after osteochondral autografting (mosaicplasty) in articular cartilage defects in the knee. Knee 20: 287-290.
85. McCoy B, Miniaci A (2012) Osteochondral autograft transplantation/mosaicplasty. J Knee Surg 25: 99-108.

86. Bader S, Miniaci A (2011) Mosaicplasty. Orthopedics 34: e491-493.
87. Wajid MA, Shah MI, Mohsin e A, Ahmad T (2011) Osteochondral grafting of knee joint using mosaicplasty. J Coll Physicians Surg Pak 21: 184-186.
88. Hangody L, Kish G, Karpati Z, Szerb I, Udvarhelyi I (1997) Arthroscopic autogenous osteochondral mosaicplasty for the treatment of femoral condylar articular defects. A preliminary report. Knee Surg Sports Traumatol Arthrosc 5: 262-267.
89. Huang H, Yin Q, Zhang Y, Zhang Y, Cao Z, et al. (2002) [Mosaicplasty osteochondral grafting to repair cartilaginous defects under arthroscopy]. Zhonghua Wai Ke Za Zhi 40: 662-664.
90. Huntley JS, Bush PG, McBirnie JM, Simpson AH, Hall AC (2005) Chondrocyte death associated with human femoral osteochondral harvest as performed for mosaicplasty. J Bone Joint Surg Am 87: 351-360.
91. Bentley G, Minas T (2000) Science, medicine, and the future: Treating joint damage in young people. BMJ: British Medical Journal 320: 1585.
92. Grande DA, Pitman MI, Peterson L, Menche D, Klein M (1989) The repair of experimentally produced defects in rabbit articular cartilage by autologous chondrocyte transplantation. J Orthop Res 7: 208-218.
93. Brittberg M, Lindahl A, Nilsson A, Ohlsson C, Isaksson O, et al. (1994) Treatment of deep cartilage defects in the knee with autologous chondrocyte transplantation. N Engl J Med 331: 889-895.
94. Peterson L, Minas T, Brittberg M, Nilsson A, Sjogren-Jansson E, et al. (2000) Two- to 9-year outcome after autologous chondrocyte transplantation of the knee. Clin Orthop Relat Res: 212-234.
95. Browne JE, Anderson AF, Arciero R, Mandelbaum B, Moseley JB, Jr., et al. (2005) Clinical outcome of autologous chondrocyte implantation at 5 years in US subjects. Clin Orthop Relat Res: 237-245.
96. Marlovits S, Striessnig G, Resinger CT, Aldrian SM, Vecsei V, et al. (2004) Definition of pertinent parameters for the evaluation of articular cartilage repair tissue with high-resolution magnetic resonance imaging. Eur J Radiol 52: 310-319.
97. Marlovits S, Zeller P, Singer P, Resinger C, Vecsei V (2006) Cartilage repair: generations of autologous chondrocyte transplantation. Eur J Radiol 57: 24-31.
98. Haddo O, Mahroof S, Higgs D, David L, Pringle J, et al. (2004) The use of chondrogide membrane in autologous chondrocyte implantation. The Knee 11: 51-55.
99. Robertson WB, Fick D, Wood DJ, Linklater JM, Zheng MH, et al. (2007) MRI and clinical evaluation of collagen-covered autologous chondrocyte implantation (CACI) at two years. Knee 14: 117-127.
100. Behrens P, Ehlers E, Köchermann K, Rohwedel J, Russlies M, et al. (1999) New therapy procedure for localized cartilage defects. Encouraging results with autologous chondrocyte implantation. MMW Fortschritte der Medizin 141: 49-51.
101. Behrens P, Bitter T, Kurz B, Russlies M (2006) Matrix-associated autologous chondrocyte transplantation/implantation (MACT/MACI)--5-year follow-up. Knee 13: 194-202.

102. Bachmann G, Basad E, Lommel D, Steinmeyer J (2004) [MRI in the follow-up of matrix-supported autologous chondrocyte transplantation (MACI) and microfracture]. Radiologe 44: 773-782.
103. Bartlett W, Skinner JA, Gooding CR, Carrington RW, Flanagan AM, et al. (2005) Autologous chondrocyte implantation versus matrix-induced autologous chondrocyte implantation for osteochondral defects of the knee: a prospective, randomised study. J Bone Joint Surg Br 87: 640-645.
104. Marlovits S, Striessnig G, Kutscha-Lissberg F, Resinger C, Aldrian SM, et al. (2005) Early postoperative adherence of matrix-induced autologous chondrocyte implantation for the treatment of full-thickness cartilage defects of the femoral condyle. Knee Surg Sports Traumatol Arthrosc 13: 451-457.
105. Trattnig S, Ba-Ssalamah A, Pinker K, Plank C, Vecsei V, et al. (2005) Matrix-based autologous chondrocyte implantation for cartilage repair: noninvasive monitoring by high-resolution magnetic resonance imaging. Magn Reson Imaging 23: 779-787.
106. Zheng M-H, Willers C, Kirilak L, Yates P, Xu J, et al. (2007) Matrix-induced autologous chondrocyte implantation (MACI®): biological and histological assessment. Tissue engineering 13: 737-746.
107. Zhang Z, Ye Q, Yang Z, Yin M, Bai J, et al. (2006) Matrix-induced autologous chondrocyte implantation for treatment of chondral defects of knee: a preliminary report. Journal of musculoskeletal research 10: 95-101.
108. Brittberg M (2010) Cell carriers as the next generation of cell therapy for cartilage repair: a review of the matrix-induced autologous chondrocyte implantation procedure. Am J Sports Med 38: 1259-1271.
109. Gille J, Schuseil E, Wimmer J, Gellissen J, Schulz AP, et al. (2010) Mid-term results of Autologous Matrix-Induced Chondrogenesis for treatment of focal cartilage defects in the knee. Knee Surg Sports Traumatol Arthrosc 18: 1456-1464.
110. Libera J, Luethi U, Alasevic O (2006) Co. don chondrosphere (Co. don AG) autologous matrix engineered cartilage transplantation. Basic Science, Clinical Repair, and Reconstruction of Articular Cartilage Defects: Current Status and Prospects Bologna, Italy: Timeo Editore: 591-600.
111. Bernstein P, Dong M, Corbeil D, Gelinsky M, Gunther KP, et al. (2009) Pellet culture elicits superior chondrogenic redifferentiation than alginate-based systems. Biotechnol Prog 25: 1146-1152.
112. Martinez I, Elvenes J, Olsen R, Bertheussen K, Johansen O (2008) Redifferentiation of in vitro expanded adult articular chondrocytes by combining the hanging-drop cultivation method with hypoxic environment. Cell Transplant 17: 987-996.
113. Furukawa KS, Suenaga H, Toita K, Numata A, Tanaka J, et al. (2003) Rapid and large-scale formation of chondrocyte aggregates by rotational culture. Cell Transplant 12: 475-479.
114. Mahmoudifar N, Doran PM (2012) Chondrogenesis and cartilage tissue engineering: the longer road to technology development. Trends Biotechnol 30: 166-176.

115. von der Mark K, Gauss V, von der Mark H, Müller P (1977) Relationship between cell shape and type of collagen synthesised as chondrocytes lose their cartilage phenotype in culture.
116. Lin Z, Fitzgerald JB, Xu J, Willers C, Wood D, et al. (2008) Gene expression profiles of human chondrocytes during passaged monolayer cultivation. Journal of Orthopaedic Research 26: 1230-1237.
117. Glowacki J, Trepman E, Folkman J (1983) Cell shape and phenotypic expression in chondrocytes. Experimental Biology and Medicine 172: 93-98.
118. Xu C, Oyajobi BO, Frazer A, Kozaci LD, Russell RG, et al. (1996) Effects of growth factors and interleukin-1 alpha on proteoglycan and type II collagen turnover in bovine nasal and articular chondrocyte pellet cultures. Endocrinology 137: 3557-3565.
119. Hilfiker A, Kasper C, Hass R, Haverich A (2011) Mesenchymal stem cells and progenitor cells in connective tissue engineering and regenerative medicine: is there a future for transplantation? Langenbecks Arch Surg 396: 489-497.
120. Guilak F, Awad HA, Fermor B, Leddy HA, Gimble JM (2004) Adipose-derived adult stem cells for cartilage tissue engineering. Biorheology 41: 389-399.
121. Gimble J, Guilak F (2003) Adipose-derived adult stem cells: isolation, characterization, and differentiation potential. Cytotherapy 5: 362-369.
122. Lee RH, Kim B, Choi I, Kim H, Choi H, et al. (2004) Characterization and expression analysis of mesenchymal stem cells from human bone marrow and adipose tissue. Cellular Physiology and Biochemistry 14: 311-324.
123. Im G-I, Shin Y-W, Lee K-B (2005) Do adipose tissue-derived mesenchymal stem cells have the same osteogenic and chondrogenic potential as bone marrow-derived cells? Osteoarthritis and cartilage 13: 845-853.
124. Sorensen AL, Jacobsen BM, Reiner AH, Andersen IS, Collas P (2010) Promoter DNA methylation patterns of differentiated cells are largely programmed at the progenitor stage. Mol Biol Cell 21: 2066-2077.
125. Sorensen AL, Timoskainen S, West FD, Vekterud K, Boquest AC, et al. (2010) Lineage-specific promoter DNA methylation patterns segregate adult progenitor cell types. Stem Cells Dev 19: 1257-1266.
126. Mackie E, Ahmed Y, Tatarczuch L, Chen K-S, Mirams M (2008) Endochondral ossification: how cartilage is converted into bone in the developing skeleton. The international journal of biochemistry & cell biology 40: 46-62.
127. Ortega N, Behonick DJ, Werb Z (2004) Matrix remodeling during endochondral ossification. Trends in cell biology 14: 86-93.
128. Kolf CM, Cho E, Tuan RS (2007) Biology of adult mesenchymal stem cells: regulation of niche, self-renewal and differentiation. Arthritis Res Ther 9: 204.
129. Neuhuber B, Gallo G, Howard L, Kostura L, Mackay A, et al. (2004) Reevaluation of in vitro differentiation protocols for bone marrow stromal cells: disruption of actin cytoskeleton induces rapid morphological changes and mimics neuronal phenotype. Journal of Neuroscience Research 77: 192-204.
130. Mackay AM, Beck SC, Murphy JM, Barry FP, Chichester CO, et al. (1998) Chondrogenic differentiation of cultured human mesenchymal stem cells from marrow. Tissue engineering 4: 415-428.

131. Phinney DG, Prockop DJ (2007) Concise review: mesenchymal stem/multipotent stromal cells: the state of transdifferentiation and modes of tissue repair—current views. Stem cells 25: 2896-2902.
132. Vogel W, Grunebach F, Messam CA, Kanz L, Brugger W, et al. (2003) Heterogeneity among human bone marrow-derived mesenchymal stem cells and neural progenitor cells. Haematologica 88: 126-133.
133. Engler AJ, Sen S, Sweeney HL, Discher DE (2006) Matrix elasticity directs stem cell lineage specification. Cell 126: 677-689.
134. Dominici M, Le Blanc K, Mueller I, Slaper-Cortenbach I, Marini F, et al. (2006) Minimal criteria for defining multipotent mesenchymal stromal cells. The International Society for Cellular Therapy position statement. Cytotherapy 8: 315-317.
135. Simmons PJ, Torok-Storb B (1991) Identification of stromal cell precursors in human bone marrow by a novel monoclonal antibody, STRO-1. Blood 78: 55-62.
136. Gronthos S, Graves S, Ohta S, Simmons P (1994) The STRO-1+ fraction of adult human bone marrow contains the osteogenic precursors. Blood 84: 4164-4173.
137. Stewart K, Walsh S, Screen J, Jefferiss CM, Chainey J, et al. (1999) Further characterization of cells expressing STRO−1 in cultures of adult human bone marrow stromal cells. Journal of Bone and Mineral Research 14: 1345-1356.
138. Lin G, Liu G, Banie L, Wang G, Ning H, et al. (2011) Tissue distribution of mesenchymal stem cell marker Stro-1. Stem cells and development 20: 1747-1752.
139. Pinho S, Lacombe J, Hanoun M, Mizoguchi T, Bruns I, et al. (2013) PDGFRα and CD51 mark human Nestin+ sphere-forming mesenchymal stem cells capable of hematopoietic progenitor cell expansion. The Journal of experimental medicine 210: 1351-1367.
140. Wislet−Gendebien S, Hans G, Leprince P, Rigo JM, Moonen G, et al. (2005) Plasticity of cultured mesenchymal stem cells: Switch from nestin−positive to excitable neuron−like phenotype. Stem cells 23: 392-402.
141. Wislet-Gendebien S, Wautier F, Leprince P, Rogister B (2005) Astrocytic and neuronal fate of mesenchymal stem cells expressing nestin. Brain research bulletin 68: 95-102.
142. Battula VL, Treml S, Bareiss PM, Gieseke F, Roelofs H, et al. (2009) Isolation of functionally distinct mesenchymal stem cell subsets using antibodies against CD56, CD271, and mesenchymal stem cell antigen-1. Haematologica 94: 173-184.
143. Basciano L, Nemos C, Foliguet B, de Isla N, de Carvalho M, et al. (2011) Long term culture of mesenchymal stem cells in hypoxia promotes a genetic program maintaining their undifferentiated and multipotent status. BMC cell biology 12: 12.
144. Centola M, Tonnarelli B, Schären S, Glaser N, Barbero A, et al. (2013) Priming 3D cultures of human mesenchymal stromal cells toward cartilage formation via developmental pathways. Stem cells and development 22: 2849-2858.
145. Baraniak PR, McDevitt TC (2012) Scaffold-free culture of mesenchymal stem cell spheroids in suspension preserves multilineage potential. Cell and tissue research 347: 701-711.

146. Chase LG, Lakshmipathy U, Solchaga LA, Rao MS, Vemuri MC (2010) A novel serum-free medium for the expansion of human mesenchymal stem cells. Stem cell research & therapy 1: 8.
147. Lange C, Cakiroglu F, Spiess AN, Cappallo−Obermann H, Dierlamm J, et al. (2007) Accelerated and safe expansion of human mesenchymal stromal cells in animal serum−free medium for transplantation and regenerative medicine. Journal of cellular physiology 213: 18-26.
148. Ho STB, Tanavde VM, Hui JH, Lee EH (2011) Upregulation of adipogenesis and chondrogenesis in MSC serum-free culture. Cell Medicine 2: 27-41.
149. Giovannini S, Diaz-Romero J, Aigner T, Heini P, Mainil-Varlet P, et al. (2010) Micromass co-culture of human articular chondrocytes and human bone marrow mesenchymal stem cells to investigate stable neocartilage tissue formation in vitro. Eur Cell Mater 20: 59.
150. Acharya C, Adesida A, Zajac P, Mumme M, Riesle J, et al. (2012) Enhanced chondrocyte proliferation and mesenchymal stromal cells chondrogenesis in coculture pellets mediate improved cartilage formation. Journal of cellular physiology 227: 88-97.
151. Bian L, Zhai DY, Mauck RL, Burdick JA (2011) Coculture of human mesenchymal stem cells and articular chondrocytes reduces hypertrophy and enhances functional properties of engineered cartilage. Tissue Engineering Part A 17: 1137-1145.
152. Tsuchiya K, Chen G, Ushida T, Matsuno T, Tateishi T (2004) The effect of coculture of chondrocytes with mesenchymal stem cells on their cartilaginous phenotype in vitro. Materials Science and Engineering: C 24: 391-396.
153. Georgi N, van Blitterswijk C, Karperien M (2014) MSC or chondrocyte seeded microcarriers as building blocks for cartilage tissue engineering. Tissue Eng Part A.
154. Wu L, Leijten JC, Georgi N, Post JN, van Blitterswijk CA, et al. (2011) Trophic effects of mesenchymal stem cells increase chondrocyte proliferation and matrix formation. Tissue Engineering Part A 17: 1425-1436.
155. Wu L, Prins H-J, Helder MN, van Blitterswijk CA, Karperien M (2012) Trophic effects of mesenchymal stem cells in chondrocyte co-cultures are independent of culture conditions and cell sources. Tissue engineering Part A 18: 1542-1551.
156. Quarto R, Campanile G, Cancedda R, Dozin B (1997) Modulation of commitment, proliferation, and differentiation of chondrogenic cells in defined culture medium. Endocrinology 138: 4966-4976.
157. Johnstone B, Hering TM, Caplan AI, Goldberg VM, Yoo JU (1998) In vitro chondrogenesis of bone marrow-derived mesenchymal progenitor cells. Exp Cell Res 238: 265-272.
158. Dong YF, Soung do Y, Chang Y, Enomoto-Iwamoto M, Paris M, et al. (2007) Transforming growth factor-beta and Wnt signals regulate chondrocyte differentiation through Twist1 in a stage-specific manner. Mol Endocrinol 21: 2805-2820.
159. Kato Y, Iwamoto M, Koike T, Suzuki F, Takano Y (1988) Terminal differentiation and calcification in rabbit chondrocyte cultures grown in centrifuge tubes: regulation by transforming growth factor beta and serum factors. Proc Natl Acad Sci U S A 85: 9552-9556.

160. Kocamaz E, Gok D, Cetinkaya A, Tufan AC (2012) Implication of C-type natriuretic peptide-3 signaling in glycosaminoglycan synthesis and chondrocyte hypertrophy during TGF-beta1 induced chondrogenic differentiation of chicken bone marrow-derived mesenchymal stem cells. J Mol Histol 43: 497-508.
161. van Beuningen HM, van der Kraan PM, Arntz OJ, van den Berg WB (1994) Transforming growth factor-beta 1 stimulates articular chondrocyte proteoglycan synthesis and induces osteophyte formation in the murine knee joint. Lab Invest 71: 279-290.
162. Yonekura A, Osaki M, Hirota Y, Tsukazaki T, Miyazaki Y, et al. (1999) Transforming growth factor-beta stimulates articular chondrocyte cell growth through p44/42 MAP kinase (ERK) activation. Endocr J 46: 545-553.
163. Zeiter S, Lezuo P, Ito K (2009) Effect of TGF beta1, BMP-2 and hydraulic pressure on chondrogenic differentiation of bovine bone marrow mesenchymal stromal cells. Biorheology 46: 45-55.
164. Huang AH, Stein A, Tuan RS, Mauck RL (2009) Transient Exposure to Transforming Growth Factor Beta 3 Improves the Mechanical Properties of Mesenchymal Stem Cell–Laden Cartilage Constructs in a Density-Dependent Manner. Tissue Engineering Part A 15: 3461-3472.
165. Miyanishi K, Trindade MC, Lindsey DP, Beaupré GS, Carter DR, et al. (2006) Effects of hydrostatic pressure and transforming growth factor-β 3 on adult human mesenchymal stem cell chondrogenesis in vitro. Tissue Engineering 12: 1419-1428.
166. Byers BA, Mauck RL, Chiang IE, Tuan RS (2008) Transient exposure to transforming growth factor beta 3 under serum-free conditions enhances the biomechanical and biochemical maturation of tissue-engineered cartilage. Tissue Engineering Part A 14: 1821-1834.
167. Thorpe SD, Buckley CT, Vinardell T, O'Brien FJ, Campbell VA, et al. (2010) The response of bone marrow-derived mesenchymal stem cells to dynamic compression following TGF-β3 induced chondrogenic differentiation. Annals of biomedical engineering 38: 2896-2909.
168. Haas AR, Tuan RS (1999) Chondrogenic differentiation of murine C3H10T1/2 multipotential mesenchymal cells: II. Stimulation by bone morphogenetic protein-2 requires modulation of N-cadherin expression and function. Differentiation 64: 77-89.
169. Hatakeyama Y, Nguyen J, Wang X, Nuckolls GH, Shum L (2003) Smad signaling in mesenchymal and chondroprogenitor cells. The Journal of Bone & Joint Surgery 85: 13-18.
170. Elshaier AM, Hakimiyan AA, Rappoport L, Rueger DC, Chubinskaya S (2009) Effect of interleukin-1beta on osteogenic protein 1-induced signaling in adult human articular chondrocytes. Arthritis Rheum 60: 143-154.
171. Solchaga LA, Penick K, Porter JD, Goldberg VM, Caplan AI, et al. (2005) FGF−2 enhances the mitotic and chondrogenic potentials of human adult bone marrow−derived mesenchymal stem cells. Journal of cellular physiology 203: 398-409.
172. Longobardi L, O'Rear L, Aakula S, Johnstone B, Shimer K, et al. (2006) Effect of IGF−I in the Chondrogenesis of Bone Marrow Mesenchymal Stem Cells in the

Presence or Absence of TGF−β Signaling. Journal of bone and mineral research 21: 626-636.
173. Davies LC, Blain EJ, Gilbert SJ, Caterson B, Duance VC (2008) The Potential of IGF-1 and TGFβ1 for Promoting "Adult" Articular Cartilage Repair: An In Vitro Study. Tissue Engineering Part A 14: 1251-1261.
174. Fortier LA, Barker JU, Strauss EJ, McCarrel TM, Cole BJ (2011) The role of growth factors in cartilage repair. Clinical Orthopaedics and Related Research® 469: 2706-2715.
175. Hall MP, Band PA, Meislin RJ, Jazrawi LM, Cardone DA (2009) Platelet-rich plasma: current concepts and application in sports medicine. Journal of the American Academy of Orthopaedic Surgeons 17: 602-608.
176. Gigante A, Calcagno S, Cecconi S, Ramazzotti D, Manzotti S, et al. (2010) Use of collagen scaffold and autologous bone marrow concentrate as a one-step cartilage repair in the knee: histological results of second-look biopsies at 1 year follow-up. International journal of immunopathology and pharmacology 24: 69-72.
177. Malda J, Martens DE, Tramper J, van Blitterswijk CA, Riesle J (2003) Cartilage tissue engineering: controversy in the effect of oxygen. Critical reviews in biotechnology 23: 175-194.
178. Henrotin Y, Kurz B, Aigner T (2005) Oxygen and reactive oxygen species in cartilage degradation: friends or foes? Osteoarthritis and Cartilage 13: 643-654.
179. Archer CW, Francis-West P (2003) The chondrocyte. The international journal of biochemistry & cell biology 35: 401-404.
180. Henderson JH, Ginley NM, Caplan AI, Niyibizi C, Dennis JE (2010) Low oxygen tension during incubation periods of chondrocyte expansion is sufficient to enhance postexpansion chondrogenesis. Tissue Eng Part A 16: 1585-1593.
181. Zscharnack M, Poesel C, Galle J, Bader A (2009) Low oxygen expansion improves subsequent chondrogenesis of ovine bone-marrow-derived mesenchymal stem cells in collagen type I hydrogel. Cells Tissues Organs 190: 81-93.
182. Mohyeldin A, Garzón-Muvdi T, Quiñones-Hinojosa A (2010) Oxygen in stem cell biology: a critical component of the stem cell niche. Cell stem cell 7: 150-161.
183. Schipani E. Hypoxia and HIF-1α in chondrogenesis; 2005. Elsevier. pp. 539-546.
184. Schipani E, Ryan HE, Didrickson S, Kobayashi T, Knight M, et al. (2001) Hypoxia in cartilage: HIF-1α is essential for chondrocyte growth arrest and survival. Genes & Development 15: 2865-2876.
185. Lafont JE, Talma S, Murphy CL (2007) Hypoxia−inducible factor 2α is essential for hypoxic induction of the human articular chondrocyte phenotype. Arthritis & Rheumatism 56: 3297-3306.
186. Lafont JE, Talma S, Hopfgarten C, Murphy CL (2008) Hypoxia promotes the differentiated human articular chondrocyte phenotype through SOX9-dependent and-independent pathways. Journal of Biological Chemistry 283: 4778-4786.
187. Derfoul A, Perkins GL, Hall DJ, Tuan RS (2006) Glucocorticoids promote chondrogenic differentiation of adult human mesenchymal stem cells by enhancing expression of cartilage extracellular matrix genes. Stem cells 24: 1487-1495.

188. Schwarz RI, Kleinman P, Owens N (1987) Ascorbate Can Act as an Inducer of the Collagen Pathway Because Most Steps Are Tightly Coupleda. Annals of the New York Academy of Sciences 498: 172-185.
189. Kozhemyakina E, Cohen T, Yao T-P, Lassar AB (2009) Parathyroid hormone-related peptide represses chondrocyte hypertrophy through a protein phosphatase 2A/histone deacetylase 4/MEF2 pathway. Molecular and cellular biology 29: 5751-5762.
190. Shahin K, Doran PM (2012) Tissue engineering of cartilage using a mechanobioreactor exerting simultaneous mechanical shear and compression to simulate the rolling action of articular joints. Biotechnol Bioeng 109: 1060-1073.
191. Ryan JA, Eisner EA, DuRaine G, You Z, Reddi AH (2009) Mechanical compression of articular cartilage induces chondrocyte proliferation and inhibits proteoglycan synthesis by activation of the ERK pathway: implications for tissue engineering and regenerative medicine. J Tissue Eng Regen Med 3: 107-116.
192. Angele P, Schumann D, Angele M, Kinner B, Englert C, et al. (2004) Cyclic, mechanical compression enhances chondrogenesis of mesenchymal progenitor cells in tissue engineering scaffolds. Biorheology 41: 335-346.
193. Grad S, Lee CR, Wimmer MA, Alini M (2006) Chondrocyte gene expression under applied surface motion. Biorheology 43: 259-269.
194. Grad S, Lee CR, Gorna K, Gogolewski S, Wimmer MA, et al. (2005) Surface motion upregulates superficial zone protein and hyaluronan production in chondrocyte-seeded three-dimensional scaffolds. Tissue Eng 11: 249-256.
195. Correia C, Pereira AL, Duarte AR, Frias AM, Pedro AJ, et al. (2012) Dynamic culturing of cartilage tissue: the significance of hydrostatic pressure. Tissue Eng Part A 18: 1979-1991.
196. Jang KW, Ding L, Seol D, Lim TH, Buckwalter JA, et al. (2014) Low-Intensity Pulsed Ultrasound Promotes Chondrogenic Progenitor Cell Migration via Focal Adhesion Kinase Pathway. Ultrasound Med Biol.
197. Choi JW, Choi BH, Park SH, Pai KS, Li TZ, et al. (2013) Mechanical stimulation by ultrasound enhances chondrogenic differentiation of mesenchymal stem cells in a fibrin-hyaluronic acid hydrogel. Artif Organs 37: 648-655.
198. Noriega S, Mamedov T, Turner JA, Subramanian A (2007) Intermittent applications of continuous ultrasound on the viability, proliferation, morphology, and matrix production of chondrocytes in 3D matrices. Tissue engineering 13: 611-618.
199. Leong DJ, Hardin JA, Cobelli NJ, Sun HB (2011) Mechanotransduction and cartilage integrity. Ann N Y Acad Sci 1240: 32-37.
200. McGlashan SR, Jensen CG, Poole CA (2006) Localization of extracellular matrix receptors on the chondrocyte primary cilium. Journal of Histochemistry & Cytochemistry 54: 1005-1014.
201. Millward-Sadler S, Salter D (2004) Integrin-dependent signal cascades in chondrocyte mechanotransduction. Annals of biomedical engineering 32: 435-446.
202. Hutmacher DW (2000) Scaffolds in tissue engineering bone and cartilage. Biomaterials 21: 2529-2543.
203. Cancedda R, Dozin B, Giannoni P, Quarto R (2003) Tissue engineering and cell therapy of cartilage and bone. Matrix Biology 22: 81-91.

204. Glowacki J, Mizuno S (2008) Collagen scaffolds for tissue engineering. Biopolymers 89: 338-344.
205. Fujisato T, Sajiki T, Liu Q, Ikada Y (1996) Effect of basic fibroblast growth factor on cartilage regeneration in chondrocyte-seeded collagen sponge scaffold. Biomaterials 17: 155-162.
206. Kawamura S, Wakitani S, Kimura T, Maeda A, Caplan AI, et al. (1998) Articular cartilage repair: rabbit experiments with a collagen gel-biomatrix and chondrocytes cultured in it. Acta Orthopaedica 69: 56-62.
207. Matthews JA, Wnek GE, Simpson DG, Bowlin GL (2002) Electrospinning of collagen nanofibers. Biomacromolecules 3: 232-238.
208. Cai Y, Li J, Poh CK, Tan HC, San Thian E, et al. (2013) Collagen grafted 3D polycaprolactone scaffolds for enhanced cartilage regeneration. Journal of Materials Chemistry B 1: 5971-5976.
209. Ma Z, Gao C, Gong Y, Shen J (2005) Cartilage tissue engineering PLLA scaffold with surface immobilized collagen and basic fibroblast growth factor. Biomaterials 26: 1253-1259.
210. Xiao W, He J, Nichol JW, Wang L, Hutson CB, et al. (2011) Synthesis and characterization of photocrosslinkable gelatin and silk fibroin interpenetrating polymer network hydrogels. Acta biomaterialia 7: 2384-2393.
211. Nichol JW, Koshy ST, Bae H, Hwang CM, Yamanlar S, et al. (2010) Cell-laden microengineered gelatin methacrylate hydrogels. Biomaterials 31: 5536-5544.
212. Son TI, Sakuragi M, Takahashi S, Obuse S, Kang J, et al. (2010) Visible light-induced crosslinkable gelatin. Acta biomaterialia 6: 4005-4010.
213. Schuurman W, Levett PA, Pot MW, van Weeren PR, Dhert WJ, et al. (2013) Gelatin−Methacrylamide Hydrogels as Potential Biomaterials for Fabrication of Tissue−Engineered Cartilage Constructs. Macromolecular bioscience 13: 551-561.
214. Spotnitz WD (2010) Fibrin sealant: past, present, and future: a brief review. World journal of surgery 34: 632-634.
215. Ting V, Sims CD, Brecht LE, McCarthy JG, Kasabian AK, et al. (1998) In vitro prefabrication of human cartilage shapes using fibrin glue and human chondrocytes. Annals of plastic surgery 40: 413-421.
216. Homminga GN, Buma P, Koot HW, van der Kraan PM, van den Berg WB (1993) Chondrocyte behavior in fibrin glue in vitro. Acta Orthopaedica 64: 441-445.
217. Silverman RP, Passaretti D, Huang W, Randolph MA, Yaremchuk MJ (1999) Injectable tissue-engineered cartilage using a fibrin glue polymer. Plastic and reconstructive surgery 103: 1809-1818.
218. Collins MN, Birkinshaw C (2013) Hyaluronic acid based scaffolds for tissue engineering—A review. Carbohydrate polymers 92: 1262-1279.
219. Zawko SA, Suri S, Truong Q, Schmidt CE (2009) Photopatterned anisotropic swelling of dual-crosslinked hyaluronic acid hydrogels. Acta Biomaterialia 5: 14-22.
220. Prestwich GD (2011) Hyaluronic acid-based clinical biomaterials derived for cell and molecule delivery in regenerative medicine. Journal of Controlled Release 155: 193-199.
221. Aigner J, Tegeler J, Hutzler P, Campoccia D, Pavesio A, et al. (1998) Cartilage tissue engineering with novel nonwoven structured biomaterial based on

hyaluronic acid benzyl ester. Journal of biomedical materials research 42: 172-181.
222. Nehrer S, Domayer S, Dorotka R, Schatz K, Bindreiter U, et al. (2006) Three-year clinical outcome after chondrocyte transplantation using a hyaluronan matrix for cartilage repair. European journal of radiology 57: 3-8.
223. Jakobsen RB, Shahdadfar A, Reinholt FP, Brinchmann JE (2010) Chondrogenesis in a hyaluronic acid scaffold: comparison between chondrocytes and MSC from bone marrow and adipose tissue. Knee Surgery, Sports Traumatology, Arthroscopy 18: 1407-1416.
224. Francis Suh J-K, Matthew HW (2000) Application of chitosan-based polysaccharide biomaterials in cartilage tissue engineering: a review. Biomaterials 21: 2589-2598.
225. Sechriest VF, Miao YJ, Niyibizi C, Westerhausen–Larson A, Matthew HW, et al. (2000) GAG−augmented polysaccharide hydrogel: A novel biocompatible and biodegradable material to support chondrogenesis. Journal of biomedical materials research 49: 534-541.
226. Madihally SV, Matthew HW (1999) Porous chitosan scaffolds for tissue engineering. Biomaterials 20: 1133-1142.
227. Soppimath K, Aminabhavi T, Dave A, Kumbar S, Rudzinski W (2002) Stimulus-Responsive "Smart" Hydrogels as Novel Drug Delivery Systems*. Drug Development and Industrial Pharmacy 28: 957-974.
228. Drury JL, Mooney DJ (2003) Hydrogels for tissue engineering: scaffold design variables and applications. Biomaterials 24: 4337-4351.
229. Guilak F, Cohen DM, Estes BT, Gimble JM, Liedtke W, et al. (2009) Control of stem cell fate by physical interactions with the extracellular matrix. Cell stem cell 5: 17-26.
230. Guo J, Jourdian GW, Maccallum DK (1989) Culture and growth characteristics of chondrocytes encapsulated in alginate beads. Connective tissue research 19: 277-297.
231. LeRoux MA, Guilak F, Setton LA (1999) Compressive and shear properties of alginate gel: effects of sodium ions and alginate concentration. Journal of biomedical materials research 47: 46-53.
232. Soon-Shiong P, Feldman E, Nelson R, Heintz R, Yao Q, et al. (1993) Long-term reversal of diabetes by the injection of immunoprotected islets. Proceedings of the National Academy of Sciences 90: 5843-5847.
233. Agrawal CM, Athanasiou KA (1997) Technique to control pH in vicinity of biodegrading PLA-PGA implants. Journal of biomedical materials research 38: 105-114.
234. Thomson R, Wake M, Yaszemski M, Mikos A (1995) Biodegradable polymer scaffolds to regenerate organs. Biopolymers Ii: Springer. pp. 245-274.
235. Sittinger M, Reitzel D, Dauner M, Hierlemann H, Hammer C, et al. (1996) Resorbable polyesters in cartilage engineering: affinity and biocompatibility of polymer fiber structures to chondrocytes. Journal of biomedical materials research 33: 57-63.
236. Freed LE, Marquis J, Nohria A, Emmanual J, Mikos A, et al. (1993) Neocartilage formation in vitro and in vivo using cells cultured on synthetic biodegradable polymers. Journal of biomedical materials research 27: 11-23.

237. Andreas K, Zehbe R, Kazubek M, Grzeschik K, Sternberg N, et al. (2011) Biodegradable insulin-loaded PLGA microspheres fabricated by three different emulsification techniques: Investigation for cartilage tissue engineering. Acta biomaterialia 7: 1485-1495.
238. Park JS, Yang HN, Woo DG, Jeon SY, Park K-H (2012) SOX9 gene plus heparinized TGF-β 3 coated dexamethasone loaded PLGA microspheres for inducement of chondrogenesis of hMSCs. Biomaterials 33: 7151-7163.
239. Zhang Y, Yang F, Liu K, Shen H, Zhu Y, et al. (2012) The impact of PLGA scaffold orientation on in vitro cartilage regeneration. Biomaterials 33: 2926-2935.
240. Wang W, Li B, Li Y, Jiang Y, Ouyang H, et al. (2010) In vivo restoration of full-thickness cartilage defects by poly (lactide-co-glycolide) sponges filled with fibrin gel, bone marrow mesenchymal stem cells and DNA complexes. Biomaterials 31: 5953-5965.
241. Dai W, Kawazoe N, Lin X, Dong J, Chen G (2010) The influence of structural design of PLGA/collagen hybrid scaffolds in cartilage tissue engineering. Biomaterials 31: 2141-2152.
242. Dai W, Yao Z, Dong J, Kawazoe N, Zhang C, et al. (2013) Cartilage tissue engineering with controllable shape using a poly (lactic-co-glycolic acid)/collagen hybrid scaffold. Journal of Bioactive and Compatible Polymers 28: 247-257.
243. Kim IL, Mauck RL, Burdick JA (2011) Hydrogel design for cartilage tissue engineering: a case study with hyaluronic acid. Biomaterials 32: 8771-8782.
244. Koepsell L, Remund T, Bao J, Neufeld D, Fong H, et al. (2011) Tissue engineering of annulus fibrosus using electrospun fibrous scaffolds with aligned polycaprolactone fibers. Journal of Biomedical Materials Research Part A 99: 564-575.
245. Nam J, Johnson J, Lannutti JJ, Agarwal S (2011) Modulation of embryonic mesenchymal progenitor cell differentiation via control over pure mechanical modulus in electrospun nanofibers. Acta biomaterialia 7: 1516-1524.
246. Harris JM, Chess RB (2003) Effect of pegylation on pharmaceuticals. Nature Reviews Drug Discovery 2: 214-221.
247. Roberts M, Bentley M, Harris J (2002) Chemistry for peptide and protein PEGylation. Advanced drug delivery reviews 54: 459-476.
248. Bryant SJ, Anseth KS (2003) Controlling the spatial distribution of ECM components in degradable PEG hydrogels for tissue engineering cartilage. Journal of Biomedical Materials Research Part A 64: 70-79.
249. Bryant SJ, Bender RJ, Durand KL, Anseth KS (2004) Encapsulating chondrocytes in degrading PEG hydrogels with high modulus: engineering gel structural changes to facilitate cartilaginous tissue production. Biotechnology and bioengineering 86: 747-755.
250. Nguyen KT, West JL (2002) Photopolymerizable hydrogels for tissue engineering applications. Biomaterials 23: 4307-4314.
251. Villanueva I, Weigel CA, Bryant SJ (2009) Cell–matrix interactions and dynamic mechanical loading influence chondrocyte gene expression and bioactivity in PEG-RGD hydrogels. Acta biomaterialia 5: 2832-2846.

252. Fan H, Hu Y, Zhang C, Li X, Lv R, et al. (2006) Cartilage regeneration using mesenchymal stem cells and a PLGA–gelatin/chondroitin/hyaluronate hybrid scaffold. Biomaterials 27: 4573-4580.
253. Sato T, Chen G, Ushida T, Ishii T, Ochiai N, et al. (2001) Tissue-engineered cartilage by in vivo culturing of chondrocytes in PLGA–collagen hybrid sponge. Materials Science and Engineering: C 17: 83-89.
254. Chen G, Sato T, Ushida T, Hirochika R, Shirasaki Y, et al. (2003) The use of a novel PLGA fiber/collagen composite web as a scaffold for engineering of articular cartilage tissue with adjustable thickness. Journal of Biomedical Materials Research Part A 67: 1170-1180.
255. Chen G, Sato T, Ushida T, Hirochika R, Tateishi T (2003) Redifferentiation of dedifferentiated bovine chondrocytes when cultured in vitro in a PLGA–collagen hybrid mesh. FEBS letters 542: 95-99.
256. Kawazoe N, Inoue C, Tateishi T, Chen G (2010) A cell leakproof PLGA−collagen hybrid scaffold for cartilage tissue engineering. Biotechnology progress 26: 819-826.
257. Chang KY, Hung LH, Chu I, Ko CS, Lee YD (2010) The application of type II collagen and chondroitin sulfate grafted PCL porous scaffold in cartilage tissue engineering. Journal of Biomedical Materials Research Part A 92: 712-723.
258. Song JJ, Ott HC (2011) Organ engineering based on decellularized matrix scaffolds. Trends Mol Med 17: 424-432.
259. Assmann A, Delfs C, Munakata H, Schiffer F, Horstkotter K, et al. (2013) Acceleration of autologous in vivo recellularization of decellularized aortic conduits by fibronectin surface coating. Biomaterials 34: 6015-6026.
260. Sun F, Zhou K, Mi WJ, Qiu JH (2011) Combined use of decellularized allogeneic artery conduits with autologous transdifferentiated adipose-derived stem cells for facial nerve regeneration in rats. Biomaterials 32: 8118-8128.
261. Youngstrom DW, Barrett JG, Jose RR, Kaplan DL (2013) Functional characterization of detergent-decellularized equine tendon extracellular matrix for tissue engineering applications. PLoS One 8: e64151.
262. Sawkins MJ, Bowen W, Dhadda P, Markides H, Sidney LE, et al. (2013) Hydrogels derived from demineralized and decellularized bone extracellular matrix. Acta Biomater 9: 7865-7873.
263. Schwarz S, Koerber L, Elsaesser AF, Goldberg-Bockhorn E, Seitz AM, et al. (2012) Decellularized cartilage matrix as a novel biomatrix for cartilage tissue-engineering applications. Tissue Eng Part A 18: 2195-2209.
264. Bayyoud T, Thaler S, Hofmann J, Maurus C, Spitzer MS, et al. (2012) Decellularized bovine corneal posterior lamellae as carrier matrix for cultivated human corneal endothelial cells. Curr Eye Res 37: 179-186.
265. Remlinger NT, Czajka CA, Juhas ME, Vorp DA, Stolz DB, et al. (2010) Hydrated xenogeneic decellularized tracheal matrix as a scaffold for tracheal reconstruction. Biomaterials 31: 3520-3526.
266. He H, Liu X, Peng L, Gao Z, Ye Y, et al. (2013) Promotion of hepatic differentiation of bone marrow mesenchymal stem cells on decellularized cell-deposited extracellular matrix. Biomed Res Int 2013: 406871.
267. Wang Y, Huang YC, Gertzman AA, Xie L, Nizkorodov A, et al. (2012) Endogenous regeneration of critical-size chondral defects in

immunocompromised rat xiphoid cartilage using decellularized human bone matrix scaffolds. Tissue Eng Part A 18: 2332-2342.
268. Burgkart R, Tron AC, Prodinger P, Culmes M, Tuebel J, et al. (2013) Decellularized kidney matrix for perfused bone engineering. Tissue Eng Part C Methods.
269. Wang L, Johnson JA, Zhang Q, Beahm EK (2013) Combining decellularized human adipose tissue extracellular matrix and adipose-derived stem cells for adipose tissue engineering. Acta Biomater 9: 8921-8931.
270. Hoganson DM, O'Doherty EM, Owens GE, Harilal DO, Goldman SM, et al. (2010) The retention of extracellular matrix proteins and angiogenic and mitogenic cytokines in a decellularized porcine dermis. Biomaterials 31: 6730-6737.
271. Kimuli M, Eardley I, Southgate J (2004) In vitro assessment of decellularized porcine dermis as a matrix for urinary tract reconstruction. BJU Int 94: 859-866.
272. Cheng CW, Solorio LD, Alsberg E (2014) Decellularized tissue and cell-derived extracellular matrices as scaffolds for orthopedic tissue engineering. Biotechnol Adv.
273. Elder BD, Kim DH, Athanasiou KA (2010) Developing an articular cartilage decellularization process toward facet joint cartilage replacement. Neurosurgery 66: 722-727; discussion 727.
274. Elder BD, Eleswarapu SV, Athanasiou KA (2009) Extraction techniques for the decellularization of tissue engineered articular cartilage constructs. Biomaterials 30: 3749-3756.
275. Visser CE, Boon ME, Visser PE, Kok LP (1989) Microwave treatment of xenogeneic cartilage transplants. Biomaterials 10: 507-510.
276. Revell CM, Athanasiou KA (2009) Success rates and immunologic responses of autogenic, allogenic, and xenogenic treatments to repair articular cartilage defects. Tissue Eng Part B Rev 15: 1-15.
277. Peretti GM, Randolph MA, Caruso EM, Rossetti F, Zaleske DJ (1998) Bonding of cartilage matrices with cultured chondrocytes: an experimental model. J Orthop Res 16: 89-95.
278. Peretti GM, Zaporojan V, Spangenberg KM, Randolph MA, Fellers J, et al. (2003) Cell-based bonding of articular cartilage: An extended study. J Biomed Mater Res A 64: 517-524.
279. Gong YY, Xue JX, Zhang WJ, Zhou GD, Liu W, et al. (2011) A sandwich model for engineering cartilage with acellular cartilage sheets and chondrocytes. Biomaterials 32: 2265-2273.
280. Yang Q, Peng J, Guo Q, Huang J, Zhang L, et al. (2008) A cartilage ECM-derived 3-D porous acellular matrix scaffold for in vivo cartilage tissue engineering with PKH26-labeled chondrogenic bone marrow-derived mesenchymal stem cells. Biomaterials 29: 2378-2387.
281. Zheng X, Yang F, Wang S, Lu S, Zhang W, et al. (2011) Fabrication and cell affinity of biomimetic structured PLGA/articular cartilage ECM composite scaffold. J Mater Sci Mater Med 22: 693-704.
282. Ghanavi P, Kabiri M, Doran MR (2012) The rationale for using microscopic units of a donor matrix in cartilage defect repair. Cell Tissue Res 347: 643-648.
283. Geistlich Biomaterials Chondro-Gide Collagen Membrane for Articular Cartilage Repair [internet, cited 2015 Jan 9]. Available from:

http://www.educell.si/medicinski-pripomocki/chondro-gide/media/chondro-gide_act_e2.pdf.
284. Anderson JM, Rodriguez A, Chang DT. Foreign body reaction to biomaterials; 2008. Elsevier. pp. 86-100.
285. Burkersroda Fv, Schedl L, Göpferich A (2002) Why degradable polymers undergo surface erosion or bulk erosion. Biomaterials 23: 4221-4231.
286. Lardner A (2001) The effects of extracellular pH on immune function. Journal of leukocyte biology 69: 522-530.
287. Solursh M, Linsenmayer TF, Jensen KL (1982) Chondrogenesis from single limb mesenchyme cells. Dev Biol 94: 259-264.
288. Jakob M, Demarteau O, Schäfer D, Hintermann B, Dick W, et al. (2001) Specific growth factors during the expansion and redifferentiation of adult human articular chondrocytes enhance chondrogenesis and cartilaginous tissue formation in vitro. Journal of cellular biochemistry 81: 368-377.
289. Mauck R, Yuan X, Tuan R (2006) Chondrogenic differentiation and functional maturation of bovine mesenchymal stem cells in long-term agarose culture. Osteoarthritis and cartilage 14: 179-189.
290. Harris JD, Siston RA, Brophy RH, Lattermann C, Carey JL, et al. (2011) Failures, re-operations, and complications after autologous chondrocyte implantation--a systematic review. Osteoarthritis Cartilage 19: 779-791.
291. Vavken P, Samartzis D (2010) Effectiveness of autologous chondrocyte implantation in cartilage repair of the knee: a systematic review of controlled trials. Osteoarthritis Cartilage 18: 857-863.
292. Lutzner J, Kasten P, Gunther KP, Kirschner S (2009) Surgical options for patients with osteoarthritis of the knee. Nat Rev Rheumatol 5: 309-316.
293. Perrot S, Menkes CJ (1996) Nonpharmacological approaches to pain in osteoarthritis. Available options. Drugs 52 Suppl 3: 21-26.
294. Cameron HU, Botsford DJ, Park YS (1997) Prognostic factors in the outcome of supracondylar femoral osteotomy for lateral compartment osteoarthritis of the knee. Can J Surg 40: 114-118.
295. Gillogly SD, Voight M, Blackburn T (1998) Treatment of articular cartilage defects of the knee with autologous chondrocyte implantation. J Orthop Sports Phys Ther 28: 241-251.
296. Kon E, Gobbi A, Filardo G, Delcogliano M, Zaffagnini S, et al. (2009) Arthroscopic second-generation autologous chondrocyte implantation compared with microfracture for chondral lesions of the knee: prospective nonrandomized study at 5 years. Am J Sports Med 37: 33-41.
297. Van Assche D, Staes F, Van Caspel D, Vanlauwe J, Bellemans J, et al. (2010) Autologous chondrocyte implantation versus microfracture for knee cartilage injury: a prospective randomized trial, with 2-year follow-up. Knee Surg Sports Traumatol Arthrosc 18: 486-495.
298. Boeuf S, Richter W (2010) Chondrogenesis of mesenchymal stem cells: role of tissue source and inducing factors. Stem Cell Res Ther 1: 31.
299. Cherubino P, Grassi FA, Bulgheroni P, Ronga M (2003) Autologous chondrocyte implantation using a bilayer collagen membrane: a preliminary report. J Orthop Surg (Hong Kong) 11: 10-15.

300. Darling EM, Athanasiou KA (2005) Rapid phenotypic changes in passaged articular chondrocyte subpopulations. J Orthop Res 23: 425-432.
301. Holtzer H, Abbott J, Lash J, Holtzer S (1960) The Loss of Phenotypic Traits by Differentiated Cells in Vitro, I. Dedifferentiation of Cartilage Cells. Proc Natl Acad Sci U S A 46: 1533-1542.
302. Malda J, Kreijveld E, Temenoff JS, van Blitterswijk CA, Riesle J (2003) Expansion of human nasal chondrocytes on macroporous microcarriers enhances redifferentiation. Biomaterials 24: 5153-5161.
303. Yen CN, Lin YR, Chang MDT, Tien CW, Wu YC, et al. (2008) Use of porous alginate sponges for substantial chondrocyte expansion and matrix production: Effects of seeding density. Biotechnology Progress 24: 452-457.
304. Malda J, van Blitterswijk CA, Grojec M, Martens DE, Tramper J, et al. (2003) Expansion of bovine chondrocytes on microcarriers enhances redifferentiation. Tissue engineering 9: 939-948.
305. Banu N, Tsuchiya T (2007) Markedly different effects of hyaluronic acid and chondroitin sulfate-A on the differentiation of human articular chondrocytes in micromass and 3-D honeycomb rotation cultures. J Biomed Mater Res A 80: 257-267.
306. Goldberg AJ, Lee DA, Bader DL, Bentley G (2005) Autologous chondrocyte implantation. Culture in a TGF-beta-containing medium enhances the re-expression of a chondrocytic phenotype in passaged human chondrocytes in pellet culture. J Bone Joint Surg Br 87: 128-134.
307. Hsieh-Bonassera ND, Wu I, Lin JK, Schumacher BL, Chen AC, et al. (2009) Expansion and redifferentiation of chondrocytes from osteoarthritic cartilage: cells for human cartilage tissue engineering. Tissue Eng Part A 15: 3513-3523.
308. Imabayashi H, Mori T, Gojo S, Kiyono T, Sugiyama T, et al. (2003) Redifferentiation of dedifferentiated chondrocytes and chondrogenesis of human bone marrow stromal cells via chondrosphere formation with expression profiling by large-scale cDNA analysis. Exp Cell Res 288: 35-50.
309. Tallheden T, Karlsson C, Brunner A, Van Der Lee J, Hagg R, et al. (2004) Gene expression during redifferentiation of human articular chondrocytes. Osteoarthritis Cartilage 12: 525-535.
310. Tare RS, Howard D, Pound JC, Roach HI, Oreffo RO (2005) Tissue engineering strategies for cartilage generation--micromass and three dimensional cultures using human chondrocytes and a continuous cell line. Biochem Biophys Res Commun 333: 609-621.
311. Giovannini S, Diaz-Romero J, Aigner T, Heini P, Mainil-Varlet P, et al. (2010) Micromass co-culture of human articular chondrocytes and human bone marrow mesenchymal stem cells to investigate stable neocartilage tissue formation in vitro. Eur Cell Mater 20: 245-259.
312. Croucher LJ, Crawford A, Hatton PV, Russell RG, Buttle DJ (2000) Extracellular ATP and UTP stimulate cartilage proteoglycan and collagen accumulation in bovine articular chondrocyte pellet cultures. Biochim Biophys Acta 1502: 297-306.
313. Anderer U, Libera J (2002) In vitro engineering of human autogenous cartilage. J Bone Miner Res 17: 1420-1429.

314. Siebold R, Sartory N, Yang Y, Feil S, Paessler HH (2011) Prone position for minimal invasive or all-arthroscopic autologous chondrocyte implantation at the patella. Knee Surg Sports Traumatol Arthrosc 19: 2036-2039.
315. Whitesides GM, Ostuni E, Takayama S, Jiang X, Ingber DE (2001) Soft lithography in biology and biochemistry. Annu Rev Biomed Eng 3: 335-373.
316. Fu YQ, Colli A, Fasoli A, Luo JK, Flewitt AJ, et al. (2009) Deep reactive ion etching as a tool for nanostructure fabrication. Journal of Vacuum Science & Technology B 27: 1520-1526.
317. Cook MM, Futrega K, Osiecki M, Kabiri M, Kul B, et al. (2012) Micromarrows--three-dimensional coculture of hematopoietic stem cells and mesenchymal stromal cells. Tissue Eng Part C Methods 18: 319-328.
318. Doran MR, Frith JE, Prowse AB, Fitzpatrick J, Wolvetang EJ, et al. (2010) Defined high protein content surfaces for stem cell culture. Biomaterials 31: 5137-5142.
319. Bhattacharya S, Datta A, Berg JM, Gangopadhyay S (2005) Studies on surface wettability of poly(dimethyl) siloxane (PDMS) and glass under oxygen-plasma treatment and correlation with bond strength. Journal of Microelectromechanical Systems 14: 590-597.
320. Bongaerts JH, Cooper-White JJ, Stokes JR (2009) Low biofouling chitosan-hyaluronic acid multilayers with ultra-low friction coefficients. Biomacromolecules 10: 1287-1294.
321. Tan GK, Dinnes DL, Butler LN, Cooper-White JJ (2010) Interactions between meniscal cells and a self assembled biomimetic surface composed of hyaluronic acid, chitosan and meniscal extracellular matrix molecules. Biomaterials 31: 6104-6118.
322. Ungrin MD, Joshi C, Nica A, Bauwens C, Zandstra PW (2008) Reproducible, ultra high-throughput formation of multicellular organization from single cell suspension-derived human embryonic stem cell aggregates. PLoS One 3: e1565.
323. Liebman J, Goldberg RL (2001) Chondrocyte Culture and Assay. Current Protocols in Pharmacology: John Wiley & Sons, Inc.
324. Bookout AL, Mangelsdorf DJ (2003) Quantitative real-time PCR protocol for analysis of nuclear receptor signaling pathways. Nucl Recept Signal 1: e012.
325. Lin RZ, Chang HY (2008) Recent advances in three-dimensional multicellular spheroid culture for biomedical research. Biotechnol J 3: 1172-1184.
326. Moreira Teixeira LS, Leijten JC, Sobral J, Jin R, van Apeldoorn AA, et al. (2012) High throughput generated micro-aggregates of chondrocytes stimulate cartilage formation in vitro and in vivo. European cells & materials 23: 387-399.
327. Hirao M, Tamai N, Tsumaki N, Yoshikawa H, Myoui A (2006) Oxygen tension regulates chondrocyte differentiation and function during endochondral ossification. J Biol Chem 281: 31079-31092.
328. Coyle CH, Izzo NJ, Chu CR (2009) Sustained hypoxia enhances chondrocyte matrix synthesis. J Orthop Res 27: 793-799.
329. Doran MR, Markway BD, Clark A, Athanasas-Platsis S, Brooke G, et al. (2010) Membrane bioreactors enhance microenvironmental conditioning and tissue development. Tissue Eng Part C Methods 16: 407-415.
330. Shahin K, Doran PM (2011) Strategies for enhancing the accumulation and retention of extracellular matrix in tissue-engineered cartilage cultured in bioreactors. PLoS One 6: e23119.

331. Cao Z, Hou S, Sun D, Wang X, Tang J (2012) Osteochondral regeneration by a bilayered construct in a cell-free or cell-based approach. Biotechnol Lett 34: 1151-1157.
332. Haasper C, Colditz M, Budde S, Hesse E, Tschernig T, et al. (2009) Perfusion and cyclic compression of mesenchymal cell-loaded and clinically applicable osteochondral grafts. Knee Surg Sports Traumatol Arthrosc 17: 1384-1392.
333. Grayson WL, Bhumiratana S, Grace Chao PH, Hung CT, Vunjak-Novakovic G (2010) Spatial regulation of human mesenchymal stem cell differentiation in engineered osteochondral constructs: effects of pre-differentiation, soluble factors and medium perfusion. Osteoarthritis Cartilage 18: 714-723.
334. Erisken C, Kalyon DM, Wang H, Ornek-Ballanco C, Xu J (2011) Osteochondral tissue formation through adipose-derived stromal cell differentiation on biomimetic polycaprolactone nanofibrous scaffolds with graded insulin and Beta-glycerophosphate concentrations. Tissue Eng Part A 17: 1239-1252.
335. Cheng HW, Luk KD, Cheung KM, Chan BP (2011) In vitro generation of an osteochondral interface from mesenchymal stem cell-collagen microspheres. Biomaterials 32: 1526-1535.
336. Klein TJ, Malda J, Sah RL, Hutmacher DW (2009) Tissue engineering of articular cartilage with biomimetic zones. Tissue engineering Part B, Reviews 15: 143-157.
337. Brand CA, Harrison C, Tropea J, Hinman RS, Britt H, et al. (2013) Management of osteoarthritis in general practice in australia. Arthritis Care Res (Hoboken).
338. Centers for Disease C, Prevention (2013) Prevalence of doctor-diagnosed arthritis and arthritis-attributable activity limitation--United States, 2010-2012. MMWR Morb Mortal Wkly Rep 62: 869-873.
339. Woolf AD, Pfleger B (2003) Burden of major musculoskeletal conditions. Bull World Health Organ 81: 646-656.
340. Buckwalter JA, Brown TD (2004) Joint injury, repair, and remodeling: roles in post-traumatic osteoarthritis. Clinical orthopaedics and related research 423: 7-16.
341. Behrens P, Ehlers EM, Kochermann KU, Rohwedel J, Russlies M, et al. (1999) [New therapy procedure for localized cartilage defects. Encouraging results with autologous chondrocyte implantation]. MMW Fortschr Med 141: 49-51.
342. Ebert JR, Robertson WB, Lloyd DG, Zheng MH, Wood DJ, et al. (2008) Traditional vs accelerated approaches to post-operative rehabilitation following matrix-induced autologous chondrocyte implantation (MACI): comparison of clinical, biomechanical and radiographic outcomes. Osteoarthritis Cartilage 16: 1131-1140.
343. Robertson W, Gilbey H, Ackland T (2004) Standard practice exercise rehabilitation protocols for matrix induced autologous chondrocyte implantation femoral condyles. Hollywood Functional Rehabilitation Clinic, Perth (Western Australia).
344. Minas T, Peterson L (1999) Advanced techniques in autologous chondrocyte transplantation. Clin Sports Med 18: 13-44, v-vi.
345. Peretti GM, Randolph MA, Villa MT, Buragas MS, Yaremchuk MJ (2000) Cell-based tissue-engineered allogeneic implant for cartilage repair. Tissue Eng 6: 567-576.

346. Shin YS, Lee BH, Choi JW, Min B-H, Chang JW, et al. (2014) Tissue-engineered tracheal reconstruction using chondrocyte seeded on a porcine cartilage-derived substance scaffold. International journal of pediatric otorhinolaryngology 78: 32-38.
347. Pottenger LA, Lyon NB, Hecht JD, Neustadt PM, Robinson RA (1982) Influence of cartilage particle size and proteoglycan aggregation on immobilization of proteoglycans. J Biol Chem 257: 11479-11485.
348. Video 1 can be found at: https://mediawarehouse.qut.edu.au/QMW/player/?dID=25203&dDocName=QMW_023801.
349. Video 2 can be found at: https://mediawarehouse.qut.edu.au/QMW/player/?dID=25204&dDocName=QMW_023802.
350. Murphy CM, Matsiko A, Haugh MG, Gleeson JP, O'Brien FJ (2012) Mesenchymal stem cell fate is regulated by the composition and mechanical properties of collagen-glycosaminoglycan scaffolds. J Mech Behav Biomed Mater 11: 53-62.
351. Chen CC, Liao CH, Wang YH, Hsu YM, Huang SH, et al. (2012) Cartilage fragments from osteoarthritic knee promote chondrogenesis of mesenchymal stem cells without exogenous growth factor induction. J Orthop Res 30: 393-400.
352. Chen WC, Yao CL, Chu IM, Wei YH (2011) Compare the effects of chondrogenesis by culture of human mesenchymal stem cells with various type of the chondroitin sulfate C. J Biosci Bioeng 111: 226-231.
353. Bhumiratana S, Eton RE, Oungoulian SR, Wan LQ, Ateshian GA, et al. (2014) Large, stratified, and mechanically functional human cartilage grown in vitro by mesenchymal condensation. Proceedings of the National Academy of Sciences 111: 6940-6945.
354. Schuurman W, Harimulyo E, Gawlitta D, Woodfield T, Dhert W, et al. (2013) Three−dimensional assembly of tissue−engineered cartilage constructs results in cartilaginous tissue formation without retainment of zonal characteristics. Journal of tissue engineering and regenerative medicine.
355. Johnstone B, Alini M, Cucchiarini M, Dodge GR, Eglin D, et al. (2013) Tissue engineering for articular cartilage repair–the state of the art. Eur Cell Mater 25: 248-267.
356. Archer CW, Redman S, Khan I, Bishop J, Richardson K (2006) Enhancing tissue integration in cartilage repair procedures. J Anat 209: 481-493.
357. Fisher MB, Henning EA, Soegaard NB, Dodge GR, Steinberg DR, et al. (2014) Maximizing cartilage formation and integration via a trajectory-based tissue engineering approach. Biomaterials 35: 2140-2148.
358. Muehleman C, Li J, Abe Y, Pfister B, Sah RL, et al. (2009) Effect of risedronate in a minipig cartilage defect model with allograft. J Orthop Res 27: 360-365.
359. Nooeaid P, Salih V, Beier JP, Boccaccini AR (2012) Osteochondral tissue engineering: scaffolds, stem cells and applications. J Cell Mol Med 16: 2247-2270.
360. Filardo G, Kon E, Di Martino A, Busacca M, Altadonna G, et al. (2013) Treatment of knee osteochondritis dissecans with a cell-free biomimetic osteochondral scaffold: clinical and imaging evaluation at 2-year follow-up. Am J Sports Med 41: 1786-1793.

361. Filova E, Rampichova M, Litvinec A, Drzik M, Mickova A, et al. (2013) A cell-free nanofiber composite scaffold regenerated osteochondral defects in miniature pigs. Int J Pharm 447: 139-149.
362. Gotterbarm T, Richter W, Jung M, Berardi Vilei S, Mainil-Varlet P, et al. (2006) An in vivo study of a growth-factor enhanced, cell free, two-layered collagen-tricalcium phosphate in deep osteochondral defects. Biomaterials 27: 3387-3395.
363. Erggelet C, Endres M, Neumann K, Morawietz L, Ringe J, et al. (2009) Formation of cartilage repair tissue in articular cartilage defects pretreated with microfracture and covered with cell−free polymer−based implants. Journal of Orthopaedic Research 27: 1353-1360.
364. Siclari A, Mascaro G, Gentili C, Cancedda R, Boux E (2012) A cell-free scaffold-based cartilage repair provides improved function hyaline-like repair at one year. Clinical Orthopaedics and Related Research® 470: 910-919.
365. Cheuk YC, Wong MW, Lee KM, Fu SC (2011) Use of allogeneic scaffold-free chondrocyte pellet in repair of osteochondral defect in a rabbit model. J Orthop Res 29: 1343-1350.
366. Brehm W, Aklin B, Yamashita T, Rieser F, Trub T, et al. (2006) Repair of superficial osteochondral defects with an autologous scaffold-free cartilage construct in a caprine model: implantation method and short-term results. Osteoarthritis Cartilage 14: 1214-1226.
367. Chen K, Shi P, Teh TK, Toh SL, Goh JC (2013) In vitro generation of a multilayered osteochondral construct with an osteochondral interface using rabbit bone marrow stromal cells and a silk peptide-based scaffold. J Tissue Eng Regen Med.
368. Chen K, Ng KS, Ravi S, Goh JC, Toh SL (2013) In vitro generation of whole osteochondral constructs using rabbit bone marrow stromal cells, employing a two-chambered co-culture well design. J Tissue Eng Regen Med.
369. Loken S, Jakobsen RB, Aroen A, Heir S, Shahdadfar A, et al. (2008) Bone marrow mesenchymal stem cells in a hyaluronan scaffold for treatment of an osteochondral defect in a rabbit model. Knee Surg Sports Traumatol Arthrosc 16: 896-903.
370. Liu Y, Shu XZ, Prestwich GD (2006) Osteochondral defect repair with autologous bone marrow-derived mesenchymal stem cells in an injectable, in situ, cross-linked synthetic extracellular matrix. Tissue Eng 12: 3405-3416.
371. Pittenger MF, Mackay AM, Beck SC, Jaiswal RK, Douglas R, et al. (1999) Multilineage potential of adult human mesenchymal stem cells. science 284: 143-147.
372. Liu XG, Jiang HK (2013) Preparation of an osteochondral composite with mesenchymal stem cells as the single-cell source in a double-chamber bioreactor. Biotechnol Lett 35: 1645-1653.
373. Malafaya PB, Reis RL (2009) Bilayered chitosan-based scaffolds for osteochondral tissue engineering: influence of hydroxyapatite on in vitro cytotoxicity and dynamic bioactivity studies in a specific double-chamber bioreactor. Acta Biomater 5: 644-660.
374. Abdollahi H, Harris LJ, Zhang P, McIlhenny S, Srinivas V, et al. (2011) The role of hypoxia in stem cell differentiation and therapeutics. Journal of Surgical Research 165: 112-117.

375. Dominici M, Le Blanc K, Mueller I, Slaper-Cortenbach I, Marini F, et al. (2006) Minimal criteria for defining multipotent mesenchymal stromal cells. The International Society for Cellular Therapy position statement. Cytotherapy 8: 315-317.
376. Aubin JE (2001) Regulation of osteoblast formation and function. Rev Endocr Metab Disord 2: 81-94.
377. Vejlens L (1971) Glycosaminoglycans of human bone tissue. Calcified tissue research 7: 175-190.
378. Engfeldt B, Hjerpe A (1976) Glycosaminoglycans and proteoglycans of human bone tissue at different stages of mineralization. Acta Pathologica Microbiologica Scandinavica Section A Pathology 84: 95-106.
379. Aigner T, Gebhard PM, Schmid E, Bau B, Harley V, et al. (2003) SOX9 expression does not correlate with type II collagen expression in adult articular chondrocytes. Matrix Biology 22: 363-372.
380. Sandberg M, Vuorio T, Hirvonen H, Alitalo K, Vuorio E (1988) Enhanced expression of TGF-beta and c-fos mRNAs in the growth plates of developing human long bones. Development 102: 461-470.
381. Ignotz RA, Endo T, Massague J (1987) Regulation of fibronectin and type I collagen mRNA levels by transforming growth factor-beta. Journal of Biological Chemistry 262: 6443-6446.
382. Heine U, Munoz E, Flanders K, Roberts A, Sporn M (1990) Colocalization of TGF-beta 1 and collagen I and III, fibronectin and glycosaminoglycans during lung branching morphogenesis. Development 109: 29-36.
383. Mueller MB, Fischer M, Zellner J, Berner A, Dienstknecht T, et al. (2010) Hypertrophy in mesenchymal stem cell chondrogenesis: effect of TGF-beta isoforms and chondrogenic conditioning. Cells Tissues Organs 192: 158-166.
384. Scotti C, Tonnarelli B, Papadimitropoulos A, Scherberich A, Schaeren S, et al. (2010) Recapitulation of endochondral bone formation using human adult mesenchymal stem cells as a paradigm for developmental engineering. Proc Natl Acad Sci U S A 107: 7251-7256.
385. Sart S, Tsai A-C, Li Y, Ma T (2013) Three-dimensional aggregates of mesenchymal stem cells: cellular mechanisms, biological properties, and applications. Tissue Engineering Part B: Reviews.
386. Lehmann M, Martin F, Mannigel K, Kaltschmidt K, Sack U, et al. (2013) Three-Dimensional Scaffold-Free Fusion Culture: the Way to Enhanced Chondrogenesis of in vitro Propagated Human Articular Chondrocytes. European journal of histochemistry: EJH 57.
387. El-Serafi AT, Wilson DI, Roach HI, Oreffo RO (2011) Developmental plasticity of human foetal femur-derived cells in pellet culture: self assembly of an osteoid shell around a cartilaginous core. Eur Cell Mater 21: 558-567.
388. Bekkers JE, Inklaar M, Saris DB (2009) Treatment Selection in Articular Cartilage Lesions of the Knee A Systematic Review. The American journal of sports medicine 37: 148S-155S.
389. Magnussen RA, Dunn WR, Carey JL, Spindler KP (2008) Treatment of focal articular cartilage defects in the knee. Clinical orthopaedics and related research 466: 952-962.

390. Yamaoka H, Nishizawa S, Asawa Y, Fujihara Y, Ogasawara T, et al. (2010) Involvement of fibroblast growth factor 18 in dedifferentiation of cultured human chondrocytes. Cell proliferation 43: 67-76.
391. Schnabel M, Marlovits S, Eckhoff G, Fichtel I, Gotzen L, et al. (2002) Dedifferentiation-associated changes in morphology and gene expression in primary human articular chondrocytes in cell culture. Osteoarthritis and Cartilage 10: 62-70.
392. Haudenschild DR, McPherson JM, Tubo R, Binette F (2001) Differential expression of multiple genes during articular chondrocyte redifferentiation. The Anatomical Record 263: 91-98.
393. Schuh E, Hofmann S, Stok K, Notbohm H, Müller R, et al. (2012) Chondrocyte redifferentiation in 3D: the effect of adhesion site density and substrate elasticity. Journal of Biomedical Materials Research Part A 100: 38-47.
394. Lee YA, Kang S-S, Baek S-H, Jung J-C, Jin EJ, et al. (2007) Redifferentiation of dedifferentiated chondrocytes on chitosan membranes and involvement of PKCalpha and P38 MAP kinase. Molecules and cells 24: 9.
395. Huey DJ, Hu JC, Athanasiou KA (2012) Unlike bone, cartilage regeneration remains elusive. Science 338: 917-921.
396. Mwale F, Stachura D, Roughley P, Antoniou J (2006) Limitations of using aggrecan and type X collagen as markers of chondrogenesis in mesenchymal stem cell differentiation. Journal of orthopaedic research 24: 1791-1798.
397. Weiss S, Hennig T, Bock R, Steck E, Richter W (2010) Impact of growth factors and PTHrP on early and late chondrogenic differentiation of human mesenchymal stem cells. Journal of cellular physiology 223: 84-93.
398. Curran JM, Chen R, Hunt JA (2006) The guidance of human mesenchymal stem cell differentiation in vitro by controlled modifications to the cell substrate. Biomaterials 27: 4783-4793.
399. Woodfield TB, Miot S, Martin I, van Blitterswijk CA, Riesle J (2006) The regulation of expanded human nasal chondrocyte re-differentiation capacity by substrate composition and gas plasma surface modification. Biomaterials 27: 1043-1053.
400. Chan CK, Seo EY, Chen JY, Lo D, McArdle A, et al. (2015) Identification and Specification of the Mouse Skeletal Stem Cell. Cell 160: 285-298.
401. Somoza RA, Welter JF, Correa D, Caplan AI (2014) Chondrogenic differentiation of mesenchymal stem cells: challenges and unfulfilled expectations. Tissue Engineering Part B: Reviews 20: 596-608.
402. Hoenig E, Leicht U, Winkler T, Mielke G, Beck K, et al. (2013) Mechanical Properties of Native and Tissue-Engineered Cartilage Depend on Carrier Permeability: A Bioreactor Study. Tissue Engineering Part A 19: 1534-1542.
403. Deng G-M, Nilsson M, Verdrengh M, Collins LV, Tarkowski A (1999) Intra-articularly localized bacterial DNA containing CpG motifs induces arthritis. Nature medicine 5: 702-705.
404. Krieg AM (2002) CPG motifs in bacterial dna and their immune effects*. Annual review of immunology 20: 709-760.
405. Dickhut A, Pelttari K, Janicki P, Wagner W, Eckstein V, et al. (2009) Calcification or dedifferentiation: requirement to lock mesenchymal stem cells in a desired differentiation stage. Journal of cellular physiology 219: 219-226.

406. Grande DA, Pitman MI, Peterson L, Menche D, Klein M (1989) The repair of experimentally produced defects in rabbit articular cartilage by autologous chondrocyte transplantation. Journal of Orthopaedic Research 7: 208-218.
407. Kim H, Moran M, Salter RB (1991) The potential for regeneration of articular cartilage in defects created by chondral shaving and subchondral abrasion. An experimental investigation in rabbits. The Journal of Bone & Joint Surgery 73: 1301-1315.
408. Wakitani S, Goto T, Young RG, Mansour JM, Goldberg VM, et al. (1998) Repair of large full-thickness articular cartilage defects with allograft articular chondrocytes embedded in a collagen gel. Tissue Engineering 4: 429-444.
409. Orth P, Zurakowski D, Wincheringer D, Madry H (2011) Reliability, reproducibility, and validation of five major histological scoring systems for experimental articular cartilage repair in the rabbit model. Tissue Engineering Part C: Methods 18: 329-339.
410. Qi Y, Zhao T, Xu K, Dai T, Yan W (2012) The restoration of full-thickness cartilage defects with mesenchymal stem cells (MSCs) loaded and cross-linked bilayer collagen scaffolds on rabbit model. Molecular biology reports 39: 1231-1237.
411. Brittberg M, Nilsson A, Lindahl A, Ohlsson C, Peterson L (1996) Rabbit articular cartilage defects treated with autologous cultured chondrocytes. Clinical orthopaedics and related research 326: 270-283.
412. Chu CR, Szczodry M, Bruno S (2010) Animal models for cartilage regeneration and repair. Tissue Engineering Part B: Reviews 16: 105-115.
413. Hao T, Wen N, Cao J-K, Wang H-B, Lü S-H, et al. (2010) The support of matrix accumulation and the promotion of sheep articular cartilage defects repair in vivo by chitosan hydrogels. Osteoarthritis and Cartilage 18: 257-265.
414. Manda K, Ryd L, Eriksson A (2011) Finite element simulations of a focal knee resurfacing implant applied to localized cartilage defects in a sheep model. Journal of Biomechanics 44: 794-801.
415. Milano G, Sanna Passino E, Deriu L, Careddu G, Manunta L, et al. (2010) The effect of platelet rich plasma combined with microfractures on the treatment of chondral defects: an experimental study in a sheep model. Osteoarthritis and Cartilage 18: 971-980.
416. Kon E, Delcogliano M, Filardo G, Fini M, Giavaresi G, et al. (2010) Orderly osteochondral regeneration in a sheep model using a novel nano−composite multilayered biomaterial. Journal of Orthopaedic Research 28: 116-124.
417. Miot S, Brehm W, Dickinson S, Sims T, Wixmerten A, et al. (2012) Influence of in vitro maturation of engineered cartilage on the outcome of osteochondral repair in a goat model. Eur Cell Mater 23: 222-236.
418. van Bergen CJ, Kerkhoffs GM, Marsidi N, Korstjens CM, Everts V, et al. (2013) Osteochondral defects of the talus: a novel animal model in the goat. Tissue Engineering Part C: Methods 19: 449-457.
419. Jeng L, Hsu H-P, Spector M (2013) Tissue-Engineered Cartilaginous Constructs for the Treatment of Caprine Cartilage Defects, Including Distribution of Laminin and Type IV Collagen. Tissue Engineering Part A 19: 2267-2274.

420. Lee KB, Hui JH, Song IC, Ardany L, Lee EH (2007) Injectable mesenchymal stem cell therapy for large cartilage defects—a porcine model. Stem Cells 25: 2964-2971.
421. Liu Y, Chen F, Liu W, Cui L, Shang Q, et al. (2002) Repairing large porcine full-thickness defects of articular cartilage using autologous chondrocyte-engineered cartilage. Tissue engineering 8: 709-721.
422. Chang C-H, Kuo T-F, Lin C-C, Chou C-H, Chen K-H, et al. (2006) Tissue engineering-based cartilage repair with allogenous chondrocytes and gelatin–chondroitin–hyaluronan tri-copolymer scaffold: a porcine model assessed at 18, 24, and 36 weeks. Biomaterials 27: 1876-1888.
423. Barnewitz D, Endres M, Krüger I, Becker A, Zimmermann J, et al. (2006) Treatment of articular cartilage defects in horses with polymer-based cartilage tissue engineering grafts. Biomaterials 27: 2882-2889.
424. Hunziker EB (1999) Biologic repair of articular cartilage: defect models in experimental animals and matrix requirements. Clinical orthopaedics and related research 367: S135-S146.
425. Powers MJ, Janigian DM, Wack KE, Baker CS, Stolz DB, et al. (2002) Functional behavior of primary rat liver cells in a three-dimensional perfused microarray bioreactor. Tissue engineering 8: 499-513.
426. Powers MJ, Domansky K, Kaazempur−Mofrad MR, Kalezi A, Capitano A, et al. (2002) A microfabricated array bioreactor for perfused 3D liver culture. Biotechnology and Bioengineering 78: 257-269.
427. Norotte C, Marga FS, Niklason LE, Forgacs G (2009) Scaffold-free vascular tissue engineering using bioprinting. Biomaterials 30: 5910-5917.
428. Mironov V, Visconti RP, Kasyanov V, Forgacs G, Drake CJ, et al. (2009) Organ printing: tissue spheroids as building blocks. Biomaterials 30: 2164-2174.
429. Ma PX (2004) Scaffolds for tissue fabrication. Materials today 7: 30-40.
430. Martin I, Wendt D, Heberer M (2004) The role of bioreactors in tissue engineering. TRENDS in Biotechnology 22: 80-86.

Acknowledgements

I would like to thank everyone who has contributed to this project and helped me to get through this process. First of all, it is my principal supervisor Dr. Michael Doran who trusted me and gave me the opportunity, let me into his lab and taught me how to cast PDMS (polydimethylsiloxane) for the first time in my life; I am very grateful for everything. Secondly, it is Assoc. Prof. Travis Klein who co-supervised me, always provided very accurate, critical corrections and creative suggestions; I am very thankful for everything. Thirdly, it is Dr. Bill Lott who also co-supervised me and has an admirable intellectual treasure and great writing skills; I appreciate the time and effort. I also would like to thank Prof. Justin Cooper-White for his involvement with my project and Prof. Ross Crawford for providing tissue samples and letting me into his operation room during one of his knee replacement surgeries, it was magnificently brutal and I somehow worked harder in the lab after that day.

I also would like to thank all my friends and colleagues in the lab who brought joy into my life not only with scientific brainstorming but also with social, political, religious and science-fictional discussions, I am very grateful for all the contribution and fun. Here is a chronological list of those great people: Dr. Mahboubeh Kabiri, Dr. Parisa Ghanavi, Dr. Matthew Cook, Michael Osiecki, Peter Levett, Kathryn Futrega, Dr. Karen Chambers, Myfanwy King, and Eman Othman. Additionally, I would like to acknowledge the microscope wizards Dr. Leo de Boer and Dr. Sandrine Roy for their assistance in imaging.

Finally, I would like to thank my family for supporting me in pursuing scientific research on this land very far from home. I cannot express my gratitude for my mother, that brave woman, who travelled all the way to Australia on her own, just to see me; and for my father who had a constant and genuine interest in my research and well-being. I am also very grateful that I have the best siblings in the world, my sister and brother who kept in touch and supported me whenever I needed them. And of course I am and always will be thankful to my caring, understanding, supportive, generous partner in life, my soul mate, my husband for coming with me and waiting in the office while I did long hours of tissue culture at the weekends.

Biographical Sketch

The author was born in Ankara, Turkey. She attended Bilkent University (full scholarship), and graduated with a Bachelor of Science degree in Molecular Biology and Genetics in June 2010. She was granted QUT Postgraduate Research Award and HDR Tuition Fee Sponsorship in September 2010. She began doctoral studies in Cartilage Tissue Engineering at Queensland University of Technology. She pursued her doctoral research under the direction of Dr. Michael Doran. The publications generated and conferences attended during candidature are listed below:

Publications

Babur BK, Kabiri M, Lott WB, Klein TJ, Doran MR. (2015). The rapid manufacture of uniform composite multicellular-biomaterial micropellets, their assembly into macroscopic organized tissues, and potential applications in cartilage tissue engineering. PLoS One (Submitted).

Babur BK, Futrega K, Lott WB, Klein TJ, Cooper-White J, Doran MR. (2015) High throughput bone and cartilage micropellet manufacture, followed by assembly of micropellets into a biphasic osteochondral tissue. Cell and Tissue Research (Submitted).

Osiecki MJ, Michl T, **Babur BK**, Kabiri M, Atkinson K, et al. (2015) Isolation and expansion of placenta-derived mesenchymal stromal cells in a packed bed bioreactor. Biomaterials (Submitted).

Babur BK, Ghanavi P, Levett P, Lott WB, Klein T, et al. (2013) The interplay between chondrocyte redifferentiation pellet size and oxygen concentration. PLoS One 8: e58865.

Kabiri M, **Kul B,** Lott WB, Futrega K, Ghanavi P, et al. (2012) 3D mesenchymal stem/stromal cell osteogenesis and autocrine signalling. Biochem Biophys Res Commun 419: 142-147.

Cook MM, Futrega K, Osiecki M, Kabiri M, **Kul B,** et al. (2012) Micromarrows--three-dimensional coculture of hematopoietic stem cells and mesenchymal stromal cells. Tissue Eng Part C Methods 18: 319-328.

Conferences

October 2013; Poster presentation; 6th Annual Meeting for Australasian Society for Stem Cell Research, Brisbane, Australia

June 2013; Oral presentation; TERMIS-EU 2013, Istanbul, Turkey

September 2012; Poster presentation; TERMIS-WC 2012, Vienna, Austria

May 2012; Poster presentation; MMRI Stem Cell Symposium, Brisbane, Australia

Oct 2011; Poster presentation; ASSCR (the Australian Society for Stem Cell Research) 4th annual meeting, Sydney, Australia

Appendices

Permissions:

All material used in this Thesis but not generated by the author is reused with permission of the copyright owner. These permissions are obtained either via direct e-mail or RightsLink Copyright Clearance Centre. The material is used as it is in all cases, no alterations were made and the source was referenced appropriately either in text or in figure captions. Next, the permissions of the reused material are listed in appearing order.

App. A- Permission for quotations in Chapters 1 and 6

Betul Babur

From: Samantray, Banita (ELS-CHN) <b.samantray@reedelsevier.com>
Sent: Friday, 18 April 2014 3:37 PM
To: Betul Babur
Subject: RE: text re-use in a PhD thesis (OA)

Dear Betul

Thank you for your permission request.

We hereby grant you permission to reprint the material below at no charge **in your thesis** subject to the following conditions:

1. If any part of the material to be used (for example, figures) has appeared in our publication with credit or acknowledgement to another source, permission must also be sought from that source. If such permission is not obtained then that material may not be included in your publication/copies.

2. Suitable acknowledgment to the source must be made, either as a footnote or in a reference list at the end of your publication, as follows:

   "This article was published in Publication title, Vol number, Author(s), Title of article, Page Nos, Copyright Elsevier (or appropriate Society name) (Year)."

3. Your thesis may be submitted to your institution in either print or electronic form.

4. Reproduction of this material is confined to the purpose for which permission is hereby given.

5. This permission is granted for non-exclusive world **English** rights only. For other languages please reapply separately for each one required. Permission excludes use in an electronic form other than submission. Should you have a specific electronic project in mind please reapply for permission.

6. Should your thesis be published commercially, please reapply for permission.

Regards

Banita Samantray
Global Rights Department

Elsevier
(A division of Reed Elsevier India Pvt. Ltd.)

Ascendas International Tech Park | Crest Building – 12th Floor | Taramani Road | Taramani | Chennai 600 113 | India
Tel: +91 44 42994667 | Fax: +91 44 42994701
E-mail: b.samantray@reedelsevier.com | url: www.elsevier.com

From: Betul Babur [mailto:betul.kul@student.qut.edu.au]
Sent: Friday, April 11, 2014 1:13 AM
To: Permissions Helpdesk
Subject: text re-use in a PhD thesis

Hi there,
I am a PhD student at Queensland University of Technology (QUT) in Australia, Brisbane.
I would like to quote some text from two Elsevier papers in my thesis.
When I searched for a Rightslink option I could not see it for those two papers. They both said open access or archive in Science direct.
I am writing you to understand if it is OK to use some text in my thesis as quotations from papers.
Following are the texts and papers I would like to use:
1)

Scaffolds for tissue fabrication

Peter X Ma

"Imagine that one day a patient will go to a human 'body shop' for a prescription for a lost leg, a failing liver, or a dysfunctional heart. In addition to the physiological, medical, and genetic information of the patient, the doctor will also collect three-dimensional images of the patient's remaining leg (in the case of the lost-leg patient) with detailed anatomical structures (bone, cartilage, tendons, ligaments, blood vessels, muscles, nerves, skin, and so forth) and the external shape. The doctor may collect the patient's saliva or other body fluids to extract genetic material (DNA) and also a tiny piece of tissue or bone marrow to obtain seeding cells for expansion.

After the patient leaves the body shop, a computer is used by a tissue engineer to design the structure of the mirror leg (the lost leg) based on the symmetrical remaining leg, using various materials that simulate the extracellular matrices of the tissues of the leg (known as scaffolds or templates). Then, cells – from a universal cell source, specifically designed for the patient, or banked cells grown from the patient's own cells – are seeded onto these scaffolds. These engineered cell-scaffold components are then grown separately and/or assembled in a special chamber (bioreactor) that provides the right nutrients, regulating molecules (such as proteins, growth factors, and differentiation factors), physical and mechanical stimuli, temperature, pressure, and mass transport conditions for cell proliferation, differentiation, and tissue/organ formation. While the tissue/organ is regenerating, the scaffolding materials degrade and disappear, leaving nothing foreign to the body. The regenerated leg or leg precursor will be surgically grafted onto the patient during the second visit to the human body shop (Fig. 1). The engineered tissues will have the capacity to grow, model, and remodel in concert with the dynamic changes of the physiological environment of the body. The grafted leg will integrate into the body. The new leg will grow and age as the body's natural leg. This scenario is an example of what the field of tissue engineering is hoping to do in the future."

2)

A history of the understanding of cartilage

Dr T.G. Benedek, M.D.

"Cartilages are spread on some parts of them [bones], such as the joints, to make them smooth, and Nature also uses cartilages occasionally as moderately yielding bodies…. Cartilage serves as a grease for the joints[2a]." Elsewhere it is not only cartilage but also synovial fluid that protects joints against wear: "…Nature has again searched out a double remedy, first covering each member of the joint with cartilage and then pouring over the cartilages themselves a sort of oily substance, a greasy, glutinous fluid, which gives every joint an easy movement and protection against wear"

"cartilage is a certain substance like bone, but softer which you will find at the extremities of all the bones, large and small according to the need of the member…. This cartilaginous portion was reserved for many bones at their extremities in order to keep two hard surfaces from coming into contact and being broken by movement and to maintain something between the final hardness of the bone and the soft flesh"

"The head of the right os femoris was not rounded into a globular form: and was depress'd, and not cover'd by a smooth and white cartilage, but by one of a pale ash-colour: and, indeed, this cartilage was totally deficient in the posterior part of the head; so that the bone appear'd naked in that part, and form'd into many roundish and protuberant particles."

> "We may compare the Texture of a Cartilage to the Pile of Velvet, its Fibres rising up from the Bone, as the silky Threads of that rise from the woven Cloth or Basis….
>
> Now these perpendicular Fibres make the greatest Part of the cartilaginous Substance; but without Doubt there are likewise transverse Fibrils which connect them, and make the Whole a solid Body, though these last are not easily seen, because being very tender, they are destroyed in preparing the Cartilage."

" Every Joint is invested with a Membrane, which forms a complete Bag, and gives a Covering to every thing within the Articulation…. The Blood-vessels are so small, that they do not admit the red Globules of the Blood; so that they remain in a great measure unknown."

"…an ulcerated Cartilage is universally allowed to be a very troublesome Disease; that it admits of a Cure with more difficulty than a carious Bone; and that, when destroyed, it is never recovered[11]."""

Is it OK to quote those sections in my thesis? Please let me know about the issue.

Regards,

Betul (Kul) Babur

PhD Student | Stem Cell Therapies Laboratory | QUT | IHBI |
Translational Research Institute | Level 3 West | 37 Kent St. |
Woolloongabba | Queensland Australia 4102 |
Mobile: +61401239481 | Office: +61734437297
E-mail: betul.kul@student.qut.edu.au

App. B-Permission for Figures 1, 5 and 7

Betul Babur

From: Ann <ann@sechrest.com>
Sent: Monday, 14 April 2014 9:36 PM
To: Betul Babur
Subject: Re: [Website Feedback] authorization of reproduction for an image

Permission granted...Good Luck! Ann
On 4/10/2014 10:10 PM, Betul Babur wrote:
> Hi Ann,
> Here is my hopefully final list (I will not be using the image I asked for permission at the beginning because I have found a new one also listed below),
> I would like to ask for permission of re-use for the four images listed below:
>
> http://www.eorthopod.com/sites/default/files/imagecache/product_full/k
> nee_cart_surg_intro01.jpg
> http://www.eorthopod.com/sites/default/files/imagecache/product_full/k
> nee_arthroplasty_intro01.jpg
> http://www.eorthopod.com/sites/default/files/imagecache/product_full/k
> nee_osteoarth_intro01.jpg
> http://www.eorthopod.com/sites/default/files/images/knee_anatomy02a.jp
> g
>
>
> I will not be altering any of the images, the copyright will be intact and visible.
> I will not be using any of the material on web, in software or in prints and presentations for re-sale.
> Each image will be labelled as " Image courtesy of Medical Multimedia Group LLC, www.eOrthopod.com", I will try to insert an active link if I can.
> The name of my thesis will be "Utilizing micropellets as building blocks in cartilage tissue engineering".
> Please let me know about the decision.
>
> Regards,
> Betul (Kul) Babur
> PhD Student | Stem Cell Therapies Laboratory | QUT | IHBI |
> Translational Research Institute | Level 3 West | 37 Kent St. |
> Woolloongabba | Queensland Australia 4102 |
> Mobile: +61401239481 | Office: +61734437297
> E-mail: betul.kul@student.qut.edu.au
>
> -----Original Message-----
> From: Ann [mailto:ann@sechrest.com]
> Sent: Thursday, 10 April 2014 9:54 PM
> To: Betul Babur
> Subject: Re: [Website Feedback] authorization of reproduction for an
> image
>
> Betul - We prefer that you use current images that are on our website
> http://www.eorthopod.com. Once you have established which ones you
> want to use in your thesis, send me a list for approval. Thanks, Ann
>

App. C- Permission for Figure 3

Betul Babur

From: Ed Woodward <ecw1@rice.edu>
Sent: Thursday, 3 April 2014 11:56 PM
To: Betul Babur; cnx@cnx.org
Subject: Re: [cnx@cnx.org] authorization of reproduction for an image

It is all ok.

Ed

On 4/2/14 7:18 PM, Betul Babur wrote:

> Hello Ed,
> Thanks for your quick response.
> I just wanted to be clear, I will embed the image into my document, say image is the courtesy of "Creative Commons CC-BY", reference it then list the following in my references section "OpenStax College, Bone Formation and Development. OpenStax CNX. Jun 28, 2013 http://cnx.org/contents/b601e5c1-0c20-449c-a324-a0f5ad55eb96@4."
> Would that be sufficient?
> Also my thesis will be available online after acceptance, is that also OK?
>
> Regards,
>
> Betul (Kul) Babur
>
> PhD Student | Stem Cell Therapies Laboratory | QUT | IHBI |
> Translational Research Institute | Level 3 West | 37 Kent St. |
> Woolloongabba | Queensland Australia 4102 |
> Mobile: +61401239481 | Office: +61734437297
> E-mail: betul.kul@student.qut.edu.au
>
> **From:** Ed Woodward [mailto:ecw1@rice.edu]
> **Sent:** Thursday, 3 April 2014 12:20 AM
> **To:** Betul Babur; cnx@cnx.org
> **Subject:** Re:[cnx@cnx.org] authorization of reproduction for an image
>
> All of our content is licensed Creative Commons CC-BY which means you are free to reuse our content as long as you give proper attribution to OpenStax CNX and the author. Please use the URL to the new version of our site which is http://cnx.org/contents/b601e5c1-0c20-449c-a324-a0f5ad55eb96@4. At the bottom of the page, there is an Attribution tab that has examples of proper attribution for this Page.
>
> Ed
> OpenStax CNX Team

App. D- Permission for Figure 4

SPRINGER LICENSE
TERMS AND CONDITIONS

Apr 15, 2014

This is a License Agreement between Betul Babur ("You") and Springer ("Springer") provided by Copyright Clearance Center ("CCC"). The license consists of your order details, the terms and conditions provided by Springer, and the payment terms and conditions.

All payments must be made in full to CCC. For payment instructions, please see information listed at the bottom of this form.

License Number	3364500480203
License date	Apr 08, 2014
Licensed content publisher	Springer
Licensed content publication	Stem Cell Reviews
Licensed content title	Time-Dependent Processes in Stem Cell-Based Tissue Engineering of Articular Cartilage
Licensed content author	Ivana Gadjanski
Licensed content date	Jan 1, 2011
Volume number	8
Issue number	3
Type of Use	Thesis/Dissertation
Portion	Figures
Author of this Springer article	No
Order reference number	
Original figure numbers	figure 1
Title of your thesis / dissertation	untilizing micropellets as building blocks in cartilage tissue engineering
Expected completion date	Jun 2014
Estimated size(pages)	100
Total	0.00 USD
Terms and Conditions	

Introduction

The publisher for this copyrighted material is Springer Science + Business Media. By clicking "accept" in connection with completing this licensing transaction, you agree that the following terms and conditions apply to this transaction (along with the Billing and Payment terms and conditions established by Copyright Clearance Center, Inc. ("CCC"), at the time that you opened your Rightslink account and that are available at any time at http://myaccount.copyright.com).

App. E- Permission for Figure 8

Title: Clinical Efficacy of the Microfracture Technique for Articular Cartilage Repair in the Knee:An Evidence-Based Systematic Analysis

Author: Kai Mithoefer, Timothy McAdams, Riley J. Williams, Peter C. Kreuz, Bert R. Mandelbaum

Publication: American Journal of Sports Medicine

Publisher: SAGE Publications

Date: 10/01/2009

Logged in as:
Betul Babur
Account #:
3000775536

LOGOUT

Gratis

Permission is granted at no cost for sole use in a Master's Thesis and/or Doctoral Dissertation. Additional permission is also granted for the selection to be included in the printing of said scholarly work as part of UMI's "Books on Demand" program. For any further usage or publication, please contact the publisher.

App. F- Permission for Figure 9

BMJ PUBLISHING GROUP LTD. LICENSE TERMS AND CONDITIONS

Apr 15, 2014

This is a License Agreement between Betul Babur ("You") and BMJ Publishing Group Ltd. ("BMJ Publishing Group Ltd.") provided by Copyright Clearance Center ("CCC"). The license consists of your order details, the terms and conditions provided by BMJ Publishing Group Ltd., and the payment terms and conditions.

All payments must be made in full to CCC. For payment instructions, please see information listed at the bottom of this form.

License Number	3364520347802
License date	Apr 08, 2014
Licensed content publisher	BMJ Publishing Group Ltd.
Licensed content publication	The BMJ
Licensed content title	Treating joint damage in young people
Licensed content author	George Bentley, Tom Minas
Licensed content date	Jun 10, 2000
Volume number	320
Type of Use	Thesis/Dissertation
Requestor type	Individual
Format	Print and electronic
Portion	Figure/table/extract
Number of figure/table/extracts	3
Will you be translating?	No
Circulation/distribution	4
Title of your thesis / dissertation	untilizing micropellets as building blocks in cartilage tissue engineering
Expected completion date	Jun 2014
Estimated size(pages)	100
BMJ VAT number	674738491
Billing Type	Invoice
Billing address	TRI Level 3 West 37 Kent St. Woolloongabba , QLD 4102 Australia
Permissions Cost	0.00 USD
VAT (0.00%)	0.00 USD
Total	0.00 USD
Terms and Conditions	

App. G- Permission for Figure 36

WOLTERS KLUWER HEALTH LICENSE TERMS AND CONDITIONS

Apr 15, 2014

This is a License Agreement between Betul Babur ("You") and Wolters Kluwer Health ("Wolters Kluwer Health") provided by Copyright Clearance Center ("CCC"). The license consists of your order details, the terms and conditions provided by Wolters Kluwer Health, and the payment terms and conditions.

All payments must be made in full to CCC. For payment instructions, please see information listed at the bottom of this form.

License Number	3364500014899
License date	Apr 08, 2014
Licensed content publisher	Wolters Kluwer Health
Licensed content publication	Current Orthopaedic Practice
Licensed content title	Biologic Repair of Articular Cartilage: Defect Models in Experimental Animals and Matrix Requirements
Licensed content author	Ernst Hunziker
Licensed content date	Jan 1, 1999
Volume Number	367
Type of Use	Dissertation/Thesis
Requestor type	Individual
Portion	Figures/table/illustration
Number of figures/tables/illustrations	1
Figures/tables/illustrations used	figure 5
Author of this Wolters Kluwer article	No
Title of your thesis / dissertation	untilizing micropellets as building blocks in cartilage tissue engineering
Expected completion date	Jun 2014
Estimated size(pages)	100
Billing Type	Invoice
Billing address	TRI Level 3 West 37 Kent St. Woolloongabba , QLD 4102 Australia
Total	0.00 USD
Terms and Conditions	

App. H- Permission for Figure 37

ELSEVIER LICENSE
TERMS AND CONDITIONS

Apr 15, 2014

This is a License Agreement between Betul Babur ("You") and Elsevier ("Elsevier") provided by Copyright Clearance Center ("CCC"). The license consists of your order details, the terms and conditions provided by Elsevier, and the payment terms and conditions.

All payments must be made in full to CCC. For payment instructions, please see information listed at the bottom of this form.

Supplier	Elsevier Limited The Boulevard,Langford Lane Kidlington,Oxford,OX5 1GB,UK
Registered Company Number	1982084
Customer name	Betul Babur
Customer address	TRI Level 3 West 37 Kent St. Woolloongabba , QLD 4102
License number	3370540684606
License date	Apr 15, 2014
Licensed content publisher	Elsevier
Licensed content publication	Biomaterials
Licensed content title	Organ printing: Tissue spheroids as building blocks
Licensed content author	Vladimir Mironov,Richard P. Visconti,Vladimir Kasyanov,Gabor Forgacs,Christopher J. Drake,Roger R. Markwald
Licensed content date	April 2009
Licensed content volume number	30
Licensed content issue number	12
Number of pages	11
Start Page	2164
End Page	2174
Type of Use	reuse in a thesis/dissertation
Intended publisher of new work	other
Portion	figures/tables/illustrations
Number of figures/tables/illustrations	1
Format	both print and electronic
Are you the author of this Elsevier article?	No
Will you be translating?	No

App. I- Permission for Figure 38

ELSEVIER LICENSE
TERMS AND CONDITIONS

Apr 21, 2014

This is a License Agreement between Betul Babur ("You") and Elsevier ("Elsevier") provided by Copyright Clearance Center ("CCC"). The license consists of your order details, the terms and conditions provided by Elsevier, and the payment terms and conditions.

All payments must be made in full to CCC. For payment instructions, please see information listed at the bottom of this form.

Supplier	Elsevier Limited The Boulevard,Langford Lane Kidlington,Oxford,OX5 1GB,UK
Registered Company Number	1982084
Customer name	Betul Babur
Customer address	TRI Level 3 West 37 Kent St. Woolloongabba , QLD 4102
License number	3373961507577
License date	Apr 21, 2014
Licensed content publisher	Elsevier
Licensed content publication	Trends in Biotechnology
Licensed content title	The role of bioreactors in tissue engineering
Licensed content author	Ivan Martin,David Wendt,Michael Heberer
Licensed content date	February 2004
Licensed content volume number	22
Licensed content issue number	2
Number of pages	7
Start Page	80
End Page	86
Type of Use	reuse in a thesis/dissertation
Portion	figures/tables/illustrations
Number of figures/tables/illustrations	1
Format	both print and electronic
Are you the author of this Elsevier article?	No
Will you be translating?	No
Title of your thesis/dissertation	untilizing micropellets as building blocks in cartilage tissue engineering
Expected completion date	Jun 2014